March 2019

POPULATION VIABILITY AND CONNECTIVITY OF THE FEDERALLY THREATENED EASTERN INDIGO SNAKE IN CENTRAL PENINSULAR FLORIDA

Javan Bauder

POPULATION VIABILITY AND CONNECTIVITY OF THE FEDERALLY THREATENED EASTERN INDIGO SNAKE IN CENTRAL PENINSULAR FLORIDA

A Dissertation Presented

by

JAVAN MATHIAS BAUDER

Submitted to the Graduate School of the

University of Massachusetts Amherst in partial fulfillment

of the requirement for the degree of

DOCTOR OF PHILOSOPHY

February 2019

Department of Environmental Conservation
Wildlife, Fish, and Conservation Biology

POPULATION VIABILITY AND CONNECTIVITY OF THE FEDERALLY THREATENED EASTERN INDIGO SNAKE IN CENTRAL PENINSULAR FLORIDA

A Dissertation Presented

By

JAVAN MATHAIS BAUDER

Approved as to style and content by:

_____
Kevin McGarigal, Chair

_____
John T. Finn, Member

_____
Andrew R. Whiteley, Member

_____
Daniel R. Sheldon, Member

_____
Christopher L. Jenkins

_____
Curtice R. Griffin, Department Head
Environmental Conservation

DEDICATION

To my wife, Kelsey, and my daughters, Adalyn Jane and Stella Grace, for their love, support, and encouragement through this whole process. I love you all!

ACKNOWLEDGEMENTS

I would first like to thank my Lord and Savior Jesus Christ whose grace and mercy has allowed me to complete this process. To God be the glory! I would also like to thank my wife, Kelsey, for her love and encouragement while spending the first five years of our marriage as the wife of a graduate student. I also thank my daughters, Adalyn Jane and Stella Grace, for the joy and fulfillment they have brought.

I would like to give a special thanks to my dissertation committee chair, Dr. Kevin McGarigal, for his mentorship and incredible support. I have learned so much from him and feel very blessed to have been one of his students. I would also like to give special acknowledgement to my committee member and long-time friend and mentor, Dr. Chris Jenkins. Chris has encouraged and supported me in my academic and career development for over 12 years. He provided the initial opportunity and funding for me to return to school for my Ph.D., and I am very thankful for his continuous support throughout this process. Special thanks go to my other committee members, Dr. Andrew Whiteley, Dr. Jack Finn, and Dr. Dan Sheldon, for their insight and guidance on this project.

This project could not have been accomplished without the help of many collaborators and colleagues, and I am very thankful for their support and assistance. Dr. Dave Breininger, Becky Bolt, and Mike Legare generously provided me with their 5-year eastern indigo snake data set without which this project, in its current form, would not have been possible. They have been patient with my incessant questions and generous with their contributions. Dr. Betsie Rothermel was instrumental in developing our eastern

indigo snake research program at the Archbold Biological Station and provided invaluable support throughout our work there. These people have been, and continue to be, models of supportive collaborators.

Linda LaClaire at the U.S. Fish and Wildlife Service obtained funding for much of this project through a Cooperative Agreement under the Endangered Species Conservation-Recovery Implementation Fund and she has been an enthusiastic supporter of this project from its inception. I would like to thank the Explorer's Club, the Society for the Study of Amphibians and Reptiles, and The Herpetologist's League for additional funding. Very special thanks go to the Department of Environmental Conservation at the University of Massachusetts for providing me with a graduate research fellowship and Drs. Kevin McGarigal and Chris Sutherland for multiple teaching assistantships.

I would also like to thank Dr. Hillary Swain and the Archbold Biological Station for allowing use of their facilities. Zach Forsburg, Lance Paden, Patrick Barnhardt, and Ed Stowe were outstanding field technicians and numerous staff, students, and volunteers at The Archbold Biological Station and in Highlands County assisted with field work. Wade Ulrey, Kevin Main, and Kye Ewing assisted in accessing many private properties in Highlands County. Numerous private land owners in Highlands County allowed us access to their property to radio-track eastern indigo snakes and I am very thankful for their support. The Florida Fish and Wildlife Conservation Commission provided access to additional properties and contributed many genetic samples. Nicole Ranalli, Brad Kolhoff, and Joseph Sage were particularly helpful and supportive. The Florida Department of Environmental Protection Division of Parks, The Florida Forest Service, The Nature Conservancy, and Lykes Bros., Inc. provided access to their properties to

search for eastern indigo snakes and I thank Dave Butcher, Steven Dale, Steve Morrison, Jennifer Navarra, Beatriz Pace-Aldana, Adam Peterson, and Brian Pinson for helping to facilitate access. Daniel Parker provided valuable insights and assistance in searching for eastern indigo snakes in central Florida. Andy Day, Kevin Enge, Greg Graziani, and Steve Godley provided additional field assistance collecting genetics samples. A very special acknowledgment goes to Dr. Chris Jenkins and the Orianne Society for allowing me to return to school for my Ph.D. while still an employee and continuing their financial and logistical support thereafter. I would like to thank my former Orianne Society coworkers, Heidi Hall, Dirk Stevenson, Karen McLain, Sue Bottoms, Patty Li, Jerry Medlock, and Kevin Croom, for all their administrative and technical support over the years. Dr. Kenney Krysko and the Florida Museum of Natural History provided additional genetics samples. Dr. Steve Spear conducted the laboratory work for the genetics portion of this project and provided additional guidance on data analyses. Dr. Bill Peterman provided substantial guidance on the use of his R package RESISTANCEGA for use in our genetics analysis. Special thanks to Dr. Jim Hines and Dr. Marc Mazerolle who re-analyzed our eastern indigo snake survival data.

I would also like to thank everyone in Dr. McGarigal's lab. I feel very blessed to have been part of such an outstanding group and I learned so much from everyone. I want to thank my fellow graduate students Dr. Kathy Zeller, Blake Massey, and Kris Winiarski. A very special thanks goes to Brad Compton and Ethan Plunkett for their invaluable help with all things computational. Their patience with me on the lab's cluster is amazing, and I could never have completed this project without their support.

Finally, I would like to thank the rest of my family for their love and support in so many different ways over these past six years, ranging from running some of my analyses on their computers to providing us with a place to live: my parents Rudy and Carolyn Bauder; my brothers, Jared and Jesse Bauder; my wife's parents, Dexter and Patricia James; and my in-law's, David and Katrina Lent. Their support has truly made this dissertation a family project.

ABSTRACT

POPULATION VIABILITY AND CONNECTIVITY OF THE FEDERALLY THREATENED EASTERN INDIGO SNAKE IN CENTRAL PENINSULAR FLORIDA

FEBRUARY 2019

JAVAN MATHIAS BAUDER, B.S., UNIVERSITY OF IDAHO

M.S., IDAHO STATE UNIVERSITY

PH.D., UNIVERSITY OF MASSACHUSETTS AMHERST

Directed by: Professor Kevin McGarigal

Understanding the factors influencing the likelihood of persistence of real-world populations requires both an accurate understanding of the traits and behaviors of individuals within those populations (e.g., movement, habitat selection, survival, fecundity, dispersal) but also an understanding of how those traits and behaviors are influenced by landscape features. The federally threatened eastern indigo snake (EIS, *Drymarchon couperi*) has declined throughout its range primarily due to anthropogenically-induced habitat loss and fragmentation making spatially-explicit assessments of population viability and connectivity essential for understanding its current status and directing future conservation efforts.

The primary goal of my dissertation was to understand how landscape features influence EIS population viability and connectivity in central peninsular Florida. I accomplished this through four components. First, I evaluated EIS movement patterns and space use including daily movement distance, home range size, within-individual home range overlap, and among-individual home range overlap and how these patterns varied by sex and season. Second, I conducted a multi-level, multi-scale habitat selection analysis to create spatially-explicit estimates of EIS habitat selection. Third, using the aforementioned data and previously published data, I developed an agent-based model for simulating EIS movement, survival, reproduction, and dispersal in central Florida. I used this model to determine how landscape features and conservation lands influence EIS occupancy across our study landscape. Finally, I used landscape genetics to determine how landscape features influenced genetic connectivity and to estimate resistance surfaces with which to model potential corridors.

I found that male EIS maintain larger home ranges than females and move extensively during the breeding season in search of females. While seasonal home ranges within an individual strongly overlapped, individuals avoided home ranges of same-sex conspecifics. EIS selected home ranges and within-home range locations in areas of undeveloped upland habitat with high habitat heterogeneity and generally avoided urban. While EIS did not avoid roads, they rarely crossed primary and secondary roads. I used observed patterns of movement and habitat selection to calibrate my ABM. My ABM simulated larger male home ranges and smaller home ranges and lower survival in urbanized landscapes although simulated effect sizes were weaker than observed effect sizes. My model was unable to simulate observed patterns of within-individual home

range overlap but accurately simulated survival in developed and undeveloped landscapes. EIS occupancy after a 15 year simulation was 56% and occupancy was most strongly affected, negatively, by urbanization. While the presence of conservation lands was not a strong driver of EIS occupancy, EIS occupancy was more consistently higher on conservation lands. EIS gene flow was most strongly associated with undeveloped uplands, urbanization, and habitat edge at the broadest scales we evaluated. Potential corridors were widespread in the southern half of our study area with substantial areas of potential habitat and corridor occurring outside of the existing conservation network. This work indicates that the LWR contains extensive areas capable of supporting EIS although increasing urbanization may have a negative impact on future persistence of EIS.

TABLE OF CONTENTS

LIST OF TABLES

Table Page

LIST OF FIGURES

Figure Page

CHAPTER 1

EFFECTS OF SEX AND SEASON ON EASTERN INDIGO SNAKE (*DRYMARCHON COUPERI*) MOVEMENT PATTERNS AND SPATIAL OVERLAP AT MULTIPLE SPATIO-TEMPORAL SCALES

1.1. Introduction

Animal movements can vary across multiple spatio-temporal scales in response to variation in resource availability or the relative importance of a given resource (e.g., Lister and Aguayo 1992; Trierweiler et al. 2013). Seasonal variation in movement patterns is widespread throughout many snake taxa and can occur in response to spatio-temporal variation in hibernacula (Gregory 1982), prey (Madsen and Shine 1996a; Sperry and Weatherhead 2009b), mates (King and Duvall 1990; Glaudas and Rodriguez-Robles 2011), gestation or oviposition sites (Blouin-Demers and Weatherhead 2002; Brown et al. 2005), and thermally suitable shelters (Croak et al. 2013). As ectotherms, snake activity is also strongly influenced by environmental temperature (Peterson et al. 1993; George et al. 2015) and seasonal variation in temperature may constrain their activity to periods of thermally conducive weather (Sperry et al. 2010). Some of the most pronounced seasonal movements in snakes occur in populations in north-temperate regions in the form of seasonal migrations between communal hibernacula and summer foraging/breeding habitats (Larsen 1987; Jorgensen et al. 2008; Gardiner et al. 2013). Many snake species with broad geographical ranges appear to exhibit more pronounced migratory behavior at higher latitudes (Reed and Douglas 2002; Rodriguez-Robles 2003; Carfagno and Weatherhead 2008; Klug et al. 2011; Gardiner et al. 2013). Nevertheless, species in mild

climates might still undertake lengthy migrations in response to seasonal variation in other resources, such as prey (Madsen and Shine 1996a).

The nature of interactions among conspecifics has a strong influence on their degree of spatial overlap, which in turn influences multiple ecological processes, including social behaviors (MacDonald et al. 2010), mating systems (Owen-Smith 1977), and population density and regulation (Wolff 1997; Fryxell et al. 1999). The degree of spatial overlap among conspecifics can vary widely within and among species (Rogers 1987; Ostfeld 1990; Gehrt and Fritzell 1998; McLoughlin et al. 2000; MacDonald et al. 2010), ranging from extensive overlap to exclusive space use (Maher and Lott 1995). Patterns of conspecific spatial overlap and the factors influencing those patterns are described for many terrestrial taxa, including mammalian carnivores (Powell 1979; Rogers 1987; Powell 1994; Gese 2001; MacDonald et al. 2010) and herbivores (Owen-Smith 1977), small mammals (Smith 1968; Ostfeld 1986; Ostfeld 1990), birds (Brown 1969), and lizards (Stamps 1983). However, relatively little is known about the factors influencing spatial overlap in snakes.

Studies on snake movement patterns and space use have reported widely varying levels of spatial overlap, ranging from extensive home range overlap (Diffendorfer et al. 2005; Mitrovich et al. 2009; Anguiano and Diffendorfer 2015) to low levels of overlap (Webb and Shine 1997; Steen and Smith 2009; Cottone and Bauer 2013). Other studies have reported extensive home range overlap but conspecific avoidance at the scale of specific shelters (Fitzgerald et al. 2002; Whitaker and Shine 2003). However, active defense of and conspecific exclusion from an area (i.e., territoriality) (Maher and Lott 1995) appears very rare in snakes (Gregory et al. 1987; Greene 1997; Huang et al. 2011;

Webb et al. 2015). Indeed, many species of snakes show very dense conspecific aggregations (Gregory et al. 1987) yet these aggregations often occur near high concentrations of resources such as communal hibernacula, gestation sites, distinct habitats (e.g., wetlands or riparian habitats), cover objects, prey, or potential mates (Gregory 1984; Gillingham 1987; Gregory et al. 1987; Graves and Duvall 1995). In such cases, the benefits and efficacy of maintaining exclusive access to those resources may be far below the costs (Maher and Lott 2000) although the only two studies demonstrating territorial behavior in snakes both involved spatially clustered resources, i.e., sea turtle nests (Huang et al. 2011) and shelter sites (Webb et al. 2015). Excluding individuals from an area where resources are widely dispersed may prove similarly uneconomical. Nevertheless, despite the variability in patterns of spatial overlap reported for snakes, most studies reporting information on inter-individual home range overlap in snakes merely report population-level summary statistics and do not examine how overlap varied temporally or by sex. Describing patterns of home range overlap within and between sexes and how those patterns vary seasonally may provide insights into the mechanisms driving the degree of observed overlap.

Eastern Indigo Snakes (*Drymarchon couperi*) are large (> 2 m) colubrids endemic to the southeastern coastal plain of the U.S. (Smith 1941; Conant and Collins 1998; Enge et al. 2013) and listed as Threatened under the U.S. Endangered Species Act (U. S. Fish and Wildlife Service 1978). This species shows male-biased sexual dimorphism with males being longer and heavier than females (Stevenson et al. 2009). In the northern part of their range (southern Georgia), *D. couperi* exhibit strong seasonal variation in movement patterns (Speake et al. 1978; Hyslop et al. 2014). In this region, *D. couperi*

maintained small (< 10 ha) winter home ranges on xeric sandhills that support Gopher Tortoises (*Gopherus polyphemus*), but used much larger (≤ 1500 ha) home ranges and a greater diversity of habitat types during Spring through Autumn (Speake et al. 1978; Stevenson et al. 2003; Hyslop et al. 2009a; Stevenson et al. 2009; Hyslop et al. 2014). In one study, several individuals undertook lengthy (1.5–7.5 km) linear migrations between winter and summer home ranges in a manner analogous to many north-temperate snake species (Hyslop et al. 2014). However, less is understood about seasonal variation in *D. couperi* movements in peninsular Florida. Breininger et al. (Breininger et al. 2011) reported smaller home range sizes (≤ 538 ha) than those reported for southern Georgia and noted that *D. couperi* did not make seasonal migrations. Additionally, very little is known about how individual home ranges overlap spatially or what factors may affect the degree of overlap. Hyslop et al. (2014) reported that several *D. couperi* in southern Georgia had overlapping year-round home ranges. No studies have to-date discussed inter- or intra-individual home range overlap for *D. couperi* in peninsular Florida. More detailed descriptions are therefore needed to quantify seasonal variation in *D. couperi* spatial ecology in peninsular Florida.

Reproductive behavior is also known to have a strong influence on seasonal variation in snake movements both within and between sexes. Males in many species search for females during the breeding season and therefore move more extensively during those times (Waldron et al. 2006; Glaudas and Rodriguez-Robles 2011; Lelievre et al. 2012; Putman et al. 2013). Females might also move more extensively during the breeding season (Blouin-Demers and Weatherhead 2002; Brown et al. 2005) or exhibit reduced movement while gestating or prior to oviposition (Reinert and Zappalorti 1988b;

Graves and Duvall 1993; Carfagno and Weatherhead 2008). *Drymarchon couperi* appear to maintain a late fall through early spring breeding season throughout their range, during which males engage in mate-searching, male–male ritualized combat, and, possibly, guarding of females (Moler 1992; Stevenson et al. 2003; Hyslop 2007; Stevenson et al. 2009; D.S. Stevenson, personal observation). In southern Georgia, however, breeding activity is largely confined to overwintering sites presumably because of *D. couperi*'s cool-season reliance on Gopher Tortoise burrows (Stevenson et al. 2003; Hyslop et al. 2009a; Hyslop et al. 2014). In contrast, *D. couperi* breeding activity in peninsular Florida could potentially occur over a broader spatial extent because individuals can move throughout their home ranges during both the breeding and non-breeding seasons (Breininger et al. 2011). While Breininger et al. (2011) found that male *D. couperi* had larger home ranges than females, they did not examine the extent to which this might have been related to male breeding season movements, nor did they quantify the degree of within-individual seasonal home range overlap.

Our goals were to describe seasonal variation in the spatial ecology of *D. couperi* in central Florida at multiple temporal scales, and to ascertain the degree to which seasonal variation in spatial parameters differs between sexes. Given that male *D. couperi* appear to search for females during the breeding season in southern Georgia (Stevenson et al. 2009), we hypothesized that male *D. couperi* in central Florida would also exhibit mate-searching behavior. However, given the greater potential for year-round surface activity in peninsular Florida (Breininger et al. 2011),we predicted that male mate-searching behavior in our study would result in longer, more frequent movements and larger home ranges during the breeding season compared to the non-breeding season. We

also expected that females would show either seasonally invariant movement patterns or increased movements during spring oviposition (e.g., Blouin-Demers and Weatherhead 2002). We also predicted that within-individual home range overlap would be moderate to high (Breininger et al. 2011), but that such overlap would be lowest for males when comparing breeding and non-breeding seasons, indicating that males expanded and/or shifted their breeding season home ranges in their search for females. Finally, we predicted that *D. couperi* would show relatively little inter-individual home range overlap within sexes and that the degree of inter-individual home range overlap for males would increase during the breeding season.

1.2. Methods

1.2.1. Study Site and Data Collection

We used radio telemetry data collected from two separate studies. The first study occurred on the southern 40 km of the Lake Wales Ridge in Highlands County, Florida (27°17′N, 81°21′W; datum = WGS84 in all cases) from 2011–2013. This study area included both state and private lands and was a mix of natural habitats (scrub, scrubby flatwoods, mesic flatwoods, forested and non-forested wetlands), cattle ranches, citrus groves, and rural and urban development. Abrahamson et al. (1984) and Layne and Steiner (1996) provide additional details about this study area. Sampling methodologies including *D. couperi* capture, surgical implantation of radio transmitters, and radio telemetry procedures were described in Bauder and Barnhart (2014). While the majority of our telemetry fixes were obtained via homing, a small number (113 of 3219 = 3.5%)

were obtained via triangulation (White and Garrott 1990) with Lenth's maximum likelihood estimator (Lenth 1981) using LOAS (v4.0, Ecological Software Solutions LLC, Hegymagas, Hungary). We then predicted the linear error of these locations as described in Bauder and Barnhart (Bauder and Barnhart 2014).

The second study occurred primarily at three locations in central peninsular Florida including Brevard (28°38′N, 80°42′W), Indian River (27°50′N, 80°35′W), and Polk counties (27°37′N, 81°19′W). These study areas included federal, state, and private lands and a diversity of natural habitats (scrub, scrubby flatwoods, mesic flatwoods, hammocks, forested and non-forested wetlands, coastal scrub) and rural and urban development. Data were collected from 1998–2003 as described in Breininger et al. (2011). We hereafter refer to these two datasets as Highlands and Brevard, respectively.

1.2.2. Movement Patterns

We used the Highlands data to analyze fine-scale movement patterns because the data were collected more frequently (approximately every 2 d) than the Brevard data (approximately weekly). We further restricted our movement analyses to telemetry fixes obtained via homing and separated by ≤ 7 d (n = 2735). All analyses were conducted in R (R Core Team 2017) and values are reported as mean ± 1 SE unless otherwise noted.

We estimated daily probability of movement (DPM) as the per day probability of a snake leaving its current location. Because we did not obtain daily locations on our telemetered snakes we considered the probability of a snake leaving its current location as a binomial probability with trial size equal to the number of days until the next consecutive telemetry fix (Days) and per trial (i.e., per day) probability (P) of moving

from that location as DPM. We estimated DPM by first calculating the sum of the squared error (SSE) between our observed data (0 or 1 denoting whether or not the snake moved from that location) and the predicted probability of the snake moving from that location with trial size equal to Days and per trial probability equal to *P*. We then used the R function *optimize* to find the value of *P* that minimized the SSE which we then retained as our estimate of DPM. To determine how DPM varied seasonally, we used a 40-d moving window to calculate DPM and a bootstrapped 95% confidence interval for each day of the year (DOY). We selected a 40-d window because it was the smallest window size that allowed model convergence in subsequent analysis, although we found that window size had little effect on the overall pattern of our results. To create a smoothed fit to our time series of DPM, we fit a generalized additive model (GAM) to DPM for males and females separately using the MGCV package (v. 1.8-5; Wood 2011; Wood 2015). We used a cyclic P-spline smooth term to ensure that the predicted DPM for DOY = 1 and DOY = 365 were equal, and a generalized approximate cross-validation to select the degree of smoothing. We calculated bootstrapped prediction intervals by randomly sampling our data with replacement, calculating the DPM for each DOY using a 40-d moving window, fitting a GAM to the new estimates of DPM, and then calculating the predicted DPM for each DOY. We repeated this process 1000 times and took the 2.5 and 97.5 percentiles of each DOY's predicted values.

We calculated daily movement rate as meters moved per day. Although most researchers obtain this value by dividing the distance between consecutive telemetry observations by the number days between those observations, this approach assumes the distance was covered equally over each day, an assumption that is unrealistic in nature.

Therefore, we used our predicted DPM from the GAM to adjust our uncorrected estimates of daily movement rate, as follows:

1. We measured the distance between consecutive telemetry locations with the package ADEHABITATLT in R (v. 0.3.23; Calenge 2006).
2. For each telemetry location, we calculated the probability that the telemetered snake moved from that location (P_{moved}) as a binomial probability with trial size equal to Days and P equal to the GAM-predicted DPM for that snake's sex and DOY.
3. For 1,…n where n = Days, we multiplied the uncorrected movement rate (distance/n) by the cumulative binomial probability of moving from that location with trial size n = Days and per trial probability P normalized by P_{moved}. For example, if Days = 3, P = 0.50, and distance between locations = 100 m then P_{moved} = 0.875. We would then calculate the probability of moving 100 m over one day (0.375), normalize that value by P_{moved} (i.e., 0.375 / 0.875 = 0.429), and then multiply the resulting value by 100/1. We would then calculate the probability of moving 100 m over 2 d (0.375), normalize that value by P_{moved}, and multiply the resulting value by 100/2. Lastly, we would calculate the probability of moving 100 m over 3 d (0.125), normalize that value by P_{moved}, and multiply the resulting value by 100/3. Finally, we would sum these values to obtain the adjusted daily movement rate (i.e., [0.429 × 100 m / day] + [0.429 × 50 m / day] + [0.143 × 33 m / day] = 69.07 m / day compared to 100 m / 3 days = 33.33 m / day).

Because the frequency distribution of daily movement rate was highly right-skewed, we modeled our data using a generalized Pareto distribution (GPD) with the package TEXMEX (v. 2.1; Southworth and Heffernan 2013). TEXMEX uses a GPD with two parameters, scale and shape. The scale controls the spread of the distribution while the shape controls the shape of the distribution and can be positive or negative. In our application, both an increasing scale and shape indicate a greater frequency of longer daily movement rate although shape had a trivial effect on the overall form of our distributions so we only report the estimates of scale. To determine how daily movement rate varied seasonally, we used a 40-d moving window to calculate scale and its bootstrapped 95% CI for each DOY.

1.2.3. Home Range Estimation

We estimated annual and seasonal home ranges for both Highlands and Brevard data. We used triangulated locations from Highlands County with predicted linear error ≤ 150 m (Bauder and Barnhart 2014) because fixed kernel home range estimates are robust to triangulation error at the scale observed in our study (Moser and Garton 2007). We estimated annual (i.e., 9–12 mo) home ranges using fixes from individuals tracked ≥ 255 consecutive days (~9 mo) because home range estimates are unbiased these sampling durations (i.e., home range size estimated with 9 mo of data is ≥ 0.90 of home range size estimated with 12 mo of data; Bauder et al. 2015). We defined the breeding season as October–March and the non-breeding season as April–September based on observations of *D. couperi* breeding activity throughout its range (Layne and Steiner 1996; Stevenson et al. 2009; Hyslop et al. 2014). We estimated seasonal home ranges for each 6-mo

season using individuals tracked for ≥ 105 consecutive days (~3.5 mo) because estimates are unbiased at these sampling durations (i.e., home range size estimated with 3.5 mo of data is ≥ 0.90 of home range size estimated with 6 mo of data; Bauder et al. 2015), and our results were similar for individuals tracked for 6 mo. The greater sampling intensity for Highlands snakes also allowed us to calculate 3-mo home ranges for Winter (January–March), Spring (April–June), Summer (July–September), and Autumn (October–December). We used individuals tracked for ≥ 73 consecutive days (~2.5 mo) and our results were similar to those using individuals tracked for 3 mo. We did not estimate 3-mo home ranges for Brevard because of insufficient telemetry fixes.

We estimated home ranges using 95% fixed kernel utilization distributions (UD) and 100% minimum convex polygons (MCP). We used the plug-in and reference bandwidths with unconstrained bandwidth matrices (Duong and Hazelton 2003) because they were robust to variation in sampling intensity and allowed for a more flexible degree of smoothing compared to single-parameter bandwidth matrices (Bauder et al. 2015). We estimated the bandwidth matrix using the KS package (v. 1.9.2; Duong 2007; Duong 2014). Home range sizes estimated using the reference bandwidth were highly correlated with home range sizes estimated using the plug-in bandwidth ($r_s \geq 0.97$) and MCP ($r_s \geq 0.97$), so we report the results of the home range size analyses using the reference bandwidth. Because some seasonal home ranges in the Brevard data had as few as 10 fixes, we calculated area-observation plots for all seasonal home ranges by subsampling the data for each home range at 5, …, $n - 1$ fixes where n is the total number of fixes for that home range (Harris et al. 1990; Laver and Kelly 2008). We ran 500 iterations at each number of subsampled fixes and considered our home range estimates to have reached an

asymptote if the mean home range size for ≥ (n × 0.50) subsampled fixes was within 0.10 of the full home range size. The number of fixes for seasonal home ranges reaching an asymptote ranged from 11–84. We found that the results of our subsequent analyses were similar to those obtained using all seasonal home ranges with ≥ 10 fixes.

We tested for effects of sex, study site (Highlands and Brevard), and their interaction on annual home range size using linear mixed-effects models with individual treated as a random effect in the NLME package (v. 3.1–111; Pinheiro et al. 2013) and ranked models using AIC adjusted for small sample sizes (AIC_c; Burnham and Anderson 2002). We report model-averaged parameter estimates and 95% CI. We also tested for an effect of sex, season, and their interaction on seasonal home range size using linear mixed-effects models. Preliminary analyses indicated a 3-way interaction between sex, season, and study site for 6-mo home range size, so we analyzed those data separately for Highlands and Brevard. The number of fixes was not correlated with home range size for any of our analyses ($|r_s| \leq 0.12$, $P \geq 0.19$), but we nevertheless included it in our models to control for unequal sampling intensities within individuals. We also tested for an effect of body size (snout–vent length [SVL]) in all analyses because Hyslop et al. (2014) found SVL was positively associated with annual home range size for *D. couperi* in southern Georgia. We used mean SVL values for individuals for which we had >1 measure of body size (31 of 71 subjects = 46%).

1.2.4. Within-Individual Spatial Overlap

We used individuals with multiple seasonal home ranges meeting the aforementioned criteria to measure the degree of spatial overlap within individuals over

time. We calculated the percentage of home range overlap at the 95% volume contour between pairs of home ranges (dyads) following Chaverri et al. (2007). However, the percentage of home range overlap does not incorporate information provided by the UD about variation in the intensity of space use within the home range. Therefore, we calculated the volume of intersection (VI) and utilization overlap index (UDOI) at the 95% volume contour to quantify the degree of UD overlap (Fieberg and Kochanny 2005; Fieberg 2014). As an additional measure of spatial overlap, we measured the Euclidean distance between home range centroids defined as the mean x/y coordinates for a given home range.

We used linear mixed-effects models to test for effects of sex, seasonal combinations (e.g., breeding–breeding, non-breeding–breeding), and their interaction on the degree of spatial overlap with individual as a random effect. The effect of body size had virtually no model support and was not included the analyses. For 6-mo home ranges, seasonal combination was a four-level categorical variable consisting of non-breeding vs. breeding, breeding vs. breeding, non-breeding vs. non-breeding, and non-breeding vs. non-breeding with two intervening seasons (i.e., non-breeding 2011 to breeding 2012). We excluded home range dyads that were separated by > 2 intervening seasons. We had insufficient data within the Highlands 6-mo seasonal home ranges to fit our models, so we combined the Highlands and Brevard data (results were similar regardless). We represented seasonal combinations for the 3-mo home ranges as a seven-level categorical variable with the following combinations: "B–B" = within the same breeding season (e.g., Fall 2011 to Winter 2011), "NB–NB" = within the same non-breeding season, "B–NB" = adjacent 3-mo seasons within adjacent breeding and non-breeding seasons, and

"B–NB1" = non-adjacent 3-mo seasons within adjacent breeding and non-breeding seasons separated by one 3-mo season (e.g., Autumn 2011 to Spring 2012). We compared models using AIC_c and report model-averaged parameter estimates and 95% CI. We examined our model residuals for homogeneity of variances and specified alternate variance structures available in the lme function as necessary to meet the assumption of homogeneity of variances. We also transformed our dependent variables as necessary to meet the assumption of normality.

1.2.5. Among-Individual Spatial Overlap

We evaluated among-individual home range overlap using 6-mo seasonal home ranges as previously described. We included data from two Highlands snakes that exhibited complications with the transmitter implantation site or extreme weight loss (≥ 31%) because they exhibited spatial overlap with other telemetered snakes and gave no indication that their space use patterns differed from those of other telemetered snakes. We likewise included data from a single Brevard snake that died from receiving an antibiotic combined with ivermectin during surgery. We estimated 95% and 50% fixed kernel utilization distributions (UD) using the unconstrained reference bandwidth because the reference bandwidth imposed a higher degree of smoothing, resulting in larger home range estimates that allowed more adjacent home range dyads to meet our criteria for adjacency (see below). Additionally, in a study such as ours, where the degree of inter-individual interaction may be under-represented due to infrequent sampling, imposing a higher degree of smoothing for home range estimation may be advantageous, because it incorporates areas where space use may have occurred but was not detected.

Because some of the Brevard home ranges had as few as 10 fixes, we created area-observation plots for all home ranges and retained those whose plots reached an asymptote (Harris et al. 1990; Laver and Kelly 2008). We generated 500 bootstrapped home range estimates for each number of fixes from 5 to *n* where *n* = the total number of fixes for that home range. We considered an estimate to have reached an asymptote if the mean bootstrapped home range size for at least the last 50% of subsampled fixes were within 10% of the home range size estimated with all fixes. However, this relatively conservative criterion excluded several home ranges, including some which visually appeared to reach an asymptote. Because inter-individual variability in home range sizes is often the single greatest source of variability in home range data sets, it is often advantageous to maximize the number of individuals included in an analysis (Borger et al. 2006). We therefore reran our area-observation plots using a more liberal criterion defining an asymptote as a mean bootstrapped home range size within 10% of the full home range size for the last five subsampled fixes (Laver and Kelly 2008). We ran all subsequent analyses with both data sets and obtained similar results so we report those using the more liberal criterion.

To quantify spatial overlap among individuals, we identified dyads of simultaneously adjacent home ranges, defined as home ranges within the same season with overlapping 99% UD volume contours. This ensured that individuals in the same dyad were tracked during the same temporal (season) and spatial (overlapping UD) extent. We used the 99% volume contour to define adjacency because it approximates the maximum possible area over which an individual could have moved and therefore interacted with conspecifics. We measured home range and core area overlap using the

volume of intersection (VI) and utilization distribution overlap index (UDOI) (Fieberg and Kochanny 2005; Fieberg 2014). We also calculated the distance between home range centroids for each dyad, where the centroid was the mean x and y coordinates across an individual's telemetry fixes. However, small home ranges mostly or completely overlapped by larger home ranges had low VI and UDOI despite high degrees of overlap. Therefore, for each dyad, we calculated the probability of each individual occurring within the other individual's home range (PHR) (Fieberg and Kochanny 2005) which is analogous to the proportion of home range *i* overlapped by home range *j* but accounts for non-uniform space use within the home range by using the UD. Because PHR is calculated for each individual in the dyad we used the maximum of the two values (PHR_{max}) in all analyses. The higher the PHR_{max} value, the more one home range was contained within the other home range.

We analyzed inter-individual UD overlap for home ranges and core areas separately using a permutation-based multivariate analysis of variance of distance matrices (Anderson 2001; McArdle and Anderson 2001). This accounted for both the non-normal distribution of our data and the lack of independence among dyads due to the presence of individuals within more than one dyad. We specified our data as a Euclidean distance matrix upon which the sums of squares was then partitioned between within- and among-group variance in a manner analogous to a parametric analysis of variance. We used 10,000 permutations to calculate exact *P* values with the *adonis* function in the R package VEGAN (v. 2.2-1; Oksanen et al. 2015). We tested for an interactive effect of sex (male-female, female-female, and male-male) and season (breeding and non-breeding) on UD overlap and combined Highlands and Brevard data because of sample size

limitations. If the initial test was significant, we then conducted pairwise tests using the adonis function within the significant factors and reported adjusted *P* values using sequential Bonferroni corrections (Holm 1979). Because of sample size limitations we used an uncorrected $\alpha = 0.10$.

While the above metrics quantify the degree of spatial overlap at the scale of the entire home range, we were primarily interested in describing the degree to which an individual uses space within a conspecific's simultaneously adjacent home range. Because the UD provides a probabilistic measure of space use, where each underlying pixel has a probability density value proportional to its expected probability of use, the distribution of conspecific UD densities at an individual's telemetry fix describes the manner in which that individual utilized the conspecific's home range. However, our observations of simultaneously adjacent home range overlap only included two, occasionally three, individuals. Because we did not simultaneously monitor all adjacent conspecifics, we felt that only fixes within some "zone of interaction" (ZOI), instead of all fixes, had the potential to be influenced by a conspecific. We defined the ZOI using a two-step process. First, we calculated the 99% UD volume contours for the focal individual and its simultaneously adjacent conspecifics and considered all fixes within the area of overlap as within the ZOI. For fixes outside of the area of overlap, we measured the Euclidean distance to the edge of the focal individual's 99% volume contour ($dist_{focal}$) and the edges of the 99% volume contours of the conspecifics ($dist_{consp}$). All fixes where $dist_{consp} \leq dist_{focal}$ and that overlapped the conspecific UD were also considered within the ZOI. For all fixes within the ZOI we measured the density values of the conspecific UD (D_{consp}) as the density at that fix multiplied by the area of the pixel.

We used a constant pixel size (15 × 15 m) for all individuals. We assumed the presence of two conspecifics would represent an additive effect and therefore added the UD when multiple simultaneously adjacent conspecifics were present. We measured D_{consp} twice, once using only simultaneously adjacent individuals of the same sex (i.e., male-male or female-female overlap) and once using only simultaneously adjacent individuals of the opposite sex (i.e., male-female or female-male).

Because the distribution of D_{consp} was highly right skewed, we modeled our data using a generalized Pareto distribution (GPD) using the TEXMEX package (v. 2.1; Southworth and Heffernan 2013). We again combined the Highlands and Brevard data because of small sample sizes. The GPD has two parameters, shape and scale, and we modeled both parameters as a function of overlap type, sex, season, and their respective interactions. Overlap type included same-sex (i.e., male-male or female-female) or opposite-sex (i.e., male-female or female-male) overlap. Male-female overlap represents male use of female home ranges while female-male overlap represents female use of male home ranges. Sex was a binary variable representing male use of conspecific space or female use of conspecific space. Season was also binary representing breeding or non-breeding seasons. Because data sparseness prevented us from fitting the global model with all possible interactions, we considered interactive terms of two variables with an additive effect of the third variable. We compared models using AIC_c (Burnham and Anderson 2002).

1.3. Results

1.3.1. Movement Patterns

We collected data from a total of 30 *D. couperi* from the Highlands study site. However, two females developed externally visible infections around their transmitter implantation sites within 4 mo and another male and female lost 23–31% of their body weight within 6 mo after receiving their transmitters. Therefore, we conducted all analyses with, and without, these four subjects and found that including them did not alter the overall patterns of our results. We nevertheless report the results of all analyses without these four subjects. We therefore included a total of 26 *D. couperi* from the Highlands site (18 males and 8 females) with mean number of fixes per individual of 110 (± 55 SD) in the analyses of movement patterns.

Daily probability of movement calculated across all individuals was 0.40 and overall DPM for males and females was also 0.40. Males and females moved at similar frequencies throughout the year except for two brief periods (Fig. 1). Females moved more frequently than males during March and April, whereas males moved more frequently during November.

Figure 1.1. Seasonal change in daily probability of moving for female (A) and male (B) Drymarchon couperi in Highlands County, Florida. The dotted lines and light shaded ribbons represent the observed values with their bootstrapped 95% CI, and the solid lines and dark shaded ribbons represent the predicted values and their bootstrapped 95% CI from generalized additive models fit separately to each sex. The horizontal dashed line is the overall DPM across the entire study with both sexes (0.40). The left-most vertical line is the start of the non-breeding season (March 1) and the right-most vertical line is the start of the breeding season (October 1).

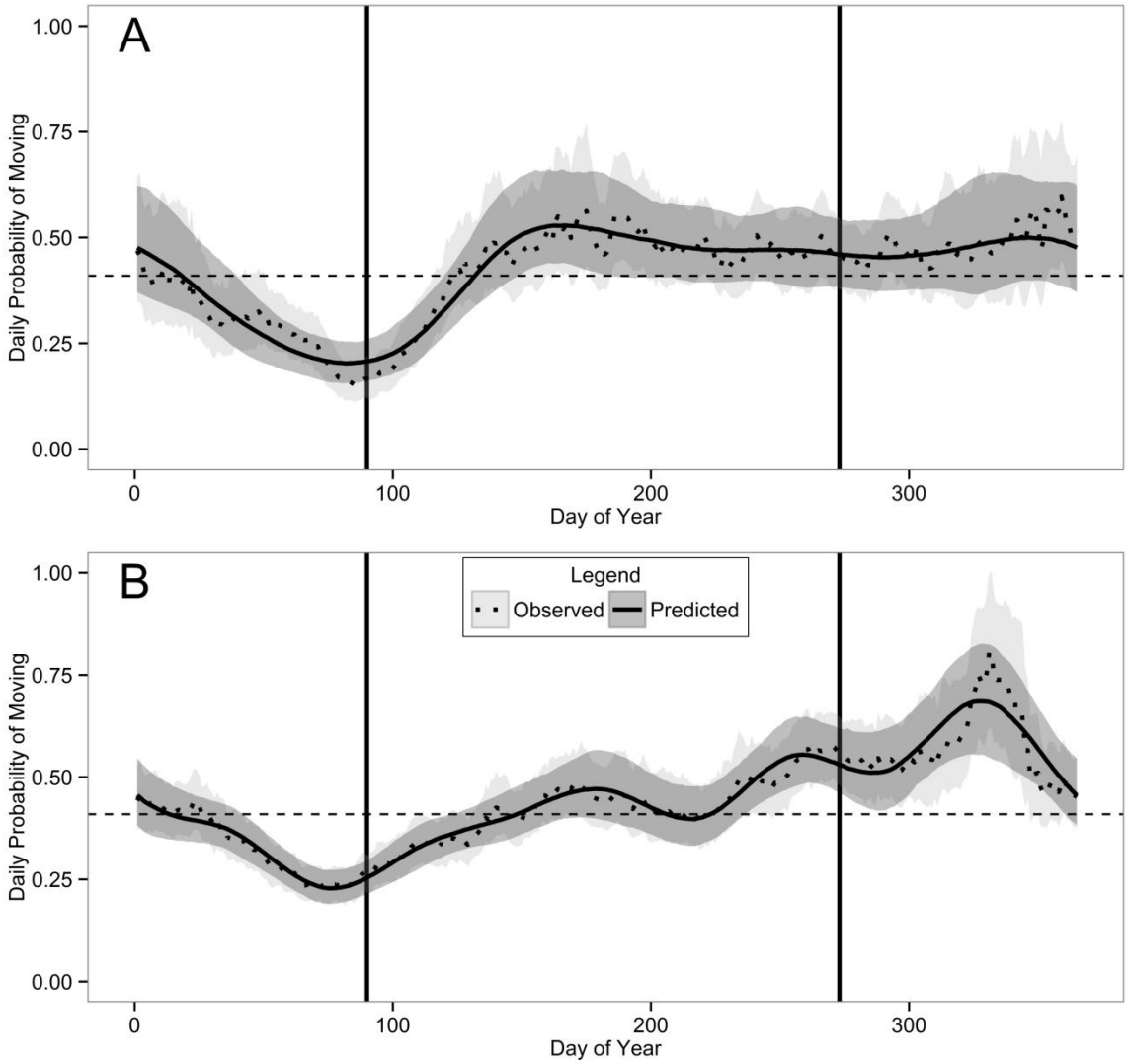

Median daily movement rate during the breeding season was 234 m/d (95th quantiles = 1.7–990.9 m/d) and 114 m/d (95th quantiles = 3.3–587.9 m/d) for males and females, respectively. During the non-breeding season, these values were 185 m/d (95th

quantiles = 4.4–745.0 m/d) and 140 m/d (95^{th} quantiles = 8.2–571.8 m/d) for males and females, respectively. Overall, males exhibited longer daily movements than females (Fig. 2). Males and females made similar daily movements during the non-breeding season as evidenced by the overlapping CI around the scale parameter (Fig. 2). During the breeding season, male daily movement distances were greater as evidenced by the higher estimates for the scale parameter of the GPD.

Figure 1.2. Movement distances and frequencies for *Drymarchon couperi* in Highlands County, Florida. (A) Estimates (solid lines) and bootstrapped 95% confidence interval (shaded ribbons) for the scale parameter from the generalized Pareto distributions (GPD) fit to subject daily movement distance for each day-of-year (DOY). Higher values of scale indicate a greater frequency of longer daily movement distances. (B) The median (solid lines) and inter-quartile range (25th and 75th percentiles, shaded ribbons) for daily movement rate (m/day). We do not present the estimates of the shape parameter from the GPD because it has a negligible effect on the overall form of the GPD distribution. The leftmost vertical line is the start of the nonbreeding season (April 1) and the rightmost vertical line is the start of the breeding season (October 1).

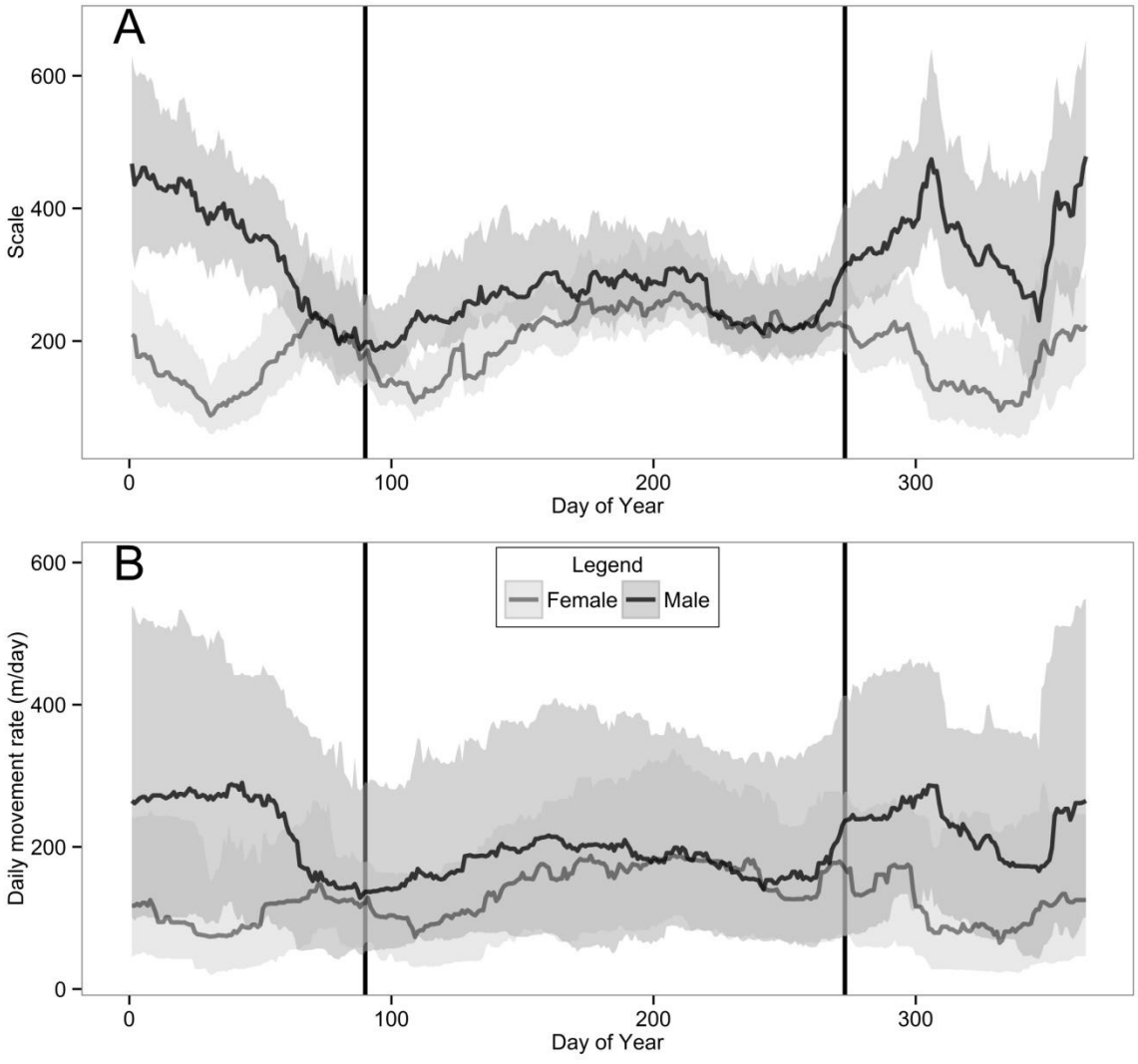

1.3.2. Annual and Seasonal Home Range Size

We had sufficient data from 12 Highlands and 59 Brevard subjects to estimate annual home ranges and estimated 12 and 84 annual home ranges from each study area, respectively (Appendix A). We removed four Highlands 6-mo home ranges because we lost contact with those subjects throughout their respective seasons and therefore estimated 36 six-month home ranges from 19 Highlands snakes. We estimated 128 six-month home ranges from 59 Brevard snakes. After removing three 3-mo ranges on account of having lost contact with those subjects, we estimated 70 three-month home ranges from 24 Highlands snakes. Males were larger than females for the pooled (male SVL = 173.4 ± 3.5 cm, female SVL = 163.9 ± 3.0 cm; $t = –2.07$, $P = 0.04$), Brevard (male SVL = 177.8 ± 4.3 cm, female SVL = 166.6 ± 2.8 cm, $t = –2.20$, $P = 0.03$), and Highlands data (male SVL = 155.3 ± 4.7 cm, female SVL = 139.5 ± 4.9 cm, $t = –2.33$, $P = 0.03$).

Models including sex were the best-supported models for all four home range analyses (Table 1.1). Males consistently had larger home ranges than females (Fig. 1.3) although the model-averaged parameter estimate for sex overlapped zero for the Highlands 6-mo home ranges (Table 1.2). However, SVL was positively correlated with 6-mo home range size in the Highlands subjects. Size only had a significant effect on Highlands 6- and 3-mo home range sizes (Table 1.2). We found no support for differences in annual home range size between study sites. However, the interactive effect of sex and season on 6-mo home range size differed between Highlands (significant) and Brevard (non-significant, although the model-averaged 95% CI for the interactive term only slightly overlapped zero; Table 1.2). Male seasonal home ranges

were larger in winter than in summer for Highlands while this trend was reduced in Brevard (Fig. 1.3). Male 3-mo home ranges from the Highlands data were also largest during the breeding season while female 3-mo home ranges remained relatively invariant (Fig. 1.3).

Table 1.1. Model selection results for annual, 6-, and 3-mo home range sizes for *Drymarchon couperi* as a function of sex, size (snout-vent length), and study site (study = Highlands or Brevard). Individual was included as a random effect in all analyses. Season in the 6-mo home range models includes the breeding (October–March) and non-breeding season (April–September) while in the 3-mo model season includes Winter (January–March), Spring (April–June), Summer (July–September), and Autumn (October–December). Number of fixes was included in all models. Deviance is –2 × log likelihood, k = number of parameters, and wi = AICc model weights. We report models whose cumulative w ≥ 0.95.

Model	Deviance	*k*	AIC_c	ΔAIC_c	w_i
Annual home range					
Sex + size	–119.97	4	250.61	0.00	0.2470
Sex + study + size	–117.77	6	250.81	0.21	0.2228
Sex + study	–119.07	5	251.09	0.48	0.1940
Sex	–119.19	5	251.32	0.71	0.1728
Sex × study + size	–117.56	7	252.77	2.16	0.0839
Sex × study	–118.84	6	252.95	2.34	0.0768
Highlands 6-mo seasonal home range					
Sex × season + size	–30.04	8	81.41	0.00	0.6563
Sex × season	–32.74	7	83.48	2.06	0.2342
Sex + size	–35.84	6	86.58	5.17	0.0495
Sex	–37.53	5	87.07	5.65	0.0389
Brevard 6-mo seasonal home range					
Sex × season	–141.34	7	297.62	0.00	0.4227
Sex × season + size	–141.09	8	299.38	1.76	0.1753
Sex + season	–143.36	6	299.41	1.79	0.1731
Sex	–144.94	5	300.37	2.75	0.1069
Sex + season + size	–143.11	7	301.15	3.53	0.0723
Highlands 3-mo seasonal home range					
Sex × season + size	–55.64	12	140.76	0.00	0.7395
Sex × season	–58.45	11	143.44	2.68	0.1932
Sex + season + size	–63.19	9	147.39	6.63	0.0269

Table 1.2. Model-averaged betas (i.e., parameter estimates) and 95% CI for fixed-effects parameters from annual and seasonal models of home range size for *Drymarchon couperi*. Parameter estimates whose model-averaged 95% CI did not overlap zero are displayed in bold. Reference levels are female (Sex), Brevard (Study), Summer (6-mo season), and Autumn (3-mo season).

Parameter	Model-averaged β	95% CI
Annual home range		
Sex	**0.86**	**0.40–1.33**
Study	0.84	–0.63–2.31
Sex × study	0.44	–0.90–1.78
Size	0.01	–0.00–0.02
Fixes	0.00	–0.02–0.01
Highlands 6-mo seasonal home range		
Sex	0.46	–0.40–1.32
Season	**–0.68**	**–1.31—0.05**
Sex × study	**1.26**	**0.46–2.07**
Size	**0.02**	**0.00–0.04**
Fixes	**0.02**	**0.00–0.04**
Brevard 6-mo seasonal home range		
Sex	**0.80**	**0.30–1.30**
Season	**–0.30**	**–0.58—0.01**
Sex × study	0.40	–0.00–0.79
Size	0.00	–0.01–0.02
Fixes	–0.01	–0.03–0.02
Highlands 3-mo seasonal home range		
Sex	**1.41**	**0.55–2.28**
Season (spring)	0.02	–0.6–0.65
Season (summer)	0.18	–0.41–0.78
Season (winter)	–0.58	–1.17–0.01
Sex × season (spring)	**–0.93**	**–1.69– –0.17**
Sex × season (summer)	**–0.94**	**–1.71– –0.18**
Sex × season (winter)	0.06	–0.73–0.85
Size	**0.02**	**0.00–0.04**
Fixes	0.02	–0.00–0.04

Figure 1.3. Seasonal home range sizes (means ± bootstrapped 95% CI) for *Drymarchon couperi* by sex and season. (A) Highlands 6-mo home ranges; (B) Brevard 6-mo home ranges; and (C) Highlands 3-mo home ranges. Home ranges were estimated using 95% fixed kernel utilization distributions with an unconstrained reference bandwidth matrix. Seasons for the 6-mo home ranges are breeding (October–March) and non-breeding (April–September) and seasons for the 3-mo range ranges are Autumn (October–December), Winter (January–March), Spring (April–June), and Summer (July–September).

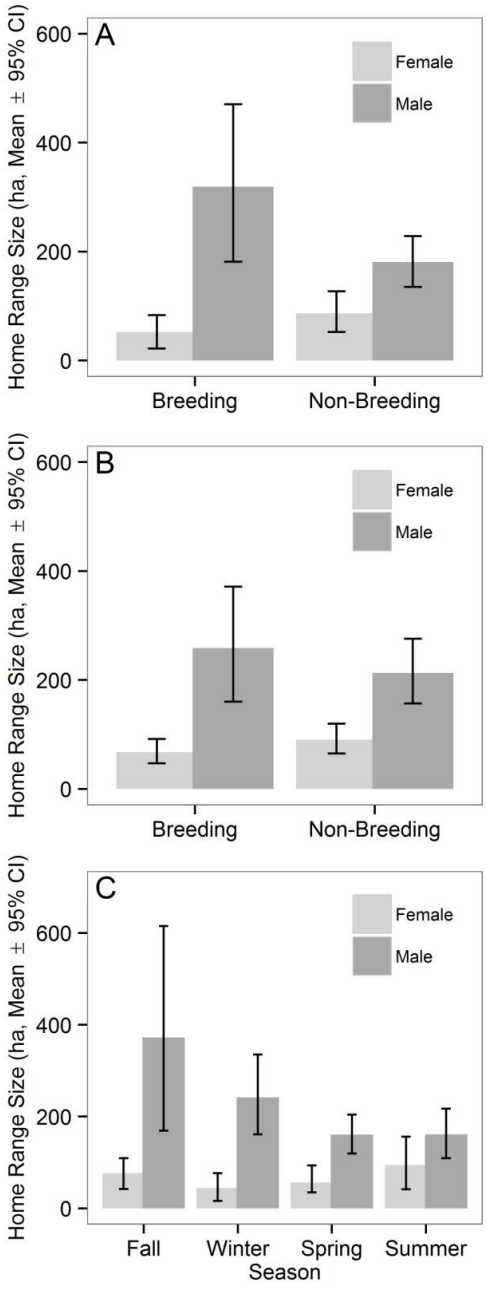

1.3.3. Within-Individual Spatial Overlap

Within the Highlands and Brevard 6-mo data, we obtained 140 home range dyads (58 males and 82 females) from 47 subjects. We obtained 74 home range dyads (41 males and 33 females) from 19 subjects in Highlands 3-mo data. The volume of intersection was highly correlated with the percentage of home range overlap ($r_s \geq 0.82$, $P < 0.0001$) and UDOI ($r_s \geq 0.96$, $P < 0.0001$), so we only report the results using VI. Mean VI across all dyads was 0.48 (0.04–0.75) and 0.46 (0.13–0.75) for 6- and 3-m dyads, respectively. Mean distance between centroids across all dyads was 296 m (11–3445 m) and 356 m (11–1469 m) for 6- and 3-mo dyads, respectively.

Models containing an effect of seasonal combination on VI between seasonal home ranges had high support for both 6- and 3-mo home ranges (Table 1.3). There was no strong support for an effect of sex on VI (Table 1.4). For 6-mo home ranges, only the degree of overlap between breeding and non-breeding seasons separated by 12 mo (i.e., two seasons) was less than the degree of overlap between adjacent breeding and non-breeding seasons (Fig. 1.4). The model-averaged 95% CI for seasonal combinations of 3-mo home ranges all overlapped zero for VI. Models containing an interactive effect of sex and season had very little support for both seasonal home ranges and overlap metrics ($w_i \leq 0.08$). We only observed two and three within-individual home range dyads, from Brevard and Highlands respectively (four male subjects), where the distance between home range centroids was > 1 km (e.g., Appendix B). For all but two subjects, there was substantial overlap between breeding and non-breeding home ranges (i.e., VI ≥ 0.21, and % home range overlap ≥ 0.40).

Table 1.3. Model selection results for *Drymarchon couperi* for factors influencing within-individual 6- and 3-mo home range overlap. Season in the 6-mo home range models includes the breeding (October–March) and non-breeding season (April–September) while in the 3-mo model season includes Winter (January–March), Spring (April–June), Summer (July–September), and Autumn (October–December). Deviance is –2 × log likelihood, k = number of parameters, and w_i = AIC_c model weights. The null model contained only a random effect of individual. The reference levels for all models are females and a breeding–non-breeding season with no intervening seasons (e.g., non-breeding 2011–breeding 2011).

Model	Deviance	k	AIC_c	ΔAIC_c	w_i
Brevard and Highlands 6-mo					
Volume of intersection					
Season	57.02	6	-101.42	0.00	0.6150
Sex + season	57.61	7	-100.38	1.04	0.3660
Sex × season	57.92	10	–94.13	7.28	0.0161
Null	48.02	3	–89.85	11.56	0.0019
Sex	48.36	4	–88.42	13.00	0.0009
Distance between centroids					
Sex + season	–171.77	7	358.40	0.00	0.5580
Sex	–175.48	4	359.25	0.85	0.3647
Sex × season	–170.33	10	362.36	3.96	0.0769
Season	–181.06	6	374.75	16.36	0.0002
Null	–184.40	3	374.97	16.57	0.0001
Highlands 3-mo					
Volume of intersection					
Season	–62.50	6	–49.25	0.00	0.4396
Sex + season	–63.33	7	–47.63	1.62	0.1956
Null	–53.87	3	–47.52	1.73	0.1854
Sex	–55.07	4	–46.49	2.76	0.1104
Sex × season	–69.04	10	–45.55	3.71	0.0689
Distance between centroids					
Sex	169.30	4	177.88	0.00	0.8944
Sex + season	168.07	7	183.76	5.88	0.0472
Sex × season	160.39	10	183.88	6.00	0.0445
Null	180.00	3	186.34	8.46	0.0130
Season	178.65	6	191.90	14.02	0.0008

Table 1.4. Model-averaged betas (i.e., parameter estimates), 95% CI, and AIC_c parameter weights for fixed-effects parameters from *Drymarchon couperi* within-individual home range overlap models. Parameter estimates whose model-averaged 95% CI did not overlap zero are displayed in bold. Reference levels are female (Sex) and breeding–non-breeding (Season). The betas and CI for the interactive effect of sex and season are not reported because models with the interactive term had low support ($w_i \leq 0.07$) and the CI for the betas all overlapped zero.

	Model-averaged β	95% CI
Brevard and Highlands 6-mo		
Volume of intersection		
Season (breeding)	–0.04	–0.12–0.04
Season (non-breeding)	0.00	–0.07–0.07
Season (breeding–non-breeding 2)	**–0.18**	**–0.26– –0.10**
Sex	–0.04	–0.12–0.04
Distance between centroids		
Sex	**0.93**	**0.52–1.34**
Season (breeding)	–0.03	–0.50–0.43
Season (non-breeding)	0.25	–0.13–0.64
Season (breeding–non-breeding 2)	**0.53**	**0.08–0.97**
Highlands 3-mo		
Volume of intersection		
Season (breeding)	0.09	–0.04–0.22
Season (non-breeding)	0.10	–0.04–0.24
Season (breeding–non-breeding 1)	–0.02	–0.11–0.07
Sex	–0.06	–0.19–0.07
Distance between centroids		
Sex	**1.15**	**0.49–1.81**
Season (breeding)	0.35	–0.44–1.15
Season (non-breeding)	0.32	–0.61–1.25
Season (breeding–non-breeding 2)	0.25	–0.23–0.73

	Model-averaged β	95% CI
Brevard and Highlands 6-mo		
Volume of intersection		
Season (breeding)	–0.04	–0.12–0.04
Season (non-breeding)	0.00	–0.07–0.07
Season (breeding–non-breeding 2)	**–0.18**	**–0.26– –0.10**
Sex	–0.04	–0.12–0.04
Distance between centroids		

Sex	**0.93**	**0.52–1.34**
Season (breeding)	–0.03	–0.50–0.43
Season (non-breeding)	0.25	–0.13–0.64
Season (breeding–non-breeding 2)	**0.53**	**0.08–0.97**
Highlands 3-mo		
Volume of intersection		
Season (breeding)	0.09	–0.04–0.22
Season (non-breeding)	0.10	–0.04–0.24
Season (breeding–non-breeding 1)	–0.02	–0.11–0.07
Sex	–0.06	–0.19–0.07
Distance between centroids		
Sex	**1.15**	**0.49–1.81**
Season (breeding)	0.35	–0.44–1.15
Season (non-breeding)	0.32	–0.61–1.25
Season (breeding–non-breeding 2)	0.25	–0.23–0.73

Figure 1.4. Within-individual seasonal overlap in home ranges of *Drymarchon couperi* measured in 6-mo (Brevard and Highlands sites combined, A and B) and 3-mo (Highlands only, B and C) intervals. Plotted values represent means ± bootstrapped 95% CI. Males and females were pooled for volume of intersection. Each 3-mo home range was reclassified into its respective 6-mo season (breeding or non-breeding). The season combination marked with an asterisk had a model-averaged parameter estimate whose 95% CI did not overlap zero. Distance between home range centroids differed between sexes for both the 6- and 3-mo data. See text for description of seasonal combinations.

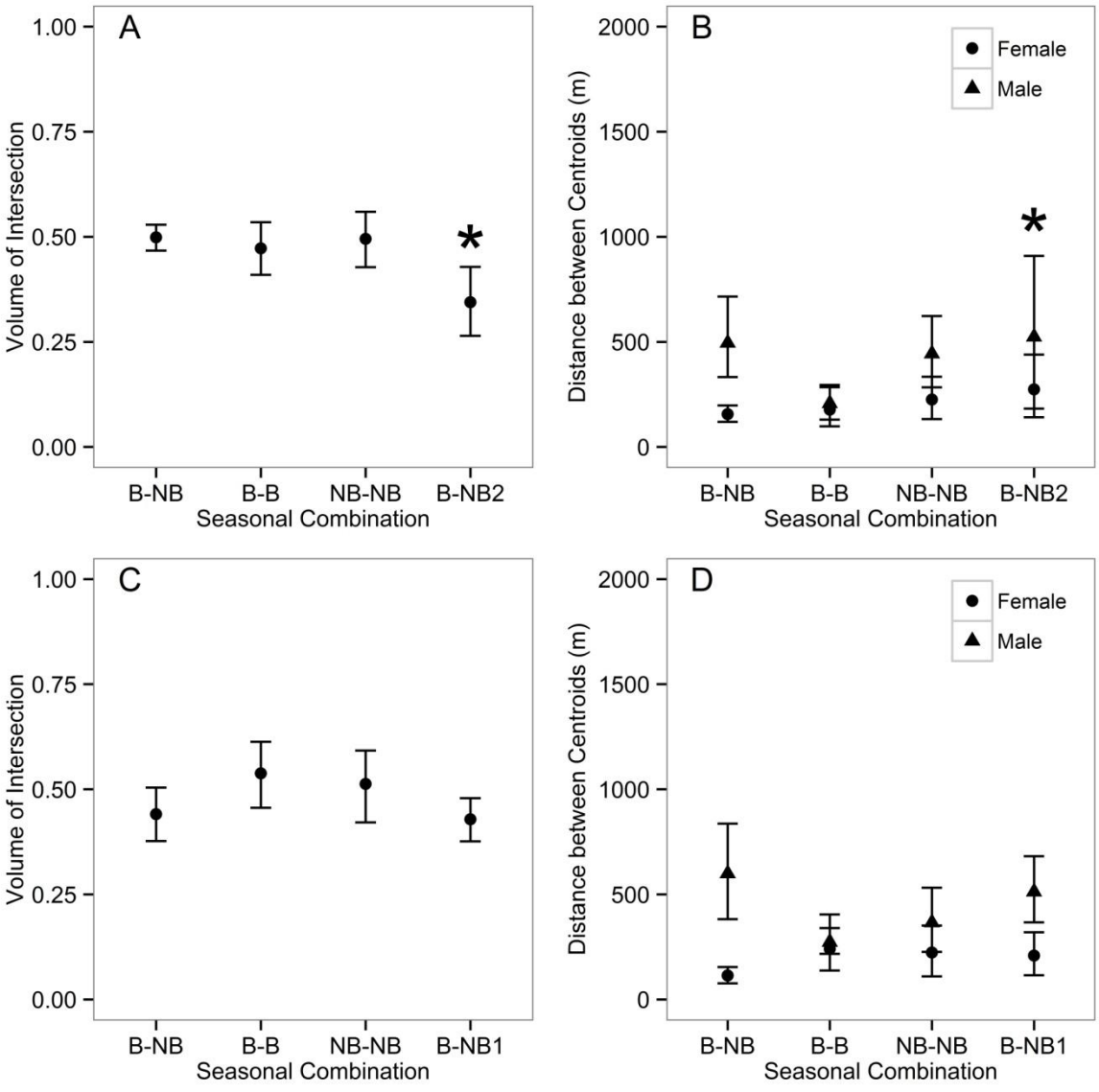

1.3.5. Among-Individual Spatial Overlap

We estimated 6-month home ranges from 41 Brevard and 16 Highlands snakes that were simultaneously adjacent with at least one other conspecific (Table 1.5). We obtained 61 conspecific 6-month home range dyads, including 36 male-female, 8 female-female, and 17 male-male dyads. All individuals were considered adults (snout-vent length [SVL] ≥ 122 cm) and we did not distinguish between gravid and non-gravid females because available data suggest that female *D. couperi* reproduce annually (Speake et al. 1987; Hyslop et al. 2009b). Males were significantly longer (SVL [mean ± SE]: males = 168.75 cm ± 3.90, females = 156.69 cm ± 3.53, t = -2.29, P = 0.0252) and heavier (males = 1.66 kg ± 0.09, females = 1.20 kg ± 0.07, t = -4.17, P < 0.0001) than females.

Table 1.5. Number of individuals, home range dyads, home range sizes, and tracking intensities for radio telemetered eastern indigo snakes (*Drymarchon couperi*) used in the analyses of conspecific spatial overlap. The mean and standard deviation of home range size, number of fixes, and tracking duration are reported. Sample sizes within each home range column are the number of simultaneously adjacent home range dyads (pooled across sexes). The maximum possible number of tracking days was 183 days for 6-month home ranges.

	Mean home range size (ha)						Mean number of fixes	Mean tracking duration (days)
	Males			Females				
	Snakes (*n*)	Breed-ing	Non-breeding	Snakes (*n*)	Breed-ing	Non-breeding		
6-month Highlands	9	313.68 (238.06) *n* = 5	183.24 (56.83) *n* = 8	7	36.99 (33.11) *n* = 7	87.3 (62.47) *n* = 4	57 (10)	163 (17)
6-month Brevard	22	426.68 (313.06) *n* = 29	235.00 (174.63) *n* = 27	19	84.51 (72.91) *n* = 19	146.26 (120.81) *n* = 21	19 (4)	157 (22)
6-month Brevard & Highlands	31	410.07 (302.78) *n* = 34	223.17 (156.44) *n* = 35	26	71.72 (67.40) *n* = 26	136.82 (114.61) *n* = 25	26 (16)	158 (21)

Volume of intersection was highly correlated with UDOI for both home ranges (UD) and core areas (50% UD) ($r_s \geq 0.94$, $P < 0.0001$) so we only report the results using VI. Mean home range VI was 0.13 (range = 0.00–0.60) across all dyads. There was no significant effect of sex ($F_{2,60} = 2.15$, $P = 0.1244$), season ($F_{1,60} = 1.49$, $P = 0.2365$), or their interaction ($F_{2,60} = 0.22$, $P = 0.8027$) on home range VI. However, there was a significant effect of sex ($F_{2,60} = 12.77$, $P = 0.0002$), season ($F_{1,60} = 2.93$, $P = 0.0904$) and sex*season ($F_{2,60} = 2.44$, $P = 0.0945$) on distance between home range centroids. Following corrections for pairwise error, the distance between breeding season male-male centroids was significantly greater than the distance between male-female centroids during both the breeding ($P = 0.0126$) and non-breeding seasons ($P = 0.0045$, Fig. 1). Sex was also significant for home range PHR_{max} ($F_{2,60} = 11.55$, $P < 0.0001$) but not for season ($F_{1,60} = 0.10$, $P = 0.7453$) or sex*season ($F_{2,60} = 1.88$, $P = 0.1502$). Male-male home range dyads had significantly lower PHR_{max} than male-female ($P = 0.0003$) and female-female dyads ($P = 0.0528$, Fig. 1.5).

Figure 1.5. Boxplots of conspecific home range overlap (95% fixed kernel utilization distribution) for simultaneously adjacent eastern indigo snake (*Drymarchon couperi*) 6-month home range dyads (Highlands and Brevard data combined). Home ranges were estimated using an unconstrained reference bandwidth matrix. The thick horizontal line indicates the median, the edges of the boxes the 25^{th} and 75^{th} percentiles, and the whiskers approximate a 95% confidence interval. Female-female dyads are denoted as "Female," male-male dyads as "Male," and male-female dyads as "Male-Female." Breeding seasons (October–March) are denoted with dark gray and non-breeding seasons (April–September) with light gray. Maximum PHR is the maximum probability of home range overlap for each dyad. Pairs of dyads marked with the same upper-case letters (e.g., A, B) are significantly different ($P < 0{\cdot}10$). All pairwise *P* values were adjusted using Holm's (1979) method. Pairwise comparisons in maximum PHR indicate a significant effect of sex; there was no significant effect of season or sex*season.

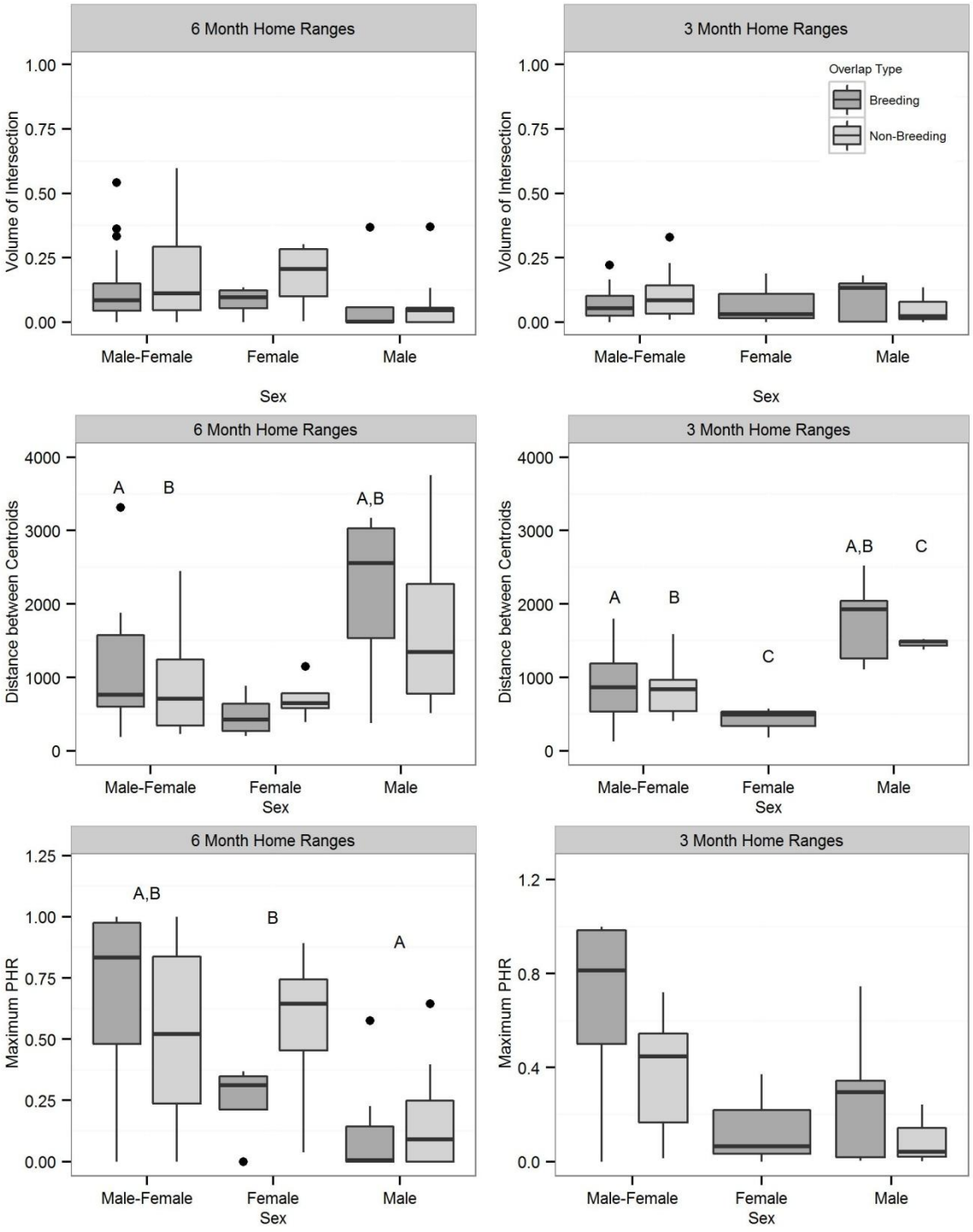
6 Month Home Ranges
3 Month Home Ranges
Volume of Intersection
Overlap Type
Breeding
Non-Breeding
Male-Female
Female
Male
Sex
Distance between Centroids
A
B
A,B
C
Maximum PHR

Mean core area VI was 0.05 (range = 0.00–0.52). There was no significant effect of sex ($F_{2,60}$ = 0.65, P = 0.5474), season ($F_{1,60}$ = 0.06, P = 0.8164), or their interaction ($F_{2,60}$ = 0.23, P = 0.7909) on core area VI. Sex was significant for core area PHR_{max} ($F_{2,60}$ = 3.27, P = 0.0421) but not for season ($F_{1,60}$ = 0.16, P = 0.6926) or sex*season ($F_{2,60}$ = 0.32, P = 0.7209). The core area PHR_{max} for male-male and male-female dyads were significantly different (P = 0.0753, Fig. 1.6).

Figure 1.6. Boxplots of conspecific core area overlap (50% fixed kernel utilization distribution) for simultaneously adjacent eastern indigo snake (Drymarchon couperi) 6-month home range dyads (Highlands and Brevard data combined). Home ranges were estimated using an unconstrained reference bandwidth matrix. The thick horizontal line indicates the median, the edges of the boxes the 25th and 75th percentiles, and the whiskers approximate a 95% confidence interval. Female-female dyads are denoted as "Female," male-male dyads as "Male," and male-female dyads as "Male-Female." Breeding seasons (October–March) are denoted with dark gray and non-breeding seasons (April–September) with light gray. Maximum PHR is the maximum probability of home range overlap for each dyad. Pairs of dyads marked with the same upper-case letters (e.g., A, B) are significantly different (P < 0.10). All pairwise P values were adjusted using Holm's (1979) method. Pairwise comparisons in maximum PHR indicate a significant effect of sex; there was no significant effect of season or sex*season.

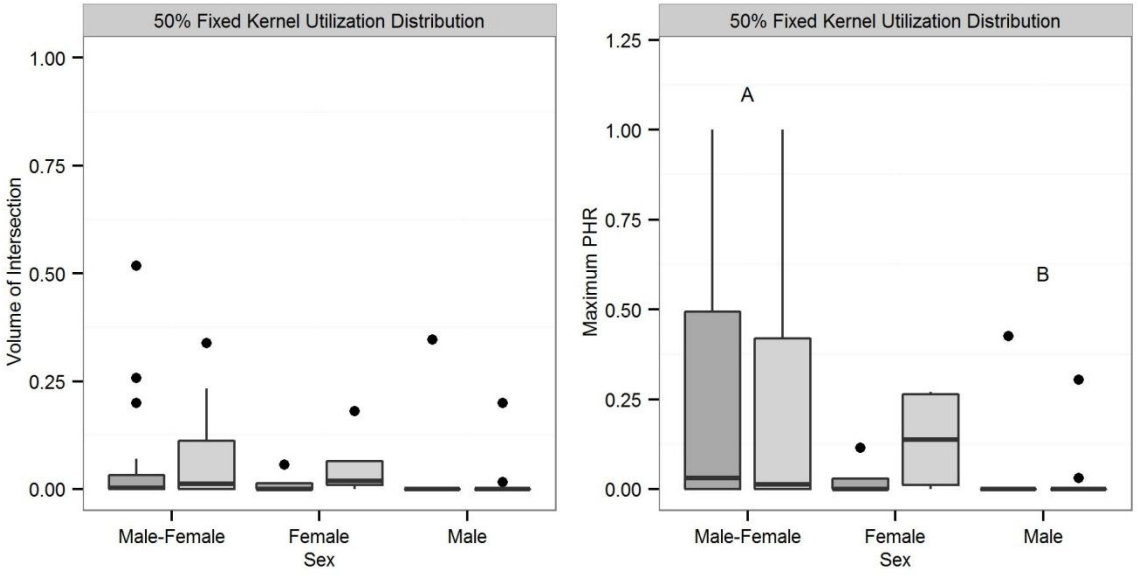

The model including an interactive effect of season and overlap type and an additive effect of sex for shape and scale received all the model support among GPD models for individual use of conspecific space (Table 1.6). Males used less of other males' home ranges compared to female use of other females' home ranges, particularly during the non-breeding season (Fig. 1.7). Female use of male home ranges was greatest during the breeding season, while male use of female home ranges was lower and more temporally consistent.

Table 1.6. Model selection results using a generalized Pareto distribution (GPD) to model conspecific UD density within the zone-of-interaction for 6-month home ranges estimated using the unconstrained reference bandwidth. The GPD has two parameters, scale (estimated here as log(scale), φ) and shape (ξ), which were both modeled as a function of season (breeding = October–March, non-breeding = April–September), sex, and overlap type (same-sex or opposite-sex). Additive effects (+) were included where model convergence would not permit interactive effects (*). Deviance (Dev) is -2*log-likelihood, *k* is the number of model parameters, and $w_i = AIC_c$ model weights.

Model	**Dev**	***k***	**AIC_c**	**ΔAIC_c**	**w_i**
φ(Season*Type + Sex), ξ(Season*Type + Sex)	12969·78	10	-25919·41	0·00	1·00
φ(Sex*Type + Season), ξ(Season*Type + Season)	12951·87	10	-25883·60	35·81	0·00
φ(Sex*Type), ξ(Sex*Type)	12948·56	8	-25881·02	38·39	0·00
φ(Sex*Season + Type), ξ(Sex*Season + Type)	12949·54	10	-25878·94	40·47	0·00
φ(Sex + Type), ξ(Sex + Type)	12934·65	6	-25857·25	62·16	0·00
φ(Sex*Season), ξ(Sex*Season)	12899·49	8	-25782·88	136·53	0·00
φ(Sex + Season), ξ(Sex + Season)	12894·01	6	-25775·97	143·43	0·00
φ(Sex), ξ(Sex)	12889·27	4	-25770·52	148·89	0·00
φ(Season*Type), ξ(Season*Type)	12840·95	8	-25665·80	253·60	0·00
φ(Type), ξ(Type)	12835·14	4	-25662·26	257·15	0·00
φ(Season + Type), ξ(Season + Type)	12836·11	6	-25660·17	259·24	0·00
φ(Season), ξ(Season)	12679·46	4	-25350·88	568·52	0·00
φ(.), ξ(.)	12676·76	2	-25349·51	569·89	0·00

Figure 1.7. Distributions of conspecific utilization distribution (UD) densities at eastern indigo snake (Drymarchon couperi) radio telemetry locations fit using a generalized Pareto distribution. Utilization distributions were calculated using the unconstrained reference bandwidth for each 6-month season (breeding = October–March, non-breeding = April–September). Male-female overlap represents male use of female UD while female-male overlap represents female use of male UD. The number of fixes for each season*overlap type combination are displayed in each panel.

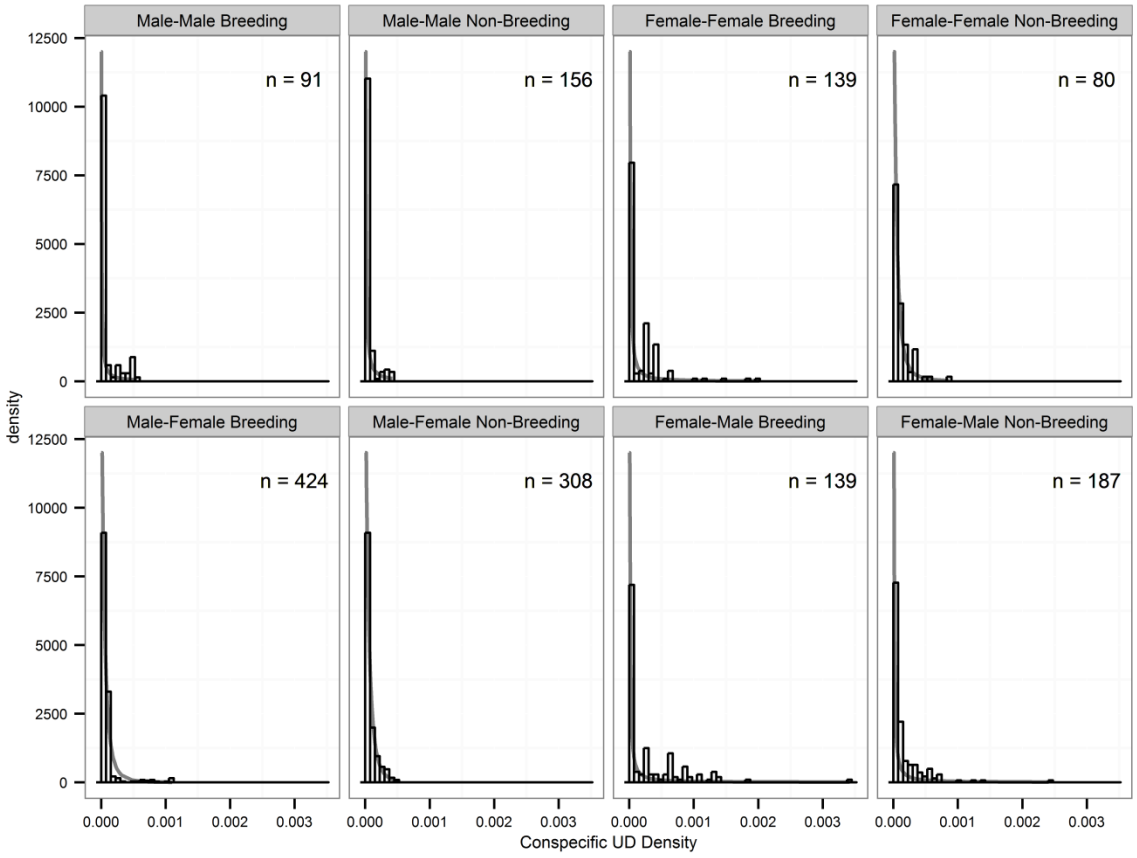

1.4. Discussion

Our study supports that male and female *D. couperi* in peninsular Florida show different degrees of seasonal variation in movement patterns. Specifically, female *D. couperi* movement patterns were relatively invariant throughout the year with the exception of a decrease in movement frequency in the late winter and early spring. In contrast, males increased their movement frequency, daily movement distances, and

home range sizes during the breeding season. These patterns are consistent with our hypothesis that male *D. couperi* undertake mate-searching movements during the breeding season. The timing of these increased movements are consistent with our observations of copulation (24 December 2012), male–male combat (26 November 2012), and apparent mating or courtship (22 February 2013) among our Highlands subjects, and with reproductive behavior reported previously across the species' range (Speake et al. 1978; Moler 1992; Layne and Steiner 1996; Stevenson et al. 2003; Hyslop 2007).

Increased male movements during the breeding season are known from many snake taxa (Waldron et al. 2006; Cardwell 2008; Sperry and Weatherhead 2009a; Lelievre et al. 2012). Increased movements might increase male reproductive success by increasing the number of females encountered (Madsen et al. 1993; Duvall and Schuett 1997; Glaudas and Rodriguez-Robles 2011; but see Smith et al. 2015). The spatial distribution of females can influence male mate-searching patterns (Duvall and Schuett 1997; Brown and Weatherhead 1999). For example, where females are widely distributed and spatially unpredictable, linear movements might maximize a male's chances of encountering a female (Duvall and Schuett 1997). At our study sites, both male and female movements throughout the year were non-directional indicating that female *D. couperi* were spatially predictable.

Females in many snake species also show an increase in movement during the breeding season (e.g., Cardwell 2008; Sperry and Weatherhead 2009a; Row et al. 2012) which may reflect travel to and from suitable oviposition sites (Blouin-Demers and Weatherhead 2002; Brown et al. 2005). Additionally, these movements might make

females more accessible to males through the deposition of chemical cues (LeMaster et al. 2001; Jellen and Aldridge 2014; Jellen et al. 2014). In our study, however, female *D. couperi* did not increase their movements or home ranges during the breeding season and moved less frequently during the late winter and early spring. The late winter–early spring (i.e., March–April) decrease in daily probability of movement for females might be associated with gestation, as *D. couperi* oviposit in April–June (Moulis 1976; Speake et al. 1978; Newberry et al. 2009). Many female snakes reduce movements when gravid (Graves and Duvall 1993; Charland and Gregory 1995; Webb and Shine 1997; Carfagno and Weatherhead 2008). Interestingly, male *D. couperi* in our study exhibited a similar decrease in movement frequency during this period suggesting that the concurrent decrease in female daily probability of movement may not be driven entirely by gestation. We are unsure of the causes behind this decrease in movement frequency. This timeframe at our study sites is typically characterized by dry conditions that might reduce activity patterns among several reptilian and amphibian prey species of *D. couperi* (Stevenson et al. 2010). Lower movement frequencies during this time might therefore have been an energy-saving strategy. Dalrymple et al. (1991) found that road-crossings of several snakes in southern peninsular Florida (Everglades National Park) remained relatively low through April and did not generally peak until May. Hyslop et al. (2014) found that the movement frequencies and distances of female *D. couperi* in southern Georgia were lowest during December through April although this might largely reflect *D. couperi* reliance on Gopher Tortoise burrows as cool-season shelter sites (Stevenson et al. 2003; Hyslop et al. 2009a; Stevenson et al. 2009).

Drymarchon couperi in peninsular Florida remained surface active year-round. Many snake species in the southern portion of North America are surface-active during periods of warmer weather in Winter, but these levels are generally much less than those observed during Spring–Autumn (Timmerman 1995; Cardwell 2008; Sperry and Weatherhead 2009a, 2012). While studies have reported year-round snake activity in southern peninsular Florida (Dalrymple et al. 1991; Bernardino and Dalrymple 1992; May et al. 1996), activity levels still showed a decrease during the winter. With the exception of the late winter–early spring decrease in movement frequency, *D. couperi* at our study sites exhibited similar or increased activity levels during the winter months compared to the rest of the year. The pattern of winter breeding, and concurrent increases in male movements and home range size, in *D. couperi* is different from Spring and/or Autumn breeding reported for most North American snakes (e.g., Aldridge and Duvall 2002). It is unclear why *D. couperi* show this divergent behavior. Dry-season breeding (i.e., Winter) has been reported or inferred for several tropical species (Madsen and Shine 1996b; Aldridge and Duvall 2002; Brown and Shine 2002; Bertona and Chiaraviglio 2003; Fearn et al. 2005). The genus *Drymarchon* is found primarily in Mexico, Central and South America (Wuster et al. 2001), so winter breeding in *D. couperi* might reflect the tropical origins of this genus. However, some tropical species also breed during spring/summer months (Maciel et al. 2003; Marques et al. 2014) or show increased activity during Spring–Autumn compared to Winter (Brown et al. 2005; Abom et al. 2012). Additionally, we note that our study did not examine the seasonality of other reproductive processes (e.g., vitellogenesis, ovulation).

The home ranges of male *D. couperi* were larger than those of female subjects during the non-breeding season, although this difference was smallest during the Summer (July–September; mean values for males and females = 161.15 ha and 93.98 ha, respectively; $\beta = 0.65$, 95% CI = 0.03–1.28). This indicates that the larger annual home range sizes we observed for males were not entirely attributable to male mate-searching movements. Similarly, Hyslop et al. (2014) found that mean Spring–Autumn home range sizes for male *D. couperi* in southern Georgia were approximately 2–5 times larger than those of females. We are unsure why males would maintain larger home ranges outside of the breeding season, although other studies have also reported increased movements and/or larger home ranges for male snakes outside of the breeding season (Brown et al. 2005; Smith et al. 2009). This pattern might reflect the larger body sizes of male *D. couperi* (Layne and Steiner 1996; Stevenson et al. 2009). We found a positive effect of body size, but not sex, on seasonal home range size at the Highlands site. However, we suspect this effect is attributable to low overlap in SVL between males and females (inter-quartile range, males = 145.0–162.9 cm vs. females = 126.3–141.5 cm), resulting in a high correlation between sex and SVL. Indeed, both of these covariates had similar effects on home range size when examined separately. Hyslop et al. (2014) found that body size, in addition to sex, had a positive effect on *D. couperi* annual home range size, and suggested that larger male home range sizes were not attributable solely to greater resource needs of larger individuals. This hypothesis is supported by the effect of sex, but not size, on annual (Highlands and Brevard sites combined) and Brevard seasonal home range size, despite males being larger.

Although our study was not designed to directly compare seasonal variation in *D. couperi* movement patterns between the southern and northern parts of their range, we note several qualitative differences between their movement patterns in peninsular Florida and southern Georgia (Hyslop et al. 2014). Consistent with results from Breininger et al. (2011), *D. couperi* in peninsular Florida maintained smaller mean annual home ranges than those in southern Georgia (males, 149.12 vs. 510 ha; females, 48.97 vs. 102 ha; Hyslop et al. 2014). While our annual home range sizes were smaller than those reported by Breininger et al. (2011) this is likely because they reported home range sizes with tracking durations of up to 2 yr. However, 3-mo home range sizes, movement frequency, and distance were all lowest during the Winter (December–March) in southern Georgia despite breeding occurring during that time (Speake et al. 1978; Stevenson et al. 2003; Stevenson et al. 2009; Hyslop et al. 2014). Mean 3-mo home range size at that locality ranged from ≤ 10 ha for both males and females in the Winter to approximately 150–275 ha and 25–50 ha during Spring–Autumn for males and females, respectively (Hyslop et al. 2014). In contrast, mean Winter 3-mo home ranges at our study sites were 100.58 ha and 16.10 ha for male and female subjects, respectively. Additionally, six males in the south Georgia study undertook lengthy (1.5–7 km) migrations between overwintering sites on sandhills and Summer foraging habitat (Hyslop et al. 2014). These results contrast with the increased movement frequency, distance, and home range size of *D. couperi* in peninsular Florida during the Autumn–Winter breeding season, and the lack of distinct migratory behavior.

While our study cannot directly test hypotheses responsible for latitudinal variation in seasonal movement patterns of *D. couperi*, we suspect that this variation is

driven by cooler winter temperatures in southern Georgia which, in turn, might dictate *D. couperi* dependence on Gopher Tortoise burrows for winter shelter sites. In southern Georgia, > 80% of Autumn–Winter shelter sites were in Gopher Tortoise burrows (Hyslop et al. 2009a). In contrast, among the Highlands snakes monitored > 105 d during the breeding season (n = 13), Gopher Tortoise burrows comprised a mean of 61% of shelter sites. Similarly, 29% of the Brevard snakes were never observed using a tortoise burrow for shelter (M.R. Bolt, personal observation).

Our study suggests that *D. couperi* in peninsular Florida maintain generally low levels of spatial overlap but that the degree of overlap varies interactively by sex and, to a lesser extent, season. Male home ranges would often mostly or completely overlap one or more female home ranges, whereas male-male and, to a lesser extent, female-female overlap was much less (Figs. 1.5, 1.6, & 1.8). These patterns persisted when examining core area overlap as only three of 17 (18%) male-male dyads had overlapping core areas (50% UD) compared to four of eight (50%) female-female and 20 of 36 male-female dyads (56%). The probability of occurring within a conspecific's home range (PHR_{max}) was significantly greater for male-female dyads compared to female-female or male-male dyads (Fig. 1.5). This pattern persisted, albeit at reduced levels, when examining core area overlap as PHR_{max} differed significantly between male-male and male-female dyads. There was also evidence for increasing male-female overlap during the breeding season and, while this trend was not statistically significant, it was consistent with our expectations based on *D. couperi* mating systems. Webb and Shine (1997) report similar patterns with regards to male-male home range overlap in broad-headed snakes (*Hoplocephalus bungaroides*). During the spring and early summer, when individuals

inhabited rocky outcrops, male home ranges showed virtually no overlap while female home ranges were contained within male home ranges. Home range overlap was greater within and between sexes during the summer, when individuals moved into adjacent woodlands, but individuals appeared to avoid conspecifics of either sex temporally. Steen and Smith (2009) reported low annual home range overlap for eastern kingsnakes (*Lampropeltis g. getula*) and also found that male-female overlap was higher than male-male overlap. Similarly, Cottone and Bauer (2013) reported that female home ranges were often contained within male home ranges during the breeding season for rhombic skaapstekers (*Psammophylax r. rhombeatus*).

Figure 1.8. Six-month home range overlap among simultaneously adjacent male and female eastern indigo snakes (*Drymarchon couperi*) for consecutive breeding (October–March) and non-breeding (April–September) seasons from Highlands County, Florida. Panels A and B, C and D, and E and F depict the same individuals. Panels A and B depict an example of reduced male-male overlap between the breeding and non-breeding season. Panels C and D depict the maximum observed male-male overlap during both the breeding and non-breeding season. Panels E and F depict an example of high female-female overlap. Note that not all of the home range estimates depicted here met our criteria for inclusion in the statistical analyses (i.e., were not monitored for ≥ 105 days and/or home range size did not asymptote). Individuals depicted in panel E but not F were lost due to transmitter removal/failure or mortality.

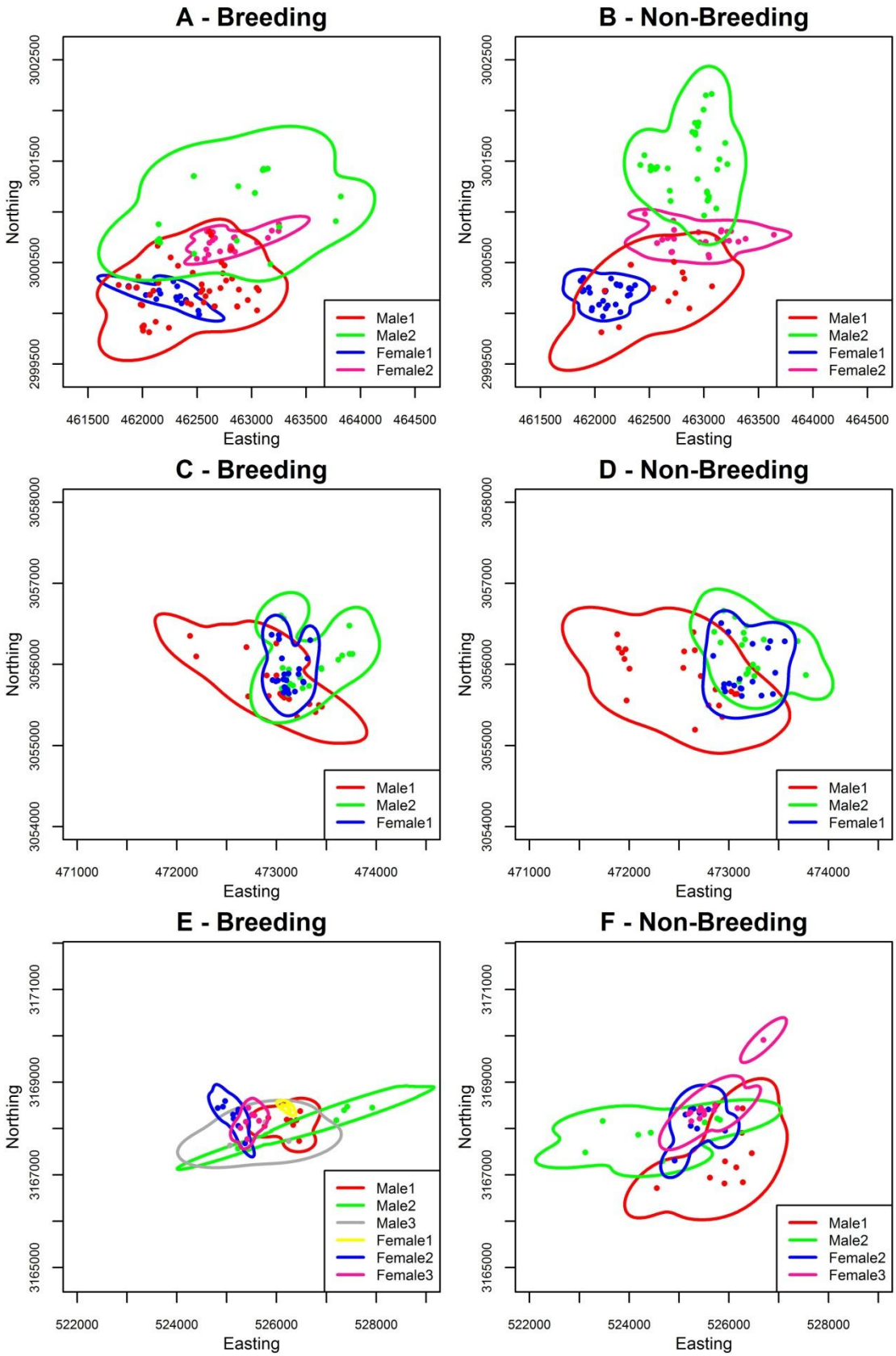
A - Breeding
B - Non-Breeding
C - Breeding
D - Non-Breeding
E - Breeding
F - Non-Breeding
Northing
Easting
Male1
Male2
Male3
Female1
Female2
Female3

In contrast to males, females showed higher overlap in the non-breeding season than the breeding season (Figs. 1.5 & 1.6). Although only four female-female non-breeding season dyads met our criteria for inclusion in our analyses, another three Brevard females monitored during the non-breeding seasons of 1999 and 2000 had relatively high home range overlap (median VI = 0.09 and 0.35 for core area and home ranges, respectively, e.g., Fig. 1.8F). In contrast, home range overlap among these same three females during the breeding season was lower (median VI = 0.06 and 0.18 for core area and home ranges, respectively, e.g., Fig. 1.8E), a pattern consistent with the results of our analyses. Cottone and Bauer (2013) did not observe breeding season home range overlap in female rhombic skaapstekers. Low levels of female home range overlap may reflect efforts to minimize competition for food so that females can secure sufficient resources for reproduction (Ostfeld 1990). Yet if this was the case in our system we would expect female-female home range overlap to be lowest during the non-breeding season when temperatures are warmer and most foraging occurs (Hyslop et al. 2014). Whitaker and Shine (2003) found that female brownsnakes (*Pseudonaja textilis*) often cohabited burrows while males were never observed to do so, a pattern analogous to that seen by Webb et al. (2015) with regard to small-eyed snakes (*Cryptophis nigrescens*) using shelter rocks. However, we note that spatial overlap does not imply the lack of temporal avoidance (Fitzgerald et al. 2002; Whitaker and Shine 2003).

Studies reporting low home range overlap in snakes are a minority. It is difficult to make direct comparisons of home range overlap among studies because of differences in home range estimators and methods used to calculate overlap. For example, most snake studies estimated home ranges using minimum convex polygons (MCP) instead of

fixed kernels even though the latter provides a probabilistic representation of space use that provides a more accurate measure of spatial overlap (Fieberg and Kochanny 2005). Nevertheless, we suggest that qualitative comparisons are still possible, particularly of factors influencing home range overlap (e.g., sex, season). Of 19 published studies that addressed home range overlap in snakes, 15 (79%) inferred high levels of home range overlap (e.g., non-exclusive home ranges). However, two of these studies found that, despite broad home range overlap (11–89% MCP overlap), snakes avoided using shelter sites that were or had previously been occupied by conspecifics (Fitzgerald et al. 2002; Whitaker and Shine 2003). Seven of these 15 studies quantified the degree of home range overlap either as a percentage of the home range overlapped by one or more individuals (Fitzgerald et al. 2002; Whitaker and Shine 2003; Wilson et al. 2006; Mitrovich et al. 2009; Anguiano and Diffendorfer 2015) or the number overlapping home ranges (Secor 1994; Hyslop et al. 2014). For example, Hyslop et al. (2014) reported that *D. couperi* home ranges in southern Georgia were overlapped by the annual home ranges of at least six other individuals. Mitrovich et al. (2009) calculated the proportion of an individual's home range overlapped by other individuals for coachwhips (*Coluber flagellum fuliginosus*) in southern California and found that mean overlap was 0.49–0.89 across three sites. Eight studies that did not quantify the degree of home range overlap reported overlap as "substantial" or "extensive" (Slip and Shine 1988; Weatherhead and Hoysak 1989; Plummer and Congdon 1994; Blouin-Demers and Weatherhead 2002; Diffendorfer et al. 2005; Pearson et al. 2005; Carfagno and Weatherhead 2008; Corey and Doody 2010). Anguiano and Diffendorfer (2015) found that female California kingsnakes shared a greater percentage of their MCP home range with males (mean = 63%) than males did

with females (19%) or other males (27%). However, males never shared core areas. In contrast, "extensive" home range overlap was reported between male and female carpet pythons (*Morelia spilota*, (Slip and Shine 1988; Pearson et al. 2005)) and green pythons (*Morelia viridis*) (Wilson et al. 2006).

Patterns of low spatial overlap among males combined with relatively higher inter-sexual spatial overlap are seen in many mammalian carnivores (Powell 1979; Sandell 1989; Powell 1994; Ferreras et al. 1997). Powell (1993, 1994) hypothesized that high spatial overlap between males and females in a species where males search for females could confer a net advantage to males by providing easy access to females even if breeding occurs seasonally. Low year-round home range overlap among male *D. couperi* combined with high male-female overlap may therefore act to increase male reproductive success. While high levels of male-female overlap outside of the breeding season could lead to intraspecific competition for food resources, the advantages of such overlap to males may exceed the costs (Weatherhead and Hoysak 1989; Mitrovich et al. 2009). Powell (1993, 1994) hypothesized that, in species with male-biased sexual-size dimorphism, males may force spatial overlap on females. Additionally, the costs of inter-sexual home range overlap are expected to decrease if male foraging movements within their home range avoid widespread behavioral or numerical suppression of prey (Powell 1993, 1994). The patterns of *D. couperi* spatial overlap we observed are consistent with these hypotheses, particularly since *D. couperi* males are larger than females (Layne and Steiner 1996; Stevenson et al. 2009). In our study, males also maintained larger home ranges than females during both the breeding and non-breeding seasons which could serve as a means to reduce inter-sexual competition. However, explicitly testing these

hypotheses requires information on mating success and the degree of dietary overlap between males and females.

Resource abundance and competition may also influence spatial overlap. Low levels of spatial overlap are theoretically most beneficial when resource abundance and availability is neither extremely low nor extremely high, because in each instance the costs of excluding conspecifics may exceed the benefits (Carpenter and MacMillen 1976; Maher and Lott 2000). While data from mammalian carnivores often supports this hypothesis (McLoughlin et al. 2000; Eide et al. 2004; Lopez-Bao et al. 2014), it is less clear if this pattern should hold for snakes because, as ectotherms, they have lower energetic requirements, greater conversion efficiencies, are able to consume larger meals, and are more resilient to fasting than similarly-sized endotherms (Pough 1980; McCue 2007; Nowak et al. 2008). However, snake species with larger body sizes, home ranges, and more active foraging strategies generally have higher energetic requirements (Ruben 1976; Secor and Nagy 1994; Plummer and Congdon 1996; Nagy 2005; Carfagno and Weatherhead 2008; Lelievre et al. 2010; Lelievre et al. 2012), which may make exclusive use of foraging habitats more advantageous if it reduces intraspecific competition for prey. While data on *D. couperi* energetic requirements are unavailable, *D. couperi* is a large (> 2 m SVL), actively foraging species with some of the longest daily movement distances and home range sizes reported for snakes (Breininger et al. 2011; Hyslop et al. 2014). The relatively low levels of spatial overlap observed in our study are consistent with the hypothesis that reduced spatial overlap is more advantageous for snake species with higher energetic requirements. While high home range overlap has been reported in ambush foragers (Secor 1994; Pearson et al. 2005) or species with small home ranges (<

25 ha, (Fitzgerald et al. 2002; Diffendorfer et al. 2005; Wilson et al. 2006; Anguiano and Diffendorfer 2015), other active foraging species of snakes also show high levels of spatial overlap (Plummer and Congdon 1994; Carfagno and Weatherhead 2008; Mitrovich et al. 2009). Additionally, Hyslop et al. (2014) found broad overlap among *D. couperi* home ranges in southern Georgia although they did not specify how much of this overlap was due to shared use of overwintering habitat or migration routes. It is therefore less clear how energetic requirements may influence home range overlap in snakes.

Alternatively, low spatial overlap may be driven by a "bet-hedging" strategy where exclusive home ranges are maintained despite temporal fluctuations in prey abundance (White and Ralls 1993; Bateson 2002; Jenkins 2007; Lopez-Bao et al. 2014). Jenkins (2007) hypothesized that such a strategy might explain inter-annual fidelity in western rattlesnake (*Crotalus oreganus*) summer home ranges despite changing prey availability. Similarly, *D. couperi* appear to show inter-annual fidelity to non-breeding season home ranges within our study area. However, additional data on energetics and variation in prey availability are needed to test these alternative hypotheses. Another factor potentially contributing to low spatial overlap in *D. couperi* is the potential for cannibalism. Snakes comprise a major portion of *D. couperi* diets and cannibalism has been documented (Smith 1987; Stevenson et al. 2010). However, if individuals avoided conspecifics to reduce the threat of cannibalism, we would then expect very little male-female overlap because males are larger and more able to prey on females than other males.

We acknowledge that our study suffers from the limitation of not simultaneously monitoring all individuals within our study areas. The presence of non-telemetered

individuals could result in greater spatial overlap among individuals than we observed. *Drymarchon couperi* in our study areas are difficult to detect, which makes it difficult to assess the degree of bias in our results. However, non-telemetered snakes and telemetered snakes that did not meet the criteria for inclusion in our analyses still displayed behaviors consistent with our results. For example, in our Highlands study, we captured nine unmarked adult males overlapping the home ranges of telemetered males. Although this may suggest higher rates of male-male home range overlap than our results indicate, seven of these captures (78%) occurred during the breeding season when males are most likely to overlap spatially. We implanted transmitters in four of the nine snakes and found that their home ranges overlapped little with simultaneously adjacent telemetered males during the subsequent non-breeding season (e.g., Fig 1.8A & 1.8B). Patterns of home range overlap among Brevard snakes not included in our analyses were also consistent with our results. While anecdotal, we suggest that these observations lend confidence to the results of our analyses.

Landscape composition could influence conspecific overlap, although our sample sizes did not permit us to examine this factor. Developed landscapes may compress home ranges and inflate population densities relative to less-disturbed landscapes (Salek et al. 2015), potentially leading to greater levels of home range overlap. This pattern was observed in coachwhips in isolated habitat fragments (Mitrovich et al. 2009). Breininger et al. (2011) found that *D. couperi* home ranges were smaller for both sexes in developed landscapes. This may have confounded the degree of spatial overlap among the Brevard snakes because many were monitored in developed landscapes. One of our two broadest overlapping male-male dyads (non-breeding season, VI = 0.37) was in an urbanized

landscape. However, we observed another broadly overlapping male-male dyad in an undeveloped landscape (breeding season, VI = 0.37). Furthermore, urban red foxes (*Vulpes vulpes*) maintained exclusive home ranges similar to those of rural foxes despite continuous shifts in the urban home ranges, possibly caused by fluctuating food resources (Doncaster and MacDonald 1991).

We also note that our study did not examine the behavioral mechanisms responsible for maintaining the observed levels of spatial overlap. The mechanisms responsible for spatial segregation are diverse and include antagonistic physical interactions, physical or auditory display, or passive actions such as scent marking (Smith 1968; Gese 2001; Wronski et al. 2006; Giuggioli et al. 2011). We think it is unlikely that *D. couperi* engage in active defense of their home ranges as we did not observe movement patterns consistent with territoriality, such as patrolling the edge of the home range (Giuggioli et al. 2011). Nor did we observe antagonistic interactions outside of the breeding season suggestive of territorial defense. Nevertheless, exclusive space use may be maintained passively through scent markings (e.g., Gese 2001). Snakes have excellent olfactory capabilities that are used in foraging (Duvall et al. 1990; Theodoratus and Chiszar 2000; Clark 2004), mate selection (LeMaster et al. 2001), and refuge selection (Reinert and Zappalorti 1988a; Scott et al. 2013). Furthermore, multiple studies have demonstrated that snakes can obtain information about conspecific body size from scent (Shine et al. 2003; Scott et al. 2013), which could allow smaller, subordinate individuals to avoid areas occupied by larger, dominant individuals (Scott et al. 2013). It is possible that the within-home range movements we observed were sufficient to maintain scent markings that conspecifics could detect. Alternatively, individuals may retain some

spatial memory of areas used by conspecifics and avoid those areas. Investigating the mechanisms responsible for maintaining reduced spatial overlap in snakes could provide greater insights into the costs and benefits of maintaining reduced overlap. This could in turn contribute to a more comprehensive understanding of snake social systems and how they contrast with those of ecologically comparable terrestrial vertebrates (e.g., small- to medium-sized mammalian carnivores).

In summary, we found that seasonal variation in *D. couperi* movements are influenced by differences in reproductive behavior between males and females, specifically male mate-searching. Our results also indicate differences in the movement and spatial ecology of *D. couperi* between the southern and northern edges of its distribution. While we hypothesize that these differences are climatically driven, additional research is needed to fully examine the contributing factors. Understanding latitudinal and seasonal patterns can also provide information useful for species management and conservation given the potential negative impacts of anthropogenic landscape changes on species movements at multiple spatio-temporal scales (Gillies et al. 2011; Beyer et al. 2013).

CHAPTER 2

MULTI-LEVEL, MULTI-SCALE HABITAT SELECTION OF EASTERN INDIGO SNAKES IN CENTRAL PENINSULAR FLORIDA

2.1. Introduction

Ecological patterns and processes are influenced by factors operating at multiple spatial scales (Wiens 1989; Bowyer and Kie 2006; Martin et al. 2016). For example, species often respond to habitat features at multiple spatio-temporal scales (Boyce 2006; Mayor et al. 2009; Wheatley and Johnson 2009) or even show multi-scale responses to specific habitat features (Thompson and McGarigal 2002; Leblond et al. 2011; Shirk et al. 2014). Assessing habitat selection at one or a few spatio-temporal scales, even based on biologically-relevant criteria, may result in weak or misleading inferences regarding species-habitat relationships (e.g., Grand and Cushman 2004; McClure et al. 2012). Multi-scale habitat models often outperform single-scale models (Graf et al. 2005; Martin and Fahrig 2012; Timm et al. 2016). Characteristic scales (sensu Holland et al. 2004) may vary seasonally (Boyce et al. 2002; Zweifel-Schielly et al. 2009; Leblond et al. 2011), by sex, and behavioral state (Zeller et al. 2014). Despite the growing awareness of spatial scale in wildlife-habitat relationships, many studies fail to consider multi-scale relationships or do so at too few scales (McGarigal et al. 2016).

In their review of multi-scale habitat selection modeling, McGarigal et al. (2016) identified two non-exclusive approaches for assessing multi-scale wildlife-habitat relationships. The first and most common approach assessed selection at hierarchically nested levels reflecting different behavioral processes (Johnson 1980; Meyer and Thuiller

2006; Mayor et al. 2009). For example, researchers might examine home range selection within a study area (i.e., Johnson's (1980) second order of selection) and selection of resource patches within a home range (i.e., Johnson's third order of selection). While levels vary in their spatial extent, and therefore scale, these extents vary among species or populations. The second approach assesses multi-scale selection by varying the spatial size (i.e., grain) of the observation unit and/or extent of analysis (e.g., Leblond et al. 2011). While scales may be selected to correspond to particular behavioral processes (e.g., home range selection), multi-level analyses explicitly link selection with different behavioral processes occurring over different spatial extents. Although multi-level studies are implicitly multi-scale (but see Wheatley and Johnson 2009), habitat covariates within each hierarchical level are predominately measured at a single spatial scale (e.g., Johnson et al. 2004). Yet multi-scale relationships may still be present within a given hierarchical level (e.g., DeCesare et al. 2012; Shirk et al. 2014; Zeller et al. 2017). Because characteristic scales may differ among covariates, using a single *a priori* scale for each covariate and each level may lead to misleading inferences. An alternative, and arguably more ideal, approach is to assess selection for each covariate at each level across a gradient of scales to identify the characteristic scale of each covariate at each level (e.g, Leblond et al. 2011; Bellamy et al. 2013). McGarigal et al. (2016) described this approach as a "multi-level scale optimized" approach. Despite its advantages, multi-level scale-optimized studies remain a minority among habitat selection studies (but see Zeller et al. 2017).

We examine multi-level scale-optimized habitat selection by the federally threatened eastern indigo snake (EIS, *Drymarchon couperi*). Endemic to the southeastern

Coastal Plain of the U.S.A. (Enge et al. 2013), the EIS has declined throughout its range primarily due to anthropogenically induced habitat loss and fragmentation (U.S. Fish and Wildlife Service 2008). Its large body size (>2 m), large home range sizes (Breininger et al. 2011; Hyslop et al. 2014), and year-round active foraging behavior, particularly in peninsular Florida (Bauder et al. 2016a), increasing its vulnerability to anthropogenic landscape changes. Quantitative data on EIS habitat selection within peninsular Florida are lacking. Anecdotal observations suggest that EIS in peninsular Florida use a variety of natural and anthropogenically disturbed habitats including rural and suburban development (Steiner et al. 1983; Moler 1992; Breininger et al. 2011; Enge et al. 2013). While flexible habitat use may mitigate population-level effects of anthropogenic landscape changes (e.g., Knopff et al. 2014), disturbed habitats may also act as population sinks (Mumme et al. 2000; Breininger et al. 2004), particularly if individuals select anthropogenic landscape features that increase mortality. Many snake species regularly cross roads (Andrews and Gibbons 2008) and selection for habitats containing roads combined with high road crossing rates may negatively impact population viability and connectivity (Row et al. 2007; Fahrig and Rytwinski 2009). Multi-level, multi-scale assessments of EIS habitat selection are therefore needed to better understand the impacts of anthropogenic landscape changes.

Our goal was to evaluate EIS second- and third-order selection (hereafter Level II and Level III, respectively) to provide a multi-level, scale-optimized assessment of EIS habitat selection in central peninsular Florida. We also estimated the probability of EIS road crossings to provide a fine-scale assessment of EIS responses to roads. We predicted that EIS would show negative associations with anthropogenic development and low

probabilities of road crossing (Breininger et al. 2011, 2012; Hyslop et al. 2014). While EIS in peninsular Florida are surface-active year-round, they nevertheless utilize a variety of winter retreat sites, including gopher tortoise (*Gopherus polyphemus*) burrows (Bauder et al. 2016a). Because tortoises primarily occupy terrestrial upland habitats (Auffenberg and Franz 1982; Castellon et al. 2015), mosaics of wetland and upland habitats may increase resource concentrations for EIS. We therefore predicted that EIS would show positive selection for natural habitat heterogeneity (e.g., Hoss et al. 2010; Steen et al. 2012) and comparatively stronger selection for upland habitats compared to wetlands during the winter. We predicted that males and females would show seasonally-variant patterns of Level III selection resulting from differences in breeding season (i.e., winter) reproductive behavior between males and females (Bauder et al. 2016a).

2.2. Methods

2.2.1. Study Area

We used VHF telemetry data from two EIS studies occurring in a similar suite of habitats across central peninsular Florida. The Brevard study (1998–2002) encompassed Cape Canaveral/Titusville (28.63°N, 80.70°W; datum = WGS84 in all cases), southern Brevard County (27.83°N, 80.58°W), and the Avon Park Air Force Range (27.62°N, 81.32°W). The Highlands study (2011–2013) took place in central and southern Highlands County (27.28°N, 81.35°W). Natural habitats included xeric oak scrub, mesic pine flatwoods, hardwood hammocks, maritime scrub and hammocks, and various wetland habitats. Anthropogenic habitats present included improved cattle pasture,

unimproved pasture/woodlands, citrus groves, commercial agriculture, and rural and urban development. Additional descriptions of the study areas and these habitats are provided elsewhere (Abrahamson et al. 1984; Myers and Ewel 1990; Breininger et al. 2011; Bauder and Barnhart 2014).

2.2.2. Telemetry Data

Descriptions of telemetry data collection procedures are provided in Bauder and Barnhart (2014) and Breininger (2011) and briefly recounted here. We monitored a total of 137 snakes (Highlands: $n = 30$, Cape Canaveral: $n = 71$, Indian River: $n = 12$, Avon Park: $n = 25$). Most snakes (> 90%) were captured opportunistically although a small number were captured through road-cruising, visual encounter surveys, or constant-effort trapping. Radio transmitters were surgically implanted into adult snakes weighing ≥ 500 g by professional veterinarians following standard surgical procedures (Reinert and Cundall 1982; Hyslop et al. 2009b). Transmitter battery duration ranged from 12–24 months and a subset of individuals was recaptured and received new transmitters to extend their tracking duration. We located individuals approximately weekly in the Brevard study and once every two days in the Highlands study. We visually confirmed each snake's location for the majority of telemetry fixes (113 of 3,219 [3.5%]) and estimated the remaining using triangulation (White and Garrott 1990), retaining only those with predicted linear error ≤ 150 m (Bauder and Barnhart 2014).

2.2.3. Home Range Estimation

We estimated "total" home ranges from all telemetry locations for each snake using the 95% volume contour polygon of a fixed kernel utilization distribution. Given that our data were collected at relatively infrequent intervals, we used the unconstrained reference bandwidth to provide a relatively high degree of smoothing and account for the uncertainty of an individual's location between telemetry fixes (Bauder et al. 2015). We estimated bandwidths using the package ks (Duong 2007; Duong 2014) in R (R Core Team 2013). We used snakes that were monitored for ≥ 255 consecutive days because this duration provides an unbiased estimate of annual home range size (Bauder et al. 2015). However, some individuals meeting this criterion from the Brevard study had as few as 10 fixes. We therefore calculated area-observation plots to determine the number of fixes needed to reach a stable estimate of home range size (Bauder et al. 2016a). Of the individuals from the Brevard study with ≥ 20 fixes, 90% (57 of 63) reached 90% of their observed home range size with < 17 fixes. We therefore assumed that ≥ 17 fixes would provide a reasonable estimate of the home range while still maximizing the number of individuals included in our analyses. We therefore estimated home ranges for 83 individuals (Highlands: n = 18, Cape Canaveral: n = 36, Indian River: n = 8, Avon Park: n = 21). Most variation in home range size is due to inter-individual variation rather than variation in sampling intensity making it important to maximize the number of individuals (Borger et al. 2006). Additionally, other studies have found that < 20 fixes can still provide unbiased fixed kernel home range estimates (Said et al. 2005; Borger et al. 2006).

2.2.4. Habitat Covariates

We used several habitat covariates that we predicted would influence EIS habitat selection (Table 2.1). Although, we used land cover data from multiple sources and years, we took steps to ensure our habitat data were representative of conditions during each telemetry study period. We used the Cooperative Land Cover Map v. 3.0 (CLC, collected 2014) from the Florida Natural Areas Inventory and Florida Fish and Wildlife Conservation Commission (Knight 2010; Kawula 2014) for the Highlands study area and protected conservation areas in the remaining study areas. We used the St. John's (2000), South Florida (2004), and Southwest Florida Water Management District (2004) land cover data for remaining areas (additional details provided in Appendix A). We also used the 2014 National Wetlands Inventory (NWI) data (U.S. Fish and Wildlife Service 2014) after visually confirming that the NWI data reflected land cover conditions when the telemetry data were collected in each study area. We classified a pixel as wetland if it was mapped as a wetland by any data source. We combined and reclassified the CLC and WMD data following Knight (2010) and considered five land cover types in our analyses: urban, undeveloped, wetlands, citrus, and improved pasture. We considered urban, wetland, and citrus edge as additional land cover types. We included paved roads (collected 1998), linear wetland features (i.e., rivers, streams, canals, and ditches < 15 m wide, hereafter "canals"), soil moisture (available water storage (AWS) at 150 cm), and winter and spring normalized differenced vegetation index (NDVI) as habitat covariates (Appendices B, C). We calculated NDVI using imagery concurrent with our telemetry data collection. Lastly, we also calculated the standard deviation (SD) in AWS and NDVI to represent habitat heterogeneity. All GIS data, except NDVI, were obtained in vector

format and converted to 15-m rasters. We assigned different weights to different road classes, urban densities, and undeveloped land covers to test if EIS responded differently to different development intensities (Table 2.2).

Table 2.1. Habitat covariates used to assess multi-level, multi-scale eastern indigo snake (*Drymarchon couperi*) habitat selection in central peninsular Florida.

Class	Covariate	Description	Source
Land cover	Undeveloped	Natural (e.g., scrub, flatwoods, dry prairie) and anthropogenic (e.g., unimproved pasture/woodland, rural)	CLC (Knight 2010; Kawula 2014) and WMD land cover
Land cover	Wetlands	Forested and unforested wetland	CLC and WMD land cover, Archbold Biological Station wetlands map (unpublished data), National Wetlands Inventory (USFWS 2014)
Land cover	Urban	High, medium, and low density urban	CLC and WMD land cover
Land cover	Citrus	Citrus groves	CLC and WMD land cover
Land cover	Pasture	Improved pasture	CLC and WMD land cover
Land cover	Canals	Permanent and intermittent canals and ditches ≤15 m wide	1:24,000 scale National Hydrography flowline data (USGS 2014)
Land cover	Roads	Paved roads (primary, secondary, tertiary)	1998 1:24,000 roads layer (USGS 1990)
Habitat edge	Wetland Edge	Wetland pixels adjacent to other land covers	CLC and WMD, Archbold Biological Station wetlands map (unpublished data), National Wetlands Inventory (USFWS 2014)
Habitat edge	Urban Edge	Urban pixels adjacent to other land covers	CLC and WMD
Habitat edge	Citrus Edge	Citrus pixels adjacent to other land covers	CLC and WMD
Soil moisture	AWS	Available water storage at 150 cm	Soil Survey Geographic Database (ESRI 2014)
Vegetation cover	Spring NDVI	Normalized differenced vegetation index (NDVI , Apr-May)	USGS Earth Explorer (http://earthexplorer.usgs.gov/)
Vegetation cover	Winter NDVI	NDVI (Dec-Jan)	USGS Earth Explorer

Table 2.2. Weighting scenarios for different road classes and urban and undeveloped land covers. Weights were assigned to each class/category prior to Gaussian smoothing. Undeveloped includes sandhill, scrub, flatwoods, hammock, and dry prairie land covers while rural includes unimproved pasture, mixed rangeland, and rural land covers. See Appendices 2 and 4 for additional details.

	Equal Weights	Strong Differences	Weak Differences	Strong Effect	Weak Effect	No Rural
Roads						
Primary	1	5	3	5	2	NA
Secondary	1	2.5	2	5	2	NA
Tertiary	1	1	1	1	1	NA
Urban/Urban Edge						
High Density	1	5	3	5	2	NA
Medium Density	1	2.5	2	5	2	NA
Low Density	1	1	1	1	1	NA
Undeveloped Upland						
Undeveloped	1	NA	NA	5	2	1
Rural	1	NA	NA	1	1	0

2.2.5. Characteriziation of Spatial Scales

To characterize scale-specific responses to our habitat covariates, we used Gaussian kernels to calculate the amount of each habitat covariate within ecological neighborhoods of varying sizes (Addicott et al. 1987). We used Uniform kernels to calculate the SD of AWS and NDVI as measures of habitat heterogeneity. We systematically varied the Gaussian bandwidth from 15–75 m using 15-m increments and from 100-2000 m using 100-m increments (e.g., DeCesare et al. 2012; Shirk et al. 2014). We varied the uniform kernel radii from 30–150 m using 30–m increments and from 200–4000 m using 200-m increments. We masked out open water pixels prior to

smoothing our continuous raster surfaces and following the smoothing of all raster surfaces.

2.2.6. Measuring Habitat Use and Availability

For our Level II analyses, we estimate home range selection functions (HRSF, Zeller et al. 2012). We measured habitat use by taking the home range-wide average of each habitat covariate measured at each scale and habitat availability by randomly shifting and rotating each home range 250 times within each snake's respective study area. We defined the extent of our study areas by buffering all telemetry fixes within each study area and then merging all the buffers within each study area. To select the buffer radius, we measured the maximum distance between the telemetry fixes for each individual as an approximation of home range width. We used the 95^{th} percentile of this distribution as our buffer radius (3,860 m). We down-weighted each random UD so that the sum of the weights of the used UD equaled the sum of the weights of the available UD, ensuring a 1:1 ratio of used to available observations (Barbet-Massin et al. 2012; Squires et al. 2013).

For the Level III analyses, we evaluated how individuals selected locations relative to available habitats conditional upon the individual's current location and movement potential. We deemed it best to treat our data as points given our relatively low tracking intensity and therefore estimated point selection functions (PSF, Zeller et al. 2012) implemented conceptually as step-selection functions (Johnson et al. 2004; Thurfjell et al. 2014). We measured an individual's habitat use at time *t* and paired that value with a measure of the habitat available to that individual at time *t*–1, thereby

comparing habitat use to what an individual could have used. We measured use at each individual's unique telemetry location. For triangulated locations, we centered a Uniform kernel on the estimated location with a radius equal to that location's predicted linear error (Bauder and Barnhart 2014) and took the mean habitat value within that kernel. We measured availability using empirically-derived generalized Pareto distribution (GPD) kernels centered on the location at *t*–1 (Zeller et al. 2014). Because the durations between successive telemetry locations varied, we allowed the size of the GPD kernel to increase as step duration increased. We modeled the relationship between the scale parameter of the GPD and the duration (i.e., number of days) between successive telemetry locations which showed scale increasing asymptotically with increasing duration (Appendix 5). We estimated separate PSFs for each sex and each 6-month season (breeding, Oct.–Mar., and non-breeding, Apr.–Sep., Bauder et al. 2016). We used data from individuals monitored ≥ 105 days during a given season (n = 80), following Bauder et al. (2016a), because our home range estimates are unbiased at these sampling durations (Bauder et al. 2015) and to ensure the seasonal home range was adequately sampled. This resulted in 728 observations for breeding season females (n = 34), 969 observations for non-breeding season females (n = 28), 841 observations for breeding season males (n = 28), and 983 observations for non-breeding season males (n = 37).

2.2.7. Resource Selection Analyses

We used a pseudo-optimization approach (McGarigal et al. 2016) to identify the characteristic scale for each covariate by fitting a series of single-variable models for each covariate across all scales and then retaining the scale with the lowest AIC as the

characteristic scale (sensu Holland et al. 2004). For covariates with multiple weighting scenarios (Table 2.2) we retained the lowest-AIC scenario. We combined all covariates at their characteristic scales to create a multi-variable, multi-scale model for each level. We used a non-parametric Kruskal-Wallis test to test for differences in Level III characteristic scales among sex*season groups.

We constrained the range of scales considered for Level III to avoid confounding the effects of Level II and Level III selection. We defined the maximum scale for each sex*season group by taking the lower 5^{th} percentile of seasonal home range size (HR5) for each group and then calculating the radius of a circular home range whose area equaled HR5. We then selected the maximum Gaussian bandwidth (h) such that $2 \times h$ equaled the radius of the circular home range and the maximum Uniform kernel radius equaled the radius of the circular home range. The size of HR5 was 12.07 ha (females – breeding season), 23.41 ha (females – non-breeding season), 46.44 ha (males – breeding season), and 35.10 ha (males – non-breeding season), which corresponded to maximum h's of 105, 135, 195, and 165 m, respectively, and maximum radii of 210, 270, 390, and 330 m, respectively. We identified the characteristic scale as the scale with the lowest AIC that was not part of a monotonic decrease extending beyond the maximum scale. We tested for collinearity among covariates at their characteristic scales using Pearson's correlation coefficients (r). If two variables had $|r| > 0.60$ we retained the variable with the lowest AIC. Because urban and roads were moderately correlated with SD of NDVI at Level II ($r = 0.69$ and 0.65, respectively) and yet were of specific interest with regards to EIS habitat selection, we evaluated their effects post-hoc by rerunning the analyses (see below) including urban or roads as well as SD NDVI. Variance inflation factors

were ≤ 3.07 and ≤ 2.95 for the Level II and Level III analyses, including post-hoc analyses, respectively.

We estimated HRSFs using fixed-effects generalized linear models in R's glm function. We estimated PSFs using paired logistic regression (Compton et al. 2002; Zeller et al. 2014) and weighted each pair of used and available locations by the number of telemetry fixes observed at that location (median = 1, range = 1–10). We controlled for within-individual autocorrelation by grouping all observations by individual and computing robust (i.e., empirical) standard errors (Nielson et al. 2002; Hardin and Hilbe 2003; Fortin et al. 2005) using the coxph function in the R package survival (v. 2.38, Therneau 2015).

We fit all combinations of our covariates for both Level II and Level III because all covariates reflected *a priori* hypotheses, yet we had no reason to consider any particular combination of our covariates. We ranked models using AIC and used AIC parameter weights to assess relative variable importance (Burnham and Anderson 2002; Giam and Olden 2016). We standardized our data by subtracting each observation from the median and dividing it by its 0.05–0.90 quantile range. We report model-averaged standardized beta estimates, following Lukacs et al. (2010), across models whose cumulative weight summed to > 90% and deemed effects "significant" if their model-averaged 95% CI did not include zero.

2.2.8. Predicted Surfaces

When creating predicted surfaces (e.g., Boyce et al. 2002), the data used to create each surface must be of the same type (i.e., have the same interpretation) as the data used

to estimate the RSF (e.g., Zeller et al. 2016; Holbrook et al. 2017). For our Level II analyses, we therefore re-smoothed our Gaussian/Uniform kernel-smoothed rasters by a Uniform kernel equal in area to the median EIS home range (144 ha, radius = 677 m). Studies using paired logistic regression typically calculate predicted surfaces using the parameter estimates from paired logistic regression in an unpaired framework by applying the parameter estimates to habitat data without first differencing used and available data (Zeller et al. 2016). Thus, to create Level III predicted surfaces, we followed Zeller et al. (2016) to create raster surfaces representing the differences between habitat use and context-dependent availability. We used the GPD kernel corresponding to a 1-day step duration and applied it to every pixel in our kernel-smoothed raster surfaces. We then differenced these GPD kernel-smoothed surfaces (representing availability) from the original Gaussian/Uniform kernel-smoothed surfaces (representing use). We created Level III predicted surfaces for each sex*season group. We created model-averaged predicted surfaces using the models in the 90% model set. We also calculated the proportion of deviance explained (D^2) for each model.

We evaluated the predictive performances of our Level II and Level III RSF using Johnson et al.'s (2006) *v*-fold cross-validation procedure. Briefly, this approach divides relative probability of selection into equal-interval bins and compares the proportion of used observations within each bin to the area-weighted expected proportion of available points within each bin. We quantified the relationship between used and expected proportions using Lin's (1989) concordance correlation coefficient (CCC) following Zeller et al. (2014). Because we were interested in applying the results of our models beyond our study areas, we cross-validated our models across study sites ($v = 4$) such that

for $v = i$, the i^{th} site was used as testing data and the remaining sites as training data. For the Level III models, we created our available data by sampling our differenced raster surfaces using random points drawn from each study area at a density of 2.5 points/ha. For breeding season females, most training models did not converge when cross-validating by site so we used 4-fold cross-validation without regard to site.

We multiplied our Level II and Level III predicted surfaces to create a multi-level, scale-optimized predicted surface of EIS relative probability of selection (Johnson et al. 2004). While not truly conditionally nested (DeCesare et al. 2012), our hierarchical multi-level design ensures that our surfaces are conceptually hierarchically nested (e.g., Johnson et al. 2004; Zeller et al. 2017).

2.2.9. Road Crossing Analysis

We modeled the daily probability of crossing a road as a binomial probability using the straight-line distance between consecutive telemetry fixes (i.e., one movement step) as the sample, trial size equal to step duration (i.e., the number of days between consecutive telemetry locations), and number of successes per sample as the number of observed road crossings for each step. We only used steps where an individual had moved (i.e., step length >0). We assumed that we observed the true number of road crossings within each step and that no more than one crossing occurred per day. Because the validity of these assumptions decreases with increasing step duration, we only considered steps with 2–3 day durations to balance the accuracy of our observations with maximizing the number of individuals and steps included. We fit separate models for each sex*season group using road class (primary, secondary, tertiary) and Euclidean

distance from road as covariates. If the snake did not move during the step, we measured the distance to the nearest road. We only included distances that were less than the diameter of a circular home range equal in area to the median seasonal home range for each group. To account for uncertainty due to maximum step duration, we fit two models for each group, one using 2 days and another 3 days as the maximum step duration. We then calculated D^2 for each model and used the normalized D^2 to calculate weighted average predicted probabilities of road crossing.

2.3. Results

2.3.1. Level II

The characteristic scales of 13 of our 18 covariates (including quadratic effects) were ≤ 100 m (Table 2.3). Among the remaining five covariates, model support for a single characteristic scale was weak (max. ΔAIC ≤0.90, e.g., AWS in Fig. 2.1). The best supported weighting scenarios for undeveloped and urban land covers and urban edge was the equal weights scenario while the best supported scenario for roads was the strong effect scenario (Table 2.3). Model support was equivocal across all scenarios (max. ΔAIC ≤2.84, Appendix B)

Table 2.3. Characteristic scales (m) for Level II and III selection for 18 habitat covariates. Scales refer to Gaussian kernel bandwidth or Uniform kernel radius (*). Wetlands and wetland edge were evaluated using linear and quadratic effects (†). Superscripts denote the following weighting scenarios (Table 2.2): [a] = equal weight, [b] = weak differences, [c] = strong effect, [d] = strong differences.

	Level II	Level III			
		Males		Females	
		Non-breeding	Breeding	Non-breeding	Breeding
Terrestrial	45[a]	15[b]	15[a]	15[b]	15[d]
Urban	15[a]	15[a]	15[a]	15[d]	15[c]
Spring NDVI	60	15	15	15	75
Winter NDVI	60	15	15	15	90
Citrus	15	15	15	15	15
Pasture	15	15	15	15	15
Canals	1200	15	60	15	45
Wetland Edge	15	45	135	30	75
Wetland Edge†	15	NA	NA	NA	NA
AWS	800	15	30	15	45
Roads	15[c]	15[d]	180[d]	30[c]	30[c]
Citrus Edge	1400	60	15	15	15
Urban Edge	1100[a]	165[a]	30[a]	15[a]	75[a]
Wetlands	400	90	15	30	15
Wetlands†	100	NA	NA	NA	NA
SD of Spring NDVI*	60	45	15	75	75
SD of Winter NDVI*	60	60	225	90	90
SD of AWS*	60	150	90	105	150

Figure 2.1. Change in ΔAIC across scales for select Level II covariates. Undeveloped includes rural land covers. Urban and urban edge use the equal weights scenario.

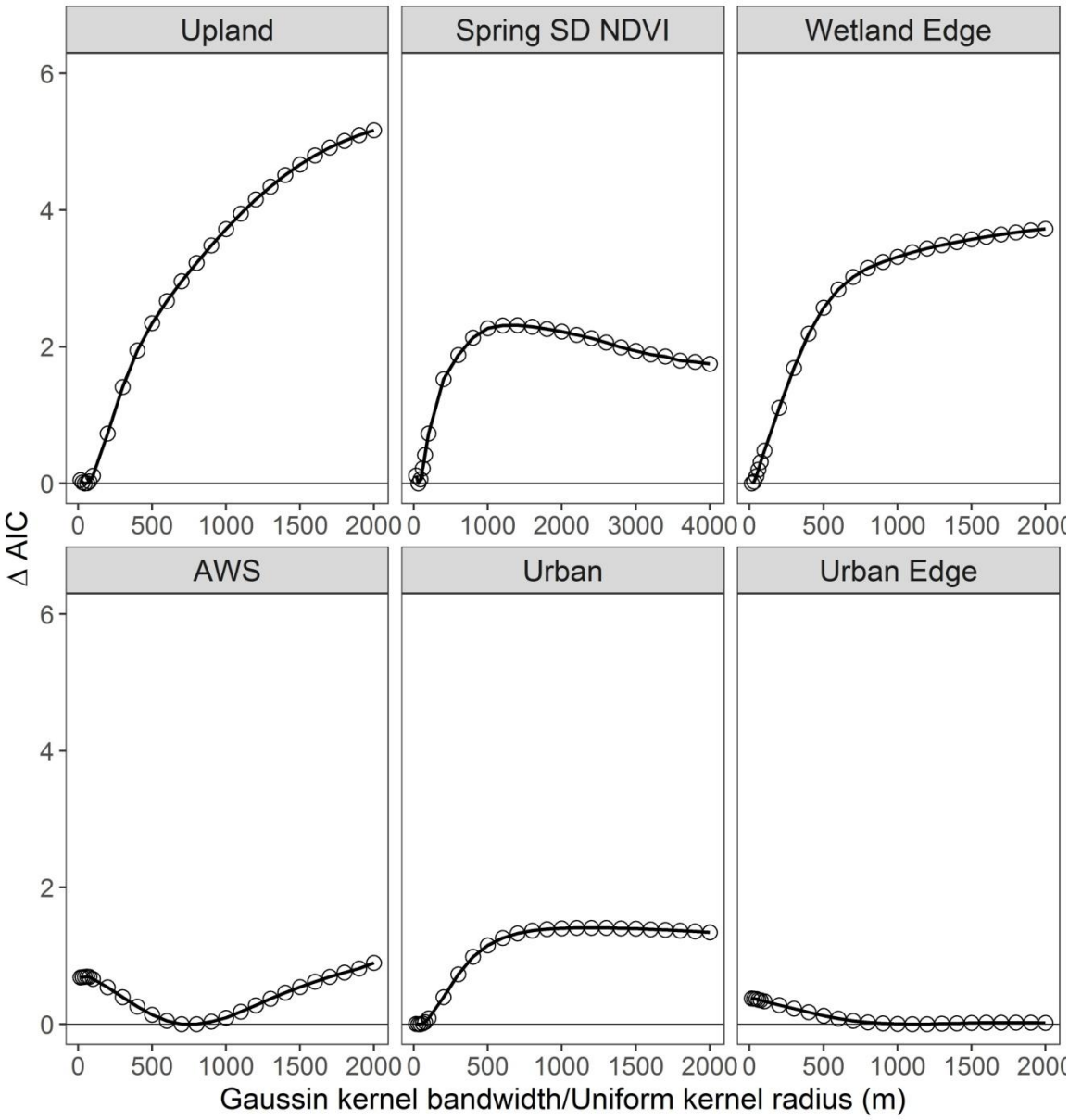

Undeveloped (h = 60 m), SD of spring NDVI (radius = 60 m), and wetland edge (h = 15 m) received the strongest support (parameter weights ≥0.54) although only undeveloped had model-averaged 95% CI that did not overlap zero (Table 2.4, Fig. 2.2). When urban (h = 15 m) was included in the analysis with SD of spring NDVI, SD spring

NDVI, undeveloped, and urban had parameter weights of 0.82, 0.72, and 0.66, respectively, although the 95% CI for all covariates then included zero (Table 2.4, Fig. 2.2). When SD spring NDVI was excluded from the analysis, the effect size of urban markedly decreased. Roads had very low support when included in the analysis (parameter weights = 0.33). The predictive performance of the top model was high (CCC = 0.91, 0.54-0.98) when cross-validating by site and D^2 = 0.11. Model-averaged CCC and D^2 across the 90% model set (n = 125) was 0.88 (range = 0.47–0.99) and 0.09 (range = 0.03–0.11), respectively. When SD spring NDVI and urban were included together, predictive performance decreased slightly (top model: CCC = 0.68, -0.27–0.96, 90% model set = 0.72, range = -0.24–0.99) although D^2 increased slightly (top model = 0.12; 90% model set = 0.11). The correlation between the predicted surfaces across our four study areas with and without urban was high (median r = 0.94, range = 0.88–0.95).

Table 2.4. Model-averaged standardized beta estimates, 95% CI, odds ratios, and AIC weights (*w*) for Level II covariates. *Estimates obtained via post-hoc analyses (see text for details). Data were standardized by subtracting each observation from the median and dividing by the 0.05–0.90 percentile. Estimates were model-averaged across the 90% model set

Excluding Urban				
	Betas	95% CI	Odds ratio	*w*
Undeveloped	1.79	0.23-3.35	5.99	0.87
SD Spring NDVI	1.06	-0.70-2.82	2.89	0.65
Wetland Edge	0.67	-0.82-2.16	1.95	0.54
SD AWS	0.27	-0.82-1.36	1.31	0.36
Citrus	-0.17	-1.26-0.92	0.84	0.33
AWS	-0.13	-1.14-0.88	0.88	0.33
Winter NDVI	0.08	-0.73-0.89	1.08	0.30
Pasture	0.02	-0.76-0.80	1.02	0.28
Urban (without SD NDVI)*	-0.31	-1.63-1.01	0.73	0.38
Roads (with SD NDVI)*	-0.12	-1.01-0.77	0.89	0.33

Including Urban				
	Betas	95% CI	Odds ratio	*w*
SD Spring NDVI	2.22	-0.20-4.63	9.17	0.82
Undeveloped	1.22	-0.61-3.06	3.40	0.72
Urban	-1.85	-5.02-1.32	0.16	0.66
Citrus	-0.51	-2.24-1.22	0.60	0.44
Wetland Edge	0.40	-0.86-1.66	1.49	0.44
AWS	-0.18	-1.29-0.92	0.83	0.35
SD AWS	0.08	-0.68-0.83	1.08	0.31
Winter NDVI	0.18	-0.78-1.14	1.20	0.30

Figure 2.2. Model-averaged predicted relative probabilities selection and 95% CI for Level II using the 90% model set. Values for urban and roads were obtained via post-hoc analyses. Covariates were standardized by subtracting each observation from the median and dividing by the 0.05–0.90 percentile.

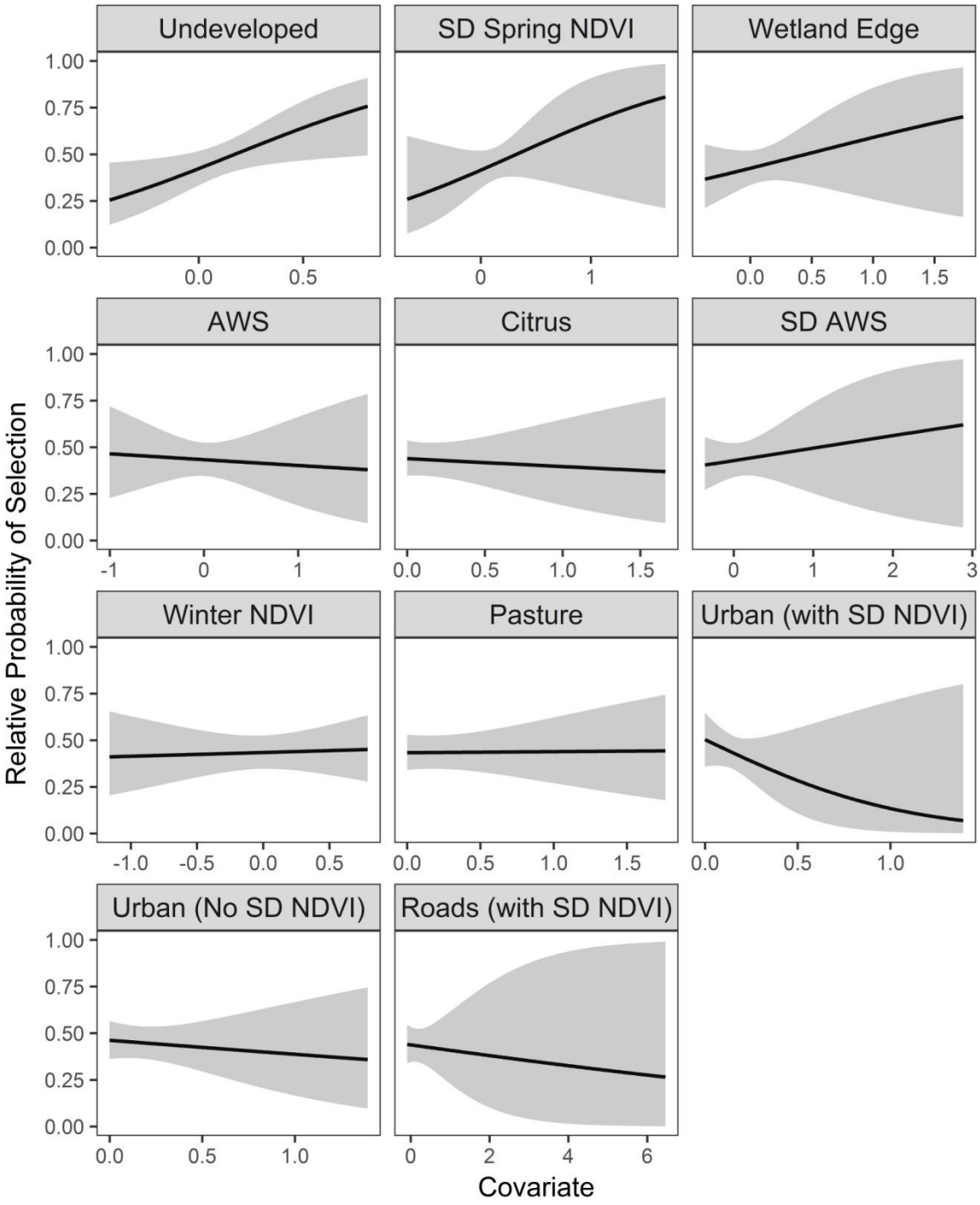

2.3.2. Level III

Although Level III characteristic scales spanned nearly the entire range of scales we considered, the 15-m bandwidth was the most common across all groups (53%, Table 2.3, Fig. 2.3). This percentage increased slightly when we only considered significant covariates (58%) and covariates with parameter weights >0.90 (66%). There was no significant difference in characteristic scales among groups (significant covariates only, $\chi^2 = 0.64$, $p = 0.89$). Model-averaged D^2 across the 90% model set was 0.22, 0.21, 0.32, and 0.22 for breeding and non-breeding season females and males, respectively.

Three covariates (SD of NDVI, undeveloped, and urban) received consistently strong support ($w \geq 0.99$) across all groups (Table 2.5). While not significant in each group, all groups selected increasing SD of NDVI and undeveloped and decreasing urban (Fig. 2.4). The degree and direction of selection for the remaining covariates varied among groups. Citrus and NDVI received strong support among three groups, with avoidance of the former and positive selection for the latter. Both sexes avoided pasture, especially during the breeding season (Table 2.5, Fig. 2.4). Males selected wetland edge while females tended to select increasing SD of AWS while showing neutral selection for roads. While breeding season males showed broad scale (h = 180 m) selection for roads (Fig. 2.4) they also exhibited a secondary characteristic scale (h = 15 m, Fig. 2.3) and post-hoc analyses indicated avoidance at this finer scale (model-averaged beta = -0.16, 95% CI -0.54–0.23, w = 0.85). Breeding season males appeared most selective of their habitat use showing significant selection for 7 of 12 covariates included in their analysis (Table 2.5).

Figure 2.3. Change in ΔAIC across scales for select Level III covariates by sex and season. ΔAIC for each group is rescaled so zero represents that group's characteristic scale. Undeveloped, urban, urban edge, and roads use the lowest-AIC weighting scenario (see text for details).

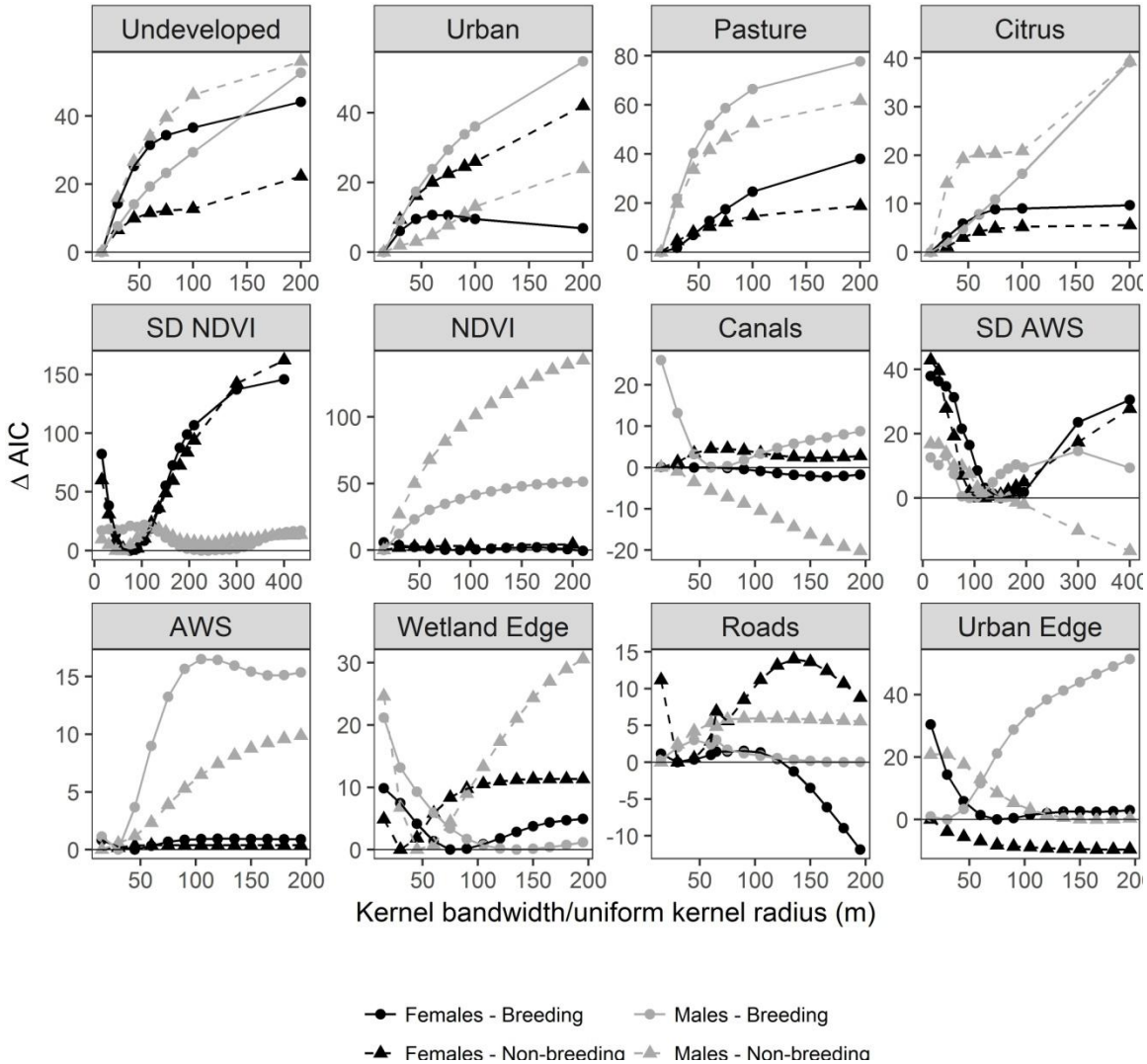

Table 2.5a. Model-averaged standardized beta estimates, 95% CI, odds ratios (OR), and AIC weights (*w*) for Level III covariates for males. *Estimates obtained via post-hoc analyses (see text for details) and were not included in the final model set. Data were standardized by subtracting each observation from the median and dividing by the 0.05–0.90 percentile. Estimates were model-averaged across the 90% model set.

	Males							
	Non-breeding				Breeding			
	Betas	CI	OR	*w*	Betas	CI	OR	*w*
SD Winter NDVI	1.50	0.87-2.13	4.48	1.00	1.93	0.6-3.25	6.87	1.00
Urban	-1.21	-2.57-0.16	0.30	1.00	-1.80	-3.25--0.35	0.17	1.00
Undeveloped	0.90	-0.21-2.02	2.46	0.99	1.16	0.17-2.14	3.18	1.00
Citrus	-1.76	-2.54--0.97	0.17	1.00	-1.51	-3.26-0.24	0.22	1.00
Winter NDVI	2.19	1.03-3.36	8.94	1.00	1.49	0.47-2.5	4.42	1.00
Pasture	-0.19*	-1.02-0.63	0.83	0.53	-0.48	-1.48-0.52	0.62	0.79
Canals	0.12	-0.35-0.59	1.13	0.47	1.49	0.32-2.66	4.45	1.00
SD AWS	0.09	-0.42-0.60	1.09	0.39	0.21	-0.71-1.12	1.23	0.58
Wetland Edge	0.79	0.12-1.47	2.20	1.00	1.43	0.33-2.53	4.17	1.00
AWS	-0.06	-0.69-0.56	0.94	0.34	-2.03	-3.85--0.21	0.13	1.00
Roads	-0.18	-0.60-0.25	0.84	0.69	0.43	-0.09-0.96	1.54	0.89
Urban Edge	NA	NA	NA	NA	NA	NA	NA	NA
Wetland	-0.18	-1.12-0.76	0.84	0.44	NA	NA	NA	NA
Citrus Edge	NA	NA	NA	NA	0.14	-0.07-0.36	1.15	0.98

Table 2.5b. Model-averaged standardized beta estimates, 95% CI, odds ratios (OR), and AIC weights (*w*) for Level III covariates for females. *Estimates obtained via post-hoc analyses (see text for details) and were not included in the final model set. Data were standardized by subtracting each observation from the median and dividing by the 0.05–0.90 percentile. Estimates were model-averaged across the 90% model set.

	Females							
	Non-breeding				Breeding			
	Betas	CI	OR	*w*	Betas	CI	OR	*w*
SD Winter NDVI	NA	NA	NA	NA	NA	NA	NA	NA
SD Spring NDVI	2.86	1.75-3.98	17.46	1.00	3.40	1.84-4.97	29.96	1.00
Urban	-1.75	-3.40--0.10	0.17	1.00	-0.73	-1.74-0.27	0.48	0.98
Un-developed	1.30	0.29-2.30	3.67	1.00	1.22	0.10-2.34	3.39	1.00
Citrus	-0.06	-0.74-0.61	0.94	0.38	-0.56	-2.21-1.08	0.57	1.00
Winter NDVI	1.08	0.26-1.88	2.94	1.00	0.18	-1.63-2.00	1.20	0.39
Spring NDVI	NA	NA	NA	NA	NA	NA	NA	NA
Pasture	-0.02*	-0.31-0.27	0.98	0.28	-0.68	-1.69-0.33	0.51	1.00
Canals	0.52	-0.14-1.17	1.68	0.99	0.19	-1.06-1.44	1.21	0.53
SD AWS	0.68	-0.11-1.46	1.97	0.93	1.67	0.03-3.32	5.31	1.00
Wetland Edge	0.01	-0.35-0.35	1.01	0.27	0.02	-0.84-0.89	1.02	0.28
AWS	-0.10	-0.70-0.50	0.90	0.39	-0.24	-1.39-0.90	0.79	0.53
Roads	0.03	-0.20-0.26	1.03	0.33	0.04	-0.25-0.32	1.04	0.36
Urban Edge	0.29	-0.11-0.69	1.34	0.96	NA	NA	NA	NA
Citrus Edge	0.02	-0.07-0.11	1.02	0.41	0.01	-0.05-0.06	1.01	0.29

Figure 2.4. Model-averaged predicted relative probabilities of selection for Level III by sex and season using the 90% model set. Covariates were standardized by subtracting each observation from the median and dividing by the 0.05–0.90 percentile. Missing covariates were excluded from final analyses due to multicollinearity.

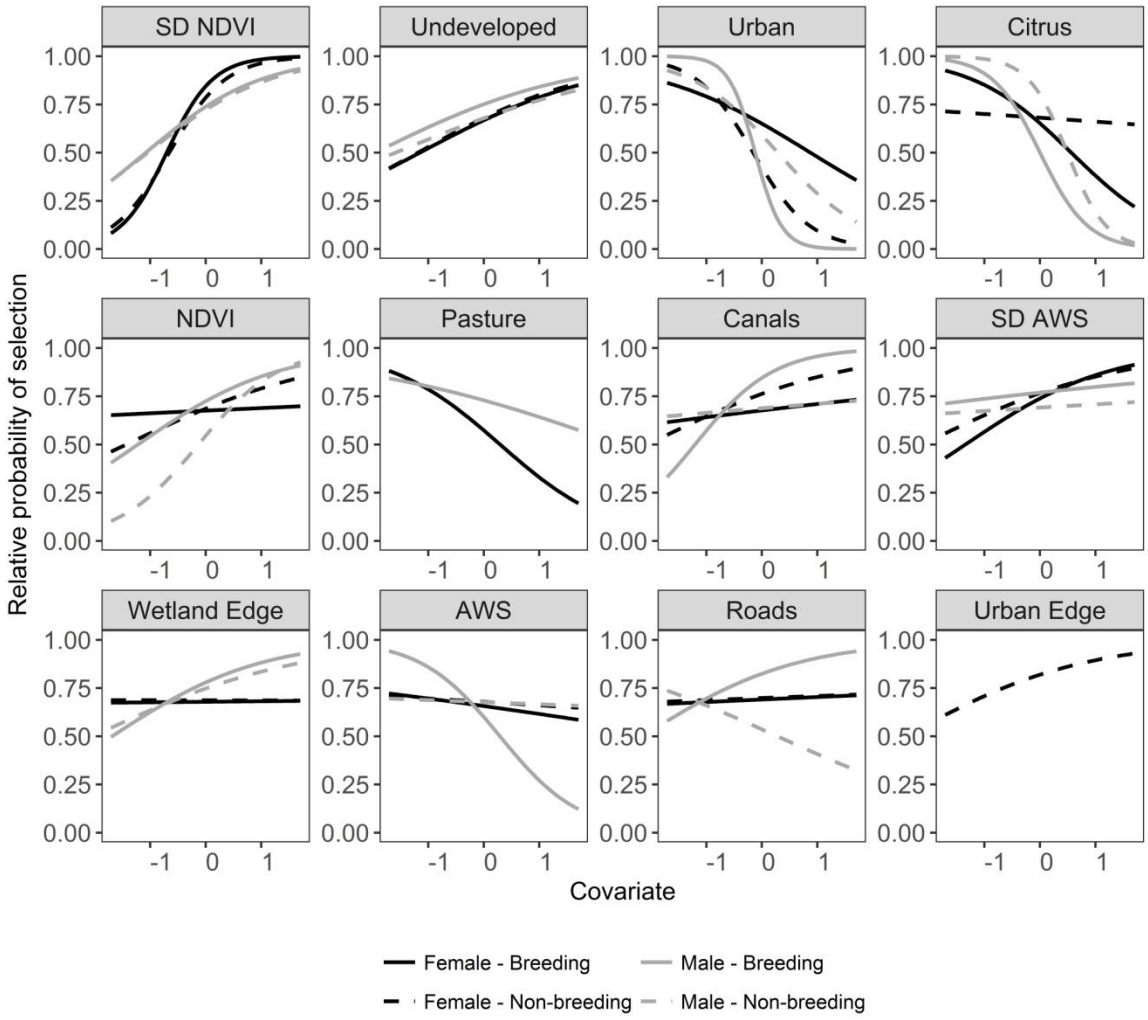

Predictive performance varied across groups. We initially included pasture in our analyses for non-breeding season females and males but doing so reduced the model-averaged CCC from 0.73 to 0.70 and 0.78 to 0.59, respectively. Because the parameter weights for pasture were low to moderate (w = 0.28 and 0.53, respectively) and the model-averaged 95% CI included zero (β = -0.02, 95% CI = -0.58–0.98, β = -0.19, -1.65–0.83, respectively), we removed pasture from our final analyses of non-breeding season

females and males. Model-averaged CCC was 0.62 (0.56–0.68), 0.70 (0.57–0.79), 0.89 (0.87–0.96), and 0.73 (0.59–0.82) for breeding and non-breeding season females and males, respectively. The correlation between the predicted surfaces across our four study areas with and without pasture for non-breeding season females and males was high (r > 0.99).

2.3.3. Road Crossing

The probability of road crossing decreased with increasing distance from road and differed among groups and road classes (Fig. 2.5). All groups had a near-zero probability of crossing primary roads and males had a near-zero probability of crossing secondary roads. Probability of crossing tertiary roads was 0.23–0.35 when an individual was adjacent to a road and became ≤0.01 when distance from road exceeded 340 m for breeding season females, 400 m for non-breeding season females, 1,160 m for breeding season males, and 880 m for non-breeding season males.

Figure 2.5. Predicted probability of road crossing by sex and season as a function of Euclidean distance from road and road class. Probabilities were obtained using D^2-weighted averages of predicted values using 2 and 3 day step durations.

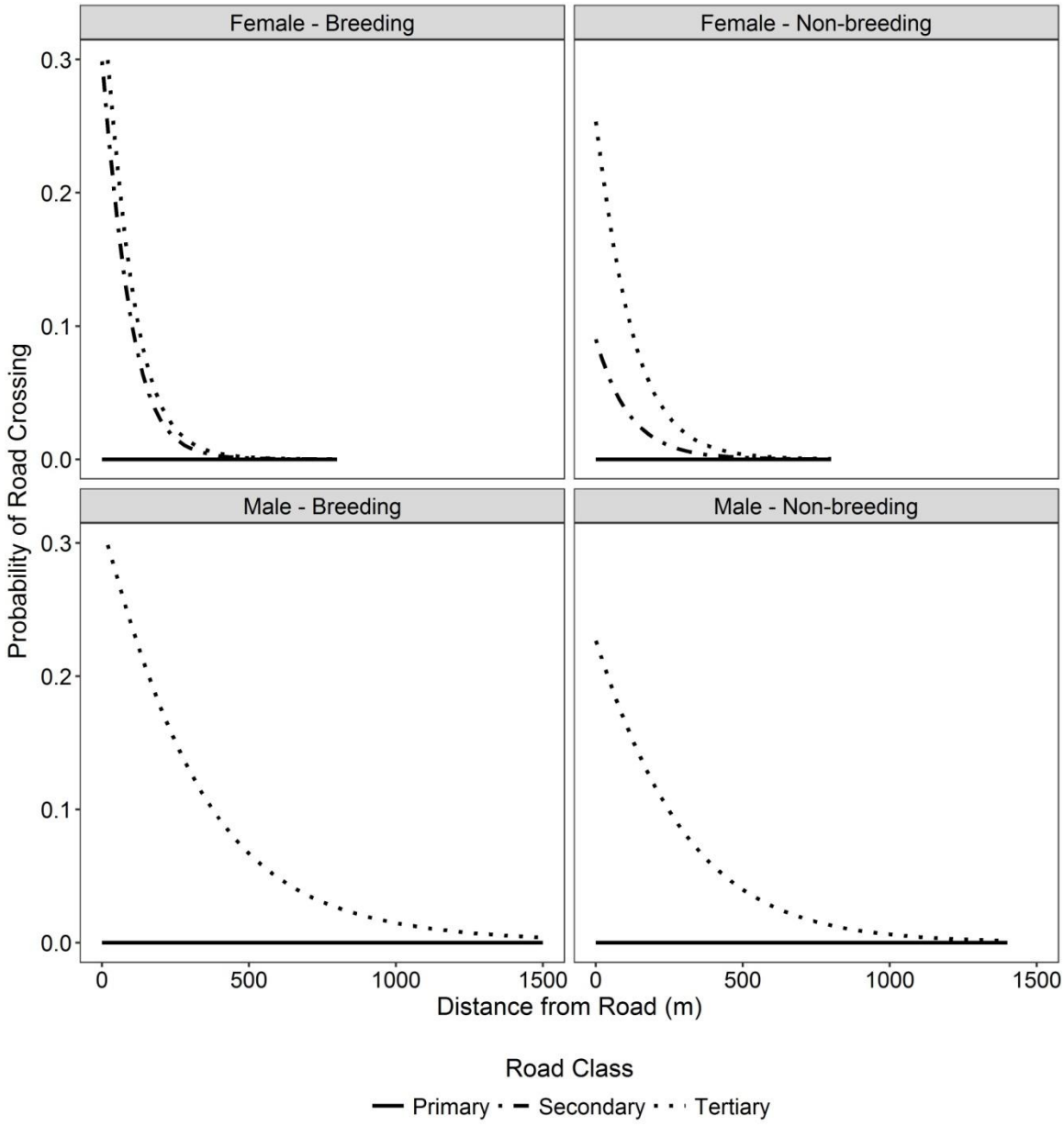

2.4. Discussion

Our results indicate that EIS in central peninsular Florida showed consistent scale-specific responses to habitat selection within two hierarchical levels of selection. Within each level, the characteristic scales of selection were predominately the finest scales we considered. Because we used the home range as the observation unit in the Level II analysis, selection at fine scales suggests that EIS respond most strongly to covariates across and slightly beyond the extent of the home range. This equivocal support across scales in our Level II analysis may suggest that a multi-scale approach using the home range as the observation unit was unnecessary. However, we still recommend that researchers conduct multi-scale Level II analyses because species may respond to habitat features beyond the extent of their home range (Kie et al. 2002; Anderson et al. 2005; Zeller et al. 2017). This may be particularly important if Level II selection is assessed using telemetry locations rather than home ranges as the observation units.

In contrast, we observed markedly different support across scales for some covariates in our Level III analysis. For example, ΔAIC between the 15- and 30-m bandwidth for undeveloped land cover ranged from 6.51–16.00. These results caution against using single-scale analyses of habitat selection and highlight the importance of scale optimization for all covariates within a given hierarchical level. We recommend that researchers constrain the range of potential scales to correspond to a particular hierarchical level to avoid confounding selection across hierarchical levels. The broad (i.e., h >200 m) characteristic scales we observed in our Level III analyses likely reflect confounding effects of second- and third-order selection. These confounding effects can

be minimized by using observation units whose grain (i.e., spatial extent) corresponds to the hierarchical level of interest (e.g., assessing Level II selection using home ranges as the observation unit, Meyer and Thuiller 2006; Meyer 2007). Such an approach also ensures that relative probabilities of selection from each level are conditionally nested, thereby allowing selection at multiple hierarchical levels to be incorporated into a single predicted surface (Fig. 2.6)

Figure 2.6. Multi-level scale-optimized predicted surfaces from the Cape Canaveral study area. **a** Level II predicted surface, **b–d** the normalized products of Level II (excluding urban) and III predicted surfaces (rescaled from 0–1) for breeding season females, non-breeding season males, and breeding season males, respectively.

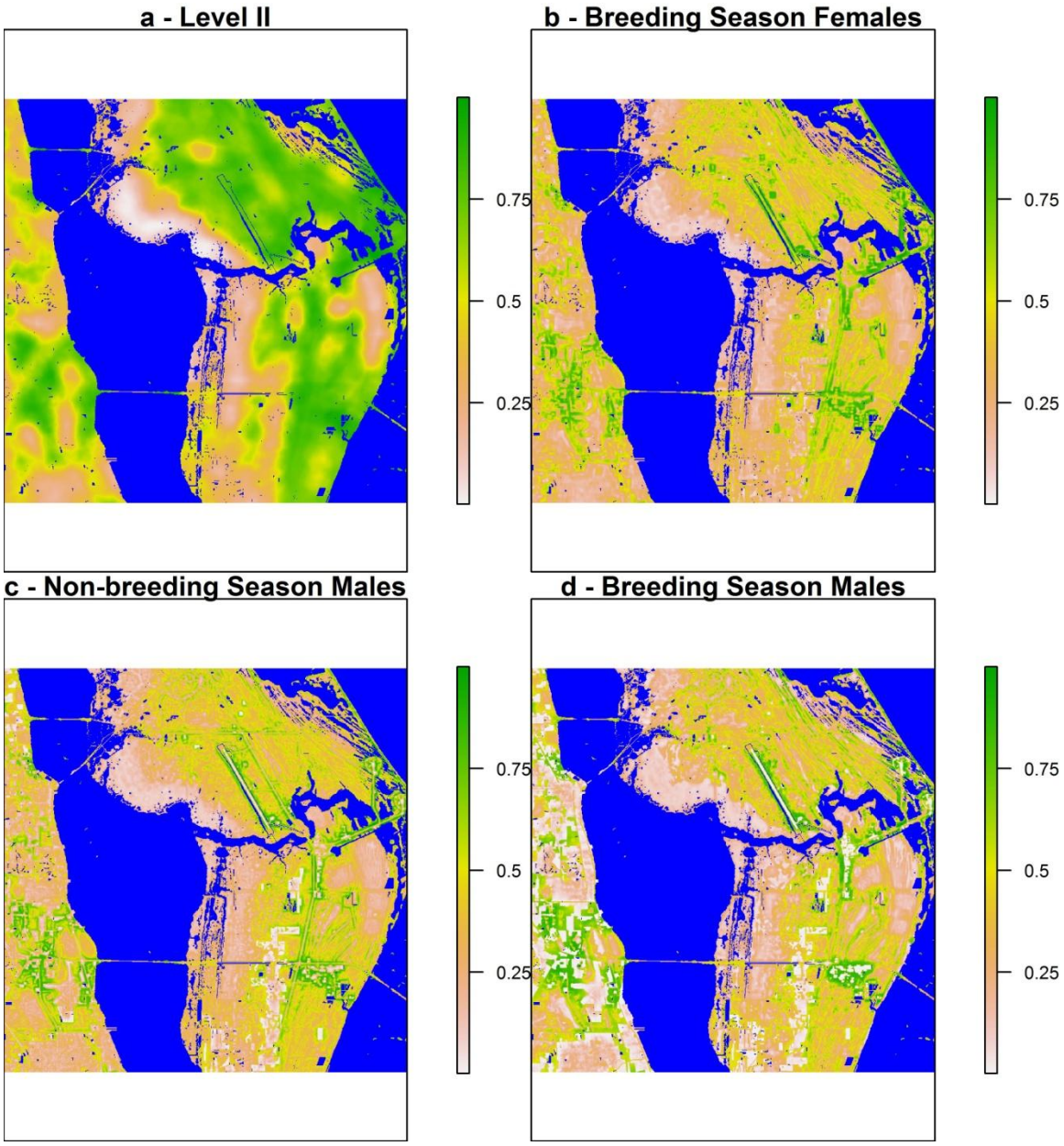

The need to consider habitat selection at multiple spatial scales is widely recognized and many wildlife habitat selection studies employ either multi-level single-scale or single-level multi-scale analyses. However, McGarigal et al. (2016) found that

out of 173 “multi-scale” studies, only 8 were multi-level and scale-optimized. Multi-level, scale-optimized studies may be implemented in various ways depending on the study’s particular objectives (e.g., Leblond et al. 2011; McNew et al. 2013). For example, researchers may optimize scale for a subset of covariates at each hierarchical level, particularly if previous research can inform the appropriate scale for the remaining covariates (Polfus et al. 2011; DeCesare et al. 2012). Alternatively, measuring covariates at a single scale within one hierarchical level while optimizing scale for covariates at other hierarchical levels may be appropriate in some applications, such as evaluating the importance of nest- or location-level factors relative to landscape-level factors (Irvin et al. 2013). However, we suggest that, for many research questions, scale-optimization across all covariates within each hierarchical level (Zeller et al. 2017) will lead to the strongest inferences and predictive abilities.

Eastern indigo snakes also showed consistent patterns of habitat selection across levels, selecting undeveloped upland habitats and habitat edge (measured using SD of NDVI) and avoiding urbanized areas. Furthermore, EIS generally avoided citrus and pastures and selected increasing NDVI at Level III. The greater support for the equal weights scenario for urban at both levels suggest that EIS consistently avoid urbanized habitat regardless of development intensity. However, when SD NDVI was excluded from the Level II analysis, avoidance of urban was relatively weak while selection for undeveloped, wetland edge, and SD AWS increased slightly. Urban was positively correlated with SD NDVI at Level II which is consistent with SD NDVI representing developed-undeveloped interfaces. Despite their positive correlation, the opposite direction of selection for urban and SD NDVI suggests that while EIS select home ranges

in areas with high habitat edge they simultaneously avoid selecting home ranges in highly urbanized landscapes. The reduced predictive performance of our Level II models when urban was included are likely due to cross-validating by study area because the Cape Canaveral study area contains a much higher proportion of urban than the other three study areas. When our Level II models were cross-validated using 4-fold cross validation without regards to study area model performance was high (model averaged CCC = 0.89). This suggests that the transferability of our Level II HRSF may be limited when urban is included in the analysis.

The best supported weighting scenario for undeveloped upland for Level II included natural and rural land covers, suggesting that EIS select upland habitats with relatively low levels of anthropogenic disturbance. Multiple studies of medium-bodied mammalian carnivores in urbanized landscapes have also reported fine-scale avoidance of urban habitats (Riley et al. 2003; Gehrt et al. 2009; Gross et al. 2012). The fine-scale Level III avoidance of urban land cover may allow EIS to utilize relatively small patches of natural habitats within a matrix of urban land covers, a pattern seen in other snakes in urban landscapes (Mitrovich et al. 2009; Anguiano and Diffendorfer 2015). Breininger et al. (2011) found that EIS home ranges in suburban landscapes were significantly smaller than those in natural landscapes, a pattern consistent with our results.

We are limited in our ability to discern the mechanisms responsible for EIS avoidance of anthropogenic habitats. While it could reflect scarcity of resources, anthropogenic habitats often support numerous potential prey and shelter sites (Koenig et al. 2001; Kwiatkowski et al. 2008; Pattishall and Cundall 2009). Like other researchers (Enge et al. 2013), we have observed EIS in all three urban development classes as well

as citrus and pasture. Avoidance of anthropogenic habitats may also reflect risk avoidance behavior and/or cumulative effects of road mortality and human persecution (Breininger et al. 2012). However, EIS appeared to avoid urban more strongly than roads as suggested by the relatively low support for roads across levels. Only non-breeding season males avoided roads (albeit non-significantly) and all groups had relatively high daily probabilities (≥0.23) of crossing adjacent tertiary roads.

Eastern indigo snakes also selected increasing SD of NDVI at both levels, which represents selection for habitat edges, either between vegetation communities or between vegetated and impervious surfaces (e.g., roads, urban development). Wetland edge and SD of AWS were also significantly selected at Level III by males and females, respectively. These results are also consistent with our prediction of selection for natural habitat heterogeneity. Urban edge was positively correlated with SD NDVI (r = 0.72 at Level II and r = 0.51–0.72 at Level III) suggesting that EIS may select urban edges while avoidance directly using urban areas. Indeed, predicted Level III surfaces consistently showed high predicted selection along developed-undeveloped interfaces. We offer several hypotheses to explain these patterns of edge selection. First, heterogeneous habitats may spatially concentrate resources and compress home range sizes (Law and Dickman 1998; Kie et al. 2002; Hoss et al. 2010). Second, EIS are dietary generalists (Stevenson et al. 2010) and habitat edges may increase the diversity and abundance of potential prey species. Edge selection has been noted for dietary generalists in many mammalian and avian taxa (Marzluff et al. 2004; Stewart et al. 2013; Beatty et al. 2014). Third, habitat edges may increase opportunities for thermoregulation, a pattern noted in many north-temperate snakes (Blouin-Demers and Weatherhead 2001a; Row and Blouin-

Demers 2006). However, ectotherms in mild climates may be more flexible in their thermoregulation (Shine and Madsen 1996) and therefore less reliant on edges or habitat openings for thermoregulation (Anderson and Rosenberg 2011). We did not observe a consistent increase in selection for SD NDVI during the winter breeding season, although the resolution of our land cover data may be poorly suited for testing this thermoregulatory hypothesis.

Our predicted surfaces often showed strong selection along road and urban edges reflecting high SD NDVI values. Given that EIS will readily cross tertiary roads, selection for anthropogenically-induced habitat edges may prove maladaptive (e.g., Mumme et al. 2000). Because EIS are active foragers with large home ranges and high movement potential (Breininger et al. 2011; Bauder et al. 2016a), selection for these edges likely increases their risk for road mortality and human persecution (Whitaker and Shine 2000; Andrews and Gibbons 2008). In particular, male EIS, despite their near-zero probability of crossing primary and secondary roads, may be at greater risk of road mortality than females because of their greater movement potential and positive selection for roads at broader scales, which may lead to a greater absolute number of attempted road crossings over tertiary roads.

We found little evidence to support our prediction that the strength of selection for undeveloped uplands increased relative to that of wetlands during the breeding season. Level III selection for uplands was consistently strong year-round, whereas only males avoided areas with high soil moisture during the breeding season. However, some individuals in the Cape Canaveral study area used large expanses of salt marshes during the summer and used predominately uplands during the winter. We were unable to

directly evaluate Level III selection for wetland in most groups because of multicollinearity. While the wetland parameter estimates from single-variable models were consistent with our prediction, these estimates were non-significant ($P \geq 0.152$). This lack of consistent seasonal variation in Level III selection differs from patterns of EIS habitat selection at the northern edge of their range (i.e., southern Georgia). During the winter, EIS in southern Georgia showed near-exclusive use of xeric sandhills supporting gopher tortoise burrows (Speake et al. 1978; Stevenson et al. 2003; Hyslop et al. 2014). During the summer, EIS used a greater diversity of habitats particularly wetlands where most foraging events were observed (Hyslop et al. 2014). The lack of distinct seasonal differences in habitat selection by EIS in central peninsular Florida may be driven, at least in part, by relatively mild winter temperatures that allow them to use a greater diversity of winter shelter sites (Bauder et al. 2016a).

Inter-sex differences in habitat selection can result from differences in reproductive behavior, selection of suitable gestation, nesting, or birthing sites, and/or differences in resource needs (e.g., Charland and Gregory 1995; Blouin-Demers and Weatherhead 2001b; Harvey and Weatherhead 2006). Patterns of selection for the most influential covariates (undeveloped upland and urban land covers, SD of NDVI) were consistent between sexes, highlighting the importance of these features. The greatest difference in patterns of Level III selection between sexes was the greater degree of selection by breeding-season males, for which all but one covariate was either significant or strongly supported ($w > 0.90$). We suspect this is due to larger male home ranges and movement potential during the breeding season (Bauder et al. 2016a) which may therefore entail a greater degree of selective use of both preferred and avoided habitats.

Varying patterns of selection as a function of home range size have been reported in other taxa (Herfindal et al. 2009). Breeding season males strongly selected the weighting scenario for undeveloped upland and selected roads at broad scales. This may be due to males' priority in locating females during the breeding season, which may lead them to traverse a greater diversity of habitats even if those habitats may be less suitable for other activities (e.g., foraging). Variation in home range size may explain other inter-sex differences in Level III selection. For example, males selected wetland edge in both seasons whereas females exhibited neutral selection of wetland edge and roads. This may reflect a hierarchical process of habitat selection wherein smaller female home ranges are selected in areas with optimal densities of wetland edge and roads, thereby resulting in neutral selection of these features within the home range.

We acknowledge limitations in our study that may influence our results and inferences. Several factors may have influenced the accuracy of our GIS data. First, there may have been some degree of temporal mismatch between our telemetry data and GIS data may have occurred, although we attempted to minimize this by using GIS data contemporaneous with our telemetry data. Visual inspections of our GIS data using aerial imagery indicated that our GIS data accurately reflected land cover conditions when our telemetry data were collected. Second, within-class heterogeneity in land covers may have limited our ability to detect relationships (Gaston et al. 2017). Vegetation cover and building densities within urban and rural land covers were highly variable; however, our use of multiple weighting scenarios and other covariates (AWS, NDVI) should have mitigated this variability. Use of multiple land cover data sources may have introduced additional variability, although our reclassification of land cover into five classes should

also have reduced this variability. Finally, combining different data types with different minimum mapping units may have also obscured Level III relationships. However, our use of Gaussian-smoothed surfaces should have reduced this effect by effectively increasing grain size. Moreover, the strong Level III relationships we observed suggest that insufficient data resolution was not a primary cause of weak relationships. Logistical constraints prevented us from assessing selection for field-based microhabitat features (e.g., shrub cover, retreat site abundance). Many snake studies have demonstrated selection for microhabitat features (Reinert 1984; Moore and Gillingham 2006; Martino et al. 2012; Croak et al. 2013) which may be more important than selection for broader-scale habitat features (Harvey and Weatherhead 2006). The moderate predictive performances of our models may reflect our inability to model EIS responses to microhabitat features. While it is possible that large home range sizes and high movement potential cause EIS to respond more strongly to relatively broad-scale habitat features compared to microhabitat features, our study was unable to test this hypothesis.

Large tracts of undeveloped upland habitats containing a mosaic of natural habitats, particularly wetland-upland mosaics, are likely to prove essential for EIS conservation. While EIS exhibit flexible habitat use at multiple levels, our results corroborate previously noted negative impacts of habitat loss and fragmentation (Moler 1992; Breininger et al. 2004). In particular, despite avoidance of urban land covers, EIS will readily cross small paved roads and potentially select roadside habitats which may increase road mortality. While conservation of "rural" land covers may benefit EIS, such benefits are likely contingent upon low road densities and low rates of road-induced mortality. Nevertheless, even infrequent road mortality may still contribute to population-

level declines (Mumme et al. 2000; Row et al. 2007; Fahrig and Rytwinski 2009). Given the development pressures on upland habitats within peninsular Florida (Turner et al. 2006a; Swain and Martin 2014) maintaining and expanding existing conservation networks will likely benefit EIS conservation. We encourage additional research to determine the spatial requirements for viable EIS populations and the degree of EIS connectivity among protected lands within peninsular Florida.

CHAPTER 3

AN INDIVIDUAL-BASED MODEL TO EXAMINE THE POPULATION VIABILITY OF EASTERN INDIGO SNAKES IN CENTRAL FLORIDA

3.1. Introduction

Understanding the likelihood that populations will persist into the future (i.e., population viability) is a key component of many wildlife management and conservation efforts (e.g., Bonnot et al. 2011; Bonnot et al. 2013; Olsen et al. 2014). As a population-level characteristic, population viability is the manifestation of traits and behaviors of individuals within those populations. As a result, an accurate understanding of population-level processes requires an accurate understanding of individual-level traits and behaviors. Moreover, individual-level traits and behaviors are strongly influenced by characteristics of the external environment including climate, topography, and habitat conditions (Morellet et al. 2013; DeCesare et al. 2014). Anthropogenically-induced landscape changes can have strong impacts on individual-level traits that in turn may influence population viability such as survival, fecundity, and dispersal (Robinson et al. 1995; Mumme et al. 2000; Breininger et al. 2012). As a result, spatially-explicit assessments of population viability are often required to incorporate the influence of landscape characteristics, particularly with regards to real-world populations (e.g., Wiegand et al. 2004; Zurell et al. 2012).

This understanding has been greatly aided in recent decades by population viability analyses (PVA, Boyce 1992; Beissinger and Westphal 1998), particularly spatially-explicit PVA. Dunning et al. (1995) identified two broad classes of spatially-

explicit population models, population- and individual-based, which represent two ends of a continuum of how variation in individual-level traits and behaviors are represented (Bolker et al. 1997). Population-based models (PBM) combine individuals into populations or patches within which individuals are assumed to share some or all individual-level traits (e.g., survival, reproduction, dispersal rates). However, it is often advantageous to explicitly incorporate variation in individual-level traits and behaviors by directly simulating the behavior of individuals which can be accomplished using individual- or agent-based models (I/ABM). Agent-based models treat individuals as unique entities and allow them to interact with other agents and their unique environment according to a pre-defined set of rules designed to increase agent fitness (Grimm and Railsback 2005; Railsback and Grimm 2011). Individuals may respond according to intrinsic (e.g., age, sex, reproductive condition) and/extrinsic (e.g., habitat quality, presence of competitors, predators, or mates) conditions (Grimm and Railsback 2005; McLane et al. 2011). ABMs therefore allow population-level traits to emerge as the result of individual-level processes which makes them well suited to understanding how population viability is influenced by landscape factors. Individual-based models have been widely used in ecological applications diverse as evaluating foraging theory (Lewison and Carter 2004), comparing alternative management options (Toral et al. 2012), understanding population genetics (Landguth and Cushman 2010), testing theories of habitat selection (Railsback and Harvey 2002), and understanding the effects of climate change (Stodola and Ward 2017). Additionally, ABMs are increasingly used in PVA (e.g., Letcher et al. 1998; Kramer-Schadt et al. 2005; Rossmanith et al. 2007).

Despite their potential, developing ABMs present several challenges, notably the requirement of sufficient data on individual traits and behaviors. Such data may be difficult to obtain in many situations, particularly for rare or secretive species. However, ABMs can benefit from the application of pattern oriented modeling (Wiegand et al. 2003; Grimm et al. 2005; Grimm and Railsback 2012). POM focuses on identifying multiple patterns in the system of interest which represent the underlying structure and processes of interest in the system and using these patterns the guide the development, complexity, and testing of the model. Developing a model to capture specific patterns can ensure structural realism in the model and avoid developing an overly complex model (Wiegand et al. 2003). Importantly, observed patterns can be used to calibrate a model to ensure that key patterns are satisfactorily reproduced (Wiegand et al. 2003; Topping et al. 2010). Calibration may also be used to identify unknown parameters (e.g., Watkins et al. 2015; Bauduin et al. 2016) in a process also known as indirect parameterization or inverse modeling (Grimm et al. 2005). For example, Rossmanith et al. (2007) identified optimal values of an unknown parameter (pre-breeding survival rate) by identifying a narrow range of possible parameter values that allowed the model to accurately reproduce the observed values for five population-level patterns (e.g., population age structure, nesting success). Chapron et al. (2016) expanded upon this concept by using Approximate Bayesian Computation where observed data were used to create model informative priors and potential parameter values were retained or rejected based on the similarity between observed and simulated summary statistics. In this manner, the authors estimated a conversion factor between number of gray wolf (*Canis lupus*) packs and population size that closely matched an observed time-series of population size.

The eastern indigo snake (*Drymarchon couperi*, EIS) is a federally threatened species native to the Coastal Plain of the Southeastern United States but has declined throughout its range, primarily due to habitat loss and fragmentation as well as historical over-collection for the pet trade (U. S. Fish and Wildlife Service 1978, 2008; Enge et al. 2013). This species has several life-history attributes that increase its susceptibility to anthropogenically-induced landscape changes including a large body size (> 2 m in length), a high degree of surface activity, and large home range sizes (Speake et al. 1978; Moler 1985; Breininger et al. 2011; Hyslop et al. 2014; Bauder et al. 2016a). Breininger et al. (2011) found that EIS home ranges in peninsular Florida were smaller in urbanized landscapes while Breininger et al. (2012) found that annual EIS survival was markedly less for individuals whose home ranges overlapped primary roads or urban development. Studies in the northern part of the EIS' range (i.e., southern Georgia) found that EIS in these areas differ markedly in their habitat use and movement patterns compared to peninsular Florida. Specifically, in southern Georgia EIS maintain small home ranges (ca. 10 ha) centered on xeric sandhills supporting gopher tortoise (*Gopherus polyphemus*) burrows, which are used as overwintering sites, and may undertake long-distance (5–8 km) migrations between winter and summer habitats resulting in very large annual home ranges (up to 1,500 ha, Speake et al. 1978; Stevenson et al. 2003; Hyslop et al. 2009a; Stevenson et al. 2009; Hyslop et al. 2014; Bauder et al. 2017). In contrast, EIS in peninsular Florida are not dependent upon tortoise burrows for overwintering sites, maintain smaller annual home ranges (< ca. 500 ha), move more extensive during the winter, and use a greater diversity of habitats (Moler 1985; Breininger et al. 2011; Bauder et al. 2016a, 2018). Given this variation in movement and habitat use patterns, regional

assessments of EIS population status are essential for an accurate understanding of the species' status.

Despite its threatened status, relatively few studies have evaluated EIS population viability. Hyslop et al. (2012) conducted a PVA for a single population of EIS on protected lands in southeastern Georgia using a stage-transition matrix model which suggested that the population was stable although population growth rate was most sensitive to changes in adult survival. Breininger et al. (2004) created a spatially-explicit population model for EIS in eastern peninsular Florida using the software RAMAS GIS (Akcakaya 2002). Adopting a population-based approach with a high degree of spatial resolution, they divided their landscape into grids approximating the size of an average male EIS home range. Each grid cell contained one male and four females and the survival of individuals within a grid cell varied depending on the cell's landscape context. Their model indicated that EIS population viability was highly susceptible to the degree of habitat edge which led to increased mortality from urban development and primary roads. They also identified areas where populations were likely to persist after 50 years under three different development scenarios. While the model of Breininger et al. (2004) allowed for spatial variation in survival it did not allow for spatial variation in movement patterns or space use which could influence spatial variation in population size and density. Furthermore, they classified their study area as habitat and non-habitat which ignores variation in habitat suitability.

However, neither of these population models took full advantage of an individual-based approach to incorporating inter-individual and spatial variation in individual-level traits and behaviors. An individual-based approach to modeling EIS populations may be

advantageous given the influence of landscape context on movement patterns and survival. We therefore developed an ABM for EIS in central peninsular Florida to help evaluate EIS population status in this region and to better understand the effects of landscape features on population viability. In particular, we incorporate recent data on EIS movement patterns and habitat selection (Bauder et al. 2016a, b, 2018) to simulate individual movements and space use using a series of probability surfaces representing factors hypothesized to influence EIS movements particularly habitat quality and resistance. While routinely incorporated habitat quality when simulating individual movements (e.g., Kramer-Schadt et al. 2005; Carter et al. 2015; Bauduin et al. 2016), fewer have directly incorporated landscape resistance (Watkins et al. 2015). In this paper we present an overview our model's structure calibration. Finally, we use our model to identify conservation lands within our study area capable of supporting viable EIS populations.

3.2. Methods

3.2.1. Study Species and Study Area

We designed our ABM specifically for EIS in central peninsular Florida. Within this region, EIS are surface active year round, may move several hundred meters per day, and maintain relatively large home ranges (> 500 ha) with males having larger home ranges than females (Breininger et al. 2011; Bauder et al. 2016a). During the breeding season (approximately October through March), males actively search for females and will engage in male-male combat (Bauder et al. 2016a, b). EIS are dietary generalists and

prey upon a wide range of reptiles, amphibians, and small mammals (Stevenson et al. 2010). EIS in peninsular Florida will also use a wide range of natural and anthropogenic habitats including xeric uplands, wetlands, coastal scrub, canal banks, improved and unimproved pasture, citrus, and a wide range of rural and urban development intensities. However, previous research found that EIS select undeveloped upland habitats with high habitat edge while avoiding urban, citrus, and pasture (Bauder et al. 2018). EIS home ranges are also smaller and survival is lower in urban landscapes, where individuals are at risk from vehicular and human-caused mortality, compared to undeveloped landscapes (Breininger et al. 2011; Breininger et al. 2012).

We developed our ABM using data collected from two studies in central peninsular Florida. The first study was conducted at three sites, Cape Canaveral/Titusville (28.63°N, 80.70°W; datum = WGS84 in all cases), southern Brevard County (27.83°N, 80.58°W), and the Avon Park Air Force Range (27.62°N, 81.32°W), from 1998-2003 and included radio telemetry data from 103 EIS snakes. The second study was conducted at one site, Highlands County (27.28°N, 81.35°W), from 2011-2013 and included radio telemetry data from 30 EIS snakes. Together these studies covered a wide diversity of landscape features including diverse natural habitat communities (xeric oak scrub, mesic pine flatwoods, hardwood hammocks, maritime scrub and hammocks, and various wetland habitats) and various anthropogenically disturbed habitats (improved cattle pasture, unimproved pasture/woodlands, citrus groves, commercial agriculture, and rural and urban development). These studies have produced much information of EIS ecology (Breininger et al. 2004; Breininger et al. 2011; Breininger et al. 2012; Bauder et

al. 2016a, b, 2018) and we conducted additional analyses as necessary for model development and calibration.

After calibrating our ABM using data from these studies, we applied our model to an approximately 115 × 80 km region in central peninsular Florida centered on approximately the southern half of the Lake Wales Ridge (LWR) in Polk and Highlands Counties (Fig. 3.1). The LWR is a linear topographic feature running approximately 186 km north-south through central peninsular Florida with an average width of 11.7 km and maximum elevation of 64–95 m (White 1970; Weekley et al. 2008). The LWR historically was dominated by xeric, fire-adapted scrub and sandhill communities supplemented by scrubby flatwoods, mesic flatwoods, and seasonal forested and non-forested wetlands (Abrahamson et al. 1984; Myers and Ewel 1990; Weekley et al. 2008). Areas adjacent to the ridge historically were dominated by flatwoods, prairies, and wetland habitats and currently include extensive areas of pasture and agriculture (Myers and Ewel 1990). We selected this study area for several reasons. First, it contained two of the four study sites from our radio telemetry data and therefore reduced the degree of extrapolation in our model's application. Second, an earlier population viability analysis was conducted for the remaining two study areas (Breininger et al. 2004). Third, the LWR has produced many EIS observations within at least the past 40 years and likely represents an important area for EIS within peninsular Florida (Layne and Steiner 1996; Enge et al. 2013). Finally, due to its antiquity and unique habitats, the LWR supports a high degree of plant and animal endemism (Christman 1988; Muller et al. 1989; Myers 1990). However, the LWR has lost approximately 78–85% of its original habitat from conversions to urban, citrus, and pasture (Turner et al. 2006b, a; Weekley et al. 2008;

Swain and Martin 2014) and supports a high proportion of imperiled taxa (Dobson et al. 1997). Nevertheless, the LWR features a relatively extensive network of conservation lands and connectivity networks (Turner et al. 2006a; Hoctor et al. 2010; Swain and Martin 2014; Florida Department of Environmental Protection 2017). An understanding of EIS population viability in this region could both assist future conservation efforts as well as evaluate the extent to which previous efforts are likely to benefit EIS.

Figure 3.1. Location of our ABM application study area along the southern Lake Wales Ridge in central Peninsular Florida. The insert figure shows the location of radio-tracked eastern indigo snakes whose data were used to build and calibrate the model. The boundary of the Lake Wales Ridge follows Weekley et al. (2008).

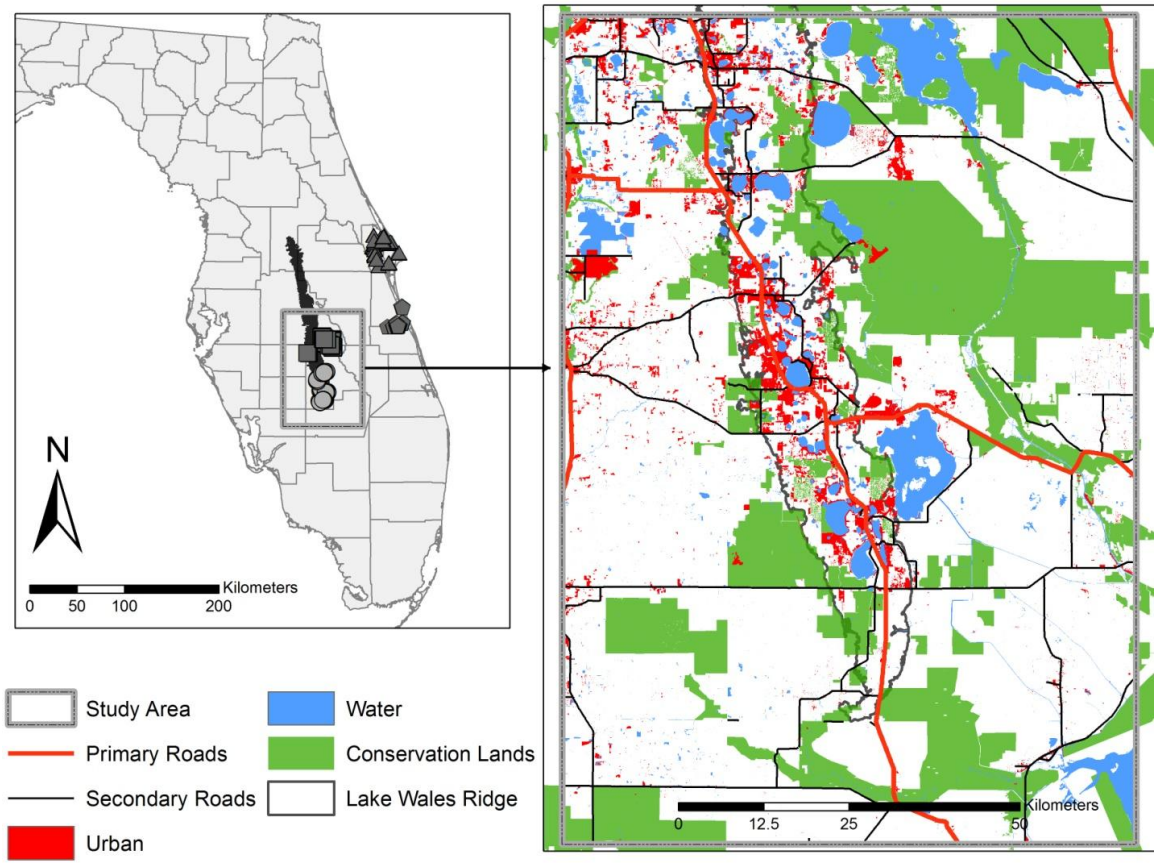

3.2.2. The Model

We wrote and implemented the model in R (R Core Team 2017) and provide a description of the model and its components following the overview, design concepts, and details (ODD) protocol of Grimm et al. (2006; 2010).

3.2.2.1. Purpose

The purpose of this model is to simulate the entire life cycle of individual EIS including birth, dispersal, maturity, home range formation, intra-home range movements, reproduction, and survival. Because the data used in model parameterization and calibration were collected from multiple sites within central peninsular Florida this model is intended for application throughout this region provided model users recognized and accept the degree of interpolation vs. extrapolation involved.

3.2.2.2. Entities, state variables, and scales

We defined our study area by buffering all telemetry observations from Bauder et al.'s (2018) Highlands and Polk County study areas (i.e., the Highlands and Avon Park study areas) by 25 km. We converted all spatial data used in the model (Appendices A–E) to 15-m pixel rasters and cropped the outer 2.5 km of our study area to minimize boundary effects. This resulted in a study area raster with 7,927 rows and 5,442 columns covering approximately 9,706 km^2. All spatial data within the model was represented as raster objects in the R package RASTER (Hijmans 2017). The model used six different types of rasters. The first raster represented Level II or second-order (Johnson 1980)

habitat selection which was used to select starting locations for new individuals (see Dispersal Submodel). The second raster represented Level III or third-order habitat selection which was used to simulate intra-home range movements. We used model-averaged resource selection surfaces (RSS) from Bauder et al. (2018) as our Level II and Level III surfaces and used four different Level III surfaces for males and females during the breeding and non-breeding seasons (Bauder et al. 2016a, 2018). The third and fourth rasters were resistance surfaces representing resistance to dispersal and intra-home range movements, respectively. We created our resistance surfaces by subtracting the Level II and Level III RSS from one, respectively. We assigned all pixels ≤ 265 m (based on the maximum confirmed observed water crossing, 263 m) from land as the maximum resistance value (see below) and all other water pixels a value of 9999 to function as a barrier. The second two rasters denoted urban land cover and roads and were used to inform survival probabilities (see Survival Submodel). We used urban land cover surfaces denoting high-, medium-, and low-density urban and a roads surface denoting primary, secondary, and tertiary roads (Appendix A). Additional rasters can be incorporated into the model depending on the spatial data needed for the models objectives. A list of model parameters are provided in Appendix F.

The model recognized two entities: agents and clutches. Agents represented individual EIS > 1 year old. We recorded the following state variables for each agent: individual identifier, age (in years), sex, date, starting spatial coordinates, birth date, date of maturity, whether or not the agent is alive or dead, the ID of the mother, and multiple landscape attributes used to calculate survival probability. We recorded whether each female's home range overlapped the home range of at least one male to determine

probability of reproduction. Additional landscape and behavioral data were recorded at each time step for each agent (see Movement Submodel) including step length, Level III RSS value, number of road crossings by class, and number of urban crossings by class. The model can be modified to record additional step-level variables as needed. Clutches were stored outside of the modeling environment because of a virtual absence of data on juvenile movements and survival and individuals did not enter the model as new agents until 1 year of age. For each clutch we recorded a unique identifier, the identifier of the mother, the spatial coordinates of the clutch, the date the clutch is laid, clutch size, expected hatch date, expected maturity date, and number of surviving juveniles reaching adulthood. New agents were added to the modeling environment as individuals mature and were probabilistically assigned a sex and starting location (see Dispersal Submodel).

3.2.2.3. Process Overview and Scheduling

Our model used a hierarchy of temporal intervals represented as nested "for" loops to control model processes and scheduling. All model scheduling followed calendar dates using the R package LUBRIDATE (v. 1.7.4, Grolemond and Wickman 2011). Each year was divided into two 6-month seasons, breeding and non-breeding beginning 1 Oct. and 1 Apr., respectively, between which model parameters and processes are allowed to vary (Bauder et al. 2016a, b, 2018). Reporting intervals were used to control the calculation of individual- and population-level metrics and state variables requiring access to all agents present in the modeling environment (e.g., identification of living, neighboring conspecifics). We used four reporting intervals per year beginning 1 Oct., 1 Jan., 1 Apr., and 1 Jul. We divided our spatial data into tiles and assigned each agent to a

tile so that each tile can be run in parallel for a given reporting interval. Spatial data for each tile were stored in list objects. Because agents may need to move beyond the extent of a given tile, a tile buffer was specified and the spatial data of all tiles within a tile buffer were merged together so that agent movements were not constrained by tile edges. The model calculated the number of step intervals within a reporting interval and the number of time steps within a step interval. The hierarchy of time steps within step intervals allowed the number of time steps to vary across step intervals (e.g., daily step intervals and 15 minute time steps where the number of time steps varies with day length). We used daily (24-hr) step intervals and time steps which were equivalent.

We began the model on 1 Oct. which we defined as the date new agents would mature and enter the modeling environment (Fig. 3.2). At each time step, each agent had some probability of moving from its current location and a new location was probabilistically selected (see Movement Submodel). Survival was then simulated as a function of the intervening landscape features (i.e., roads and urban) crossed by a straight line between point t and t+1. At the end of each reporting interval we calculated fixed kernel utilization distributions (UD) and 95% volume contour home ranges for each agent using the previous 365 days of data. We used the reference bandwidth with unconstrained bandwidth matrices (Bauder et al. 2015) in R package KS (v. 1.11.2, Duong 2007) and R code from Fieberg (2014). Simulated data were subsampled to one location every four or seven days (see Model Calibration) for consistency with our observed data (Bauder et al. 2016a). If an agent dies, its UD and home range were removed from the model environment at the end of the current reporting interval to allow other agents to utilize the vacated space.

Figure 3.2. Conceptual diagram showing the major model components and their sequence.

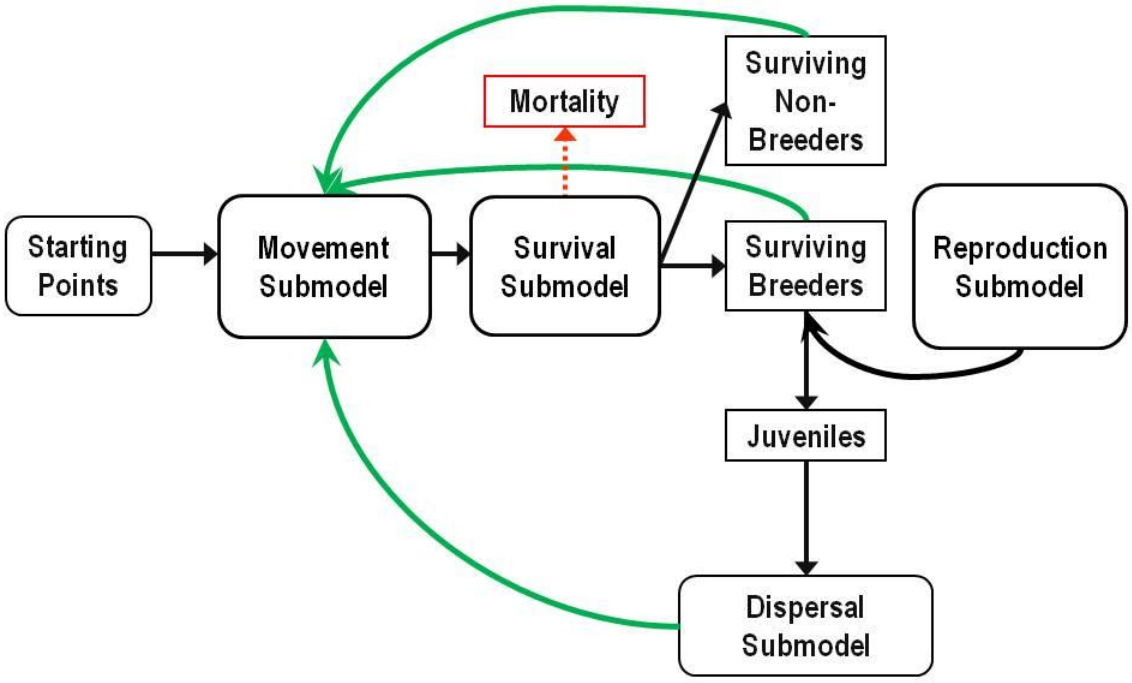

All nests were laid on 1 Apr. (see Reproduction Submodel) and all nest data were stored separate from the model environment. The date at which agents entered the model environment was also calculated and new agents entered the model environment at 1 year of age. A single survival probability was applied during their first year. All new agents were probabilistically assigned starting locations (see Dispersal Submodel) after the UDs and home ranges for existing living agents were calculated. All agents were assigned a maximum age (12 years, Stevenson et al. 2009) and agents were classified as dead upon reaching this age.

3.2.2.4. Design Concepts

3.2.2.4.1. Emergence

Simulated home range sizes emerged through interactions with the local landscape and neighboring agents. While daily movement distances were constrained as a function of sex- and season-specific parameters, the suitability and permeability of the landscape depended upon the specific landscape context which also influenced the distribution and density of conspecifics. Similarly, dispersal distance depended upon both the specific landscape context and the distribution of conspecifics. While daily survival rates were imposed based on landscape features traversed during daily movement, survival at broader temporal scales (e.g., annual survival) was a function of the specific landscape context. Population size, density, and their change over time also emerged from individual-level processes.

3.2.2.4.2. Adaptation and Fitness

Agents increased their fitness by probabilistically moving or dispersing (new agents only) to cells with high habitat suitability, low movement costs, and an absence of conspecifics. During the breeding season, males are more likely to move to cells containing females. However, because cells are selected probabilistically agents have the opportunity to select low-quality environments.

3.2.2.4.3. Learning

None

3.2.2.4.4. Prediction

None

3.2.2.4.5. Sensing

Agent sensory perception for daily movements was defined by a resistance kernel representing the daily movement potential given the resistance values of the surrounding landscape. A resistance kernel combines a probability distribution (i.e., a standard kernel) with a resistance surface and least-cost path analyses to measure the cumulative cost distance of moving from a focal cell to any other cell within the extent of the kernel (Compton et al. 2007). In a non-resistant landscape, the resistance kernel is equivalent to the standard kernel. Our standard kernel was a generalized Pareto distribution (GPD) which closely fit the distribution of observed daily movement distances (Bauder et al. 2016a) and defined the maximum extent of the resistance kernel as the 99^{th} quantile of the GPD. Because the landscape was never non-resistant, the effective scale of perception was always less than the 99^{th} quantile. For dispersal, an agent's sensory perception was defined using a resistance kernel with a half-normal kernel, following Compton et al. (2007), with a maximum extent equal to three standard deviations. We considered that this represented the area potentially available to a dispersing individual during its first year of life from which it could select and establish home range.

3.2.2.4.6. Interaction

Agents of the same sex interacted by generally avoiding other same-sex individual's UDs while males probabilistically selected cells containing females during the breeding season (Bauder et al. 2016b). New agents also avoided the UDs of same-sex individuals when dispersing to a starting location.

3.2.2.4.7. Stochasticity

All processes related to movement, survival, reproduction, and dispersal are selected probabilistically from statistical distributions.

3.2.2.4.9. Observation

The model returns a data frame for each agent where each row contains the step-level data for each agent. Step level data recorded includes agent identifier, sex, spatial coordinates, movement (yes or no), step length, the location's Level III RSF surface value, total number of road crossings cumulatively and by road class, if urban was crossed and the highest urban density level crossed, and age. The model also returns data on each nest produced including nest identifier, date laid, mother identifier, spatial coordinates, number of eggs laid, hatch date, number of eggs hatching, number of hatchlings surviving the first year of life, and the date those 1-year olds enter the model environment. Finally, the model returns population-level summary statistics at each point at which new agents are added to the model environment. These statistics include the

total number of living agents, sex ratio, home range, and dispersal distance but additional statistics can be reported as specified by the model user.

3.2.2.5. Initialization

Each simulation starts with the same number of agents with the same starting locations. The number of agents and their starting locations were selected using empirical data to approximate carrying capacity. The ages for all starting agents were drawn from a uniform distribution from 3-11 years. All simulations began on 1 Oct.

3.2.2.6. Input Data

The model initialization data consists of a data frame with the starting spatial coordinates, sex, and age of starting agents. The number of starting locations was determined separately for males and females. First, we identified suitable and non-suitable habitat using the Level II RSS surface using the 5^{th} percentile of home range-wide mean Level II RSS values as a cutoff. We then divided the total area of suitable habitat by the median total home range size for each sex and probabilistically selected starting locations using the Level II RSS surface. This data frame is add to a named list ('sim') as the first element named 'agents.' All model parameters are added to 'sim' as the second element named 'pars.' All spatial data for each tile are stored as separate named lists. Finally, all reporting intervals are stored as a separate list with each element containing a LUBRIDATE object of class period with the start and end date of each reporting interval.

3.2.2.7. Submodels

The following helper functions and submodels were executed in the following order (Fig. 3.2).

3.2.2.7.1. UpdateAgentStatesList()

This helper function computes and stores the state variables for each agent in a named list ('agent$states') using the data frame of starting locations. These lists are used to create a named list ('all') which in turn is appended to sim$agents. New agents entering the model are also appended to 'all.' The use multiple named lists allow the model to store state variables of different data types (e.g., character, numeric, date) for all agents that were ever present in the model in one list.

3.2.2.7.2. ReturnAliveSeqWithTiles()

This helper function creates and updates a data frame recording select state variables of all agents currently in the modeling environment. This data frame is used for quick access for particular state variables (e.g., identifying all agents within a particular tile or all living agents).

3.2.2.7.3. CreateAgentRDS()

Creates a data frame to store time step-level data (e.g., whether or not the agent moved, how far the agent moved, the landscape features traversed during that time step) for each agent. The number of rows equals the maximum number of allowable time steps for that

agent. The list of state variables ('states') for each agent is combined with this data frame ('step_data') into a two-element named list ('agent') and stored as an RDS file with a file name containing the agent's identifier.

3.2.2.7.4. Movement Submodel

The Movement Submodel determines if and where an agent moves during each time step. Movement from the current cell is determined using a Bernoulli draw with a separate probability for males and females for each day of the year following Bauder et al. (Bauder et al. 2016a). If the agent does not move, its spatial coordinates at time *t* are copied to those of the next time step (*t*+1) and the agent is given a daily movement distance of zero meters. If the agent does move, the maximum extent of its daily movement is defined using the 99th percentile of a GPD (see Model Calibration). We used different GPD for males and females during the breeding and non-breeding seasons (Bauder et al. 2016a).

This extent was used to create a series of probability surfaces (i.e., kernels) representing factors hypothesized to influence EIS movements. We created a habitat suitability kernel using the Level III RSS for a given sex and season. Because our Level III habitat selection analyses evaluated selection for road density rather than for cells containing roads, we depressed the RSS values on all cells containing roads by multiplying the RSS values by the probability of an EIS crossing a road of that class (primary, secondary, or tertiary) when immediately adjacent to that road. We used the road crossing probabilities from Bauder et al. (2018) which varied by sex and season. We created a resistance kernel using a resistance surface calculated as one minus the habitat

suitability kernel (i.e., Level III RSS). We allowed the resistance values for roads to vary by road class independently from the resistance values calculated from the habitat suitability kernel (i.e., background resistance). We assigned a maximum resistance value to primary roads and then reduced this value for secondary and tertiary using one minus the observed road crossing probabilities for those classes (Bauder et al. 2018). We combined the background and roads resistances layers and used the combined resistance surface to calculate a resistance kernel using a GPD kernel (Compton et al. 2007). Although we had empirical estimates of the GPD parameters (shape and scale), our observed GPD distributions came from daily movements across a resistant landscape whereas the standard kernel of a resistance kernel assumes a non-resistant landscape. Our standard GPD kernel must therefore be larger than our observed GPD kernel. To increase the size of the standard GPD kernel we used a multiplier parameter which was applied to the scale parameter since this parameter had the strongest influence on the spread of the GPD kernel. We determined the value of the scale multiplier during model calibration. Because the shape and extent of the resistance kernel are also strongly dependent upon the resistance values we varied the maximum value of the background resistance surface and roads resistance surface during model calibration (see Model Calibration).

We created a conspecific kernel using the UDs of same-sex conspecifics. Bauder et al. (Bauder et al. 2016b) modeled the probability of using a conspecifics UD using GPD models and we used these GPD models to create the conspecific kernel wherein values decreased sharply with increasing UD density. While Bauder et al. (2016b) evaluated EIS 6-month seasonal home range overlap, we used 12-month home ranges to reduce the sensitivity of the conspecific kernel to short-term shifts in space use. However,

we applied separate GPD model during the breeding and non-breeding seasons. We also updated the UDs every four months. Where multiple UDs overlapped we added their density values together. Because the data used in Bauder et al. (2016b) were not collected daily, we subsampled our simulated data to match their sampling intensity prior to estimating UDs. Finally, we created a female kernel for males during the breeding season because males actively search for females during this time (Bauder et al. 2016a, b). We assigned all cells within female home ranges a value of two and all cells outside of female home ranges a value of one.

We normalized each of these four kernels to sum to one and calculated their product to create a redistribution kernel. We set the center cell value equal to zero to ensure the agent moved from its current location. We applied an additional adjustment to the movement kernel to reflect the fact that one-dimensional probability distributions do not directly correspond to two-dimensional representations of those distributions because, in a two-dimensional distribution, surface area increases geometrically with increasing distance from the center point. Therefore, the probability density at a given distance from the one-dimensional distribution should be divided by the area of the surface corresponding to that distance. In the case of the monotonically decreasing GPD, this geometric adjustment means that a cross-section of a two-dimensional GPD would show a steeper decrease in probability density than the one-dimensional GPD. To make this adjustment, we created a raster measuring distance from the center cell and calculated the expected number of cells for each distance as $2\pi \times \text{distance}$. We then divided the redistribution kernel by this new raster and renormalized the redistribution kernel to sum to one.

We sampled a single point from this raster using the *strata* function from the SAMPLING package (Tille and Matei 2016). We set the maximum allowable movement distance to 2,020 m based on longest observed daily movement distance and selected a new location if the step length exceeded this distance. In addition to the step-level attribute data described earlier, we recorded the number of road and urban crossings, the number of road crossings by road class, and the maximum road and urban class crossed.

3.2.2.7.5. Survival Submodel

The Survival Submodel simulated survival for each agent at each time step based on the agent's state and characteristics of the landscape traversed during its previous movement step. Survival was simulated using a Bernouli draw with two possible probability values, a background survival and a road/urban crossing survival which was applied if the movement stepped crossed roads or urban. If an agent died it was removed from the model. Agents were also removed from the model if they reached the maximum age. Because daily survival rates as a function of road and urban crossings were unavailable we selected the final parameter values through a calibration process. However, we based our initial calibration values on annual survival estimates from EIS in peninsular Florida reported in Breininger et al. (2012). Breininger et al. (2012) compared survival between three landscape classes: conservation areas not intersected by highways (conservation core), conservation areas intersected by highways (conservation edge), and rural and urban development (suburb). They found that survival varied strongly by landscape class, specifically being highest in conservation core and lowest in suburb, but did vary by sex or season.

3.2.2.7.6. Reproduction Submodel

The Reproduction Submodel simulated nest laying, hatching, and first-year juvenile survival. Female agents were eligible to produce a clutch once they reached three years of age (Speake et al. 1987). One Apr. 1, immediately after the conclusion of the breeding season, we identified all adult females whose home ranges had overlapped the home range of at least one male during the previous breeding season. We used a Bernoulli draw to determine if these individuals produced a clutch. Data from captive breeding efforts using wild-caught females brought into captivity during the breeding season and held until after egg laying found that 95% (Speake et al. 1987) and 88% (Godwin et al. 2011) of females laid a clutch. Data also suggest that females are capable of reproducing annually (Speake et al. 1987; Hyslop et al. 2009b). We therefore gave females ≥ 4 years a 0.90 probability of reproducing and gave 3-year old females a 0.50 chance of reproducing (Breininger et al. 2004). All eggs were laid on 1 Apr.

We randomly selected clutch size from a normal distribution with mean = 8.62 and SD = 1.70 using data provided in Godwin et al. (2011) although this distribution is consistent with the mean clutch size of 9.4 eggs/female reported by Speake et al. (1987). We rounded all random values to the nearest integer. Although Godwin et al. (2011) had a median egg hatching rate of 80.7%, this was under captive conditions and is likely lower for wild EIS. Because data on nest survival and hatching rates for wild EIS are unavailable we followed Hyslop et al. (2012) and used a nest survival and hatching rate of 0.75. We used a first year survival rate of 0.29 calculated from estimates from captive-born EIS in Smith (1987).

For each nest we recorded nest identifier, mother identifier, date laid, the spatial coordinates of nest (defined as the spatial coordinates of the mother on 1 Apr.), spatial tile number, and clutch size. Because all nests hatched 1 Oct. of that year and all surviving juveniles would enter the model after one year on 1 Oct., we also calculated the nest hatching date, number of hatchlings surviving the first year of life, and the date at which surviving juveniles would enter the model. Because data on juvenile EIS spatial and habitat ecology are unavailable, we stored all nest data outside of the model environment until it was time for surviving agents to enter the model.

3.2.2.7.7. Hatching and Dispersal Submodel

The Hatching and Dispersal Submodel simulated the addition of new adult agents to the modeling environment. We assumed that juvenile EIS were the age class responsible for dispersal in contrast to adults which we assumed maintained relatively stable home ranges. However, EIS dispersal data is largely lacking although a small adult male of unknown age in southern Georgia was observed to move 22.2 km (Euclidean distance) between two overwintering locations (Stevenson and Hyslop 2010). We therefore assumed that this represented the maximum EIS dispersal distance. We created a dispersal kernel analogous to the redistribution kernel to probabilistically select starting locations for all new agents. We defined the extent of the dispersal kernel using the 95^{th} percentile of a half-normal kernel. We selected the standard deviation of the half-normal using model calibration (see Model Calibration).

We used three kernels to create the dispersal kernel. We created a habitat suitability kernel using the Level II RSS (Bauder et al. 2018). We created a resistance

kernel using a resistance surface calculated as one minus the habitat suitability kernel and a half-normal kernel (Compton et al. 2007). We used the maximum resistance value from the background resistance layer derived from the Level III RSS. We created a conspecific kernel using the UDs of same-sex conspecifics to reflect both the avoidance of same-sex conspecifics but also the potential for cannibalism (Smith 1987; Stevenson et al. 2010). To create the conspecific kernel we conducted a similar analysis as Bauder et al. (Bauder et al. 2016b) to estimate the probability of a seasonal (6-month) home range centroid occurring within a same-sex conspecific's home range. We calculated breeding and non-breeding home range centroids, defined as the mean of the x/y coordinates, for 85 individuals (n = 177 6-month home ranges) and then measured the UD density of adjacent same-sex conspecifics as described in Bauder et al. (2016b). This resulted in 17 centroids with non-zero values. We modeled these data using GPD in R package TEXMEX (v. 2.4, Southworth and Heffernan 2013) as a function of sex which had 100% of the AIC model support compared to the null model. We therefore used separate GPD parameters for males and females. We used 6-month home ranges in our analysis, rather than total home ranges, to obtain sufficient sample sizes. To create the dispersal kernel we normalized all three kernels before taking their product after which we again normalized the dispersal kernel to sum to one. We selected each agent's potential starting location using the *strata* function from the SAMPLING package (Tille and Matei 2016) and set the maximum allowable dispersal distance to 22.2 km (Stevenson et al. 2009).

We added mechanism to represent density dependent mechanisms by giving each new agent a probability of successfully recruiting to their potential starting location as a function of the density of conspecifics surrounding that location. We buffered each

potential starting location by 894 and 501 m for males and females, respectively. These buffers represented median total home ranges for each sex. We then overlaid all same-sex conspecific home ranges, giving pixels within home ranges values of one, and calculated conspecific home range density within each buffer. We then specified the relationship between one minus the probability of recruiting and conspecific home range density using a logistic function with an inflection and scale parameterization. The median proportion of 6-month 95% UD volume contour home range overlap across seasons was smaller for males than for females (0.09 and 0.22, respectively, Wilcoxon sign-rank test P = 0.0581, Bauder et al. 2016b). We therefore used inflection points equal to the observed median proportion of home range overlap and scale parameters of 0.05. Buffers completely overlapped by conspecific home ranges therefore had a recruitment probability of zero and buffers without conspecific home ranges had a recruitment probability of one. We used this probability in a Bernoulli draw to determine if the new individual would be added to the model at that location.

3.2.3. Analysis of Observed Patterns

We used five patterns to calibrate our ABM using a POM approach: the relationships between home range size and landscape covariates, home range size for male and female EIS, within-individual 6-month home range overlap, annual survival as a function of landscape covariates, and maximum dispersal distance. Within our ABM these patterns are emergent properties arising from interacts among individuals and between individuals and their unique landscape context.

3.2.3.1. Home Range Size Analyses

We modeled the relationships between EIS total home range size and multiple landscape covariates using a multi-scale approach. We used total home range estimates from 83 EIS used by Bauder et al. (2018). These individuals were tracked for ≥ 258 days (median = 533, max = 1,346) with ≥ 17 telemetry observations (median = 62, max = 264). Home range sizes were estimated using 95% UD volume contours and unconstrained reference bandwidth matrices and median home range size was 144 ha (15–1,129 ha). To measure landscape composition, we placed Uniform kernels of varying radii around the centroid of each snake's x/y coordinates. We systematically varied kernel radii from 50–1,600 m at 100 m increments. We measured the proportion of Urban, Undeveloped, Wetland, Citrus, Pasture, and Wetland Edge land covers within each kernel, calculated mean available water storage at 150 cm (AWS), and the mean and SD of spring NDVI. We excluded Citrus because of insufficient data. See Appendices A–D for additional descriptions of land cover data sources and covariates. We fit linear regression models using the log of home range size as the response variable and sex, number of days tracked, and one landscape covariate as independent variables. We used the beta estimates and their 95% CI as our pattern metrics (Appendix G). To describe male and female home range size we calculated the median, inter-quartile range (IQR), and range of observed total home range sizes for each sex.

3.2.3.2. Within-Individual Home Range Overlap

We used data from Bauder et al. (2016a) to calculate overlap in 6-month home ranges within individuals which included 140 home range-dyads from 47 individuals. We

calculated the volume of intersection (VI) between each dyad which ranged from 0–1 (Fieberg and Kochanny 2005). We used the VI between consecutive breeding and non-breeding seasons (B-NB), between breeding seasons (B-B), between non-breeding seasons (NB-NB), and between breeding and non-breeding seasons separated by 12 months. We quantified observed patterns using the median and IQR of VI for each sex.

3.2.2.3. Survival

We re-analyzed the survival data of Breininger et al. (2012) by combining their data and with data from 30 Highlands County snakes. We used the phi formulation of a multi-state model where survival was the probability of remaining in the observed-alive state to account for uncertainty in a snake's state (dead or alive) when detected underground (Brownie et al. 1993; Williams et al. 2002; Breininger et al. 2012). We modeled survival as a function of sex, season, and landscape class (core, edge, and suburb) and encounter probability as a function of sex, season, landscape class, state (alive or dead), and a binary covariate indicating if the snake had received a transmitter during the previous occasion (TSI). We fit models using MSURVIV (J. Hines, personal communication) and pooled data into weekly capture occasions which we then converted to annual estimates as needed. Because the model where survival varied by landscape class and encounter probability varied interactively by landscape class and TSI had an AIC_c model weight of 0.95 we made inferences solely from this model.

While annual survival for EIS in the suburb and edge classes was less than in the core class (0.5791, SE = 0.1008; 0.6584, SE = 0.1088; 0.8928, SE = 0.0456,

respectively), our primary interest was in how survival varied as a function of road and urban density. Because we had no way to disentangle the effects of each landscape feature on EIS survival, we created a binary development raster indicating if a pixel included roads or urban. To obtain survival estimates as a function of development, we first calculated the mean development value across all snakes in each landscape class. Because we were unsure of the scale at which to measure development, we measured development using the same multi-scale approach described in the home range analysis. We then fit a non-linear least-squares model to our three data points using the *nls* function in R. We used hyperbolic deterministic functions and identified the AIC-best scale for each landscape covariate. Given our very limited sample size our purpose was not to make inferences regarding scale-specific effects of landscape features on EIS survival but rather have an objective means with which to select the scale at which to measure development for model calibration.

3.2.2.4. Dispersal Distance

The only available data on EIS dispersal is a single observation from a large protected area in southeastern Georgia. An adult (140 cm snout-vent length) male was recaptured at overwintering site (i.e., xeric sandhill) 22.2 km (Euclidean) from its overwintering site the previous winter. While the age of this individual and its actual dispersal distance were unknown, we used this observation as a maximum dispersal distance in our ABM.

3.2.4. Model Calibration

We calibrated our ABM using the Cape Canaveral study area. We selected this study area particular to mitigate the computational costs of running the ABM across all four of our study areas but also because the Cape Canaveral study area had the greatest variation in roads and urban densities and the vast majority of telemetered EIS in developed landscapes were from the Cape Canaveral study area. We therefore assumed that landscape condition across our Cape Canaveral study area would be representative of the range of landscape conditions in our application study area. We defined our calibration study areas by buffering the extent of our observed telemetry observations in the Cape Canaveral study area by 5,000–8,000 m so as to obtain comprehensive coverage of available landscape features while avoiding artifacts of the study area edges. We assumed that our observed data were collected within populations at approximately carrying capacity and therefore generated agent starting locations in the following manner. First, we used our Level II RSS (Bauder et al. 2018) to quantify the area of potentially suitable habitat using the 5^{th} percentile of observed home range-wide average Level II RSS values (0.3485). For each study area, we then divided this area by the median home range size for each sex (males = 250.85 ha, females = 78.83 ha) to calculate the number of starting agents. Finally, we probabilistically selected starting locations for each agent using the Level II RSS. This resulted in 936 starting agents.

We used a POM approach estimate the values for six model parameters with unknown values: maximum resistance value for background resistance, maximum roads resistance value, the scale multiplier parameter of the GPD movement resistance kernel, daily background survival rate, daily road/urban crossing survival rate, and the standard

deviation of the half-normal dispersal resistance kernel (Appendix F). The maximum resistance value (upBound) was varied at increments of five from 5–40. The maximum roads resistance value (Roads) was either allowed to take the value of upBound or was varied at increments of 50 from 50–200. The scale multiplier (Scale) was varied at increments of 0.5 from 2–4. We parameterized daily survival rates by converted our observed survival estimates for the core and suburb landscape classes into daily survival estimates and used those daily estimates as starting values for the background and roads/urban crossing survival. We then iteratively adjusted the daily survival rates as needed. We varied the SD of the half-normal kernel used to calculate the resistance kernel for dispersal in an iterative manner beginning with SD = 11.325 which was the SD of a half-normal kernel whose 95^{th} quantile was approximately 22.2 km.

We used an iterative process to calibrate our ABM. Although calibration occurred throughout model development, key trends relating to the suitability of different parameter values were apparent even at early model development versions. We therefore report select results from early model versions to illustrate how certain parameter values and combinations influenced our simulated patterns. First, we held survival and dispersal constant at reasonable values based on our observed data and systematically varied upBound, Roads, and Scale. We calculated our home range related patterns from our simulated data for each parameter scenario and then visually compared the simulated patterns to those from our observed data. After identifying a range of parameter scenarios that reasonably reproduced our observed home range patterns we systematically varied our daily survival parameters within this relatively narrower parameter space. We estimated weekly survival rates as functions of development from our simulated data

using binomial known-fate models (Cooch and White 2017) in the R package RMark (Laake 2013). Because had only three estimates of observed survival (for snakes in core, edge, and suburb landscapes), we calculated predicted survival for our simulated agents at landscape covariate values corresponding to the mean landscape covariate values for core, edge, and suburb EIS. We then compared the observed estimates and 95% CI to the predicted simulated estimates and their 95% CI. Lastly, we adjusted the SD of the half-normal kernel for the dispersal resistance kernel until the 95th quantile of simulated dispersal distances approximated 22.2 km.

3.2.5. Model Application

We then used our final calibrated model to evaluate the effects of landscape features on EIS occupancy across our LWR study area and EIS occupancy and persistence across the current network of conservation lands. Our objective was not to evaluate occupancy or persistence on specific conservation lands but rather the use the distribution conservation lands as sampling units representing a diversity of landscape contexts.

To evaluate EIS occupancy across our LWR study area, we probabilistically selected starting points at a density approximating carrying capacity as described above and ran the ABM for 15 years. Because of computational costs we only conducted a single iteration but consider the large extent of our LWR study area and its landscape diversity to allow us to consider our simulated data as consisting of multiple replicates across different landscape conditions.

We calculated home range estimates (95% UD volume contours using the unconstrained reference bandwidth) for agents surviving to the end of the simulation period using the last 18 months of simulated data to represent the locations of surviving agents on the landscape. We then randomly selected 999 points across our LWR study area separating each point by 2,025 m to ensure a measure of spatial independence and buffered each random point by 1,013 m to represent survey plots approximating the median size of a conservation land (322 ha). We used plot sizes of 322 ha and considered a plot occupied if it was overlapped by any amount of ≥ 1 male and female home range.

To evaluate the effects of landscape features on plot occupancy, we measured several landscape covariates within concentric Uniform kernels with 977, 1277, 1577, 1877, 2177, 2477, 2777, and 3077 m radii centered on each plot. We measured the density of urban (equal weights scenario), undeveloped upland, wetland, pasture, citrus, wetland edge, and roads using the equal weights and strong effects weighting scenarios of Bauder et al. (2018, Chapter 2). We also measured the proportion of each plot/buffer overlapped by conservation lands using a GIS layer from the Florida Natural Areas Inventory (Florida Natural Areas Inventory 2018). We modeled our data using generalized linear models with binomial error distributions and conducted a multi-stage analysis to identify the most influential spatial scales and landscape covariates. First, we identified the characteristic scale (Holland et al. 2004) for each landscape covariate by fitting single-variable models and identifying the scale with the strongest AIC support. Then we fit multi-variable models to all-subsets of non-correlated covariates ($r < 0.70$) whose single model at the characteristic scale had greater AIC-support than the null (intercept only) model and calculated model-averaged effect sizes and AIC_c parameter

weights to identify influential covariates. Because roads and urban were highly correlated, we retained urban because it had the greatest AIC support.

To evaluate the extent to which conservation lands may support EIS, we calculated the model-averaged predicted occupancy for each of our 999 random plots. We then calculated the proportion of the plot that overlapped conservation land and classified plots as having 0%, 1-99%, or 100% overlap with conservation lands. We then tested for significant differences in model-averaged predicted occupancy and influential landscape covariates across these three categories. Finally, we created separate spatially-explicit estimates of simulated EIS occupancy of 322 ha plots by calculating the model-averaged predicted occupancy across the entire LWR study area.

To evaluate EIS occupancy on conservation lands, we determined occupancy for each conservation land for each year of the last 12 years of our 15-year model run. We only considered the last 12 years to minimize the impacts of initial individual starting locations on our results and to allow the first cohort one year to develop home ranges. We excluded one conservation land (Lake Wales Ridge Wildlife and Environmental Area, LWRWEA) because the GIS polygons representing the LWRWEA included approximately seven disjunct polygons or clusters of smaller polygons and spread over approximately 45 km north-south. Our final sample size was therefore 156 conservation lands. We used four criteria to determine occupancy: at least one male-female pair with $\geq$ 50% or $\geq$ 95% of their daily locations overlapping the conservation land and at least five male-female pairs with $\geq$ 50% or $\geq$ 95% of their daily locations overlapping the conservation land. The latter criteria approximate the quasi-extinction threshold of 10 adults and sub-adults used by Breininger et al. (2004). We calculated overlap using

individuals that were alive on Sept 30 of each year (the day before new recruits were added to the model) and then used their locations for the previous 365 days. We then modeled the data for each criterion using a binomial GLM with the proportion of 12 years occupied as the response variable and size of the conservation land as the independent variable. We fit our models using the bias-reduction method of Firth (1993) implemented in the BRGLM package (Kosmidis 2017) to avoid issues of complete separation. This analysis assumes recolonization can occur between years. We then calculated the size of a conservation land with a predicted probability of 0.99 which represents the probability of occurring on a conservation land for all 12 years.

To evaluate EIS persistence on conservation lands, we identified all conservation lands occupied by EIS, according to our four occupancy criteria, on the third year of simulation. We discarded the first two years of simulated data so that the data used in the persistence analysis included data only after the first recruits were added to the model environment which should minimize artifacts due to individual starting locations. We then calculated the number of years until extinction starting at the fourth year of the simulation so that an area occupied in year 3 and extinct in year 4 would have zero years until extinction. We discarded all conservation lands where individuals persisted for the remaining 12 years to allow for parametric modeling of persistence probability. We used a geometric distribution to model number of years until extinction as a function of conservation land size. Because the geometric distribution is a special case of the negative binomial distribution when the overdispersion parameter is one, we used the *glm* function specifying family using the *negative.binomial* function from the MASS package (v. 7.3-49, Venables and Ripley 2002) with theta=1. We then calculated the size of

conservation land needed for a 0.95 probability of persisting for 12 years by calculating, across a range of conservation land sizes, the predicted number of years till extinction from our negative binomial model and considering this value the expected number of "failures" before observing a single success (i.e., extinction). We then calculated the probability of persisting for all 12 trials (i.e., years) as one minus the expected probability of extinction calculated using the *pnbinom* function. We performed these calculations for each of our four occupancy criteria.

3.3. Results

3.3.1. Model Calibration

Our observed patterns indicated that male EIS had significantly larger total home ranges than females and that SD NDVI, urban, and SD AWS had significant negative relationships with total home range size (Appendix G). Total home range size was significantly positively associated with undeveloped and wetlands. Our AIC_c-best scales describing relationships between our observed survival estimates and landscape covariates were 400 m for roads, 1,100 m for urban, and 1,100 m.

Simulated total home range size and its relationship with landscape covariates were highly sensitive to the maximum background and roads resistance value and the GPD scale multiplier (Appendices H–K). Simulated total home ranges were largest when background resistance was lowest and scale multiplier was highest (Appendices H–I). Even under ideal parameter scenarios, female simulated home ranges were often larger than female observed home ranges. The negative relationships between total home range

size and SD NDVI and urban were generally best approximated when background resistance was low (5 or 10) and maximum roads resistance was high (100 or 200, Appendices J–K). While the significant negative relationships between total home range size and these covariates were reproduced under these parameter scenarios, the effect sizes were generally underestimated, particularly for SD NDVI. The degree to which relationships between total home range size and other landscape covariates were accurately simulated was more variable (Appendices J–K). While the observed direction of the relationship was often simulated correctly the magnitude of the effect was generally underrepresented.

Within-individual 6-month home range overlap was generally under simulated and this overlap decreased with increasing duration (Appendix L). Simulated weekly survival for agents in the lowest development class (i.e., low urban and road densities) was lower than observed survival while simulated weekly survival for agents in the highest development class more closely approximated observed weekly survival (Appendix M).

Based on visual assessments of our simulated patterns, we selected a maximum background resistance value of 10, a maximum roads resistance of 200, a scale multiplier of 3.5, a daily background survival of 0.99995 and a daily roads/urban crossing survival of 0.99000 as our final parameter scenario for model application (Fig. 3.3). Median dispersal distance under this scenario was 4.86 km with a maximum dispersal of 19.88 km. At the end of a 15-year simulation in the Cape Canaveral study area, population size declined from an initial 936 individuals to 292 individuals (133 males and 159 females). Sex ratio began strongly female biased (3.18:1) but became more even throughout the

simulation. Median daily step length was 100 m for males and 75 m for females. Observed and simulated annual survival for snakes in Core landscapes was 0.8928 and 0.8884, respectively, and observed and simulated annual survival for snakes in Suburb landscapes was 0.5791 and 0.6158, respectively.

Figure 3.3. Comparison of observed (Obs) and simulated (Sim) patterns under the final parameter scenario for the Cape Canaveral study area. Upper right panel show the beta estimates and 95% CI from multiple regression analyses of total home range size as a function of landscape covariates. Lower left panel shows within-individual 6-month home range overlap between consecutive breeding and non-breeding seasons (B-NB), consecutive breeding seasons (B-B), consecutive non-breeding seasons (NB-NB), and breeding and non-breeding seasons separated by 12 months (B-NB2). Lower right panel shows observed (points) and predicted (lines) weekly survival as a function of development intensity (Dvlp). Error bars represent 95% CI around the observed estimates while dashed lines represent 95% CI around the predicted values from the simulated data.

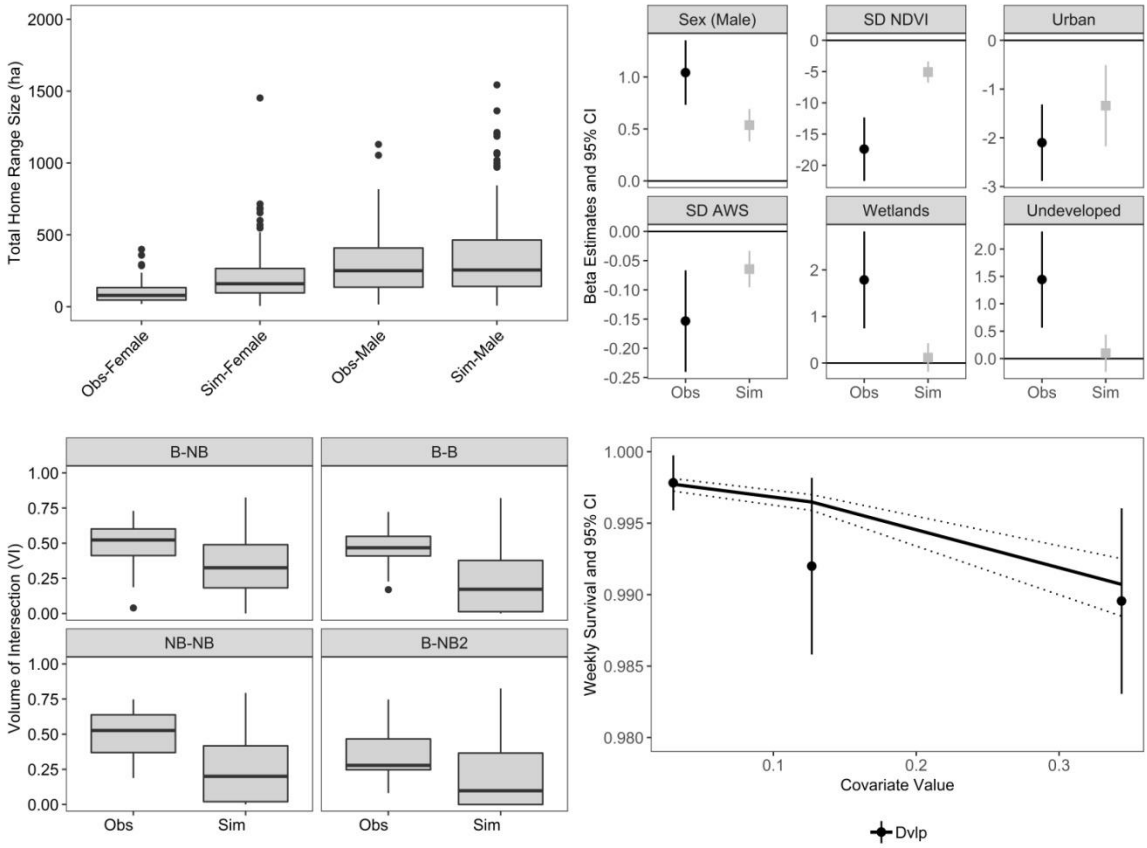

3.3.2. Model Application

Simulated EIS occupancy, defined as at least one male and one female, of 322 ha plots was 56%. Of the 13 covariates used to model simulated occupancy, the characteristic scale for 10 of those covariates was at the largest scale we considered

(3,077 m). Three covariates, urban, undeveloped upland, and SD NDVI, had the strongest influence on simulated EIS occupancy with parameter weights ≥ 0.97 and model-averaged 95% CI that excluded zero (Table 3.1). Occupancy was positively associated with undeveloped upland and negatively associated with urban and SD NDVI (Fig. 3.4). While conservation lands did not strongly influence simulated EIS occupancy and high-occupancy areas were present outside of conservation lands, model-average predicted occupancy was consistently higher on conservation lands (Fig. 3.5). Model-averaged predicted occupancy was significantly higher on plots partially or completely overlapping conservation lands than on plots not overlapping conservation lands ($P < 0.0001$). Urban was significantly lower on plots partially or completely overlapping conservation lands ($P \leq 0.0057$) while upland was significantly greater on plots partially or completely overlapping conservation lands ($P < 0.0001$). SD NDVI was significantly lower on plots completely overlapping conservation lands compared to plots not overlapping conservation lands ($P < 0.0001$) but plots partially overlapping conservation lands had significantly higher SD NDVI than plots not overlapping conservation lands ($P = 0.0118$). Our map of predicted occupancy of 322 ha plots for our study area showed lower occupancy along the more developed portions of the LWR (Fig. 3.6).

Table 3.1. Model-averaged *z*-score standardized beta estimates, 95% CI, and AIC_c parameter weights (*w*) for the effects of landscape covariates on simulated EIS occupancy of 322 ha plots across the southern LWR.

Covariate	Betas	95% CI	*w*
Urban	-0.82	-1.08 - -0.56	1.00
Upland	0.28	0.12 - 0.44	0.99
SD NDVI	-0.26	-0.43 - -0.09	0.97
SD AWS	0.04	-0.10 - 0.18	0.43
Cons Lands	0.04	-0.10 - 0.18	0.42
NDVI	0.03	-0.08 - 0.14	0.37
Citrus	-0.02	-0.13 - 0.09	0.36
Wetlands	0.02	-0.09 - 0.13	0.34
AWS	0.02	-0.09 - 0.13	0.33
Wetland Edge	0.00	-0.08 - 0.08	0.27

Figure 3.4. Model-averaged predicted relationships between simulated EIS occupancy of 322 ha plots and the top supported landscape covariates. Solid lines represent model-averaged predicted occupancy and dashed lines are model-averaged 95% CI. Different line colors represent different proportions of conservation lands in a 3,077 m buffer centered on the plot centroid. All other covariates were held constant at their mean value.

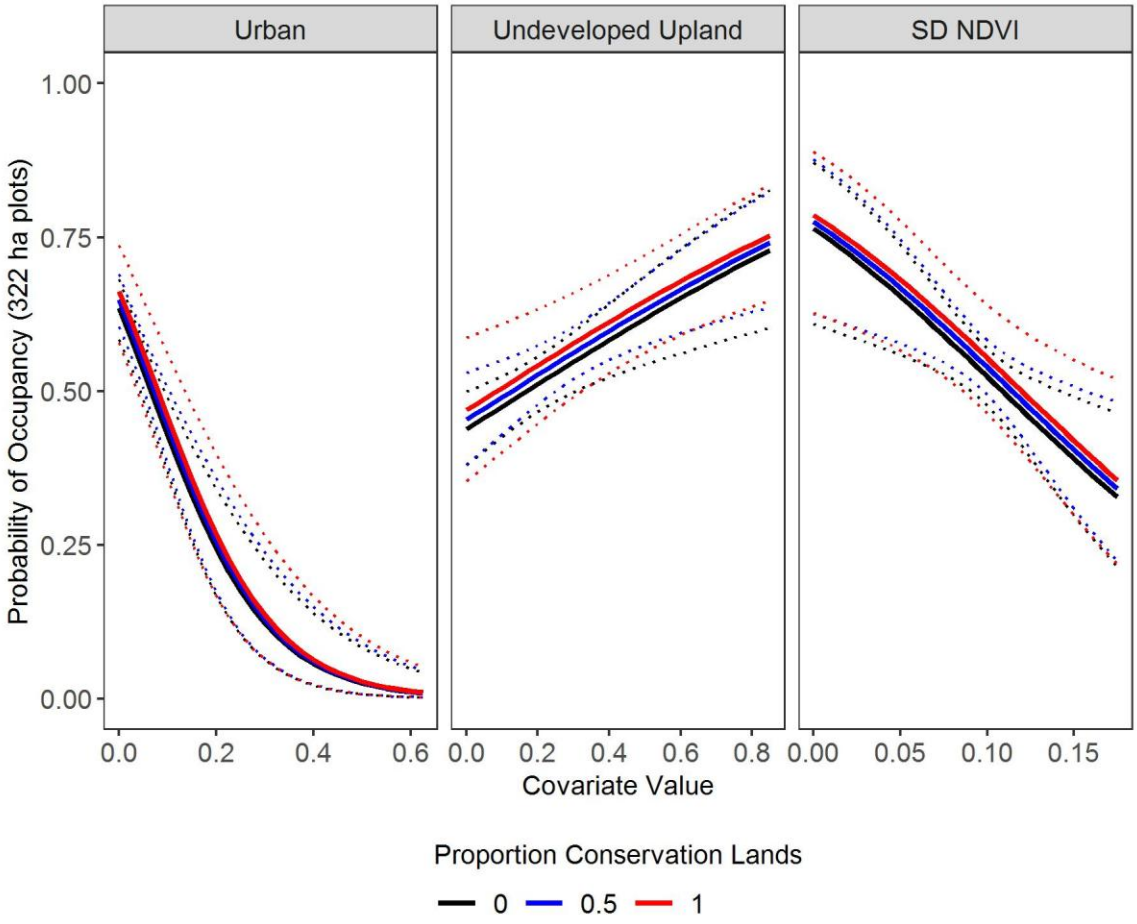

Figure 3.5. Relationships between simulated EIS occupancy, landscape covariates, and conservation lands. The top left panel shows the relationship between model-averaged predicted occupancy for all 999 random 322 ha plots as a function of the proportion of the plot overlapping conservation lands. The other three panels show the distribution of landscape covariate values for plots not overlapping (No), partially overlapping (Inter), and completely overlapping (Yes) conservation lands.

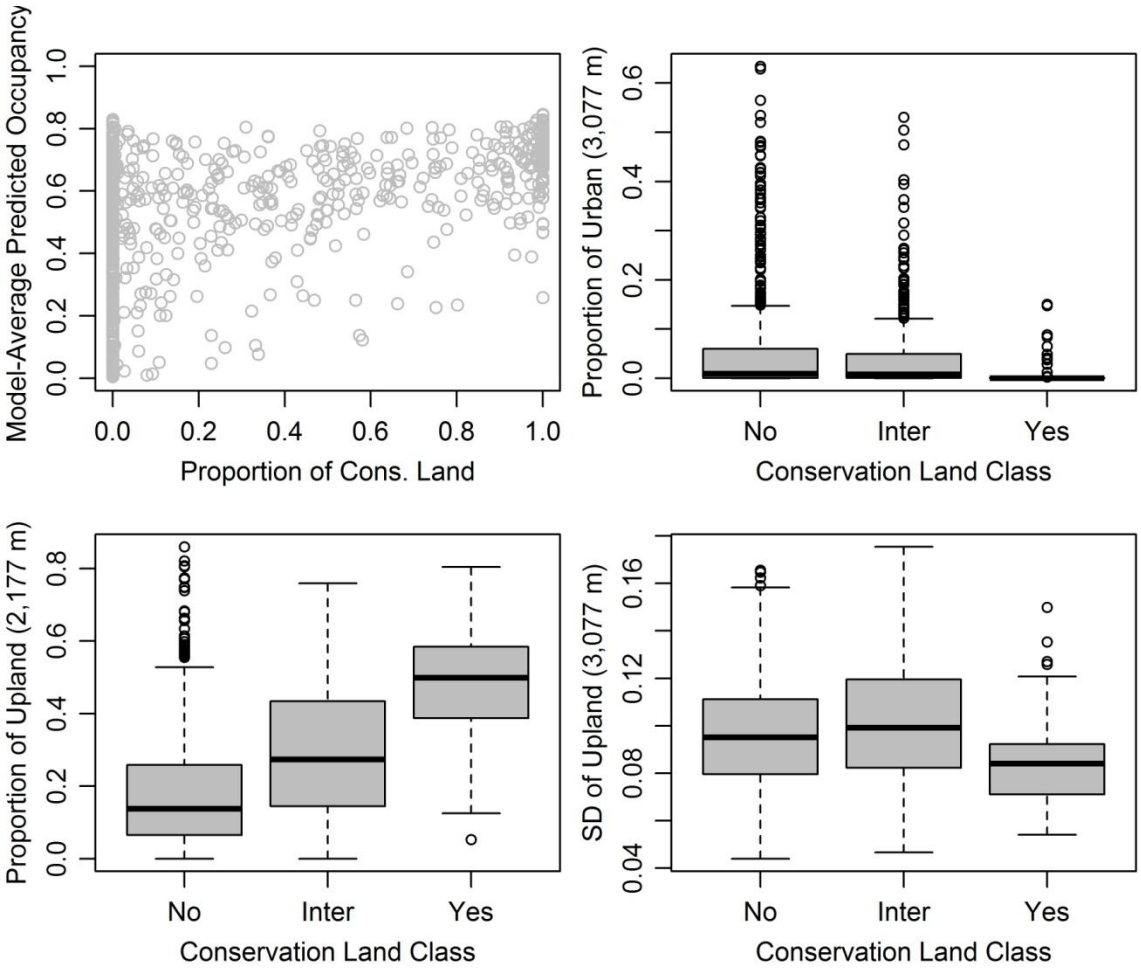

Figure 3.6. Model-averaged predicted occupancy of 322 ha plots for the Lake Wales Ridge study area. Primary, secondary, and tertiary roads are shown for reference.

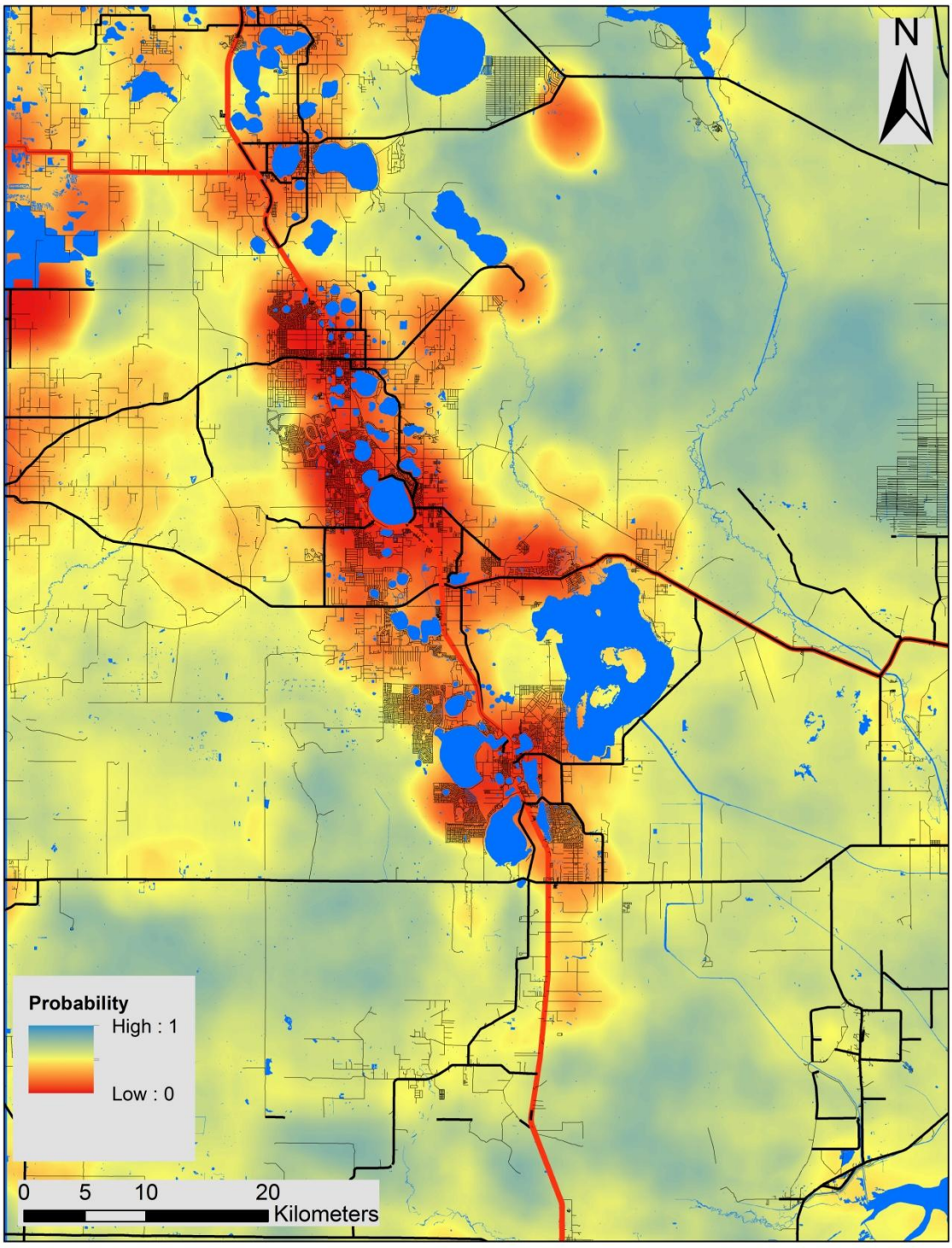

Occupancy and persistence of conservation lands showed a strong relationship with conservation land size while the strength of this relationship varied depending on our occupancy criterion (Fig. 3.7). For our analyses allowing re-colonization, the minimum sizes of conservation lands needed for 12 years of occupancy were 1,700 ha (1 pair with 50% overlap), 3,200 ha (1 pair with 95% overlap), 4,100 ha (5 pairs with 50% overlap), and 8,500 ha (5 pairs with 95% overlap). For our analyses not allowing re-colonization, the minimum sizes of conservation lands needed for EIS to persist all 12 years were 2,600 ha (1 pair with 50% overlap), 4,300 ha (1 pair with 95% overlap), 3,900 ha (5 pairs with 50% overlap), and 5,000 ha (5 pairs with 95% overlap). The median sizes of conservation lands where EIS persisted all 12 years were 3,482 ha (1 pair with 50% overlap), 10,795 ha (1 pair with 95% overlap), 11,508 ha (5 pairs with 50% overlap), and 16,792 ha (5 pairs with 95% overlap).

Figure 3.7. Relationships between simulated EIS occupancy/persistence and size of conservation lands for four different criteria of occupancy. The left panel shows the predicted proportion of years occupied for the final 12 years of a 15-year model run and assumes re-colonization. The right panel shows the predicted probability of persisting for all of the final 12 years and assumes no re-colonization after a conservation land goes extinct.

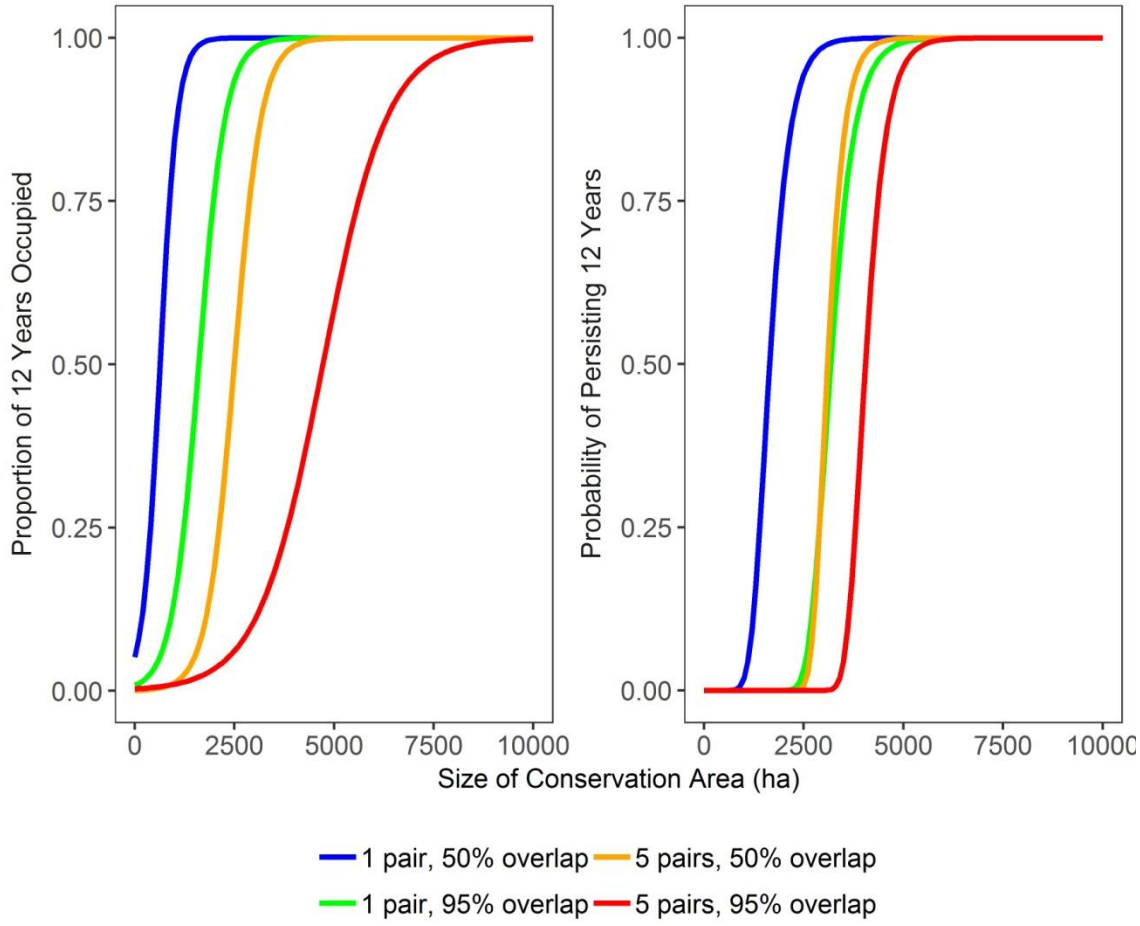

3.4. Discussion

3.4.1. Model Calibration

Our ABM builds upon previous population modeling studies for EIS (Breininger et al. 2004; Hyslop et al. 2012) by incorporating variation in individual-level traits and behaviors in a spatially explicit manner. This feature is important given the influence of landscape context on EIS home range size and survival (Breininger et al. 2011; Breininger et al. 2012). Accurately incorporating these landscape influences is important for understanding spatially explicit population dynamics for several reasons. First, spatial variation in survival directly determines spatial variation in population viability. Second, spatial variation in home range size combined with low levels of conspecific overlap directly determines population density within a given area. While it is unclear how same-sex conspecific overlap varies according to landscape development (Bauder et al. 2016b), assuming a constant home range across a range of landscape development intensities could underestimate density in more developed landscapes. This assumption would also reduce population viability in small patches of natural habitat because home ranges would be larger and road/urban crossing rate higher than expected given the landscape context which would lead to greater mortality risk. Our model therefore adds to a growing body of research using ABM to address questions related to population viability.

Using a POM approach, we were able to identify combinations of unknown parameters that produced simulated patterns of movement and survival approximating patterns from our observed data. However, among the patterns used to calibrate our model there was variation in the degree to which those patterns were approximated.

While we were able to reproduce a significant negative relationship between total home range size and SD NDVI and urban, as well as a significant effect of sex with larger male home range sizes, this required increasing the maximum resistance of roads to relatively high values. Because most urbanized areas of our calibration landscapes also had high road densities this effectively gave urban areas a higher resistance than the surrounding landscapes. This indicates that our background resistance surface, which was derived from a within-home range RSS, was a poor representation of resistance to individual movements. We suspect this is the case because avoided habitats may not necessarily have high resistance to movement. For example, wetlands were generally avoided but observed total home ranges were larger in landscapes with more wetlands. This may suggest that EIS are capable of moving through wetlands even if they do not selectively use wetlands. A more ideal approach to estimating a resistance surface for simulating within-home range movements might have been a path selection function wherein landscape features traversed across observed movement steps are compared to those from random steps (Zeller et al. 2012). However, our telemetry points were collected on average at 2–7 day intervals which makes the assumption of straight-lined movement between consecutive telemetry locations very tenuous. Additionally, we assumed a linear inverse relationship between habitat suitability and resistance which other studies may not be appropriate (Keeley et al. 2016; Zeller et al. 2018). An alternative approach was used by Watkins et al. (2015) in an ABM for jaguars (*Panthera onca*) where they used separate expert opinion-based estimates of habitat quality (i.e., food availability) and resistance. Researchers could also use a POM directly to calibrate resistances surfaces.

While increasing maximum roads resistance clearly improved our model's ability to simulate EIS home ranges, increasing the maximum roads resistance has the potential to reduce road crossing rates and therefore reduce the number of simulated road mortalities which could in turn overestimate survival of agents in more developed landscapes. However, this did not appear to be the case as we were able to identify parameter values for daily road/urban crossing survival that resulted in weekly survival estimates in our simulated data that were similar to observed weekly survival estimates for EIS in our least- and most-developed landscapes. Interestingly, our simulated data more closely approximated the relationship between survival and urban and development than the relationship between survival and roads. This may be an artifact of the high roads resistance layer which may have led to fewer than expected road crossings thereby allowing urban to be the primary driver of mortality in our ABM.

Our model was unable to reproduce the observed levels of within-individual seasonal home range overlap which suggests that simulated agents displayed a lower degree of home range fidelity than we observed in our telemetry data. This may have contributed to the larger than expected female total home ranges in our simulated data. We suspect our model's inability to reproduce within-individual home range overlap is due to the lack of an explicit mechanism for simulating home range fidelity. Rather, our model relies on the avoidance of same-sex conspecifics and the presence of a population at or near carrying capacity to constrain the movements of individuals over long temporal scales (e.g., months and years). Other ABM simulating animal home ranges rely on a resource- and/or mate-acquisition approach for generating realistic patterns of movement and home range size (Carter and Finn 1999; Wang and Grimm 2007; Malishev et al.

2018). For example, Carter et al. (2015) developed an ABM for simulating male and female tiger home ranges where within-sex home range overlap was low but male home ranges contained multiple female home ranges. Each landscape cell was assigned a resource value (prey biomass) and females sought to include sufficient pixels within their home range to reach a threshold of prey acquisition. Males then established and updated their home ranges so as to overlap the home ranges of multiple females. Under such an approach stable home ranges are possible because individuals only move beyond their home ranges if their home range no longer contains sufficient resources (e.g., through depletion or exclusion by competitors). We opted not to pursue a resource-acquisition approach in our ABM because data on EIS food intake rates, energy requirements, metabolic costs, and prey availability are unavailable although such parameters could potentially be evaluated through POM.

3.4.2. Effect of Landscape Features on Long-term EIS Occupancy

At the end of our 15 year model application run on the LWR study area EIS were present throughout our study area and all conservation lands ≥ 250 ha were occupied by 50–295 individuals during the last 18-months of model simulation. While our moderate occupancy levels suggest that much of our study area is capable of supporting EIS for at least 15 years, this also indicates that substantial portions of our study area did not support EIS for the entire simulation. EIS occupancy was most strongly influenced by the three landscape covariates that also most strongly influenced multi-level EIS habitat selection (Bauder et al. 2018). In particular, urban had the strongest effect on simulated EIS occupancy and this effect was strongest at a very broad scale (3,077 m) suggesting

that the long-term presence of EIS within an area the size of a median conservation land is affected by processes operating far beyond the boundaries of that conservation land. While the amount of conservation land surrounding the plot did not strongly influence occupancy, plots on conservation lands had more consistently higher predicted occupancy values than plots partially or not overlapping conservation lands. This indicates that while substantial potential EIS habitat occurs outside of the current network of conservation lands along the LWR, the existing network nevertheless does represent an important contribution towards EIS conservation.

Our analysis of EIS occupancy and persistence on conservation lands indicates that substantial tracts of relatively undeveloped land are required to support EIS for a relatively short period of time as the 12 years of simulated data we use approximates the life span of an EIS. As expected, the more stringent our occupancy criteria (i.e., more pairs with higher levels of overlap), the larger an area had to be to be occupied for the entire simulation period. Our simulation study provides the first empirical estimates of minimum reserve size for EIS. Moler (1992) recommended that EIS conservation focus on protecting large tracts of conservation land and suggested 1,000 ha as a minimum threshold while the U.S. Fish and Wildlife Service suggested 10,000 ha (2008). While both of these estimates appeared to lack strong empirical justification, our results suggest that 1,000 ha is too small to support even a single pair of EIS. In their PVA, Breininger et al. (2004) did not report the spatial extents of viable populations but did report that quasi-extinction (i.e., < 10 adults and subadults) occurred in many potential reserves. Using our occupancy criterion of five pairs with ≥90% overlap, our results suggest that 5,000–9,000 ha may be required to maintain EIS. Combined with our observation that the median

sizes of conservation lands occupied for all 12 years of our simulation were >10,000, our results suggest that the larger estimate provided by the U.S. Fish and Wildlife Service is more beneficial for EIS conservation. Because we used existing conservation lands for our analyses, our results do not apply to conservation lands in isolation because many conservation lands abutted other conservation lands or unprotected areas of otherwise suitable habitat. However, our persistence analysis assumes no re-colonization following extinction which is approximates completely isolated conservation lands.

3.4.3. Scope and Limitations

We acknowledge several potential limitations to our model which pertain to inferences made using our simulated data. The reliability of absolute predictions (e.g., change in population size) from population models are strongly dependent upon the accuracy and precision of life history parameter estimates (Beissinger and Westphal 1998; Brook et al. 2000; Coulson et al. 2001). Many of our model parameter values had high uncertainties or lacked empirical estimates, particularly with regards to juvenile movement and survival. Data on wild pre-adult EIS are scarce as is the case with most snake species (Parker and Plummer 1987; Shine and Bonnet 2009). However, Hyslop et al. (2012) found that predicted EIS population growth rate from a stage-transition matrix model was relatively insensitive to pre-adult survival, clutch size, nesting success, and breeding probability. Species with high adult survival, late-maturation, low fidelity, and high longevity are generally more sensitive to changes in adult survival than reproductive output (Oli and Dobson 2003; Tack et al. 2017). This trend has been observed in other snake species (Webb et al. 2002; Gregory 2009). However, we acknowledge the

uncertainty of our survival estimates and particularly in the shape and magnitude of the relationship between survival and continuous landscape covariates. An additional limitation is that we do not know the trajectories of the populations from which our observed data were collected. If our IBM was calibrated to data from a declining population our IBM would assume stable parameter values over time which might in turn lead to an overestimation of the simulated population's trajectory.

Our inferences regarding landscape effects on EIS occupancy and persistence are likewise conditional upon the parameter values and assumptions within our IBM. An arguably more ideal approach to evaluating landscape effects on EIS occupancy would be to measure occupancy directly in the field. However, EIS within peninsular Florida are extremely difficult to detect and existing occurrence records are likely biased towards areas of high field use or accessibility (e.g., with road access). Our use of an IBM therefore provides a way to measure occupancy as a result of dynamic population processes with perfect detection. This approach is arguably more informative for EIS conservation than using habitat suitability models because the latter do not incorporate demographic processes. For example, a comparison between our predicted resource selection surfaces (Chapter 2) and our predicted occupancy map (Fig. 3.6) showed that, while relative probabilities of selection could be high within developed landscapes occupancy of these areas was low. This highlights the importance of incorporating habitat selection data with demographic data when evaluating long-term occupancy or persistence.

CHAPTER 4

LANDSCAPE GENETICS OF EASTERN INDIGO SNAKES ALONG THE SOUTHERN LAKE WALES RIDGE OF CENTRAL FLORIDA

4.1. Introduction

Anthropogenic landscape changes are widely recognized as leading causes of species imperilment (Fischer and Lindenmayer 2000). In addition to reducing population viability through direct habitat loss, anthropogenic landscape changes often fragment and isolate populations (Fahrig 2003; Villard and Metzger 2014) which can in turn inhibit dispersal and reduce genetic connectivity (i.e., gene flow, Lowe and Allendorf 2010) among habitats and populations (Epps et al. 2005; Proctor et al. 2005; Clark et al. 2010). While limited gene flow may be maladaptive in some circumstances (e.g., in facilitating local adaptation, Frankham et al. 2011; Richardson et al. 2016), it is widely recognized that gene flow is beneficial under many circumstances for reducing the effects of genetic drift and inbreeding depression while maintaining future adaptive potential (Keller and Waller 2002; Hogg et al. 2006; Sexton et al. 2011). It is therefore important to understand the impacts of anthropogenic landscape features on genetic connectivity to aid in the implementation of mitigation strategies (Keller et al. 2015) and identification of potential barriers and corridors (Epps et al. 2007; Cushman et al. 2009; Zeller et al. 2017). However, species' responses to particular landscape features with regards to genetic connectivity can vary widely among taxa and landscapes (e.g., Short-Bull et al. 2011;

Balkenhol et al. 2013; Trumbo et al. 2013), highlighting the importance of species- and landscape-specific analyses.

Landscape genetics provides a conceptual and analytical framework for understanding landscape effects on genetic connectivity (Manel et al. 2003; Storfer et al. 2007). Landscape genetics analyses predominately involve three broad steps: 1) describing the genetic similarity (i.e., genetic distance) between individuals or populations, 2) describing the landscape distance (Shirk et al. 2018) between sampling units as a function of the degree to which one or more landscape feature is hypothesized to influence genetic distance, and 3) statistically relating genetic distance to landscape distance to identify the most influential landscape features driving the genetic-landscape signal (Balkenhol et al. 2016). Hypothesized effects of landscape features are often represented using resistance surfaces where landscape features (e.g., land cover, elevation) are assigned resistance values such that higher values represent a greater impediment to multi-generational gene flow (Spear et al. 2010). The relationship between the original landscape feature and resistance values may take on a variety of functional forms (e.g., linear, monomolecular, power, Peterman et al. 2014) which allow the modeling of non-linear relationships and detection of threshold effects (Keller et al. 2015). Landscape distance (i.e., cost or resistance distance) is then measured using the cumulative cost along one or more potential paths between genetic samples (i.e., isolation by resistance, Adriaensen et al. 2003; McRae 2006; McRae et al. 2008).

Because the correct resistance values and functional form are unknown, parameterizing resistance surfaces is a central issue in landscape genetics (Spear et al. 2010; Zeller et al. 2012; Spear et al. 2016). Many studies use expert opinion or previous

research to select a limit number of resistance surfaces representing different landscape features, resistance values, and/or functional forms which are then statistically evaluated against genetic data (Zeller et al. 2012; Spear et al. 2016). In some cases, predicted surfaces from habitat or species distribution models may be directly converted into resistance surfaces (e.g., Shafer et al. 2012; Weckworth et al. 2013; Mateo-Sanchez et al. 2015a). Resistance values or functional forms may be iteratively varied in univariate or multivariate space to identify optimal values (e.g., Cushman et al. 2006; Shirk et al. 2010; Wasserman et al. 2010; Castillo et al. 2014; Row et al. 2015). However, iteratively examining the complete parameter space for multiple resistance surfaces quickly becomes computationally intractable although a few studies have conducted partial optimizations with ≤ 4 surfaces over relatively large parameter spaces (Wang et al. 2009; Shirk et al. 2010). Fortunately, recent developments now allow for the formal optimization of multiple resistance surfaces, including the range of resistance values and their functional transformations, directly from the genetics data (Peterman et al. 2014; Peterman 2018).

Ecological patterns and processes can vary markedly depending on the spatio-temporal scale (i.e., grain or extent, Turner and Gardner 2015) of analysis (Wiens 1989; Levin 1992; Martin et al. 2016) and multiple studies have documented varying scale-specific effects of landscape features on animal movements and habitat selection (Thompson and McGarigal 2002; Boyce et al. 2003; Leblond et al. 2011; Zeller et al. 2016). However, the role of scale, particularly spatial scale, has received comparatively little attention in landscape genetics studies (Balkenhol et al. 2009; Anderson et al. 2010; Segelbacher et al. 2010; Jaquiery et al. 2011). Inferences regarding landscape effects on

genetic connectivity will be most reliable when the scale at which landscape features are measured (scale of analysis *sensu* Dungan et al. 2002) corresponds to the scale at which genetic connectivity responds to those features (scale of phenomenon sensu Dungan et al. 2002; Anderson et al. 2010; Galpern and Manseau 2013). Previous studies have used a variety of approaches to evaluate scale-specific landscape-genetic signals including variable-width transects between pair-wise genetic locations (Murphy et al. 2010; Emaresi et al. 2011; van Strien et al. 2014; Villemey et al. 2016), scale-specific functional transformations (Shirk et al. 2010; Wasserman et al. 2010; Castillo et al. 2014), sampling at hierarchically nested spatial scales (Millette and Keyghobadi 2014), subsampling points within pre-specified distance bins (Angelone et al. 2011; Keller et al. 2013), hierarchical Bayesian models (Coster et al. 2015), and patch-based landscape graphs (Galpern et al. 2012b). However, previous studies have generally included variables measured at a single scale within the same statistical model or measured a subset of landscape features at multiple scales. Moreover, transect-based approaches restrict inter-sample cost distances to a single linear feature and although Keller et al. (2013) used least-cost transect analysis to circumvent these shortcomings.

An alternative approach is to define the landscape surfaces in terms of ecological neighborhoods (Addicott et al. 1987) so that a single pixel conveys information about its surrounding pixels. This is analogous to varying the grain of the analysis (sensu Anderson et al. 2010; Zeller et al. 2012). Neighborhoods can be represent using kernels (e.g., Uniform or Gaussian, Row et al. 2015; Winiarski et al. In review-b) or by aggregating the original surface pixels into larger pixels (Cushman and Landguth 2010; Galpern et al. 2012b; Milanesi et al. 2017a; Milanesi et al. 2017b). Landscape distances

can then be measured at multiple scales and used to fit multi-variable, multi-scale models. Previous studies have used pseudo-optimization approaches the best scale is selected for each covariate in isolation and then covariates are combined into multi-variable, multi-scale models (Row et al. 2015; Zeller et al. 2017). Because the optimal scale may differ between single- and multi-variable models, a more ideal approach is to simultaneously optimize multiple resistance surfaces at different spatial scales. This approach was used by Winiarski et al. (In review-b) for two species of sympatric pond-breeding salamander who found that simultaneously optimized multi-scale surfaces outperformed multi-scale surfaces derived using pseudo-optimization.

Because gene flow is ultimately driven by the movements of individuals, landscape factors influencing individual movements and habitat selection may also influence genetic connectivity (Chetkiewicz et al. 2006). As a result, many studies have used predicted surfaces from habitat or species distribution models to create resistance surfaces for landscape genetics analyses (Zeller et al. 2012; Spear et al. 2016). However, habitat selection is an individual-level process whereas genetic connectivity is the manifestation of movement and successful reproduction over multiple generations. Genetic connectivity is generally driven by dispersal whereas habitat selection studies primarily examine selection at or within the level of a home range (Spear et al. 2016). Landscape features with high permeability may facilitate dispersal without providing the resources for home range establishment and reproduction. These factors may lead to discordant results between habitat selection and landscape genetic studies (Wasserman et al. 2010; Geisler et al. 2013; Reding et al. 2013; Mateo-Sanchez et al. 2015; Roffler et al. 2016). However, some studies have found that resistance surfaces from habitat selection

models may correlate well with genetic diversity (Shafer et al. 2012; Weckworth et al. 2013) or that features influencing movement also influence genetic connectivity (Cushman et al. 2006; Cushman and Lewis 2010). Because movement, habitat selection, and genetic connectivity may all have multiple scales of phenomenon (Dungan et al. 2002), it is important to incorporate multi-scale analyses when comparing landscape factors influencing these processes.

In this study, we use a recently developed optimization approach (Peterman et al. 2014; Peterman 2018) to evaluate the multi-scale influences of landscape features on genetic connectivity of a large-bodied, imperiled, terrestrial snake, the eastern indigo snake (*Drymarchon couperi*, hereafter EIS). This approach uses genetic algorithms (Scrucca 2013) and linear mixed-effects models (Clarke et al. 2002; van Strien et al. 2012) to simultaneously optimize the resistance values and functional transformations of one or more resistance surfaces. Winiarski et al. (Winiarski et al. In review-a) found that this multi-surface optimization correctly returned the true resistance surface even with correlation among landscape features. Multiple landscape features represented at different spatial scales can therefore be simultaneously optimized within a single optimization procedure. This may be important as the optimal univariate scale for a landscape feature may differ from its multi-variable optimal scale, particularly if the correlation between landscape features increases with spatial scale.

Our first objective was to evaluate hypothesized relationships between natural and anthropogenic landscape features at different spatial scales (i.e., grain sizes, Anderson et al. 2010; Zeller et al. 2012), represented by kernel-smoothed surfaces, in a multi-variable optimization. We predicted that multi-variable, multi-scale surfaces would outperform

single-variable models and multi-variable, single-scale models. Our second objective was to compare the performance of resistance surfaces derived directly from landscape features with those derived from multi-scale resource selection functions (RSF, Bauder et al. 2018) estimated at different orders or levels of selection (Johnson 1980; McGarigal et al. 2016). We predicted greater support for resistance surfaces from RSFs derived at higher levels of selection (i.e., home range selection) compared to those derived from RSFs at lower levels of selection (i.e., within home range selection). Male EIS actively search for females during the breeding season (Bauder et al. 2016a) so we also predicted that RSF surfaces for males during the breeding season would have the strongest association with genetic distance. Our third objective was to use our RSF surfaces and optimized resistance surfaces to determine the degree to which existing conservation lands facilitate EIS genetic connectivity (Cushman et al. 2009; Zeller et al. 2017) and to combine spatially-explicit estimates of EIS habitat selection (Chapter 2), occupancy (Chapter 3), and genetic connectivity to provide a spatially-explicit index of EIS conservation value. Finally, we estimated the spatial scale(s) of genetic autocorrelation across all samples and for males and females to test for evidence of sex-biased dispersal.

4.2. Methods

4.2.1. Study Species

The EIS is native to the southeastern Coastal Plain of the United States and has undergone substantial declines with robust populations persisting in southern Georgia and peninsular Florida (Enge et al. 2013) and on-going reintroduction efforts in southern

Alabama and the Florida Panhandle (Godwin et al. 2011). These declines were largely due to habitat loss, fragmentation, and degradation (U. S. Fish and Wildlife Service 1978, 2008). While previous studies have described historical range-wide patterns of genetic structure (Krysko et al. 2016; Folt et al. In review) little is known about how landscape features influence contemporary EIS genetic connectivity. EIS are large-bodied (> 2 m), active-foragers (> 1 km daily movements) with large home ranges (> 500 ha) and year-round surface activity in peninsular Florida (Breininger et al. 2011; Hyslop et al. 2014; Bauder et al. 2016a). Within peninsular Florida, males maintain larger home ranges than females, show little intra-sex home range overlap, and increase the frequency and extent of their movements to locate females during the September–March breeding season (Breininger et al. 2011; Bauder et al. 2016a, b). EIS select undeveloped terrestrial habitats and avoid urban habitats at multiple spatial scales (Bauder et al. 2018) suggesting that large tracts of terrestrial habitats are necessary for viable population (Moler 1992; Breininger et al. 2004). However, EIS in peninsular Florida will utilize a variety of anthropogenc habitats including urban and rural developments, pasture, and citrus (Breininger et al. 2011; Enge et al. 2013; Bauder et al. 2018). While such habitats may permit genetic exchange among otherwise suitable habitats, EIS in developed landscapes are at increased risk of road mortality (Breininger et al. 2012). As with many snake taxa (Parker and Plummer 1987), virtually nothing is known about EIS dispersal or how age and sex influence genetic connectivity although a 22.2 km inter-population dispersal event was documented in southern Georgia (Stevenson and Hyslop 2010). However, the presence male mate-searching movements suggest that adult males may be important

facilitators of genetic connectivity (Rivera et al. 2006; Keogh et al. 2007; Clark et al. 2008).

4.2.2. Study Area

We collected our samples across an approximately 50 × 20 km area encompassing approximately the southern third of the Lake Wales Ridge (LWR, Fig. 4.1) which has consistently produced EIS observations over the past 40 years and likely represents an important region for EIS conservation (Enge et al. 2013). The LWR is a linear topographic feature running approximately 186 km north-south through central peninsular Florida with an average width of 11.7 km and maximum elevation of 64–95 m (White 1970; Weekley et al. 2008). The LWR historically was dominated by xeric, fire-adapted scrub and sandhill communities supplemented by scrubby flatwoods, mesic flatwoods, and seasonal forested and non-forested wetlands (Abrahamson et al. 1984; Myers and Ewel 1990; Weekley et al. 2008). Lakes are widespread throughout the ridge. Due to its antiquity and unique habitats, the LWR supports a high degree of plant and animal endemism (Christman 1988; Muller et al. 1989; Myers 1990). However, the LWR has lost approximately 78–85% of its original habitat from conversions to urban, citrus, and pasture (Turner et al. 2006b, a; Weekley et al. 2008; Swain and Martin 2014) and supports a high proportion of imperiled taxa (Dobson et al. 1997). The LWR has been the focus of substantial habitat prioritization and conservation efforts (Hoctor et al. 2010; Florida Department of Environmental Protection 2017) resulting in a relatively extensive network of conservation lands (Turner et al. 2006b; Swain and Martin 2014). While many conservation areas were designated for scrub-dependent species or large

mammalian carnivores (Hoctor et al. 2010; Florida Department of Environmental Protection 2017), these lands likely benefit EIS by protected terrestrial upland habitats (Bauder et al. 2018). A spatially-explicit understanding of EIS genetic connectivity along the LWR therefore represents a timely contribution to regional conservation efforts.

Current landscape conditions within our study area include the aforementioned natural habitats as well as a range of rural and urban development intensities, citrus, improved and unimproved cattle pasture, and agriculture. Many large cattle ranches in the area provide large contiguous blocks of relatively undeveloped habitat.

Figure 4.1. Map of our landscape genetic study area along the southern Lake Wales Ridge in Highlands County, Florida. Triangles represent samples collected from the Archbold Biological Station (ABS) while circles represent all other samples. The insert map shows the location of the Lake Wales Ridge (following Weekley et al. 2008) and our study area in relation to peninsular Florida while the primary map shows the location of samples used in our analyses.

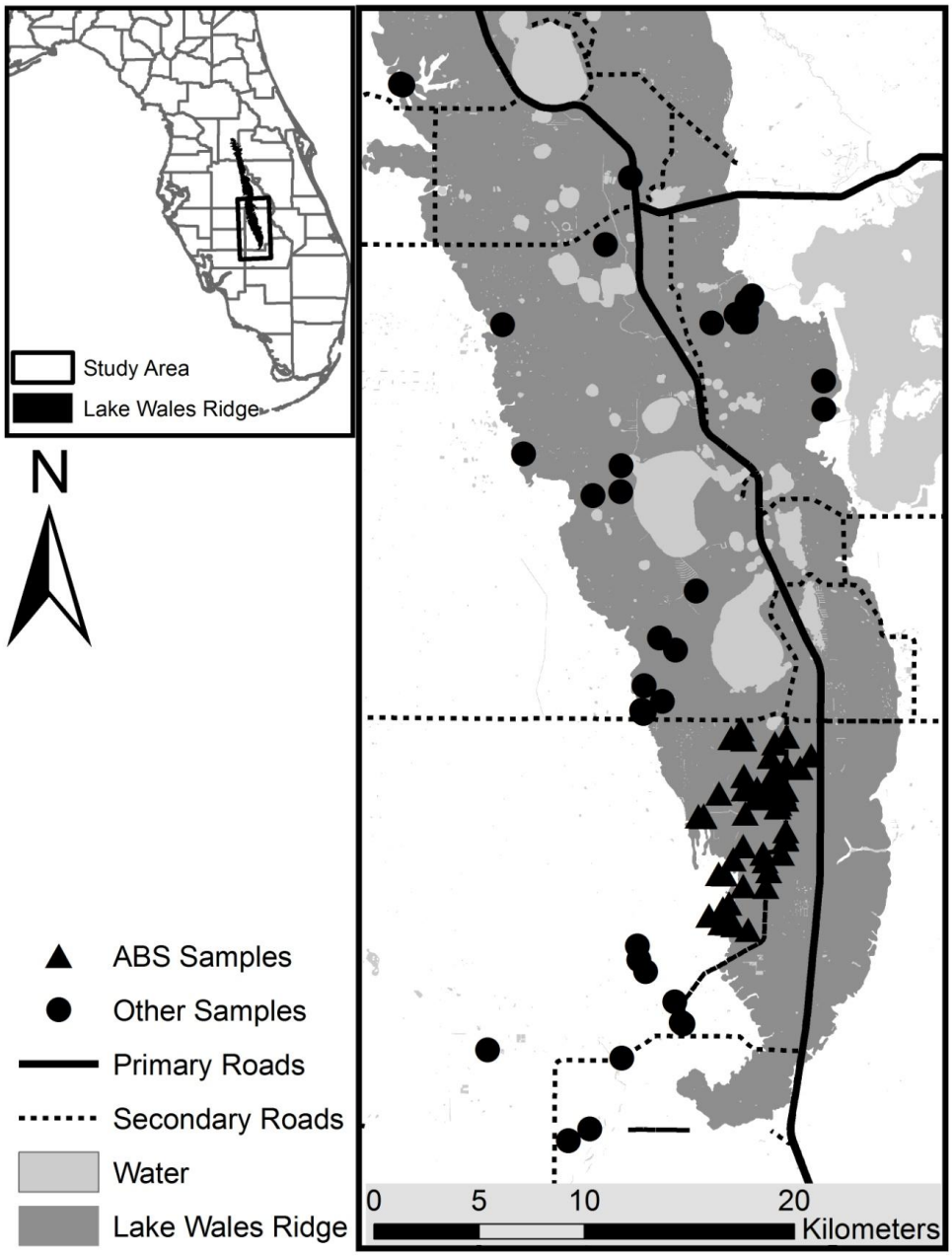

4.2.3. Sample Collection and Laboratory Methods

We collected EIS tissue samples (scale clips or shed skins) between 2010 and 2014 throughout our study area. Most samples were collected during a radio telemetry study wherein 90% of captures were opportunistic although some individuals were captured while road-cruising and during visual surveys around gopher tortoise (*Gopherus polyphemus*) burrows (Bauder and Barnhart 2014). Although we attempted to collect samples uniformly across our study area, extremely low detection rates meant that samples were often clustered in areas with greater field effort or areas with radio-tracked individuals. Additionally samples, particularly road-killed individuals, were collected by authorized project partners.

We sent samples to the University of Idaho's Laboratory for Ecological, Evolutionary, and Conservation Genetics for processing. We extracted DNA using the Oiagen DNeasy blood and tissue extraction kit and genotyped individuals at 15 microsatellite loci (Shamblin et al. 2011) using Genemapper software. Many samples did not amplify at all 15 loci so we re-ran select samples to verify questionable genotypes. We retained samples that amplified at ≥ 13 loci. Because some of our samples were from shed skins from individuals with unknown identity, we used CERVUS v.3.0.3 (Kalinowski et al. 2007) and the R (v. 3.4.2, R Core Team 2017) package ALLELEMATCH (v. 2.5, Galpern et al. 2012a) to test for potential duplicate samples after excluding loci with ≥10% null alleles. In CERVUS, we set the number of mismatching loci to five and the minimum number of loci needed for a match to three. CERVUS identified 18 pairs of potential duplicates. We used the *amUniqueProfile* function in ALLELEMATCH to select the optimal number of mismatching loci which was eight. ALLELEMATCH selected 13

clusters including 32 samples. All samples identified by CERVUS were also identified by ALLELEMATCH and all samples amplified all retained loci. After excluding scale clips from confirmed different individuals, six shed skin samples remained that were classified as potential duplicates. We excluded five of these shed skin samples but retained the sixth because it was 22.5 km from its putative duplicate samples.

4.2.4. Genetic Analyses

We calculated the proportion of null alleles per locus using MICRO-CHECKER v. 2.2.3 and the Brookfield 1 method (Van Oosterhout et al. 2004) and retained loci with < 10% null alleles. We tested for genotypic disequilibrium between all pairs of loci using GENEPOP (v. 4.2.1, Rousset 2008). We tested each locus for deviations Hardy-Weinberg proportions (HWP) using the *hw.test* function in the PEGAS package (v. 0.10, Paradis 2010), calculated F_{IS} using the *F.stat* function in the DEMELERATE package (v. 0.9-3, Kraemer and Gerlach 2017), calculated number of alleles, observed and expected heterozygosity using the *df2genind* function in the ADEGENET package (v. 2.1.1, Jombart 2008), and calculated allelic richness using the *allel.rich* function in the POPGENREPORT package (v. 3.0.0, Adamack and Gruber 2014). We tested the significance of deviations from HWP and F_{IS} using sequential Bonferroni corrections with $\alpha = 0.05$ (Holm 1979). While conformity to HWP is not required when calculating genetic distance based on mathematical dissimilarity between genotypes (Shirk et al. 2017), understanding causes of nonconformity may elucidate causes of underlying genetic structure including population (i.e., a Wahlund effect) or family structure (Allendorf et al. 2013). We therefore tested for deviations from HWP and calculated F_{IS} for individuals on the

Archbold Biological Station (ABS, Fig. 1) and the rest of the study area. We tested for isolation-by-distance (IBD) across all samples, samples from ABS, and samples outside of ABS by modeling genetic distance (see below) against Euclidean distance using linear-mixed effects models with maximum-likelihood population-effects (MLPE) (Clarke et al. 2002; van Strien et al. 2012) using the LME4 package (v. 1.1-17, Bates et al. 2014). We also report the Mantel *r* (Mantel 1967) and its exact *p* value calculated with 10,000 permutations using the *mantel* function in the VEGAN package for comparison with other studies.

4.2.5. Genetic Distance

We calculated an individual-based genetic distance using principle components (PC) analysis following Shirk et al. (2010; 2017). We converted our genotype data into a data frame with *n* columns (*n* = number of unique alleles) and specifying allelic usage as 0, 1, or 2. We replaced missing values with its respective column mean. We then calculated PC on these allelic data using the *dudi.pca* function from the ADE4 package (v. 1.7-10, Dray and Dufour 2007) and calculated genetic distance as the Euclidean distance among a particular number of PC axes. While Shirk et al. (2017) found that genetic distance calculated using > 1 PC axes approach performed as well or better than other individual-based genetic distance measures, particularly with small sample sizes and weak underlying genetic structure, little guidance currently exists for selecting an optimal number of PC axes. We therefore calculated the number of significant PC axes using the broken stick and latent root criteria and retained the smaller number of PC axes.

Furthermore, because the amount of variation explained by successive PC axes decreases, we weighted our retained axes by their eigen values.

4.2.6. Spatial Autocorrelation Analysis

To assess the spatial scale(s) of genetic relatedness, we conducted spatial autocorrelation analyses using GenAlEx 6.5 (Peakall and Smouse 2006, 2012). We calculated the genetic autocorrelation coefficient (*r*) for multiple distance bins to test the null hypothesis that genotypes are randomly distributed in space within each bin. We calculated bootstrapped 95% CI around *r* using 9,999 bootstrap iterations and calculated the 95% CI around the null hypothesis using 9,999 random permutations. We considered spatial autocorrelation significant if *r* was outside of the 95% CI for the null hypothesis and if the bootstrapped 95% CI did not include zero (Peakall et al. 2003). We performed these analyses using both the default genetic distance (Smouse and Peakall 1999) and our PC-based genetic distance. We conducted separate analyses for males and females to test for sex-biased dispersal (Banks and Peakall 2012). We identified juveniles as individual with a snout-vent length $\leq$ 90 cm and excluded these individuals from the tests of sex-biased dispersal. We used 2, 3, and 4 km distance bins for all autocorrelation analyses. To further test for evidence of sex-biased dispersal we calculated mean assignment index (mAIc) and F_{ST} between adult samples from ABS and all other samples and tested for significance with 1,000 permutations using the function *sexbias.test* in HIERFSTAT (Goudet et al. 2002).

4.2.7. Resistance Surfaces

We defined our study area by buffering the maximum extent of our samples by 8 km which is over twice the 95th percentile of observed total home range width (3,860 m, Bauder et al. 2018) and greater than the maximum observed distance between an individual's telemetry observations in our study area (7.25 km, D. Breininger, unpublished data).

We used landscape features hypothesized to influence EIS genetic connectivity based on previous research (Bauder et al. 2018, additional details provided in Chapter 3 Appendices A-E). We used a Florida land cover map (Knight 2010; Kawula 2014), National Wetlands Inventory data (U. S. Fish and Wildlife Service 2014), and the National Hydrography Dataset's GIS flowline data (U. S. Geologic Survey 2014) to represent different land cover classes. We combined and reclassified these three data sources into separate land cover surfaces for Urban, Undeveloped Upland, Wetland, Citrus, Improved Pasture, and Open Water following Bauder et al. (2018). We used the 2016 TIGER roads layer (U. S. Census Bureau 2016) to map paved roads and reclassified roads to approximate the road classes from the 1998 U.S. Geologic Survey's (USGS) 1:24,000 roads layer (U.S. Geological Survey 1990) used by Bauder et al. (2018, Chapter 3 Appendix A). We measured soil moisture using available water storage (AWS) at 150 cm from the Soil Survey Geographic Database (SSURGO) accessed through the SSURGO Downloader 2014 (ESRI 2014). We downloaded Normalized Vegetation Difference Index (NDVI) data calculated from LANDSAT 8 OLI/TIRS using the U.S. Geologic Survey's Earth Explorer data base via the bulk order service (https://espa.cr.usgs.gov/ordering/new/). We masked clouds and cloud shadows from

each image using its associated pixel_qa band which uses the Fmask algorithm of Zhu and Woodcock (2012) and Zhu et al. (2015) and a default cloud probability of 22.5%. We calculated a mean winter NDVI using images from 11 Dec. 2014, 29 Jan. 2015, 28 Nov. 2015, 16 Dec. 2016, and 2 Feb. 2017 and a mean spring NDVI using images from 14 May 2013, 2 Apr. 2015, 6 May 2016, 7 April 2017, and 9 May 2017. We resampled NDVI from 30 m to 15 m pixels and converted all vector data sources to 15 m rasters.

We smoothed our land cover, AWS, and NDVI surfaces using Gaussian kernels at 60, 600, 1200, and 1800 m bandwidths to represent different ecological neighborhoods. All surfaces were smoothed across an area whose edges were ≥ 17 km from our samples to minimize boundary effects. The 600 m bandwidth approximates the size of an average EIS home range. We also calculated the SD of AWS and NDVI using 60, 600, 1200, and 1800 m radii Uniform kernels. Because we considered Open Water as non-habitat for EIS, we masked all Open Water pixels prior and subsequent to smoothing. All pixel values therefore represent exclusively terrestrial landscape features. We aggregated all smoothed surfaces to 60 m pixels using the *aggregate* function in R package RASTER (Hijmans 2017), taking the mean pixel value, as a compromise between resolution and computing time for a total of 663,315 pixels (603 × 1105) within our study area. We created a proportional Open Water surface (Water_Prop) so that each 60-m pixel represented the proportional area of Open Water within that pixel. We likewise converted our binary 15-m roads surface into a 60-m proportional roads layer. Because Bauder et al. (2018) found that EIS responded most strongly when primary and secondary roads were weighted higher than tertiary roads, we created a weighted proportional roads layer by

first assigning all primary and secondary roads a value of five and all tertiary roads a value of one.

To create categorical land cover maps, we combined the Urban, Undeveloped, Wetland, Citrus, Pasture, and Open Water 15-m pixel surfaces. We created an additional four surfaces including roads to test different hypotheses about the restrictive effects of roads on EIS gene flow. We created 60-m pixel road surfaces directly from our TIGER roads layers to ensure that roads, as linear habitat features, would be represented without gaps. Our first surface included primary and secondary roads as a seventh category while our second surface included only primary roads as a seventh category. Our third surface included separate categories for primary and secondary roads. Our fourth surface included primary and secondary roads as a seventh category and tertiary roads not overlapping urban as an eighth category to test the hypothesis that tertiary roads had a different restrictive effect than urban.

We used predicted RSF surfaces from Bauder et al. (2018) representing selection of home ranges across the study area (second-order or Level II selection) and locations within the home range (third-order or Level III selection, Johnson 1980, Chapter 3 Appendix E). We evaluated Level II surfaces derived from analyses including and excluding urban (Bauder et al. 2018). Level III surfaces were created and evaluated for breeding and non-breeding season males and females. Because the Level II and III surfaces were hierarchically nested, we created scale-integrated resource selection functions (SRSF) following DeCesare et al. (2012) by linearly rescaling each surface from 0–1, multiplying a Level III and Level II surface together, and then normalizing the SRSF surface to sum to one. For each RSF and SRSF surface we evaluated surfaces

created using predicted values from the binomial generalized linear model and the exponential form from Manly et al. (2002) to test for differences in the functional form of the RSF surface. We therefore evaluated four Level II, 16 Level III, and 16 SRSF surfaces.

4.2.8. Resistance Surface Optimization and Evaluation

We optimized our resistance surfaces using the R package RESISTANCEGA (v. 4.0-4 to v. 4.1-11, Peterman 2018) which employs a genetic algorithm in the GA package (v. 3.0.2, Scrucca 2013) to optimize the functional transformation and maximum value of one or more resistance surfaces. Briefly, RESISTANCEGA applies one of eight functional transformations to the resistance surfaces, calculates landscape distance from the transformed surface, fits a linear mixed-effects model using the maximum likelihood population effects parameterization in LME4, and uses the log-likelihood as the objective function in the optimization. Multiple resistance surfaces are scaled from 0–10, transformed separately, and added together. The composite surface is then rescaled by dividing by the minimum value to range from one to *x* and then used to calculate landscape distance. Optimizing each resistance surface independently avoids issues of multicollinearity among surfaces. RESISTANCEGA can accommodate continuous and categorical surfaces. We initially calculated landscape distance using *commuteDistance* from the GDISTANCE package (v. 1.2-2, van Etten 2017) which is functionally equivalent to the resistance distance calculated by CIRCUITSCAPE (McRae 2006; McRae et al. 2008; Kivimaki et al. 2014) but quicker and can be run in parallel. However, we began using CIRCUITSCAPE v. 5.0.0 written with the JULIA programming language (v. 0.6.4, accessed

1 Aug 2018 at https://julialang.org/) midway through analyses to allow for increased optimization efficiency while running in parallel. We recalculate landscape distance using *commuteDistance* and the optimized resistance surfaces for all optimizations completed using JULIA and refit their MLPE models to ensure all models were fit to data on the same scale. Using *commuteDistance* or CIRCUITSCAPE avoids the assumption that individuals have complete knowledge of all potential paths and always select the lowest-cost path, as is the case with using least-cost paths (Adriaensen et al. 2003), which may be more appropriate for evaluating multi-generational gene flow. We used default parameterizations in RESISTANCEGA except that we set the maximum allowable resistance value to 3,500 and we increased the population multiplier and number of allowable runs without improvement to 20 and 30, respectively. For optimizations with four or more surfaces we required 40 runs without improvement.

We used two approaches for evaluating our RSF/SRSF surfaces. First, we linearly rescaled all RSF/SRSF surfaces from 0–1 and converted each surface to a resistance surface by subtracting all values from one. We then measured landscape distance using *commuteDistance* and used those distances to fit a MLPE model. Second, we used ResistanceGA to optimize the functional form and maximum resistance values of those RSF/SRSF surfaces. This allowed us to test the appropriateness of estimating resistance directly from a RSF/SRSF surface.

Because of computational restrictions, we specified our optimizations to evaluate a limited number of landscape features reflecting specific *a priori* hypotheses at all-possible combinations of spatial scale. We included Water_Prop in all optimizations. Our first hypothesis was that EIS genetic connectivity would be influenced by Urban,

Undeveloped, and Wetland land covers. Our second hypothesis was that EIS genetic connectivity would be influenced by landscape features most influencing EIS habitat selection, specifically Undeveloped, Urban, and SD NDVI. Our final hypothesis was that EIS genetic connectivity would be most influenced by Undeveloped, Wetlands, and Pasture which we hypothesized would most facilitate EIS genetic connectivity even though EIS showed neutral or negative selection for Wetlands and Pasture. We conducted a *post hoc* analysis testing for an effect of primary/secondary roads by re-running our top multi-surface optimizations with a binary surface denoting primary/secondary roads. We also optimized each of our five categorical land cover surfaces. Absolute values of Pearson correlation coefficients between surfaces included in the same optimization were < 0.35.

We ranked the MLPE model from each optimization using AIC adjusted for small-sample sizes (AIC_c, Burnham and Anderson 2002) and report the marginal R^2 (i.e., the proportion of variance explained by fixed-effect factors) for mixed-effects models (Nakagawa and Schielzeth 2013; Johnson 2014). To evaluate the sensitivity of model rankings to the spatial distribution of sample points we conducted a bootstrapping procedure wherein we randomly subsampled 75% of our samples without replacement, refit each model using its optimized resistance surface, and recorded the average rank of each model and the proportion of times each model was selected as the AIC_c-best model (π) using 10,000 bootstrap iterations. To evaluate the importance of each landscape feature within a multi-surface optimization, we calculated the percent contribution of each surface by dividing each transformed resistance surface by the sum of the composite resistance surface.

We conducted a multi-stage analysis to test our hypotheses. We first compared optimizations within each set of candidate surfaces (i.e., categorical surfaces, RSF-based surfaces, and smoothed-land cover surfaces representing each hypothesis) to identify the best-supported surface in each set. We determined support using π as a more conservative metric than AIC_c because π often indicated more model selection uncertainty than AIC_c. For the RSF/SRSF surfaces, we first compared all models within each model set (predicted or exponentiated values with or without optimization) and then compared the top models across all sets. For the hypotheses utilizing smoothed-land cover surfaces, we conducted an additional series of steps. We included Water_Prop in all optimizations. First, for a given land cover (e.g., undeveloped, SD NDVI), we compared optimizations at each scale to identify the characteristic scale (Holland et al. 2004) for that land cover. Second, we ran multi-surface single-scale optimizations for each of our hypotheses where each smoothed land cover surface was represented at the same scale. Finally, we ran multi-surface pseudo-optimized multi-scale optimizations for each of our four multi-surface hypotheses were each land cover surface was included at its characteristic scale.

4.2.9. Connectivity Modeling and EIS Conservation Index

We identified resource patches by taking the mean of all four Level III RSF surfaces and then multiplying them by the Level II RSF surface to create a population-level SRSF. We then calculated the HR-wide average SRSF value for our 83 total home ranges and used the 5^{th} and 50^{th} percentiles as liberal and conservative thresholds, respectively, to determine habitat suitability. We retained patches at least the size of a median male home range (251 ha) as we wanted each patch to have the potential of

supporting at least one reproductive pair (male and female). We then used a resistance kernel-based approach to identify potential corridors among patches (Compton et al. 2007; Zeller et al. 2017). We probabilistically sampled 5,000 random points across our study area using our SRSF to ensure that most points fell in areas of relatively high habitat suitability. We linearly rescaled our resistance surface from 1–100 and built resistance kernels around each source using a half-normal standard kernel and a SD equal to two times the maximum observed EIS dispersal distance (22.2 km, Stevenson and Hyslop 2010). We then linearly rescaled our resistance kernel surface from 1–100 and took the 50^{th} and 75^{th} percentiles as thresholds for identifying corridors. We visually examined the degree of spatial overlap between habitat patches, potential corridors, and conservation lands. To create a spatially-explicit index of conservation value, we linearly rescaled our population-level SRSF surface, a predicted surface for EIS occupancy of 322 ha plots (Chapter 3), and our final connectivity surfaces from 0–1 and took the geometric mean.

4.3. Results

We obtained a total of 107 samples that amplified at ≥ 13 loci. Estimated frequency of null alleles was 15% at *Dry14* and 11% at *Dry68* so we excluded these two loci when identifying potential duplicate samples. Null allele frequencies were ≤ 8% at the remaining 13 loci (Appendix A). After removing potential duplicate shed skin samples (n = 5), two of 105 tests for genotypic disequilibrium were significant following sequential Bonferroni correction. Three loci (*Dry14*, *Dyr68*, and *Dry58*) remained out of HWP following Bonferroni correction ($P \leq 0.003$) although one locus (*Dry70*) was

marginally out of HWP ($P = 0.06$, Table 4.1). Null allele frequencies estimated after removing potential duplicates were > 10% for *Dry14* (15%) and *Dry68* (11%) and ≤ 8% for all other loci (Table 4.1). Six loci had marginally significant ($p < 0.10$) F_{IS} values after Bonferroni correction. Only *Dry14* and *Dry68* were significantly out of HWP for both ABS samples and all other samples and only these two loci for ABS samples had significantly positive F_{IS} values (Appendix B). We excluded *Dry14* and *Dry68* from subsequent analyses but examined the sensitivity of our IBD and spatial genetic autocorrelation tests to the particular loci retained.

Tests for IBD were significant across all samples ($\beta_1 = 0.0417$, 95% CI = 0.0394–0.0441, $r = 0.50$, $p < 0.0001$) and all samples outside of ABS ($\beta_1 = 0.0401$, 95% CI = 0.0340–0.0462, $r = 0.15$, $p = 0.0224$) but were not significant for samples from ABS ($\beta_1 = 0.0023$, 95% CI = -0.0021–0.0066, $r = -0.05$, $p = 0.7916$). These results were similar when juveniles were excluded (all samples: $\beta_1 = 0.0449$, 95% CI = 0.0421–0.0476; $r = 0.48$, $p < 0.0001$; excluding ABS: $\beta_1 = 0.0455$, 95% CI = 0.0390–0.0520, $r = 0.18$, $p = 0.0120$; ABS: $\beta_1 = 0.0016$, 95% CI = -0.0040–0.0071, $r = -0.13$, $p = 0.9730$). These conclusions were identical regardless of the number of loci retained (Appendix C).

Table 4.1. Genetic summary statistics across all samples excluding putative duplicates (n = 102). A = number of alleles, A_R = allelic richness, H_O = observed heterozygosity, H_E = expected heterozygosity, HWP = *p* value for test of Hardy-Weinberg proportions adjusted using sequential Bonferroni correction, F_{IS} = inbreeding coefficient, F_{IS} *p* = *p* value for test significance of F_{IS} adjusted using sequential Bonferroni correction, nulls = estimated percentage of null alleles.

Locus	A	A_R	H_O	H_E	HWP	F_{IS}	F_{IS} *p*	nulls
Dry24	7	6.93	0.62	0.71	0.7024	0.14	0.0799	5.80%
Dry30	6	5.47	0.53	0.65	0.2502	0.19	0.0360	7.89%
Dry44	5	4.92	0.54	0.57	1.0000	0.05	1.0000	1.55%
Dry55	5	5.00	0.48	0.47	1.0000	0.00	1.0000	-0.12%
Dry68	7	6.67	0.55	0.73	0.0000	0.24	0.0150	11.67%
Dry06	8	7.65	0.65	0.63	1.0000	-0.01	1.0000	-0.75%
Dry48	12	11.31	0.70	0.73	1.0000	0.05	1.0000	2.22%
Dry58	14	13.63	0.75	0.87	0.0026	0.14	0.0260	6.61%
Dry59	10	9.14	0.61	0.72	0.2130	0.16	0.0549	6.99%
Dry65	8	7.66	0.39	0.45	1.0000	0.13	0.1518	4.05%
Dry69	6	5.86	0.62	0.63	1.0000	0.02	1.0000	0.67%
Dry05	8	7.65	0.67	0.68	0.0902	0.03	1.0000	1.01%
Dry14	5	4.75	0.37	0.61	0.0000	0.40	0.0150	17.70%
Dry35	8	8.00	0.75	0.79	1.0000	0.06	0.8741	2.36%
Dry70	6	5.93	0.64	0.73	0.0612	0.13	0.1169	5.75%

4.3.1. Genetic Spatial Autocorrelation

Spatial autocorrelation analyses indicated significant positive autocorrelation through 12 km (Fig. 4.2) and this pattern was identical regardless of the number of loci used (results not shown). Adult males (n = 45) showed positive autocorrelation to approximately 12 km and this pattern was significant at the 3 and 4 km distance bins (Fig. 4.3). Adult females (n = 36) showed significant positive autocorrelation only at the first two distance bins, regardless of bin width (4–8 km, Fig. 4.3). However, the bootstrapped 95% CI only slightly overlapped zero in the 4–6 km and 6–8 km bins. The

tests of Goudet et al. (2002) were not significant ($p > 0.60$). These patterns remained consistent regardless of the number of loci used (Appendix D).

Figure 4.2. Correlograms showing the spatial scale(s) of genetic autocorrelation. The genetic autocorrelation coefficient (*r*) is calculated at 2, 3, and 4 km distance bins, panels A, B, and C, respectively, up to distances of 30, 30, and 40 km. Error bars represent bootstrapped 95% CI around *r* for each distance bin and gray lines are the 95% CI around the null hypothesis of no genetic autocorrelation calculated using randomization tests. Bins with significantly positive values of *r* are distances at which genetic autocorrelation is greater than expected by chance.

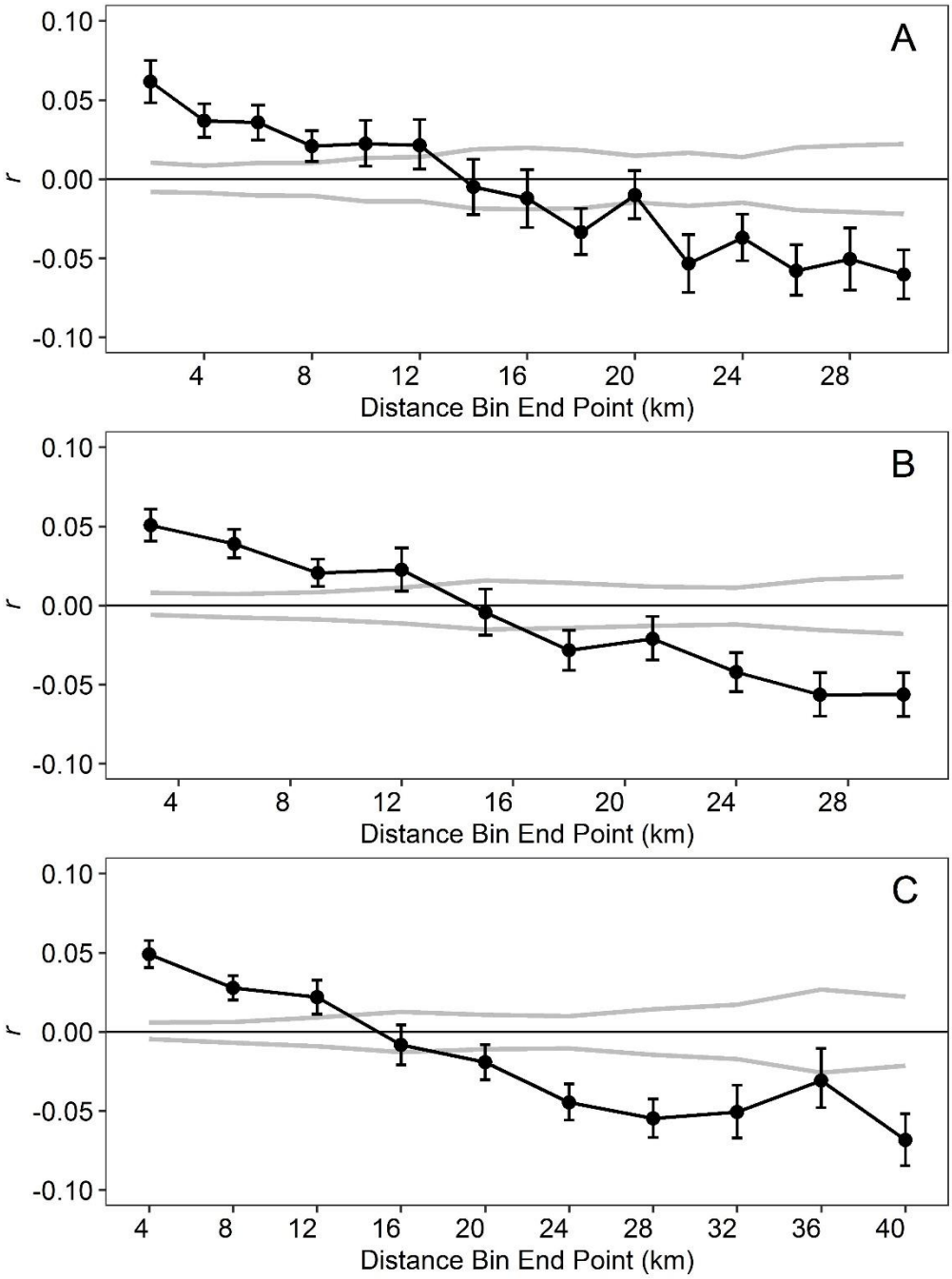

Figure 4.3. Correlograms showing the spatial scale(s) of genetic autocorrelation for adult males (n = 45, black) and adult females (n = 36, gray). The genetic autocorrelation coefficient (*r*) is calculated at 2, 3, and 4 km distance bins, panels A, B, and C, respectively, up to distances of 30, 30, and 40 km. Error bars represent bootstrapped 95% CI around *r* for each distance bin. Bins with significantly positive values of *r* are distances at which genetic autocorrelation is greater than expected by chance.

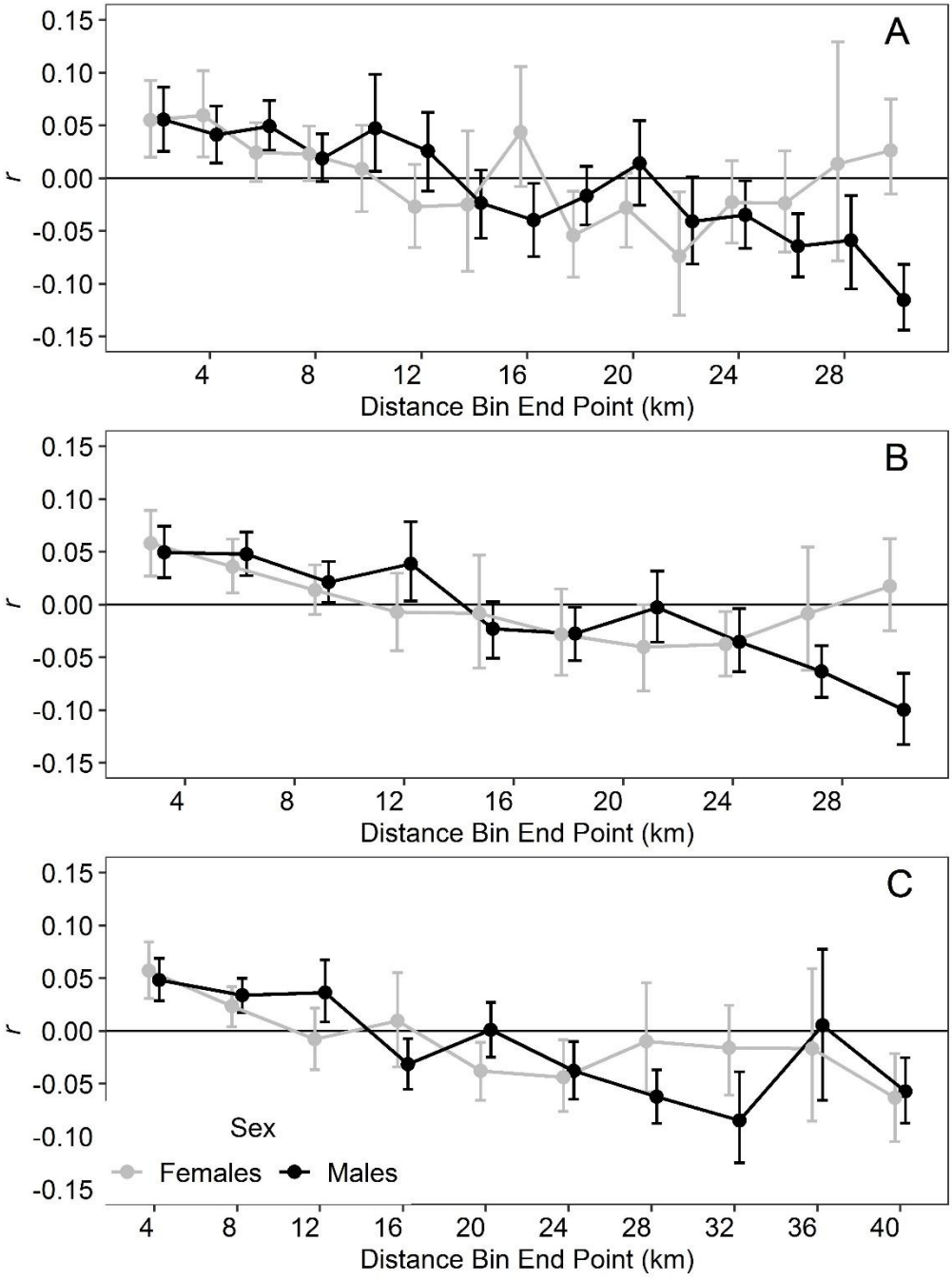

4.3.2. Categorical Surface Optimization

All optimized categorical surfaces performed better than the IBD model (ΔAIC_c = 144.70). One surface, the surface combining primary and secondary roads and keeping tertiary roads separate, had the majority of the model support (cumulative AIC_c *w* and π = 1.00 and 0.99, respectively, Table 4.2). Support for the surface without roads was low (π = 0.02). Wetland, roads, urban, and water consistently had the highest resistance values (Table 4.3).

Table 4.2. Model rankings for optimized categorical land cover surfaces. The number of model parameters is given by *K*, *w* is the AIC_c model weight, Avg. Rank is the average model ranking across 1,000 bootstrap iterations, π is the proportion of bootstrap iterations where the model was the top model, mR^2 is the marginal R^2, and cR^2 is the conditional R^2. Prim = primary roads, Sec = secondary roads, and Tert = tertiary roads.

Surface	*K*	AIC_c	ΔAIC_c	*w*	Avg. Rank	π	mR2	cR2
Prim/Sec + Tert Roads	9	-14915.11	0.00	1.0000	1.01	0.9936	0.44	0.87
Prim/Sec Roads Combined	8	-14865.98	49.13	0.0000	2.66	0.0032	0.48	0.92
Prim + Sec Roads	9	-14861.09	54.02	0.0000	2.40	0.0021	0.47	0.91
No Roads	7	-14815.79	99.32	0.0000	3.96	0.0011	0.49	0.91
Prim Roads	8	-14787.36	127.75	0.0000	4.98	0.0000	0.48	0.91
IBD	2	-14721.57	193.54	0.0000	NA	NA	0.09	0.76

Table 4.3. Optimized resistance values from the two best-supported categorical land cover surfaces. Undeveloped had the lowest resistance and therefore was assigned a value of one. Prim = primary roads, Sec = secondary roads, and Tert = tertiary roads. The order of columns from left-to-right reflects *a priori* hypothesized rankings of each land cover from lowest to highest resistance.

Surface	Wetland	Pasture	Citrus	Tert. Road	Sec. Road	Urban	Prim. Road	Water
Prim/Sec + Tert Roads	1401	1007	357	1664	2670	1629	2670	3010
Prim/Sec Roads Combined	1069	650	390	NA	2262	1448	615	2683
Prim + Sec Roads	922	765	282	NA	3203	1243	3203	2429
No Roads	628	428	144	NA	NA	1095	NA	3360
Prim Roads	675	682	340	NA	NA	1552	1717	2783

4.3.3. Resource Selection Surface Optimization

Regardless of the functional form of the RSF/SRSF surface or whether optimization was used, the Level II RSF or SRSF had greater support than the Level III RSF surfaces. Within the non-optimized surfaces, the Level II RSF surfaces contained virtually all the model support (Table 4.4 and Appendix E). Within the optimized surfaces using predicted values, the SRSF surfaces using breeding season female and non-breeding season male Level III RSF had most of the model support (cumulative w and $\pi = 1.00$ and 0.82, respectively, Table 4.5). Within the optimized surfaces using exponentiated values, the Level II RSF including urban received virtually all the model support (w and $\pi = 1.00$ and 0.98, respectively, Appendix F). The top-ranked model using optimized predicted surfaces strongly outperformed all other top-ranked RSF/SRSF models (Table 4.6). The inverse-reverse monomolecular transformation was selected for all optimized surfaces (Appendix G).

Table 4.4. Model rankings for resource selection function (RSF) and scale-integrated resource selection function (SRSF) surfaces using predicted values without optimization. RSF surfaces reflect second- and third-order habitat selection (Level II and III, respectively) while SRSF surfaces are the normalized product of Level II and Level III surfaces. Level II surfaces were estimated with and without urban land cover. Level III surfaces were estimated for breeding (Brd.) and non-breeding (NonBrd.) seasons for each sex.The number of model parameters is given by K, *w* is the AIC_c model weight, Avg. Rank is the average model ranking across 1,000 bootstrap iterations, π is the proportion of bootstrap iterations where the model was the top model, mR^2 is the marginal R^2, and cR^2 is the conditional R^2.

Surface	*K*	AIC_c	Δ AIC_c	*w*	Avg. Rank	π	mR2	cR2
Level II (w/Urban)	2	-14821.9	0	0.6593	1.25	0.6094	0.15	0.78
Level II	2	-14820.5	1.32	0.3407	1.75	0.3846	0.16	0.79
Male Brd. SRSF	2	-14797.5	24.4	0	3.33	0.0019	0.13	0.78
Male NonBrd. SRSF	2	-14795.1	26.72	0	4.04	0.0013	0.13	0.78
Female Brd. SRSF	2	-14792.9	28.92	0	5.54	0.0007	0.13	0.78
Male Brd. SRSF (w/Urban)	2	-14792.3	29.59	0	5.44	0.0009	0.12	0.77
Female NonBrd. SRSF	2	-14790.3	31.57	0	7.15	0.0004	0.12	0.78
Male NonBrd. SRSF (w/Urban)	2	-14787.6	34.22	0	7.53	0.0004	0.12	0.77
Female Brd. SRSF (w/Urban)	2	-14784	37.86	0	8.97	0.0002	0.12	0.77
Female NonBrd. SRSF (w/Urban)	2	-14782.2	39.67	0	10	0.0001	0.11	0.77
Male NonBrd. Level III	2	-14756.6	65.25	0	11.16	0	0.1	0.76
Female Brd. Level III	2	-14752.4	69.44	0	12.21	0	0.09	0.77
Female NonBrd. Level III	2	-14751	70.81	0	12.69	0	0.09	0.77
Male Brd. Level III	2	-14733.2	88.68	0	13.94	0	0.11	0.77
IBD	2	-14721.28	100.62	0	NA	NA	0.09	0.76

Table 4.5. Model rankings for resource selection function (RSF) and scale-integrated resource selection function (SRSF) surfaces using predicted values optimized using RESISTANCEGA. RSF surfaces reflect second- and third-order habitat selection (Level II and III, respectively) while SRSF surfaces are the normalized product of Level II and Level III surfaces. Level II surfaces were estimated with and without urban land cover. Level III surfaces were estimated for breeding (Brd.) and non-breeding (NonBrd.) seasons for each sex.The number of model parameters is given by *K*, *w* is the AIC_c model weight, Avg. Rank is the average model ranking across 1,000 bootstrap iterations, π is the proportion of bootstrap iterations where the model was the top model, mR^2 is the marginal R^2, and cR^2 is the conditional R^2.

Surface	*K*	AIC_c	ΔAIC_c	*w*	Avg. Rank	π	mR2	cR2
Female Brd. SRSF (w/Urban)	4	-14958.22	0.00	0.980	1.88	0.505	0.33	0.85
Male NonBrd. SRSF (w/Urban)	4	-14949.94	8.28	0.016	2.52	0.266	0.33	0.85
Female NonBrd. SRSF (w/Urban)	4	-14947.30	10.92	0.004	3.34	0.032	0.35	0.86
Level II (w/Urban)	4	-14941.57	16.65	0.000	3.78	0.056	0.33	0.85
Male Brd. SRSF (w/Urban)	4	-14937.30	20.92	0.000	3.88	0.138	0.36	0.85
Female Brd. SRSF	4	-14900.08	58.14	0.000	6.89	0.000	0.26	0.83
Male NonBrd. SRSF	4	-14896.70	61.52	0.000	7.21	0.001	0.24	0.82
Female NonBrd. SRSF	4	-14894.46	63.76	0.000	8.27	0.000	0.27	0.84
Male Brd. SRSF	4	-14892.53	65.69	0.000	8.19	0.000	0.29	0.83
Level II	4	-14887.77	70.45	0.000	9.17	0.002	0.28	0.84
Female Brd. Level III	4	-14817.99	140.23	0.000	11.36	0.000	0.15	0.79
Female NonBrd. Level III	4	-14808.47	149.75	0.000	11.62	0.000	0.20	0.80
Male NonBrd. Level III	4	-14789.36	168.86	0.000	12.90	0.000	0.17	0.78
Male Brd. Level III	4	-14768.88	189.34	0.000	13.99	0.000	0.13	0.78
IBD	2	-14721.28	236.94	0.000	NA	NA	0.09	0.76

Table 4.6. Model rankings for the top resource selection function (RSF) and scale-integrated resource selection function (SRSF) surfaces. RSF surfaces reflect second- and third-order habitat selection (Level II and III, respectively) while SRSF surfaces are the normalized product of Level II and Level III surfaces. Level II surfaces were estimated with and without urban land cover. Level III surfaces were estimated for breeding (Brd.) and non-breeding (NonBrd.) seasons for each sex.The number of model parameters is given by *K*, *w* is the AIC_c model weight, mR^2 is the marginal R^2, and cR^2 is the conditional R^2.

Surface	*K*	AIC_c	ΔAIC_c	*w*	mR2	cR2
Female Brd. SRSF (w/Urban) Pred Optim	4	-14958.22	0.00	0.984	0.33	0.85
Male NonBrd. SRSF (w/Urban) Pred Optim	4	-14949.94	8.28	0.016	0.33	0.85
Level II RSF (w/Urban) Exp Optim	4	-14903.30	54.92	0.000	0.33	0.85
Level II RSF Exp Optim	4	-14869.95	88.27	0.000	0.29	0.84
Level II RSF (w/Urban) Pred Raw	2	-14821.85	136.37	0.000	0.15	0.78
Level II RSF Pred Raw	2	-14820.53	137.69	0.000	0.16	0.79
Level II RSF Exp Raw	2	-14769.17	189.05	0.000	0.12	0.77
Level II RSF (w/Urban) Exp Raw	2	-14748.86	209.36	0.000	0.10	0.77
IBD	2	-14721.28	236.94	0.000	0.09	0.76

4.3.4. Smoothed Land Cover Optimization

The AIC_c-best scales for the single-surface optimizations with Water_prop were 1800 m for undeveloped, wetland edge, and SD NDVI, 1200 m for pasture, 600 m for urban, and 60 m for wetland (Fig. 4.4 and Appendix I). The wetland edge surfaces smoothed at 1200 and 1800 m received virtually all the model support among single surface optimizations (cumulative $w = 0.99$, Appendix I). Because the relative support for different multi-surface single-scale optimizations varied depending on whether optimizations were ranked using AIC_c or through bootstrap resampling, we used the proportion of bootstrap iterations that an optimization was selected as the AIC_c-best optimization (hereafter π) to evaluated support among candidate optimizations. The best

supported scales for the multi-surface single-scale optimizations were 1800 m for Upland+Wetland Edge+SD NDVI, 1800 m for Upland+Urban+Wetland, 1800 m for Upland+Urban+SD_NDVI, and 1200 m for Upland+Wetland+Pasture (Fig. 4.5 and Appendix J). The 1800 m multi-surface single-scale optimization was also the pseudo-optimized optimization for Upland+Wetland Edge+SD NDVI while the pseudo-optimized optimizations for the other three hypotheses included surfaces at different scales. These multi-surface multi-scale pseudo-optimized optimizations had greater empirical support for Upland+Urban+Wetland and Upland+Wetland+Pasture but not for Upland+Urban+SD NDVI (Fig. 4.5). When comparing all multi-surface optimizations, the Upland+Urban+SD NDVI optimization at 1800 m had the greatest empirical support with $\pi = 0.66$ and $w = 0.92$ (Appendix J). The second ranked optimization, using π, was the pseudo-optimized optimization for Upland+Urban+Wetland smoothed at 1800, 600, and 60 m, respectively, with $\pi = 0.13$ and $w = 0$. Across all optimizations, the median proportional contributions of surfaces to the optimized resistance surface were 0.47, 0.29, 0.18, 0.36, and 0.03 for SD NDVI, Upland, Urban, Wetland, and Water, respectively. Including a binary primary/secondary roads surface did not substantially improve empirical support for the multi-surface optimizations as the maximum π for an optimization with primary/secondary roads (Upland+Urban+SD NDVI at 1800 m) was 0.12 (additional results not presented). When we compared the best-supported optimizations across all our hypotheses, the multi-surface optimizations at broad spatial scales always outperformed single-surface, RSF-based, or categorical land cover optimizations (Table 4.7).

Figure 4.4. Model support for individual land cover surfaces smoothed with Gaussian kernels with 60, 600, 1200, and 1800 m bandwidths. Bootstrapped Proportion is the proportion of bootstrap iterations where a model was the AICc-best model in the set. Water_prop was included in each optimization.

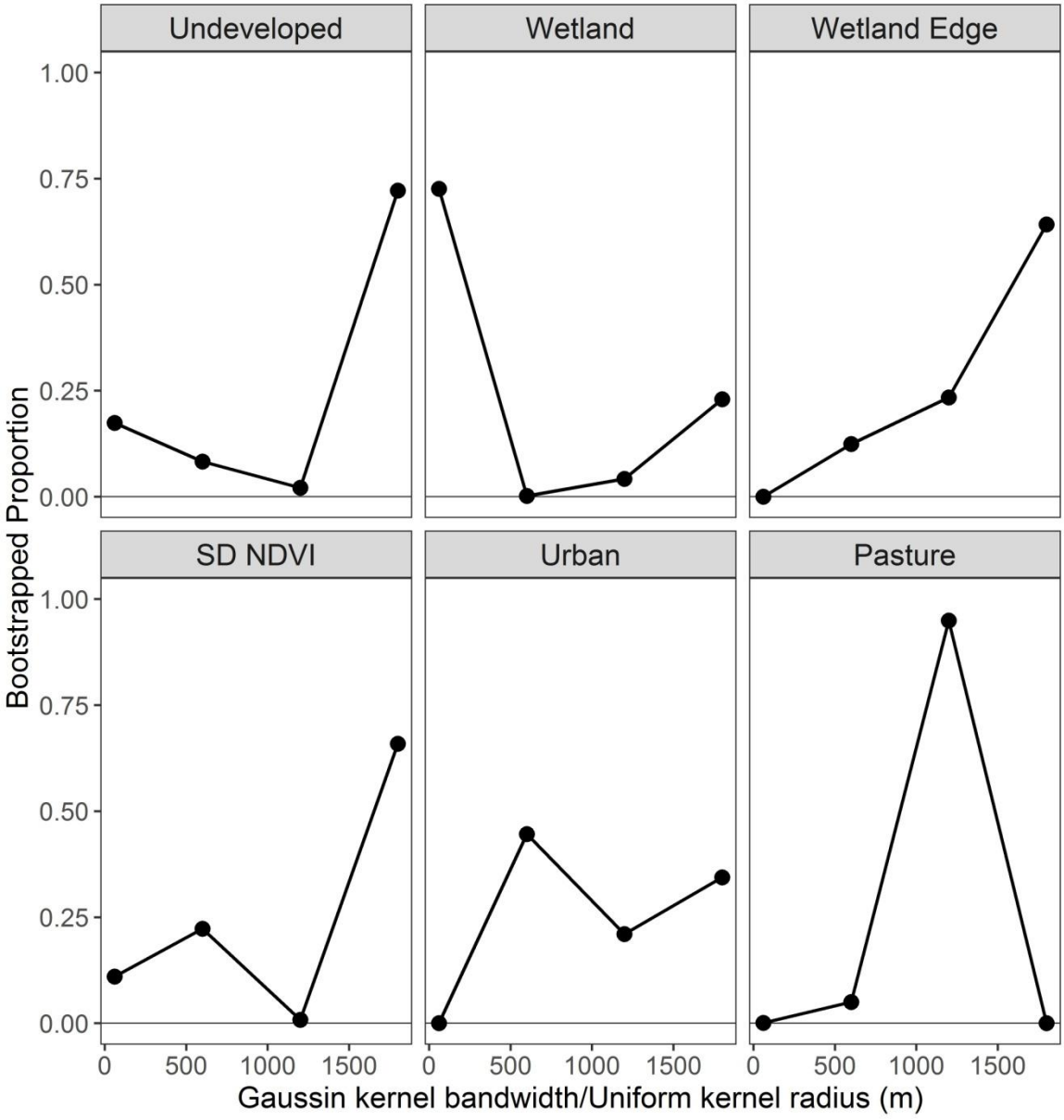

Figure 4.5. Model support for multi-surface optimizations. The first optimizations in each panel have all land cover surfaces smoothed with Gaussian kernels with 600, 1200, or 1800 m bandwidths except Water_prop which was also included in each optimization. Pseudo Opt. represents the multi-surface, multi-scale optimizations with each surface at its pseudo-optimized scale. Bootstrapped Proportion is the proportion of bootstrap iterations where a model was the AICc-best model.

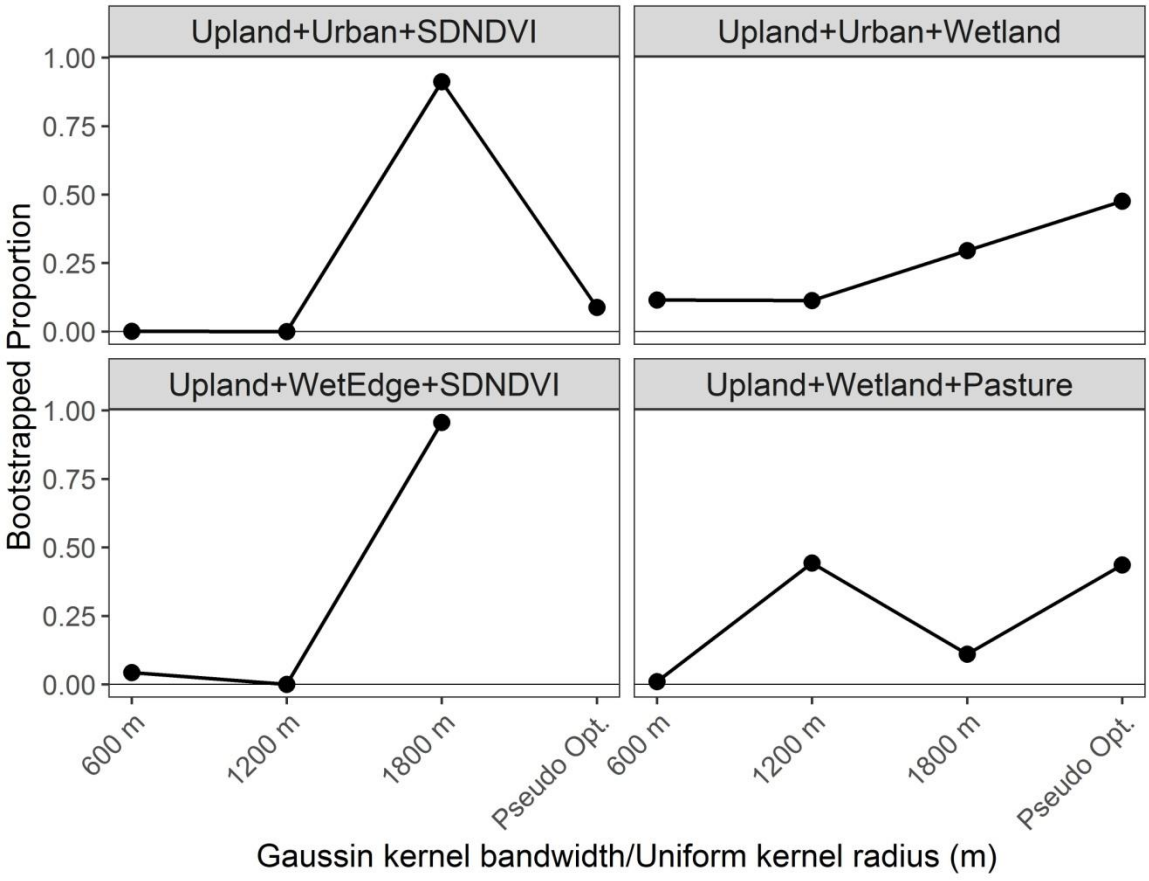

Table 4.7. Model rankings for the AICc-best ResistanceGA optimizations from each hypothesis. Surface abbreviations are: Undvlpd = Undeveloped, SRSF = scale-integrated resource selection function, NonBrd = Non-breeding season. Surfaces with Pseudo Optim for scale contain surfaces smoothed at their AICc-best scale from the single-scale analysis and are therefore multi-surface, multi-scale optimizations.The number of model parameters is given by K, w is the AICc model weight, Avg. Rank is the average model ranking across 10,000 bootstrap iterations, π is the proportion of bootstrap iterations where the model was the top model, mR2 is the marginal R2, and cR2 is the conditional R2.

Surfaces	Scale	*K*	AIC_c	ΔAIC_c	*w*	Avg. Rank	π	mR2	cR2
Undvlpd + Urban + SD NDVI	1800	13	-14987.98	0.00	0.9972	1.42	74.83	0.33	0.80
Undvlpd + Urban + Wetland	Pseudo Opt.	13	-14949.63	38.35	0.0000	3.04	17.74	0.34	0.80
Undvlpd + Wetland Edge + SD NDVI	1800	13	-14976.22	11.76	0.0028	2.44	4.85	0.28	0.81
Female NonBrd. SRSF (w/Urban) Pred	NA	4	-14958.22	29.76	0.0000	5.67	1.52	0.33	0.85
Undvlpd + Wetland + Pasture	1200	13	-14930.82	57.16	0.0000	5.18	0.65	0.34	0.83
Wetland	60	7	-14905.49	82.49	0.0000	7.95	0.28	0.35	0.80
Prim/Sec + Tert Roads	NA	9	-14915.33	72.65	0.0000	8.00	0.10	0.44	0.87
Wetland Edge	1800	7	-14940.65	47.33	0.0000	5.33	0.03	0.30	0.80
Undvlpd	1800	7	-14913.60	74.38	0.0000	8.12	0.00	0.25	0.80
SD NDVI	1800	7	-14897.63	90.35	0.0000	9.07	0.00	0.15	0.77
Urban	600	7	-14893.50	94.48	0.0000	9.83	0.00	0.29	0.82
Pasture	1200	7	-14846.74	141.24	0.0000	11.94	0.00	0.16	0.78

Figure 4.6. Functional transformations for each landscape covariate surface from the AICc-best ResistanceGA optimization. PC values represent the proportional contribution of each surface to final optimized surface.

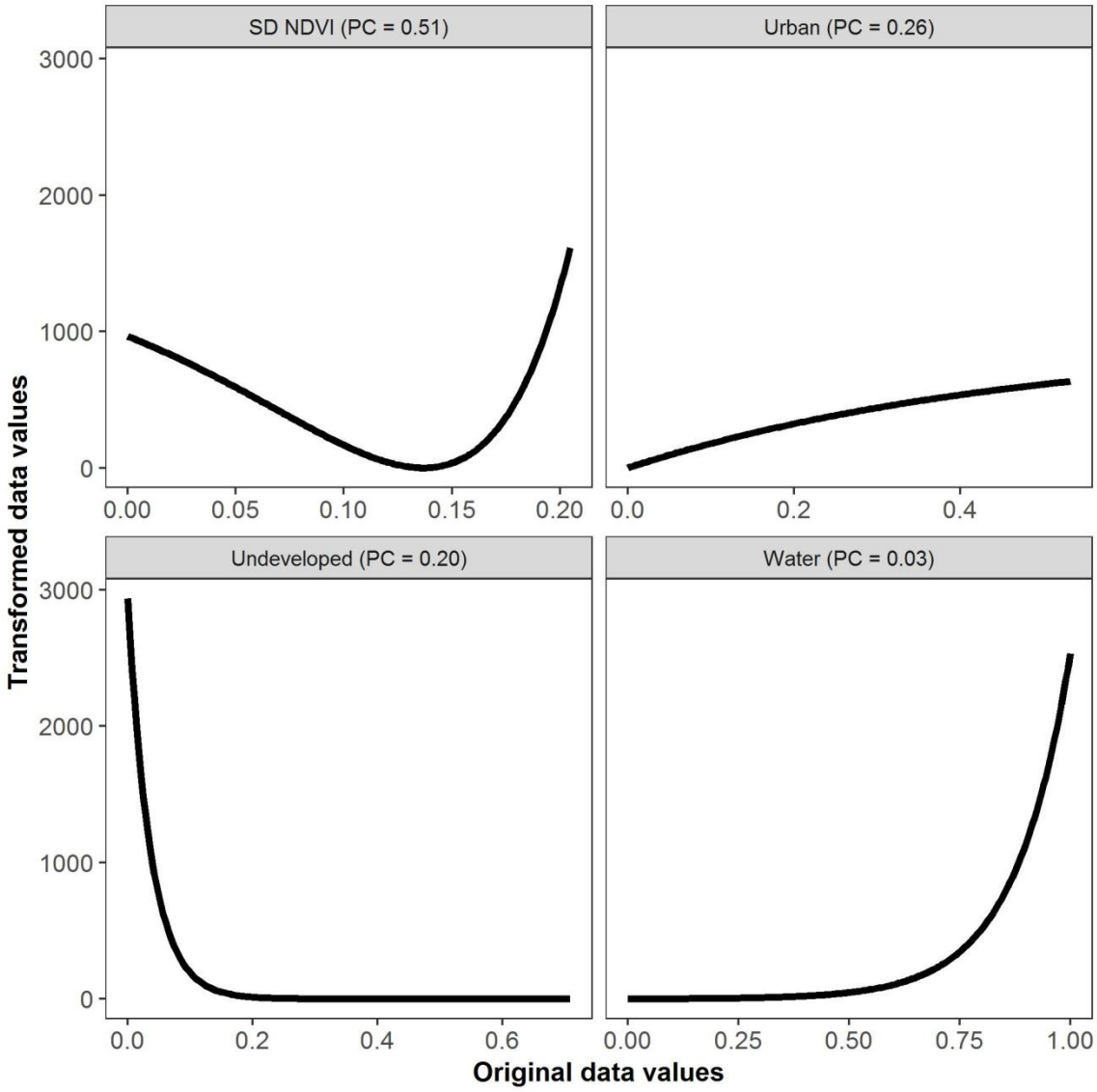

4.3.5. Connectivity Modeling

Because the optimized surface using undeveloped, urban, and SD NDVI smoothed at the 1,800 m bandwidth had the vast majority of empirical support, we used this resistance surface to map potential corridors (Fig. 4.7). Connectivity was greatest

across approximately the southern half of the study area where the vast majority of habitat patches were connected. However, connectivity was markedly reduced in the northern half of the study area. Using the 50th percentile cutoff, an area of potential corridor extended north along the western edge of the LWR. However, while most conservation lands contained both habitat patches and potential corridors, the proportion of habitat patches and corridors within conservation lands was relatively low. Our overall index of conservation value also indicates conservation lands in the southern portion of our study area have greater overall indices compared to conservation lands in the northern portion of our study area (Fig. 4.8).

Figure 4.7. Distribution of potential EIS habitat patches and corridors using the linear rescaled optimized resistance surface including undeveloped, urban, and SD NDVI smoothed with a 1,800 m bandwidth in relationship to primary and secondary roads and conservation lands. Habitat patches were defined using the 5th and 50th percentiles of a multi-level resource selection surfaces. The left panel shows the continuous connectivity surface. The middle panel shows corridors defined using the 50th percentile of the resistance kernel surface and the right panel shows corridors defined using the 75th percentile of the resistance kernel surface.

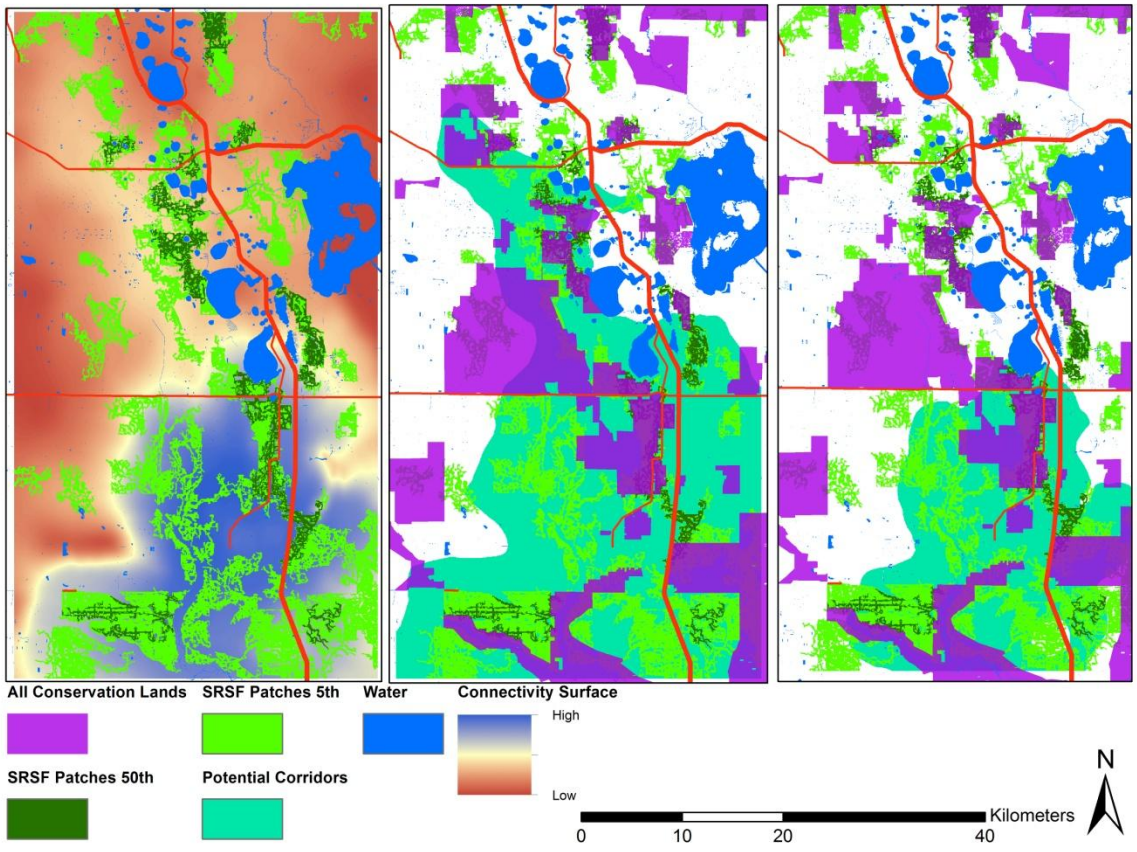

Figure 4.8. Comparison of spatially-explicit representations of different aspects of EIS ecology and an index of overall conservation value. Panel A represents a population-level scale-integrated resource selection function, Panel B represents predicted occupancy after 15 years simulated using an individual-based model, and Panel C represents the genetic connectivity surface. Panel D is the geometric mean of the three surfaces representing an index of overall conservation value.

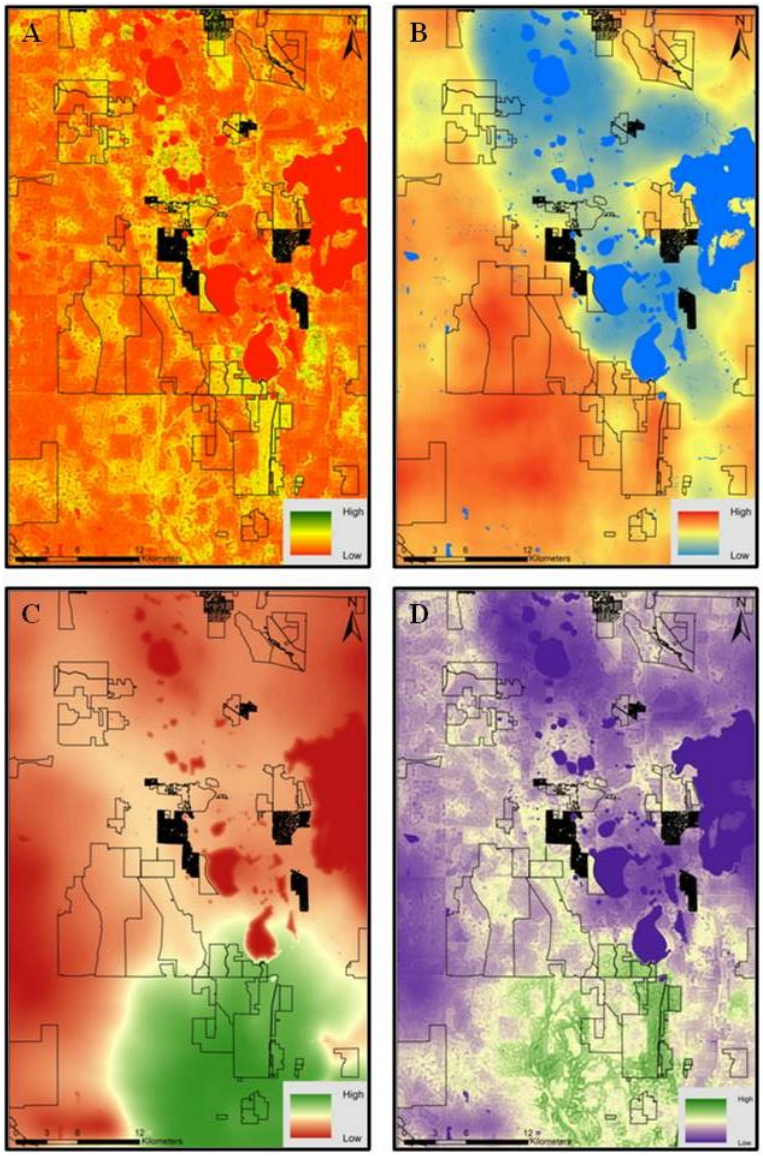

4.4. Discussion

Our results strongly indicate that EIS gene flow is influenced by multiple landscape features operating at spatial extents at or above the scale of the home range. Optimizations using multiple landscape features represented at relatively broad spatial scales out performed optimizations with multiple landscape features at relatively fine spatial scales (i.e., categorical land cover surfaces) and optimizations using two landscape features at relatively broad scales (i.e., the single surface optimizations). This suggests that even when evaluating the effects of multiple landscape features on genetic connectivity one must consider the effects of those features at multiple spatial scales. This broadly concurs with other landscape genetics studies which found that landscape features most strongly influence genetic connectivity at multiple spatial scales including scales beyond the original spatial resolution of the land cover data (Row et al. 2015; Zeller et al. 2017).

Our best multi-surface optimization included undeveloped uplands, urban, and a landscape feature representing habitat edge: SD NDVI. These three landscape features were the most influential covariates influencing EIS multi-level, multi-scale habitat selection suggesting that similar landscape features influence EIS movement at a range of biological levels ranging from within-home range movements to multi-generational gene flow. It is striking that while the landscape features influencing these processes was similar, the scale at which these features operate varied markedly. The 1800 m bandwidth received relatively strong empirical support across our analyses. Pseudo-optimized multi-surface multi-scale optimizations varied in their degree of empirical support but never strongly outperformed the single-scale multi-surface optimizations. This also indicates

that landscape influences in EIS gene flow generally operate at broad spatial scales. While the mechanisms (e.g., juvenile dispersal or male mate-searching movements) responsible for EIS gene flow are unclear, a small adult male EIS in southern Georgia was observed to disperse 22.2 km between overwintering sites within a large tract of protected lands (Stevenson and Hyslop 2010), indicating that EIS dispersal may occur at relatively broad spatial scales. Our genetic autocorrelation analysis also indicates significant positive spatial autocorrelation to approximately 12 km.

SD NDVI consistently had a relatively strong proportional contribution to the optimized resistance surface. An inverse Ricker transformation was most commonly selected for SD NDVI indicating lowest resistance at intermediate values of SD NDVI. High values of SD NDVI often represented urban-vegetation interfaces whereas low SD NDVI values often represented small amounts of habitat edge. This strong influence of habitat heterogeneity is consistent with results of Bauder et al. (2018) who found that EIS selected high habitat heterogeneity for both Level II and III selection. Moler (1985) also observed radio-tracked EIS predominately using habitat edges. Mosaics of upland and wetland habitats provide a diversity of potential foraging habitats for a dietary generalist such as the EIS (Stevenson et al. 2010) and edge-selection patterns are known in other mammalian and avian dietary generalists (Marzluff et al. 2004; Stewart et al. 2013; Beatty et al. 2014). Upland habitats (e.g., scrub, flatwoods) also often support gopher tortoises (*Gopherus polyphemus*) whose burrows are regularly used by EIS, particularly as overwintering sites (Layne and Steiner 1996; Hyslop et al. 2009a) although they are not essential as overwintering sites in peninsular Florida (Bauder et al. 2016a).

An alternative explanation for the higher performance of optimizations with broad-scale landscape features may be suggested by the distribution of anthropogenically-disturbed habitats relative to predicted corridors. Predicted corridors from our top surface formed a single contiguous area rather than exhibit discrete patches. This is consistent with the effects of smoothing landscape features in our study area with large (i.e., 1,800 m) bandwidths. However, most potential corridors (i.e., areas of low resistance) did not overlap undeveloped upland or wetland edge land covers but rather overlapped improved pasture, citrus, and, to a lesser extent, urban land covers (Fig. 4.9). This may suggest that the greater empirical support for broad spatial scales may be less a reflection of broad-scale associations with particular landscape features but rather an indication of relatively extensive gene flow across our study area. While our spatial genetic autocorrelation analysis does suggest EIS gene flow can occur over broad spatial extents (i.e., up to approximately 12 km) within our study area, we do not think this explanation is entirely sufficient to explain the greater support for the 1800 m bandwidths for several reasons. First, bootstrap resampling, which should mitigate artifacts of the spatial-distribution of sampling points, still indicated predominately strong support for the optimization with undeveloped upland, urban, and SD NDVI. Second, resistance values from our categorical land cover surfaces indicated that pasture and citrus were the second and third least resistant land cover surfaces suggesting that these land covers impede gene flow to a lesser degree than wetlands, urban, open water, and primary and secondary roads. While our results suggest that much of our study area may facilitate EIS gene flow, even in the presence of anthropogenically disturbed habitats, we nevertheless

suggest that conservation efforts target potential corridors in undeveloped habitats because of their potential to also serve as EIS habitat.

Figure 4.9. Distribution of potential EIS habitat patches and corridors using the optimized resistance surface including undeveloped, wetland edge, and SD NDVI smoothed with a 1,800 m bandwidth after removing corridors overlapping improved pasture, citrus, and urban land covers. Habitat patches were defined using the 5th and 50th percentiles of a multi-level resource selection surfaces. The left panel shows the continuous connectivity surface. The middle panel shows corridors defined using the 50th percentile of the resistance kernel surface and the right panel shows corridors defined using the 75th percentile of the resistance kernel surface.

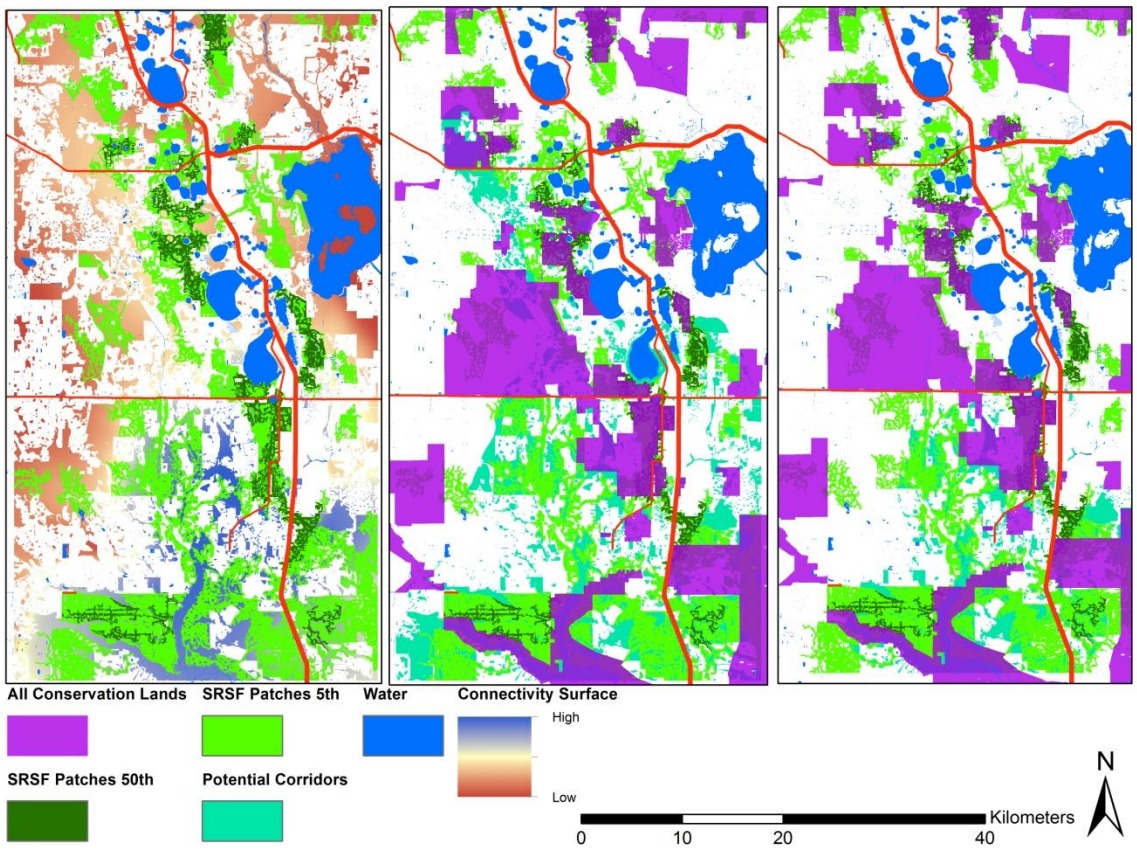

Contrary to our *a priori* expectations, wetlands were consistently negatively associated with EIS gene flow although optimizations with wetlands had comparatively low empirical support. Decreasing monomolecular transformations were most frequently

selected for wetlands and resistance values for wetlands in the categorical land cover optimizations were greater than for citrus and pasture. This restrictive effect of wetlands was surprising given observations of EIS using and foraging in wetland habitats in both peninsular Florida (Bauder et al. 2018) and southern Georgia (Speake et al. 1978; Hyslop et al. 2014). However, EIS in peninsular appeared to avoid large tracts of wetlands (Bauder et al. 2018). We are unsure of the mechanisms that might lead to wetlands restricting EIS gene flow, although given this species' range-wide association with terrestrial upland habitats it may simply reflect a species-specific avoidance of extensive mesic habitats. However, when we overlaid our wetland land cover surface on our top-ranked optimized resistance surface many wetland areas were included within potential corridors.

Although our RSF-based optimizations, particularly our SRSF-based optimizations, incorporated multiple landscape features at different spatial scales, all of these optimizations were outperformed by our top multi-surface, broad-scale optimization. This was surprising given that SRSF surfaces integrate selection occurring at different hierarchical levels (DeCesare et al. 2012; McGarigal et al. 2016) and that our habitat selection analyses evaluated selection at multiple spatial scales (i.e., extents) within each level (Bauder et al. 2018). While the optimization using female breeding season SRSF had higher AIC_c rank that our multi-surface optimization with undeveloped, urban, and wetlands, bootstrapping results suggested that the SRSF model may have had poorer performance. Our results are consistent with those of several other studies reporting that resistance surfaces derived directly from habitat models were poorly associated with genetic connectivity (Wasserman et al. 2010; Reding et al. 2013; Mateo-

Sanchez et al. 2015a; Roffler et al. 2016). We suggest two potential mechanisms for this pattern in our results. First, dispersing individuals may respond differently to landscape features than resident individuals with established home ranges (Elliot et al. 2014; Mateo-Sanchez et al. 2015a, b; Zeller et al. 2018). Several studies have found that particular landscape features showing strong associations with habitat selection showed weak associations with genetic connectivity (Coulon et al. 2008; Wasserman et al. 2010). However, two of the three landscape features in our AIC_c-best multi-surface, broad-scale optimization (Undeveloped and SD NDVI) had a strong influence on both EIS home range selection (i.e., Level II) and within-home range selection (i.e., Level III, Bauder et al. 2018). Urban also strongly influenced EIS selection at both levels. This suggests that these features are important both for habitat selection and dispersal. Keeley et al. (2016) found that resistance surfaces derived from RSF and SSF identified dispersal paths for habitat specialists (bighorn sheep) but not habitat generalists (elk). The broadly generalist patterns of EIS habitat selection in peninsular Florida may therefore contribute to the lower performance of our RSF-based optimizations. A second mechanism, therefore, is a mismatch in the scales at which particular landscape features influence dispersal versus habitat selection. While data on EIS dispersal are largely lacking, an observation of a small adult EIS in southern Georgia dispersing 22.2 km (Euclidean distance) between overwintering sites suggests that EIS dispersal may occur over broad scales (Stevenson and Hyslop 2010). It is therefore reasonable to assume that the scale at which landscape features influence dispersal is relatively large although additional data are needed to test this hypothesis.

Despite the relatively poor performance of RSF-based surfaces, our prediction that surfaces including Level II selection would outperform surfaces only reflecting Level III selection was supported, both for optimized surfaces and surfaces derived from the raw resource selection surfaces. If EIS genetic connectivity is indeed more strongly influenced by landscape features at relatively broad spatial extents, then surfaces reflecting Level II selection may more closely approximate these broader scales as Level II selection by definition represents selection at broader scales (i.e., selection of home ranges within the study area, Johnson 1980). The higher performance of optimized surfaces relative to raw resource selection surfaces was also found by Beninde et al. (2016) for common wall lizards (*Podarcis muralis*) in an urban landscape. While many studies assume a linear relationship between habitat suitability and resistance (Beier et al. 2008), more recent studies have shown that negative exponential transformations, similar to inverse-reverse monomolecular transformation, between habitat suitability and resistance also outperformed linear transformations (Keeley et al. 2016; Zeller et al. 2018). A negative exponential relationship is consistent with a tendency for dispersing individuals to traverse both marginal and high quality habitats (Elliot et al. 2014). But we also found marked differences in model performance when using predicted values from the exponential RSF or the binomial GLM used to estimate the RSF, with the latter outperforming the former regardless of whether the resistance surface was optimized. Resource selection functions using use-available designs generally assume an underlying exponential model which allows estimation of the selection coefficients using a binomial GLM or GLMM (Manly et al. 2002; Johnson et al. 2006; Avgar et al. 2017). Under a use-availability design the intercept from a binomial GLM/GLMM is non-interpretable so

predicted probabilities from the binomial GLM/GLMM do not reflect the underlying exponential model(Lele and Keim 2006; Avgar et al. 2017). However, this does not necessarily imply that the exponential model is required to generate predicted values to create resistance surfaces as evidenced both by our results and the demonstrated benefits of non-linearly transforming habitat suitability surfaces to create resistance surfaces (Keeley et al. 2016; Zeller et al. 2018). We suspect the superior performance of using the predicted GLM values may be due to logit link function of the binomial GLM/GLMM wherein the slope of the predicted relationship declines at extreme values similar to the negative exponential function at moderate-high values. However, the practice of evaluating different non-linear transformations of habitat suitability surfaces may ensure that results are robust to the manner in which the habitat suitability values were predicted.

Our prediction that SRSF or Level III surfaces for males, particularly breeding season males, was not supported. Amongst our optimized predicted surfaces, breeding season male SRSF surfaces ranked the lowest of the SRSF surfaces. While bootstrapped model weights suggested moderate model uncertainty, breeding season female and non-breeding season male SRSF surfaces received the most support. Our analysis of sex-specific dispersal did not show strong evidence for sex-biased dispersal suggesting that male mate-searching movements may not be the primary driver in EIS gene flow. However, near-absence of dispersal data for EIS limited our ability to infer the relative importance of juvenile dispersal or male-mate searching movements in influencing EIS gene flow.

We acknowledge several limitations and caveats to our methods and results which call for caution when interpreting our results. First, EIS in our study area are extremely

difficult to detect. Despite an intensive radio telemetry study and marking 38 EIS over a 35 month period, we only recaptured three non-radio tracked individuals and 7,849 km of driving roads through suitable habitat yielded only four individuals. As a result, our sampling gaps do not necessarily represent EIS distributional gaps and a lack of samples from areas where a species is present may limit one's ability to correctly infer the effects of landscape features on gene flow (Anderson et al. 2010; Oyler-McCance et al. 2013). However, our use of bootstrap resampling in evaluate model support should help mitigate against artifacts of the spatial arrangement of our sampling points. Second, our study area covered a relatively limited spatial extent, only approximately twice the distance of a maximum EIS dispersal which reduces the potential variation in genetic distance due to landscape features and limits the applicability of our results to other areas. Third, the magnitude and/or direction of the effects of particular landscape features may vary within species across different landscapes (Short-Bull et al. 2011; Richardson et al. 2016) so we stress caution when inferring the results of our study to other parts of the EIS distribution, particularly areas with known differences in EIS spatial and habitat ecology (i.e., southern Georgia). Finally, our landscape variables were represented at relatively coarse spatial resolution (i.e., 60-m pixels) and limited thematic resolution (i.e., six land cover classes), although our use of our use of NDVI and AWS should have captured additional within-class heterogeneity in vegetation structure and soil moisture. This may be important if species respond strongly to fine-scale/micro-habitat features such as vegetation structure or shelter site availability. For example, Milanesi et al. (2017) found the three-dimensional habitat models including LiDAR-derived vegetation structure

variables performed better than two-dimensional models with land cover data for capercaillie (*Tetro urogallus*).

Our study illustrates the importance of considering a multi-scale approach in landscape genetics. While scale-specific effects are now widely recognized and evaluated in wildlife habitat selection (McGarigal et al. 2016), the effects of scale have traditionally received less attention in landscape genetics (Balkenhol et al. 2009; Segelbacher et al. 2010; Jaquiery et al. 2011) although recent studies suggest that this trend is reversing (Row et al. 2015; Zeller et al. 2017). While multi-surface pseudo-optimized multi-scale optimizations did not strongly outperform broad-scale multi-surface single-scale optimizations, this pattern may be specific to our study system and we still encourage future researchers to consider a multi-scale approach. We also note that a true optimization where scale is simultaneously varied for different landscape features may outperform a pseudo-optimization approach. Winiarski et al. (Winiarski et al. In review-b) examined all possible combinations of two landscape features and six scales for two species of vernal pool breeding salamanders using RESISTANCEGA. For one species, the all-combinations best scale for one covariate (surface curvature) was different (500 m) and had greater empirical support than the pseudo-optimized scale for this covariate (1000 m). RESISTANCEGA currently incorporates an option for smoothing surfaces at different scales using a Gaussian kernel and optimizing the kernel bandwidth as an additional parameter (Peterman 2018). We recommend future research evaluating this feature as a way to simultaneously optimize the spatial scale for multiple landscape features.

Together with previous research (Bauder et al. 2018), our results highlight the importance of extensive tracts of undeveloped upland habitat with high habitat heterogeneity for both EIS habitat selection and genetic connectivity. While existing conservation lands in the southern Lake Wales Ridge should promote EIS gene flow by protecting potential corridors, our corridor modeling indicates that large areas of potential corridor do not have formal protection. Given anticipated increases in development across Florida landscapes in the near future, (Zwick and Carr 2006), additional land protection may substantially benefit EIS both in protecting habitat and in promoting genetic connectivity. However, much potential EIS habitat and/or corridors are anthropogenically-influenced land covers, predominately improved pasture, citrus, and urban. While this suggests that such lands, particularly pasture and citrus, may facilitate genetic connectivity, anthropogenic lands with high road densities may also act as population sinks for EIS (Chapter 3; Breininger et al. 2004; Breininger et al. 2012). This should lead to increased focus on remaining potential habitat and corridors in undeveloped upland land covers for conservation prioritization.

APPENDIX A. SAMPLE SIZES AND TRACKING INTENSITY FOR *DRYMARCHON COUPERI* HOME RANGE ESTIMATION.

Sample sizes for estimation of annual and seasonal home ranges of male (M) and female (F) telemetered *Drymarchon couperi* in peninsular Florida. The mean (61 SD), and range of number of fixes and number of days tracked (calculated across home ranges) are also presented.

	Number of snakes			Number of home ranges		Number of fixes		Number of days	
	Tot-al	M	F	M	F	Mean ± SD	Range	Mean ± SD	Range
Annual, Highlands	12	9	3	9	3	103 ± 20	64–131	309 ± 47	255–365
Annual, Brevard	59	31	28	43	41	30 ±11	12–64	341 ± 53	255–365
6-mo, Highlands	19	12	7	21	15	56 ±11	35–84	160 ± 22	108–180
6-mo, Brevard	59	30	29	57	71	19 ± 4.9	11–34	161 ± 19.2	105–182
3-mo, Highlands	24	17	7	45	25	32 ± 7	18–49	86 ± 4	73–91

APPENDIX B. DRYMARCHON COUPERI ANNUAL HOME RANGE ESTIMATES

Annual home range size estimates (ha, mean ± 1 SD and range) and number of radio telemetry fixes for *Drymarchon couperi* in central Florida by sex and study location (Highlands and Brevard). Home range estimators are the 100% minimum convex polygon (MCP) and the 95% volume contour of a fixed kernel utilization distribution (FK UD). Utilization distributions were estimated using the plug-in and reference bandwidths with unconstrained bandwidth matrices. For individuals with multiple annual home ranges we averaged their home range sizes and then included this value in the final average.

							95% FK UD (reference) (ha)	
	n	No. of fixes	MCP (ha)		95% FK UD (plug-in) (ha)			
Group		Mean ± SD	Mean ± SD	Range	Mean ± SD	Range	Mean ± SD	Range
Highlands, males	9	99 ± 19	245.69 ± 138.95	27.71–456.17	272.76 ± 167.03	30.28–557.51	353.84 ± 202.44	39.16–456.17
Highlands, females	3	117 ± 19	60.71 ± 49.64	27.23–117.74	66.40 ± 59.65	23.70–134.55	84.41 ± 70.85	32.48–117.74
Brevard, males	28	31 ± 9	121.08 ± 97.49	6.18–371.58	220.97 ± 187.23	11.96–679.86	270.57 ± 227.89	14.32–818.13
Brevard, females	31	30 ± 12	47.72 ± 37.65	10.27–151.11	81.28 ± 75.32	13.01–315.44	101.77 ± 85.38	19.43–352.21
Males	40	45 ± 32	149.12 ± 118.53	6.18–456.17	232.62 ± 182.12	11.96–679.86	289.30 ± 222.70	14.32–818.13
Females	31	39 ± 28	48.97 ± 38.15	10.27–151.11	79.84 ± 73.23	13.01–315.44	100.09 ± 83.20	19.43–352.21
Total	71	43 ± 30	105.40 ± 104.65	6.18–456.17	165.90 ± 163.10	11.96–679.86	206.70 ± 198.82	14.32–818.13

APPENDIX C. EXAMPLES OF DRYMARCHON COUPERI WITHIN-INDIVIDUAL SEASONAL HOME RANGE OVERLAP

Examples of 6-mo home ranges for *Drymarchon couperi* showing the degree of spatial overlap among seasons. Home ranges are the 95% volume contours of fixed kernel utlization distributions with an unconstrained reference bandwidth. Panel A is a male from Brevard, Panel B is a female from Brevard, Panel C is a male from Highlands, and Panel D is a female from Brevard. Panels A and B show the most extreme cases of seasonal shift in space observed in our study for males and females, respectively. Telemetry fixes from the non-breeding season are denoted as ●, ♦, and ○ and fixes from the breeding season are denoted as ■ and ▲.

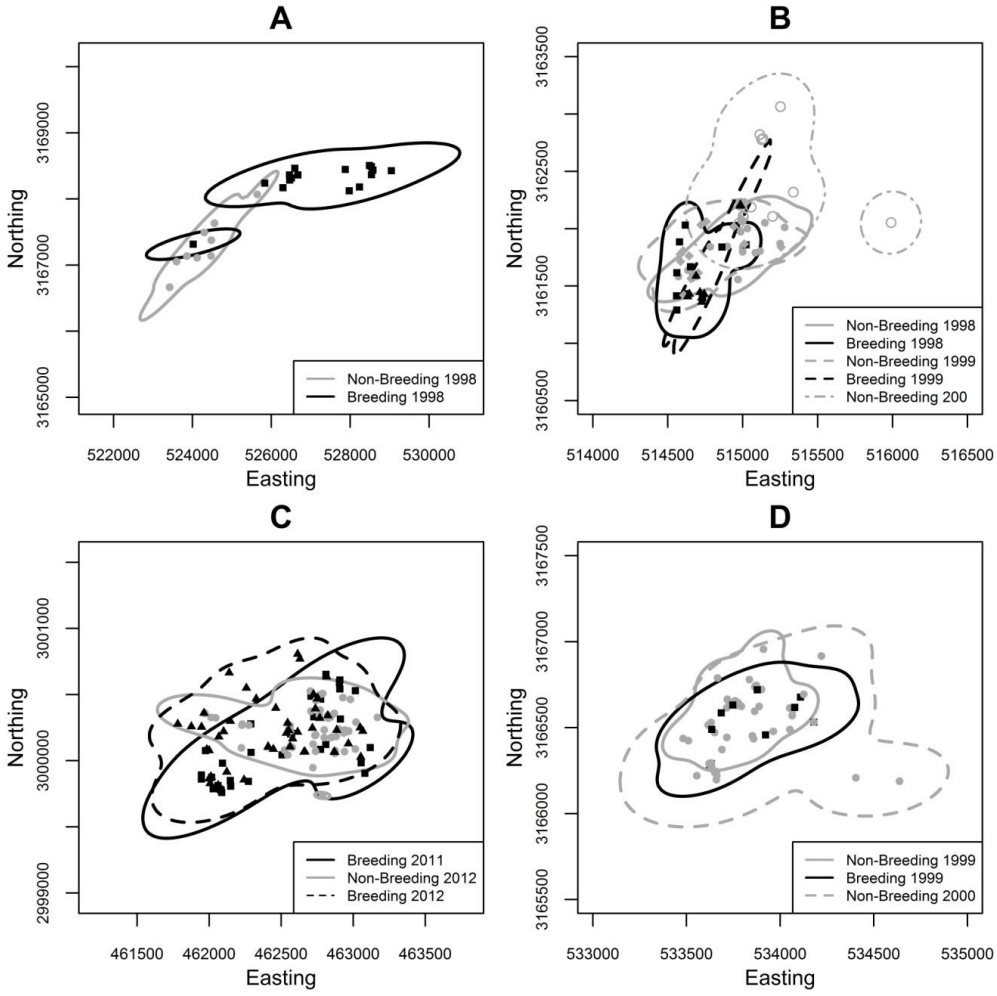

APPENDIX D. DESCRIPTION OF LAND COVER DATA SOURCES

Our first data source was the Cooperative Land Cover Map (CLC) developed by the Florida Natural Areas Inventory and Florida Fish and Wildlife Conservation Commission (Knight 2010; Kawula 2014). The CLC was based on land cover maps produced by Florida's Water Management Districts (WMD) and supplemented with local land cover maps which were often mapped with greater accuracy and thematic resolution. Minimum mapping unit was 0.20 ha. We used CLC v. 3.0 (Florida Fish and Wildlife Conservation Commission and Florida Natural Areas Inventory 2014) for our Highlands data. We assumed that land cover changes within large protected areas (e.g., Kennedy Space Center, Sebastian River State Park Buffer Preserve, Avon Park Bombing Range) were trivial between 1998–2002 and 2013 and therefore used CLC data within these areas. However, because of subsequent land cover changes in the remainder of our Brevard study area following the collection of our telemetry data, we used land cover data from regional water management districts collected at the same time as our telemetry data. We used the St. John's Water WMD from 2000 (St. John's River Water Management District [SJRWMD] 2002) for the Cape Canaveral and Indian River study areas and 2004 land cover data from the South Florida WMD (South Florida Water Management District 2004) and Southwest Florida WMD (Southwest Florida Water Management District 2004) for the Avon Park study areas. Minimum mapping units were 0.81 ha. We visually inspected all our study areas to ensure that no obvious changes were unaccounted for and manually redigitized or reclassified habitat patches where necessary to ensure that our habitat data was as accurate as possible to the on-ground conditions when our telemetry data were collected. All CLC and WMD layers were obtained as

shapefiles but because the CLC data is also provided as a 15-m raster we converted all GIS data to 15-m rasters.

We supplemented the wetlands land cover with the 2014 National Wetlands Inventory (NWI) GIS data (U. S. Fish and Wildlife Service 2014). Minimum mapping units was 0.40 ha. We visually inspected the Cape Canaveral, Indian River, and Avon Park study areas and manually removed newer water bodies, primarily anthropogenic ponds, in the NWI data that were not present when the telemetry data were collected. However, after these manual corrections, we still found some discrepancies between the NWI and CLC/WMD data. Because the direction of these discrepancies was not consistent between data sources, we adopted a conservative approach where we classified a pixel as wetland if it was mapped as a wetland by either the NWI or CLC/WMD data.

APPENDIX E. DESCRIPTION OF ADDITIONAL HABITAT COVARIATES.

We mapped paved roads using the 1998 U.S. Geologic Survey's 1:24,000 roads layer (www.fgdl.org, accessed 1 Jun 2015) and reclassified road categories into primary, secondary, and tertiary roads (U.S. Geological Survey 1990, Appendix C).

We mapped linear wetland features (i.e., rivers, streams, canals, and ditches) using the National Hydrography Dataset's GIS flowline data at the 1:24,000 scale (U. S. Geologic Survey 2014). We hypothesized that both large canals and rivers containing permanent standing water and smaller, intermittently flooded canals could both be important for eastern indigo snakes. While the NHD data mapped canals of both types, it drastically underrepresented smaller, intermittently flooded canals and ditches. One of us (JMB) manually digitized all canals, both permanent and intermittent, using natural color and color infrared aerial imagery concurrent to the telemetry data of each study area. We took a conservative approach to mapping canals in that if there was uncertainty as to the presence of a canal it was not mapped. We manually measured the width of all mapped NHD features (both canals and natural rivers/streams) and classified features >15 m wide containing standing water as open water. We classified all other canals, ditches, and streams as canals. We combined open water classes from the CLC/WMD data, permanently flooded, tidal, and subtidal wetlands from the NWI data (Federal Geographic Data Committe 2013), and NHD features > 15 m containing standing water as open water.

We measured soil moisture using available water storage (AWS) at 150 cm from the Soil Survey Geographic Database (SSURGO) accessed through the SSURGO Downloader (ESRI 2015). The minimum mapping units ranged from 0.40–4.05 ha.

Because pixel values of zero represent no data (typically open water), we first used our binary open water surface to mask out all open water pixels and filled in remaining zero-value pixels using the average of the surrounding cells in a 7x7 moving window.

We used the normalized differenced vegetation index (NDVI) to characterize vegetation cover. We calculated NDVI from LANDSAT 5 and 7 imagery converted to surface reflectance (Masek et al. 2006) and downloaded from the U.S. Geologic Survey's Earth Explorer data base (http://earthexplorer.usgs.gov/, accessed 15 May 2016). We calculated NDVI during the winter (December–January) and spring (April–May). We were unable to calculate NDVI for summer because of high cloud cover. Because telemetry data were collected over periods of approximately 3–4 yr at each study area, we calculated NDVI from 2–4 seasons from each study area and then averaged NDVI across their respective seasons to minimize the impacts of season-specific idiosyncrasies in NDVI. All habitat layers in vector format (land cover, roads, AWS) were converted to rasters with 15 m pixels and we resampled NDVI from 30 m to 15 m pixels.

APPENDIX F. RECLASSIFICATION OF ROAD CLASSES.

Reclassified road classes from the U.S. Geologic Survey's 1998 1:24,000 scale road GIS data. Additional details are provided in U.S. Geologic Survey (1990).

Major Attribute Code	Minor Attribute Code	Description	New Class
170	201	Primary route, class 1, symbol undivided	Primary
170	202	Primary route, class 1, symbol divided by center line	Primary
170	203	Primary route, class 1, symbol divided, lanes separated	Primary
170	607	Underpass	Primary
170	609	Toll road	Primary
170	613	In service facility or rest area	Primary
170	205	Secondary route, class 2, symbol undivided	Secondary
170	206	Secondary route, class 2, symbol divided by centerline	Secondary
170	207	Secondary route, class 2, symbol divided, lanes separated	Secondary
170	208	Secondary route, class 2, one way, other than divided highway	Secondary
170	402	Cloverleaf or interchange	Secondary
170	209	Road or street, class 3	Tertiary
170	217	Road or street, class 3, symbol divided by centerline	Tertiary
170	218	Road or street, class 3, divided, lanes separated	Tertiary
170	221	Road or street, class 3, one way	Tertiary
170	401	Traffic circle	Tertiary
170	210	Road or street, class 4	Not included
170	219	Road or street, class 4, one way	Not included
170	211	Trail, class 5, other than four-wheel drive vehicle	Not included
170	213	Footbridge	Not included

APPENDIX G. RELATIONSHIPS BETWEEN GENERALIZED PARETO DISTRIBUTION SCALE PARAMETER AND NUMBER OF DAYS BETWEEN TELEMETRY LOCATIONS.

To empirically estimate the relationship between duration and GPD kernel size, we subsampled our telemetry data at intervals of 1–75 days. At each subsampled interval, we calculated the step length between successive locations, estimated the two parameters of the GPD (shape and scale) and modeled their relationship with step duration. Shape was invariant with respect to step duration but scale monotonically increased with increasing step duration. We modeled this relationship using the Michaelis-Menton function to predict scale as a function of step duration. Because the parameters of the GPD varied interactively by sex and season, we estimated separate Michaelis-Menton functions for each sex*season group. We recognized a breeding (October–March) and non-breeding (April–September) season. We held scale constant at its mean value for each sex*season group.

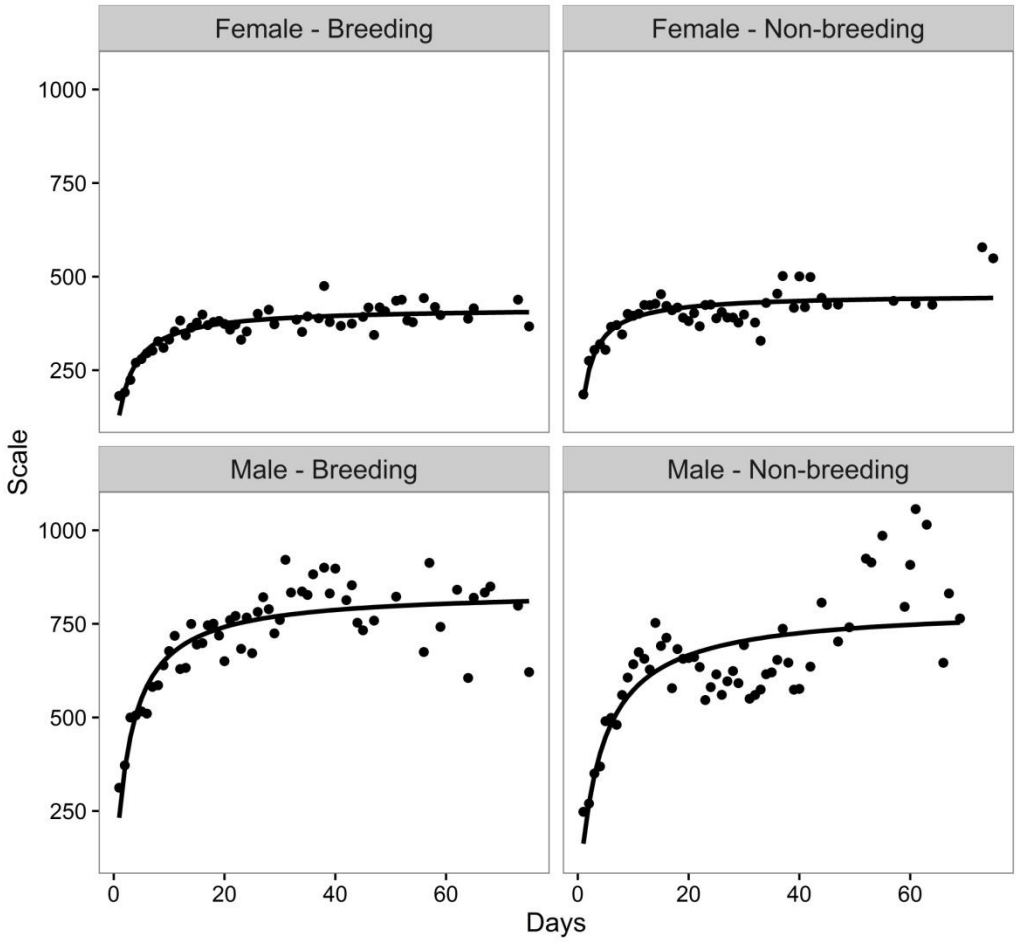

APPENDIX H. MODEL SUPPORT FOR WEIGHTING SCENARIOS.

Model support for different weighting scenarios for roads, urban, urban edge, and undeveloped upland for Level II (HRSF) and III selection. The characteristic (i.e., AIC-best) scales (m) and the ΔAIC for each scenario are reported.

	HRSF		Breeding Females		Non-breeding Females		Breeding Males		Non-breeding Males	
	ΔAIC	Scale	ΔAIC	Scale	ΔAIC	Scale	ΔAIC	Scale	ΔAIC	Scale
Roads										
Equal Weight	0.08	2000	1.03	30	12.5	30	0.56	15	5.18	75
Strong Differences	0.00	2000	0.87	30	11.68	30	0.00	180	0.00	15
Weak Differences	0.05	2000	1.34	15	10.18	30	0.38	15	2.96	15
Strong Effect	0.00	15	0.00	30	0.00	30	1.35	15	1.94	15
Weak Effect	0.08	2000	1.51	30	6.96	30	0.61	15	4.35	15
Urban										
Equal Weight	0.00	15	9.89	15	53	15	0.00	15	0.00	15
Strong Differences	0.96	15	1.14	15	0.00	15	26.52	15	23.49	45
Weak Differences	0.67	15	1.73	15	14.87	15	21.57	15	14.63	45
Strong Effect	0.58	15	0.00	15	30.72	15	39.85	15	8.73	60
Weak Effect	0.30	15	3.06	15	36.66	15	21.42	15	2.20	45
Urban Edge										
Equal Weight	0.00	1100	0.00	75	0.00	15	0.00	30	0.00	165
Strong Differences	0.11	15	15.68	45	3.43	30	36.53	60	23.37	15
Weak Differences	0.25	15	13.63	45	2.06	30	28.43	45	23.10	15
Strong Effect	0.29	15	22.90	30	3.28	30	32.69	60	23.22	15
Weak Effect	0.23	1200	14.65	45	0.46	30	19.04	45	22	15
Undeveloped Upland										
No Rural	2.93	45	2.73	15	3.98	15	62.88	15	5.05	15

Strong Difference	2.14	45	0.00	15	0.62	15	47.27	15	2.19	15
Weak Difference	1.02	45	0.94	15	0.00	15	24.71	15	0.00	15
With Rural	0.00	45	12.8	15	9.37	15	0.00	15	2.2	15

APPENDIX I. DESCRIPTION OF LAND COVER DATA SOURCES AND CREATION OF RESOURCE SELECTION FUNCTION SURFACES.

We selected our landscape covariates based on a previous study on EIS habitat selection (Bauder et al. 2018). We used the Cooperative Land Cover Map (CLC) v.3.2 shapefile (published October 2016) developed by the Florida Natural Areas Inventory and Florida Fish and Wildlife Conservation Commission (Knight 2010; Kawula 2014, accessed 19 Apr 2017 at http://myfwc.com/research/gis/applications/articles/Cooperative-Land-Cover). The CLC was based on land cover maps produced by Florida's Water Management Districts and supplemented with local land cover maps which were often mapped with greater accuracy and thematic resolution. We used the data "as-is" with the exception of four polygons classified as Roads (Site Codes 1840 and 1842) that, after visual inspection, were reclassified as Unimproved Pasture. We converted the CLC shapefile (and all subsequent shapefiles) to 15 m raster images. We then used the 2014–2016 National Wetlands Inventory (NWI) GIS data (U. S. Fish and Wildlife Service 2014, available at https://www.fws.gov/wetlands/data/Mapper.html) and the National Hydrography Dataset's (NHD) GIS flowline data at the 1:24,000 scale (U. S. Geologic Survey 2014) to define canals, wetlands, and open water. We first identified all Open Water pixels using the CLC and NWI data following the classification schemes in Appendices B and C. We then classified all NHD features as Canal or Open Water using their FCODEs and intersection with CLC/NWI Open Water or Wetland pixels as described in Appendix D. Having identified all Canal and Open Water pixels, we then removed all CLC pixels classified as Roads (Site Codes 1840–1842), Cultural Riverine

(4200), and Ditch (4220) by replacing them with the modal pixel value in a 7x7 pixel moving window.

We combined and reclassified these data sources into separate land cover surfaces for Urban, Undeveloped, Wetland, Citrus, Improved Pasture, and Open Water following Bauder et al. (2018). Because of inconsistent discrepancies between the CLC and NWI with regards to wetland classification, we adopted a conservative approach where we classified a pixel as wetland if it was mapped as a wetland by either data source. Because Bauder et al. (2018) found that different urban development intensities had no influence on multi-scale EIS habitat selection we also combined all urban development intensities.

We used the 2016 TIGER roads layer (U. S. Census Bureau 2016) to map paved roads and reclassified roads to approximate the road classes from the 1998 U.S. Geologic Survey's (USGS) 1:24,000 roads layer (U.S. Geological Survey 1990) used by Bauder et al. (2018). Specifically, we considered route type codes (i.e., RTTYP) "U" as primary roads, "S" and "C" as secondary roads, and "M" and "O" as tertiary roads. The TIGER and USGS roads were very similar for primary and secondary roads although there were some relatively minor and inconsistent differences for tertiary roads between the two data sources.

We measured soil moisture using available water storage (AWS) at 150 cm from the Soil Survey Geographic Database (SSURGO) accessed through the SSURGO Downloader 2014 (ESRI 2014, accessed 14 June 2017 at http://www.arcgis.com/home/item.html?id=4dbfecc52f1442eeb368c435251591ec). We converted the downloaded shapefiles into 15 m pixel rasters. Because pixel values of zero represent no data (typically open water or wetland), we used a two step process to fill

these pixels. First, we replace all zero-value AWS pixels that intersected wetlands with the mean AWS value across all wetland pixels. Second, we used our binary Open Water raster to mask all AWS pixels intersecting open water and filled in remaining zero-value pixels using the average of the surrounding cells in a 7x7 moving window. We then calculated the standard deviation of AWS (SD AWS) using a Uniform kernel with the *focal* function in RASTER package (Hijmans 2017).

We downloaded Normalized Vegetation Difference Index (NDVI) data calculated from LANDSAT 8 OLI/TIRS using the U.S. Geologic Survey's Earth Explorer data base via the bulk order service (https://espa.cr.usgs.gov/ordering/new/, accessed June 2016). We used LANDSAT 8 imagery to correspond as closely as possible to the date of our CLC land cover data. We masked clouds and cloud shadows from each image using its associated pixel_qa band which uses the Fmask algorithm of Zhu and Woodcock (2012) and Zhu et al. (2015) and a default cloud probability of 22.5%. Following Bauder et al. (2018), we calculated a mean winter NDVI using images from 11 Dec. 2014, 29 Jan. 2015, 28 Nov. 2015, 16 Dec. 2016, and 2 Feb. 2017 and a mean spring NDVI using images from 14 May 2013, 2 Apr. 2015, 6 May 2016, 7 April 2017, and 9 May 2017. We assigned cloud/cloud shadow pixels as NA and took the arithmetic mean for each across all images. Remaining NA pixels made up a small percentage of our study area (< 1%) and were typically associated with impervious surfaces and buildings so we assigned remaining NA pixels as the mean across all images prior to masking clouds/cloud shadows. After this step, approximately 0.01% of pixels were still NA; we replaced these with the mean of a 3 × 3 moving window. We then resampled NDVI from its original 30 m pixel resolution to 15 m pixels using ArcGIS 10.5.

APPENDIX J. CLASSIFICATION SYSTEM FOR COMBINING LAND COVER CATEGORIES FROM THE FLORIDA NATURAL AREAS INVENTORY'S COOPERATIVE LAND COVER MAP.

Reclassified land cover types and their corresponding Florida Land Cover Classification System (FLCS) categories at both the Site and State level from the Florida Natural Area Inventory's (FNAI) Cooperative Land Cover map v.3.2. Additional details of the FLCS classes are provided in Knight (2010) and Kawula (2014). We used the land covers Urban, Undeveloped, Wetland, Citrus, Improved Pasture, and Open Water to create resource selection function surfaces following Bauder et al. (2018). Land covers not listed were not included in our study area.

Site Level FLCS Code	Site Level Description	State Level Description	Reclassified Category
1110	Upland Hardwood Forest	Upland Hardwood Forest	Undeveloped
1111	Dry Upland Hardwood Forest	Upland Hardwood Forest	Undeveloped
1112	Mixed Hardwoods	Upland Hardwood Forest	Undeveloped
1120	Mesic Hammock	Mesic Hammock	Undeveloped
1122	Prairie Mesic Hammock	Mesic Hammock	Undeveloped
1123	Live Oak	Mesic Hammock	Undeveloped
1124	Pine - Mesic Oak	Mesic Hammock	Undeveloped
1125	Cabbage Palm	Mesic Hammock	Undeveloped
1130	Rockland Hammock	Rockland Hammock	Undeveloped
1131	Thorn Scrub	Rockland Hammock	Undeveloped
1140	Slope Forest	Slope Forest	Undeveloped
1150	Xeric Hammock	Xeric Hammock	Undeveloped
1200	High Pine and Scrub	High Pine and Scrub	Undeveloped
1210	Scrub	Scrub	Undeveloped
1211	Oak Scrub	Scrub	Undeveloped
1212	Rosemary Scrub	Scrub	Undeveloped
1213	Sand Pine Scrub	Sand Pine Scrub	Undeveloped
1214	Coastal Scrub	Coastal Scrub	Undeveloped
1220	Upland Mixed Woodland	High Pine and Scrub	Undeveloped
1230	Upland Coniferous	High Pine and Scrub	Undeveloped
1231	Upland Pine	Upland Pine	Undeveloped
1240	Sandhill	Sandhill	Undeveloped
1300	Pine Flatwoods and Dry Prairie	Pine Flatwoods and Dry	Undeveloped

		Prairie	
1310	Dry Flatwoods	Dry Flatwoods	Undeveloped
1311	Mesic Flatwoods	Mesic Flatwoods	Undeveloped
1312	Scrubby Flatwoods	Scrubby Flatwoods	Undeveloped
1320	Pine Rockland	Pine Rockland	Undeveloped
1330	Dry Prairie	Dry Prairie	Undeveloped
1340	Palmetto Prairie	Palmetto Prairie	Undeveloped
1400	Mixed Hardwood-Coniferous	Mixed Hardwood-Coniferous	Undeveloped
1410	Successional Hardwood Forest	Mixed Hardwood-Coniferous	Undeveloped
1500	Shrub and Brushland	Shrub and Brushland	Undeveloped
1510	Other Shrubs and Brush	Shrub and Brushland	Undeveloped
1600	Coastal Uplands	Coastal Uplands	Undeveloped
1610	Beach Dune	Coastal Uplands	Undeveloped
1620	Coastal Berm	Coastal Uplands	Undeveloped
1630	Coastal Grassland	Coastal Uplands	Undeveloped
1640	Coastal Strand	Coastal Strand	Undeveloped
1650	Maritime Hammock	Maritime Hammock	Undeveloped
1660	Shell Mound	Coastal Uplands	Undeveloped
1670	Sand Beach (Dry)	Sand Beach (Dry)	Sand
1710	Sinkhole	Barren and Outcrop Communities	Barren
1720	Upland Glade	Upland Glade	Barren
1740	Keys Cactus Barren	Barren and Outcrop Communities	Barren
1750	Bare Soil	Barren and Outcrop Communities	Barren
1760	Exposed Rock	Barren and Outcrop Communities	Barren
1800	Cultural - Terrestrial	Cultural - Terrestrial	HiUrban
1810	Mowed Grass	Cultural - Terrestrial	LowUrban
1811	Vegetative Berm	Cultural - Terrestrial	LowUrban
1812	Highway Rights of Way	Cultural - Terrestrial	LowUrban
1821	Low Intensity Urban	Low Intensity Urban	LowUrban
18211	Urban Open Land	Low Intensity Urban	Undeveloped
18211 1	Urban Open Forested	Low Intensity Urban	Undeveloped
18211 2	Urban Open Pine	Low Intensity Urban	Undeveloped
18212	Residential, Low Density	Low Intensity Urban	LowUrban
18213	Grass	Low Intensity Urban	LowUrban
18213 1	Parks and Zoos	Low Intensity Urban	LowUrban

18213 2	Golf courses	Low Intensity Urban	LowUrban
18213 3	Ballfields	Low Intensity Urban	LowUrban
18213 4	Cemeteries	Low Intensity Urban	LowUrban
18213 5	Community rec. facilities	Low Intensity Urban	LowUrban
18214	Trees	Low Intensity Urban	Undeveloped
1822	High Intensity Urban	High Intensity Urban	HiUrban
18221	Residential, Med. Density - 2-5 Dwelling Units/AC	High Intensity Urban	MedUrban
18222	Residential, High Density > 5 Dwelling Units/AC	High Intensity Urban	HiUrban
18223	Commercial and Services	High Intensity Urban	HiUrban
18224	Industrial	High Intensity Urban	HiUrban
18225	Institutional	High Intensity Urban	HiUrban
1830	Rural	Rural	Undeveloped
1831	Rural Open	Rural	Undeveloped
18311	Rural Open Forested	Rural	Undeveloped
18311 1	Oak - Cabbage Palm Forests	Rural	Undeveloped
18312	Rural Open Pine	Rural	Undeveloped
1832	Rural Structures	Rural	LowUrban
1833	Agriculture	Rural	Agriculture
18331	Cropland/Pasture	Cropland/Pasture	Agriculture
18331 1	Row Crops	Cropland/Pasture	Agriculture
18331 2	Field Crops	Cropland/Pasture	Agriculture
18331 21	Sugarcane	Sugarcane	Agriculture
18331 3	Improved Pasture	Low Intensity Urban	Improved Pasture
18331 4	Unimproved/Woodland Pasture	Rural	Undeveloped
18331 5	Other Open Lands - Rural	Cropland/Pasture	Fallow
18331 51	Fallow Cropland	Cropland/Pasture	Fallow
18332	Orchards/Groves	Orchards/Groves	Citrus
18332 1	Citrus	Orchards/Groves	Citrus
18332 2	Fruit Orchards	Orchards/Groves	Citrus

18332 3	Pecan	Orchards/Groves	Citrus
18332 4	Fallow Orchards	Orchards/Groves	AbndCitrus
18333	Tree Plantations	Tree Plantations	Undeveloped
18333 1	Hardwood Plantations	Tree Plantations	Undeveloped
18333 2	Coniferous Plantations	Tree Plantations	Undeveloped
18334	Vineyard and Nurseries	Vineyard and Nurseries	Nurs
18334 1	Tree Nurseries	Vineyard and Nurseries	Nurs
18334 2	Sod Farms	Vineyard and Nurseries	Nurs
18334 3	Ornamentals	Vineyard and Nurseries	Nurs
18334 4	Vineyards	Vineyard and Nurseries	Nurs
18334 5	Floriculture	Vineyard and Nurseries	Nurs
18335	Other Agriculture	Other Agriculture	SpecFarms
18335 1	Feeding Operations	Other Agriculture	SpecFarms
18335 2	Specialty Farms	Other Agriculture	SpecFarms
1840	Transportation	Transportation	Roads
1841	Roads	Transportation	Roads
1842	Rails	Transportation	Roads
1850	Communication	Communication	LowUrban
1860	Utilities	Utilities	LowUrban
1870	Extractive	Extractive	HiUrban
1871	Strip Mines	Extractive	HiUrban
1872	Sand & Gravel Pits	Extractive	HiUrban
1873	Rock Quarries	Extractive	HiUrban
1874	Oil & Gas Fields	Extractive	HiUrban
1875	Reclaimed Lands	Extractive	HiUrban
1876	Abandoned Mining Lands	Extractive	HiUrban
1877	Spoil Area	Extractive	Spoil
1880	Bare Soil/Clear Cut	Bare Soil/Clear Cut	Spoil
2100	Freshwater Non-Forested Wetlands	Freshwater Non-Forested Wetlands	Wetlands
2110	Prairies and Bogs	Prairies and Bogs	Wetlands
2111	Wet Prairie	Prairies and Bogs	Wetlands
21111	Wiregrass Savanna	Prairies and Bogs	Wetlands
21112	Cutthroat Seep	Prairies and Bogs	Wetlands

2112	Mixed Scrub-Shrub Wetland	Prairies and Bogs	Wetlands
21121	Shrub Bog	Prairies and Bogs	Wetlands
2113	Marl Prairie	Prairies and Bogs	Wetlands
2114	Seepage Slope	Prairies and Bogs	Wetlands
2120	Marshes	Marshes	Wetlands
2121	Isolated Freshwater Marsh	Isolated Freshwater Marsh	Wetlands
21211	Depression Marsh	Isolated Freshwater Marsh	Wetlands
21212	Basin Marsh	Isolated Freshwater Marsh	Wetlands
2122	Coastal Interdunal Swale	Marshes	Wetlands
2123	Floodplain Marsh	Floodplain Marsh	Wetlands
21231	Freshwater Tidal Marsh	Floodplain Marsh	Wetlands
2124	Slough Marsh	Marshes	Wetlands
2125	Glades Marsh	Marshes	Wetlands
2130	Marshes (Continued)	Marshes	Wetlands
2131	Sawgrass	Marshes	Wetlands
2140	Floating/Emergent Aquatic Vegetation	Freshwater Non-Forested Wetlands	Wetlands
2141	Slough	Freshwater Non-Forested Wetlands	Wetlands
2142	Water Lettuce	Freshwater Non-Forested Wetlands	Wetlands
2145	Duck Weed	Freshwater Non-Forested Wetlands	Wetlands
2146	Water Lily	Freshwater Non-Forested Wetlands	Wetlands
2150	Submergent Aquatic Vegetation	Freshwater Non-Forested Wetlands	Wetlands
2200	Freshwater Forested Wetlands	Freshwater Forested Wetlands	Wetlands
2210	Cypress/Tupelo(incl Cy/Tu mixed)	Cypress/Tupelo(incl Cy/Tu mixed)	Wetlands
2211	Cypress	Cypress	Wetlands
2212	Tupelo	Cypress/Tupelo(incl Cy/Tu mixed)	Wetlands
2213	Isolated Freshwater Swamp	Isolated Freshwater Swamp	Wetlands
22131	Dome Swamp	Dome Swamp	Wetlands
221312	Gum Pond	Dome Swamp	Wetlands
22132	Basin Swamp	Basin Swamp	Wetlands
2214	Strand Swamp	Strand Swamp	Wetlands
2215	Floodplain Swamp	Floodplain Swamp	Wetlands

22151	Freshwater Tidal Swamp	Floodplain Swamp	Wetlands
2220	Other Coniferous Wetlands	Other Coniferous Wetlands	Wetlands
2221	Wet Flatwoods	Wet Flatwoods	Wetlands
22211	Hydric Pine Flatwoods	Wet Flatwoods	Wetlands
22211 1	Cutthroat Grass Flatwoods	Wet Flatwoods	Wetlands
22211 2	Cabbage Palm Flatwoods	Wet Flatwoods	Wetlands
22212	Hydric Pine Savanna	Wet Flatwoods	Wetlands
2222	Pond Pine	Other Coniferous Wetlands	Wetlands
2230	Other Hardwood Wetlands	Other Hardwood Wetlands	Wetlands
2231	Baygall	Baygall	Wetlands
22311	Bay Swamp	Baygall	Wetlands
22312	South Florida Bayhead	Baygall	Wetlands
2232	Hydric Hammock	Hydric Hammock	Wetlands
22321	Coastal Hydric Hammock	Hydric Hammock	Wetlands
22322	Prairie Hydric Hammock	Hydric Hammock	Wetlands
22323	Cabbage Palm Hammock	Hydric Hammock	Wetlands
2233	Mixed Wetland Hardwoods	Freshwater Forested Wetlands	Wetlands
22331	Bottomland Forest	Freshwater Forested Wetlands	Wetlands
22332	Alluvial Forest	Freshwater Forested Wetlands	Wetlands
2234	Titi Swamp	Other Hardwood Wetlands	Wetlands
2240	Other Wetland Forested Mixed	Freshwater Forested Wetlands	Wetlands
2241	Cypress/Hardwood Swamps	Freshwater Forested Wetlands	Wetlands
2242	Cypress/Pine/Cabbage Palm	Freshwater Forested Wetlands	Wetlands
2300	Non-vegetated Wetland	Non-vegetated Wetland	Wetlands
2400	Cultural - Palustrine	Cultural – Palustrine	Wetlands
2410	Impounded Marsh	Cultural – Palustrine	Wetlands
2420	Impounded Swamp	Cultural – Palustrine	Wetlands
2430	Grazed Wetlands	Cultural – Palustrine	Wetlands
2440	Clearcut Wetland	Cultural – Palustrine	Wetlands
2450	Wet Coniferous Plantations	Cultural – Palustrine	Wetlands
3000	Lacustrine	Lacustrine	Open Water
3100	Natural Lakes and Ponds	Natural Lakes and Ponds	Open Water
3110	Limnetic	Natural Lakes and Ponds	Open Water

3111	Clastic Upland Lake	Natural Lakes and Ponds	Open Water
3112	Coastal Dune Lake	Natural Lakes and Ponds	Open Water
3113	Flatwoods/Prairie/Marsh Lake	Natural Lakes and Ponds	Open Water
3114	River Floodplain Lake/Swamp Lake	Natural Lakes and Ponds	Open Water
3115	Sinkhole Lake	Natural Lakes and Ponds	Open Water
3116	Coastal Rockland Lake	Natural Lakes and Ponds	Open Water
3117	Sandhill Lake	Natural Lakes and Ponds	Open Water
3118	Major Springs	Natural Lakes and Ponds	Open Water
3120	Littoral	Natural Lakes and Ponds	Open Water
3200	Cultural - Lacustrine	Cultural - Lacustrine	Open Water
3210	Artificial/Farm Pond	Cultural - Lacustrine	Open Water
3211	Aquacultural Ponds	Cultural - Lacustrine	Open Water
3220	Artificial Impoundment/Reservoir	Cultural - Lacustrine	Open Water
3230	Quarry Pond	Cultural - Lacustrine	Open Water
3240	Sewage Treatment Pond	Cultural - Lacustrine	Open Water
3250	Stormwater Treatment Areas	Cultural - Lacustrine	Open Water
3260	Industrial Cooling Pond	Cultural - Lacustrine	Open Water
4000	Riverine	Riverine	Open Water
4100	Natural Rivers and Streams	Natural Rivers and Streams	Open Water
4110	Alluvial Stream	Natural Rivers and Streams	Open Water
4120	Blackwater Stream	Natural Rivers and Streams	Open Water
4130	Spring-run Stream	Natural Rivers and Streams	Open Water
4140	Seepage Stream	Natural Rivers and Streams	Open Water
4160	Tidally-influenced Stream	Natural Rivers and Streams	Open Water
4170	Riverine Sandbar	Natural Rivers and Streams	Open Water
4200	Cultural - Riverine	Cultural – Riverine	CulturalRiverine
4210	Canal	Cultural – Riverine	Open Water
4220	Ditch/Artificial Intermittent Stream	Cultural – Riverine	Ditch
5000	Estuarine	Estuarine	Estuarine
5100	Subtidal	Estuarine	Estuarine
5200	Intertidal	Estuarine	Wetlands
5210	Exposed Limestone	Estuarine	Estuarine
52111	Keys Tidal Rock Barren	Keys Tidal Rock Barren	Estuarine
5212	Non-vegetated	Estuarine	Estuarine
5220	Tidal Flat	Tidal Flat	Wetlands
5221	Mud	Tidal Flat	Estuarine

5222	Sand	Tidal Flat	Estuarine
5230	Oyster Bar	Estuarine	Estuarine
5240	Salt Marsh	Salt Marsh	Wetlands
5250	Mangrove Swamp	Mangrove Swamp	Wetlands
5251	Buttonwood Forest	Mangrove Swamp	Wetlands
5252	Scrub Mangrove	Scrub Mangrove	Wetlands
5310	Estuarine Ditch/Channel	Cultural – Estuarine	Open Water
5320	Estuarine Artificial Impoundment	Cultural – Estuarine	Open Water
6000	Marine	Marine	Marine
6100	Surf Zone	Marine	Marine
7000	Exotic Plants	Exotic Plants	Undeveloped
7100	Australian Pine	Exotic Plants	Undeveloped
7200	Melaleuca	Exotic Plants	Undeveloped
7300	Brazilian Pepper	Exotic Plants	Undeveloped
7400	Exotic Wetland Hardwoods	Exotic Plants	Wetlands
9100	Unconsolidated Substrate	Unconsolidated Substrate	UnconSub

APPENDIX K. NATIONAL WETLANDS INVENTORY (NWI) ATTRIBUTE CODES CLASSIFIED AS OPEN WATER.

All other attribute codes within our study area were classified as Wetland.

NWI Attribute Code	Open Water
L1AB4H	Yes
L1AB4Hx	Yes
L1AB6H	Yes
L1ABH	Yes
L1ABHx	Yes
L1UBH	Yes
L1UBHh	Yes
L1UBHx	Yes
L1UBKx	Yes
L2AB3/4H	Yes
L2AB3H	Yes
L2AB3Hx	Yes
L2AB4H	Yes
L2AB4Hsx	Yes
L2AB5H	Yes
L2ABH	Yes
L2ABHx	Yes
L2ABKx	Yes
L2EMH	Yes
L2UBHh	Yes
L2UBHsx	Yes

APPENDIX L. CLASSIFICATION SYSTEM FOR CLASSIFYING PIXELS AS CANALS AND OPEN WATER.

National Hydrography Data (NHD) polylines were first reclassified into a NHD Class and converted into 15-m pixel rasters. This raster was added to a reclassified raster of the Florida Natural Area Inventory's Cooperative Land Cover (CLC) map. The summed pixel values were then used for the final classification of Canals and Open Water. See Appendix B for the CLC reclassification codes.

NHD FCODE	NHD Feature Type	Original NHD Feature Description	NHD Class
33400	Connector	Feature type only: no attributes	0
33600	Canal/Ditch	Feature type only: no attributes	1
33601	Canal/Ditch	Canal/Ditch type: aqueduct	1
46000	Stream/River	Feature type only: no attributes	1
46003	Stream/River	Hydrographic category: intermittent	1
46006	Stream/River	Hydrographic category: perennial	3
46007	Stream/River	Hydrographic category: ephemeral	1
55800	Artificial Path	Feature type only: no attributes	2

CLC Class	NHD Class	Final Classification
Other	0	None
Other	1	Canal
Other	2	None
Other	3	Canal
Open Water	0	Open Water
Open Water	1	Open Water
Open Water	2	Open Water
Open Water	3	Open Water
Wetland	0	None
Wetland	1	Canal
Wetland	2	None
Wetland	3	Canal
Stream	0	Open Water
Stream	1	Canal
Stream	2	Open Water
Stream	3	Open Water
Cultural Riverine (4200)	1	Canal
Cultural Riverine (4200)	2	Canal
Cultural Riverine (4200)	3	Canal

Canal (4210)	0	Open Water
Canal (4210)	1	Open Water
Canal (4210)	2	Open Water
Canal (4210)	3	Open Water
Ditch (4220)	1	Canal

APPENDIX M. CREATING RESOURCE SELECTION FUNCTION SURFACES.

We followed the procedures of Bauder et al. (2018) to create resource selection surfaces using the land cover data described above. We created surfaces representing Level II (i.e., second order, Johnson 1980) selection using home range selection functions where the unit of observation was an individual's "total" home range polygon estimated using the 95% volume contour of a fixed kernel utilization distribution with the unconstrained bandwidth matrix. Each land cover surface was first smoothed using Gaussian kernel with a bandwidth corresponding to its characteristic scale as described in Bauder et al. (2018). We then smoothed these surfaces again using a Uniform kernel with a 677 m radius which corresponded to an average-sized total home range. This ensured that the value of each pixel approximated the home range-wide average value. We then created predicted surfaces using the 90% model set from Bauder et al. (2018) and summed the AIC-weighted predicted values to obtain model-averaged predicted values. We used the predicted probabilities but emphasize that these probabilities represent relative, not absolute, probabilities of selection.

We created surfaces representing Level III (i.e., third-order, Johnson 1980) selection using the paired-design described in Bauder et al. (2018). Our surfaces that were Gaussian smoothed at their characteristic scales represented habitat use. Habitat availability surfaces were created by re-smoothing the Gaussian-smoothed surfaces with a generalized Pareto distribution representing the extent of available habitats within one day's movement. We then differenced the used and available surface for each landscape covariate and calculated model-averaged predicted probabilities using the 90% model set as described above. We created separate Level III surfaces for males and females during

the breeding and non-breeding season and varied the size of the generalized Pareto distribution for each group.

APPENDIX N. PARAMETER VALUES FOR THE INDIVIDUAL-BASED MODEL.

Values of POM parameters were calibrated using pattern oriented modeling.

Parameter	Value	Description/Reference
Maximum Age	12 years	Stevenson et al. (2009)
Birth Day	1-Oct	Date at which eggs hatch and new individuals enter the model (Speake et al. 1978, Godwin et al. 2011)
Female Attraction	2	Value assignd to all pixels within a female's 95% fixed kernel home range during the breeding season
Dispersal SD	POM	Standard deviation of the half-normal standard kernel used to create the resistance kernel for dispersal
Maximum Dispersal Distance	22,200 m	Stevenson and Hyslop (2010)
Maximum Background Resistance	POM	Maximum resistance value assigned to non-road pixels for calculating the resistance kernel for movement and dispersal
Maximum Roads Resistance Value	POM	Maximum resistance value assigned to road pixels for calculating the resistance kernel for movement and dispersal
Scale Multiplier	POM	Value by which the scale parameter of the generalized Pareto distribution standard kernel was multiplied to create the movement resistance kernel
Maximum Daily Movement Distance	2,020 m	D.R. Breininger (unpublished data)
Water Barrier Distance	265 m	Distance from land at which open water is considered a barrier (D.R. Breininger, unpublished data)
Male Recruitment Buffer	894 m	Radius of circular uniform kernel used to calculate conspecific home range density for males to determine probability of recruitment
Female Recruitment Buffer	501 m	Radius of circular uniform kernel used to calculate conspecific home range density for females to determine probability of recruitment
Male Logistic Scale	0.05	Scale parameter of a logistic function used to calculate probability of recruitment as a function of conspecific home range density
Male Logistic Inflection	0.09	Inflection parameter of a logistic function used to calculate probability of recruitment as a function of conspecific home range density
Female Logistic Scale	0.05	Scale parameter of a logistic function used to calculate probability of recruitment as a function of conspecific home range density

Female Logistic Inflection	0.22	Inflection parameter of a logistic function used to calculate probability of recruitment as a function of conspecific home range density
Combine Method	Product	Method used to combine probability surfaces to create the redistribution and dispersal kernels
Min. Number of Steps	10	Minimum number of daily time steps required to calculate a utilization distribution (UD)/home range
UD Bandwidth	Unconstrained Reference	Bauder et al. (2010)
UD Number of Days	365 days	Number of days prior to current date used to calcualte a UD/home range
UD Sample	7 days	Subsampling rate to calculate UD/home range
Nesting Date	1 Apr.	Speake et al. (1978), Godwin et al. (2011)
Mean Clutch Size	8.62	Godwin et al. (2011)
SD of Clutch Size	1.7	Godwin et al. (2011)
Age at First Reproduction	3 years	Speake et al. (1978), Godwin et al. (2011)
Annual Probability of Reproducing at 3 years	0.5	Breininger et al. (2004), Hyslop et al. (2012)
Annual Probability of Reproducing at ≥4 years	0.9	Speake et al. (1978), Godwin et al. (2011)
Nest Survival	0.75	Hyslop et al. (2012)
Hatching Rate	0.75	Hyslop et al. (2012)
Hatching Sex Ratio	50:50:00	
Age of Entering the Model	1 year	Age at which new agents are added to the model environment
First-year Survival	0.29	Smith (1987)
Daily Probability of Movement	Variable	Varied by day as described in Bauder et al. (2016)
Movement Kernel GPD Scale - Breeding Season Males	271.3252	Bauder et al. (2016)
Movement Kernel GPD Shape - Breeding Season Males	0.0580	Bauder et al. (2016)
Movement Kernel GPD Scale - Non-Breeding Season Males	252.0699	Bauder et al. (2016)
Movement Kernel GPD Shape - Non-Breeding Season Males	-0.0540	Bauder et al. (2016)

Movement Kernel GPD Scale - Breeding Season Females	158.2161	Bauder et al. (2016)
Movement Kernel GPD Shape - Breeding Season Females	-0.0208	Bauder et al. (2016)
Movement Kernel GPD Scale - Non-Breeding Season Females	163.8718	Bauder et al. (2016)
Movement Kernel GPD Shape - Non-Breeding Season Females	-0.0229	Bauder et al. (2016)
Consp Kernel GPD Scale - Breeding Season Males	0.0000002	Parameters for the GPD used to create the conspecific kernel for movement (Bauder et al. 2016)
Consp Kernel GPD Shape - Breeding Season Males	4.5937584	Parameters for the GPD used to create the conspecific kernel for movement (Bauder et al. 2016)
Consp Kernel GPD Scale - Non-Breeding Season Males	0.0000005	Parameters for the GPD used to create the conspecific kernel for movement (Bauder et al. 2016)
Consp Kernel GPD Shape - Non-Breeding Season Males	3.7454979	Parameters for the GPD used to create the conspecific kernel for movement (Bauder et al. 2016)
Consp Kernel GPD Scale - Breeding Season Females	0.0000034	Parameters for the GPD used to create the conspecific kernel for movement (Bauder et al. 2016)
Consp Kernel GPD Shape - Breeding Season Females	3.1503287	Parameters for the GPD used to create the conspecific kernel for movement (Bauder et al. 2016)
Consp Kernel GPD Scale - Non-Breeding Season Females	0.0000879	Parameters for the GPD used to create the conspecific kernel for movement (Bauder et al. 2016)
Consp Kernel GPD Shape - Non-Breeding Season Females	0.2461834	Parameters for the GPD used to create the conspecific kernel for movement (Bauder et al. 2016)
Primary Road Crossing - Breeding Season Females	0.000000456	Probability of crossing a road when distance from road = 0 m (Bauder et al. 2018)
Secondary Road Crossing - Breeding Season Females	0.298734900	Probability of crossing a road when distance from road = 0 m (Bauder et al. 2018)
Tertiary Road Crossing - Breeding Season Females	0.354970100	Probability of crossing a road when distance from road = 0 m (Bauder et al. 2018)
Primary Road Crossing - Non-breeding Season Females	0.000000580	Probability of crossing a road when distance from road = 0 m (Bauder et al. 2018)
Secondary Road Crossing - Non-	0.090127770	Probability of crossing a road when distance from road = 0 m (Bauder et al.

breeding Season Females		2018)
Tertiary Road Crossing - Non-breeding Season Females	0.253403900	Probability of crossing a road when distance from road = 0 m (Bauder et al. 2018)
Primary Road Crossing - Breeding Season Males	0.000000003	Probability of crossing a road when distance from road = 0 m (Bauder et al. 2018)
Secondary Road Crossing - Breeding Season Males	0.000000008	Probability of crossing a road when distance from road = 0 m (Bauder et al. 2018)
Tertiary Road Crossing - Breeding Season Males	0.314752200	Probability of crossing a road when distance from road = 0 m (Bauder et al. 2018)
Primary Road Crossing - Non-breeding Season Males	0.000000003	Probability of crossing a road when distance from road = 0 m (Bauder et al. 2018)
Secondary Road Crossing - Non-breeding Season Males	0.000000006	Probability of crossing a road when distance from road = 0 m (Bauder et al. 2018)
Tertiary Road Crossing - Non-breeding Season Males	0.226624200	Probability of crossing a road when distance from road = 0 m (Bauder et al. 2018)
Consp Kernel GPD Scale - Males (Dispersal)	6.885351E-30	Parameters for the GPD used to create the conspecific kernel for dispersal
Consp Kernel GPD Shape - Males (Dispersal)	51.0532207	Parameters for the GPD used to create the conspecific kernel for dispersal
Consp Kernel GPD Scale - Females (Dispersal)	0.0000439	Parameters for the GPD used to create the conspecific kernel for dispersal
Consp Kernel GPD Shape - Females (Dispersal)	0.8434534	Parameters for the GPD used to create the conspecific kernel for dispersal
Daily Background Survival Rate	POM	
Daily Roads/Urban Crossing Survival Rate	POM	

APPENDIX O. OBSERVED BETA ESTIMATES AND 95% CONFIDENCE INTERVALS FOR RELATIONSHIPS BETWEEN TOTAL HOME RANGE SIZE AND LANDSCAPE COVARIATES.

Beta estimates are denoted with β while "Stand." represents *z*-score standardized betas. AIC_c model weights are denoted by *w*. Beta estimates for the intercept, sex (level = Male), and Days (number of days tracked) were included in every model and model averaged across all models. A single landscape covariate was included in each model.

LC	β	Lower 95% CI	Upper 95% CI	Stand. β	Stand. Lower 95% CI	Stand. Upper 95% CI	*w*
Intercept	5.810	5.106	6.513	4.085	3.649	4.522	1.000
Sex	1.042	0.732	1.352	1.042	0.732	1.352	1.000
SD NDVI	-17.418	-22.503	-12.332	-0.525	-0.678	-0.372	0.998
Urban	-2.100	-2.885	-1.315	-0.450	-0.619	-0.282	0.002
SD AWS	-0.153	-0.240	-0.067	-0.322	-0.505	-0.140	0.000
Wetlands	1.785	0.742	2.827	0.311	0.130	0.493	0.000
Un-developed	1.442	0.562	2.321	0.300	0.117	0.484	0.000
Pasture	-1.304	-2.909	0.301	-0.155	-0.346	0.036	0.000
Wetland Edge	3.017	-1.176	7.209	0.140	-0.055	0.335	0.000
NDVI	1.104	-1.672	3.880	0.080	-0.121	0.281	0.000
Days	0.001	0.000	0.001	0.001	0.000	0.001	1.000

APPENDIX P. SIMULATED TOTAL HOME RANGE SIZES HOLDING THE SCALE MULTIPLIER CONSTANT

Scale multiplier is three while maximum background resistance (Back) and maximum roads resistance (Rds) are varied. Horizontal gray lines represent the observed median (solid) and inter-quartile ranges (dashed) of observed total home range size. Simulations were run on the Cape Canaveral study area.

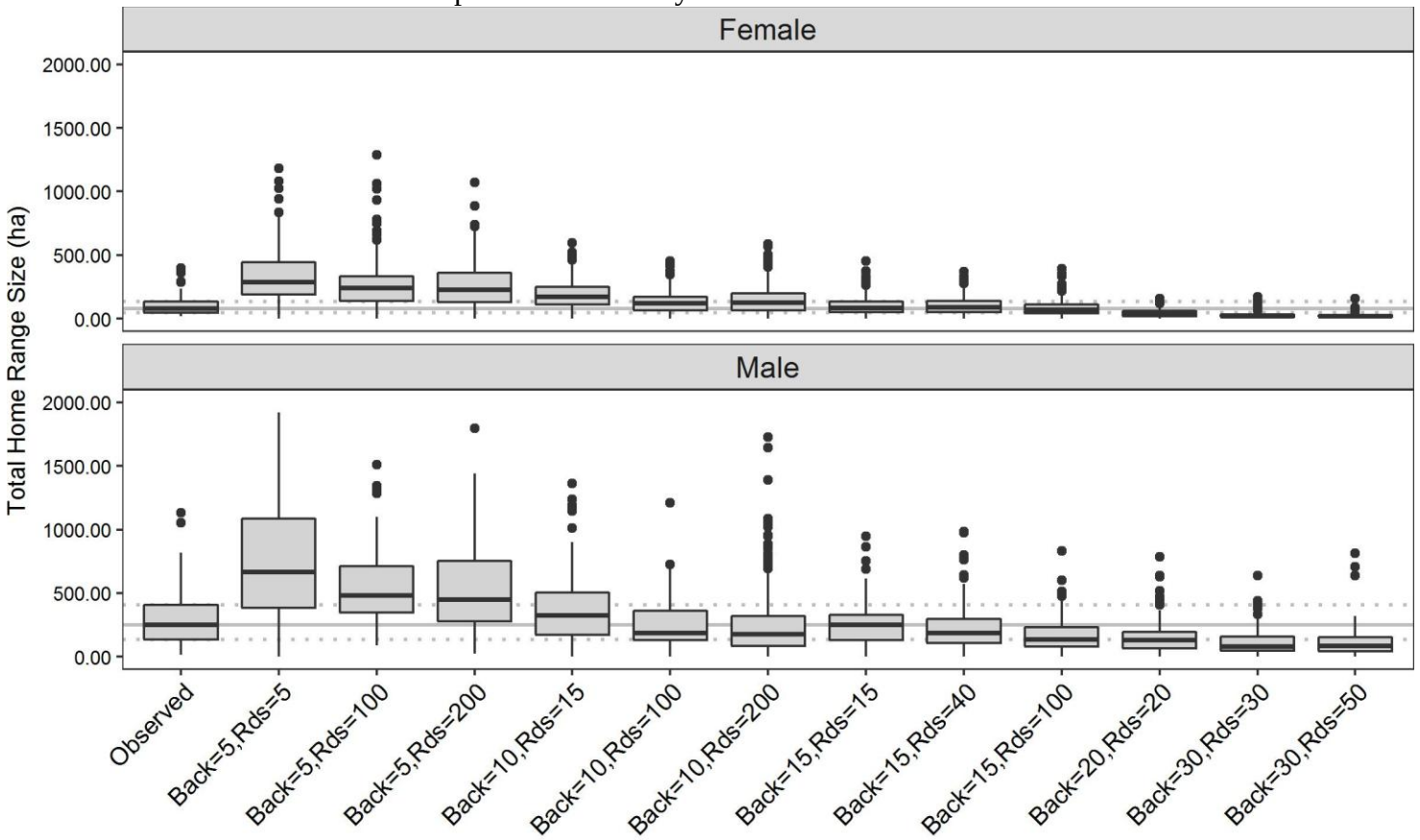

APPENDIX Q. SIMULATED TOTAL HOME RANGE SIZES VARYING THE SCALE MULTIPLIER CONSTANT

Horizontal gray lines represent the observed median (solid) and inter-quartile ranges (dashed) of observed total home range size. Simulations were run on the Cape Canaveral study area.

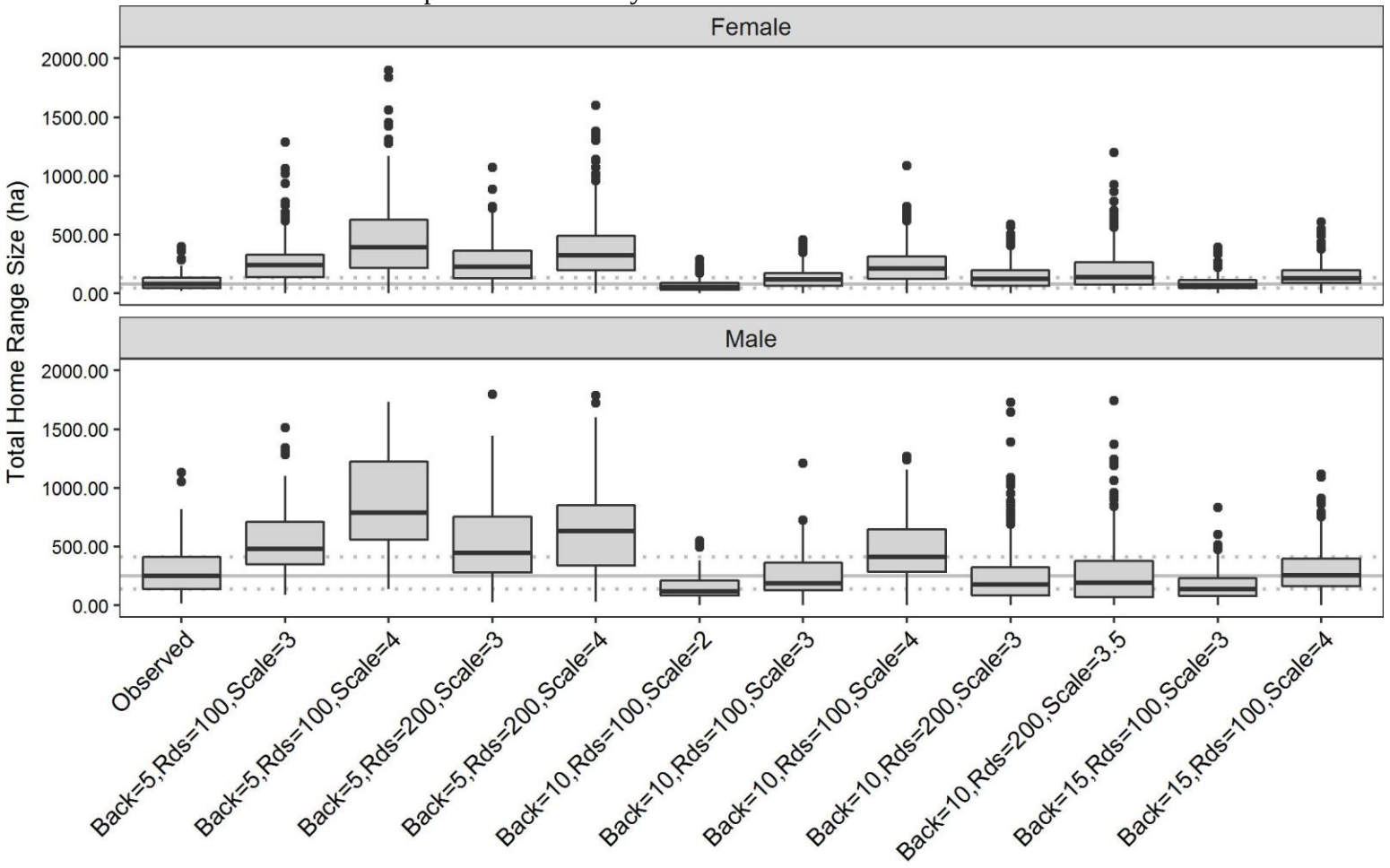

APPENDIX R. BETA ESTIMATES AND 95% CI FOR LANDSCAPE COVARIATE EFFECTS ON TOTAL HOME RANGE SIZE

Scale multiplier is three while maximum background resistance (Back) and maximum roads resistance (Rds) are varied. Simulations were run on the Cape Canaveral study area.

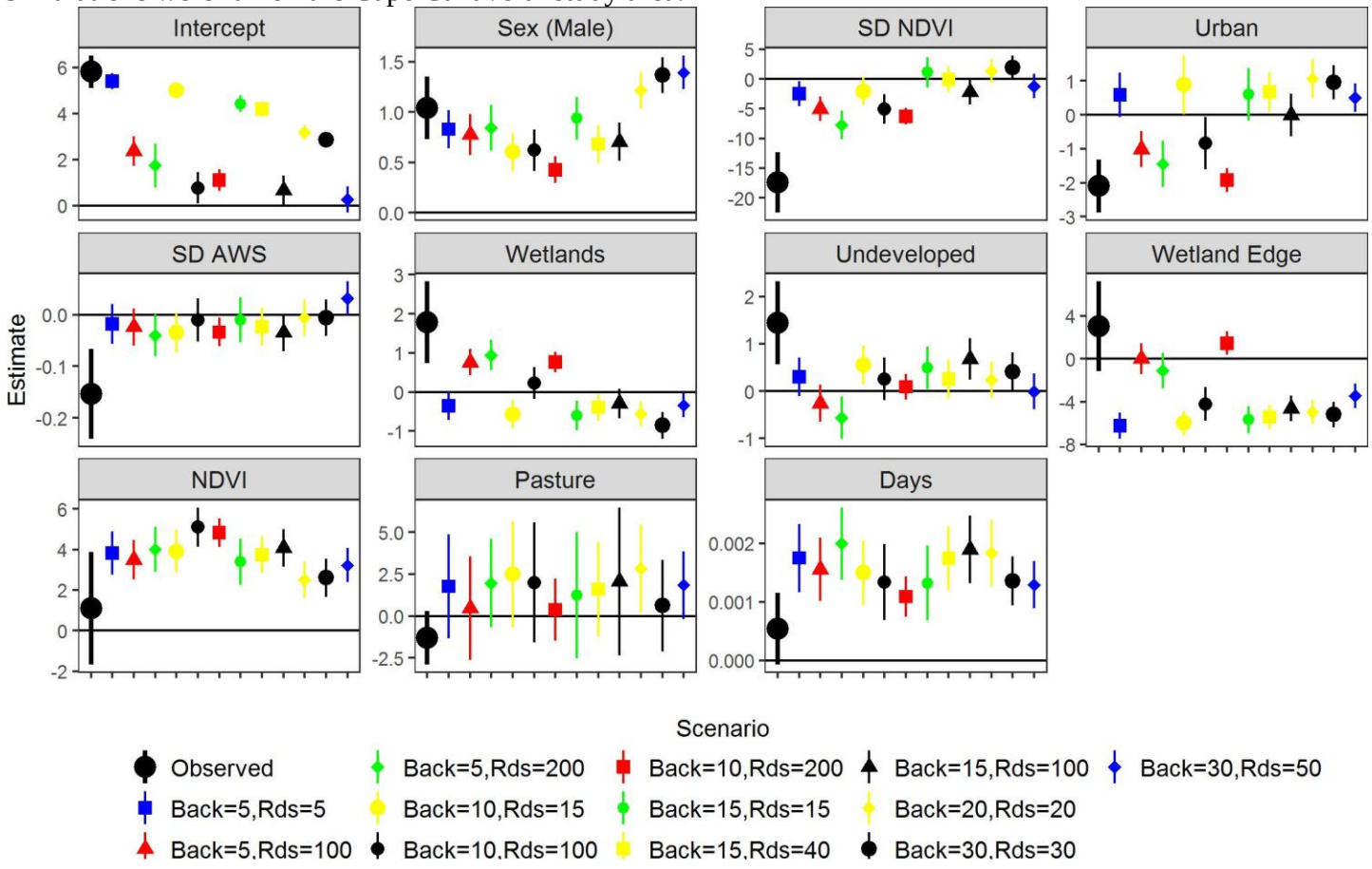

APPENDIX S. BETA ESTIMATES AND 95% CI FOR LANDSCAPE COVARIATE EFFECTS ON TOTAL HOME RANGE SIZE VARYING THE SCALE MULTIPLIER

Simulations were run on the Cape Canaveral study area

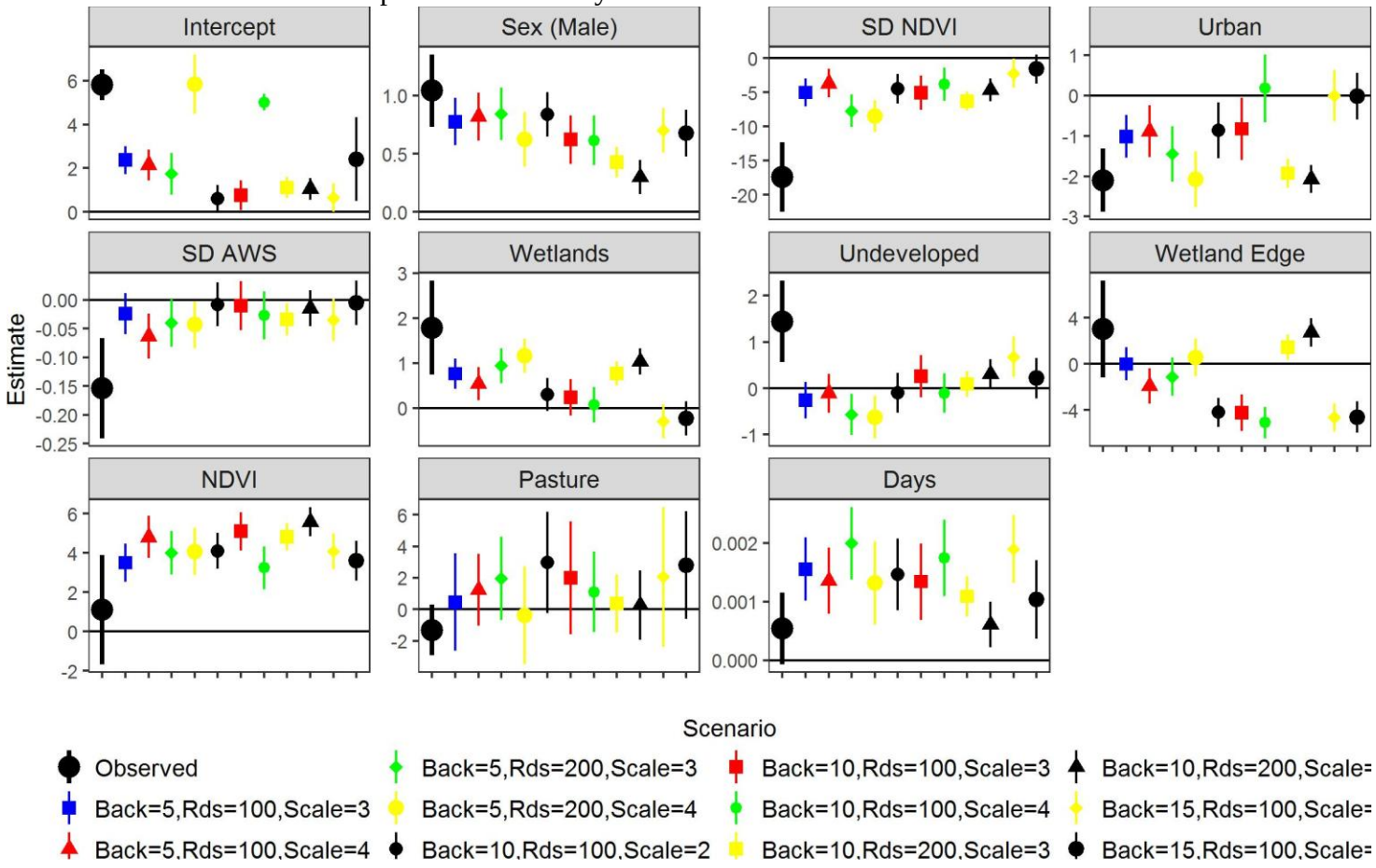

APPENDIX T. WITHIN-INDIVIDUAL 6-MONTH HOME RANGE OVERLAP

B-NB represent consecutive breeding and non-breeding season home ranges, B-B represent consecutive breeding season home ranges, NB-NB represent consecutive non-breeding season home ranges, and B-NB2 represent breeding and non-breeding seasons separated by 12 months. Horizontal gray lines represent the observed median (solid) and inter-quartile ranges (dashed) of observed total home range size. Simulations were run on the Cape Canaveral study area.

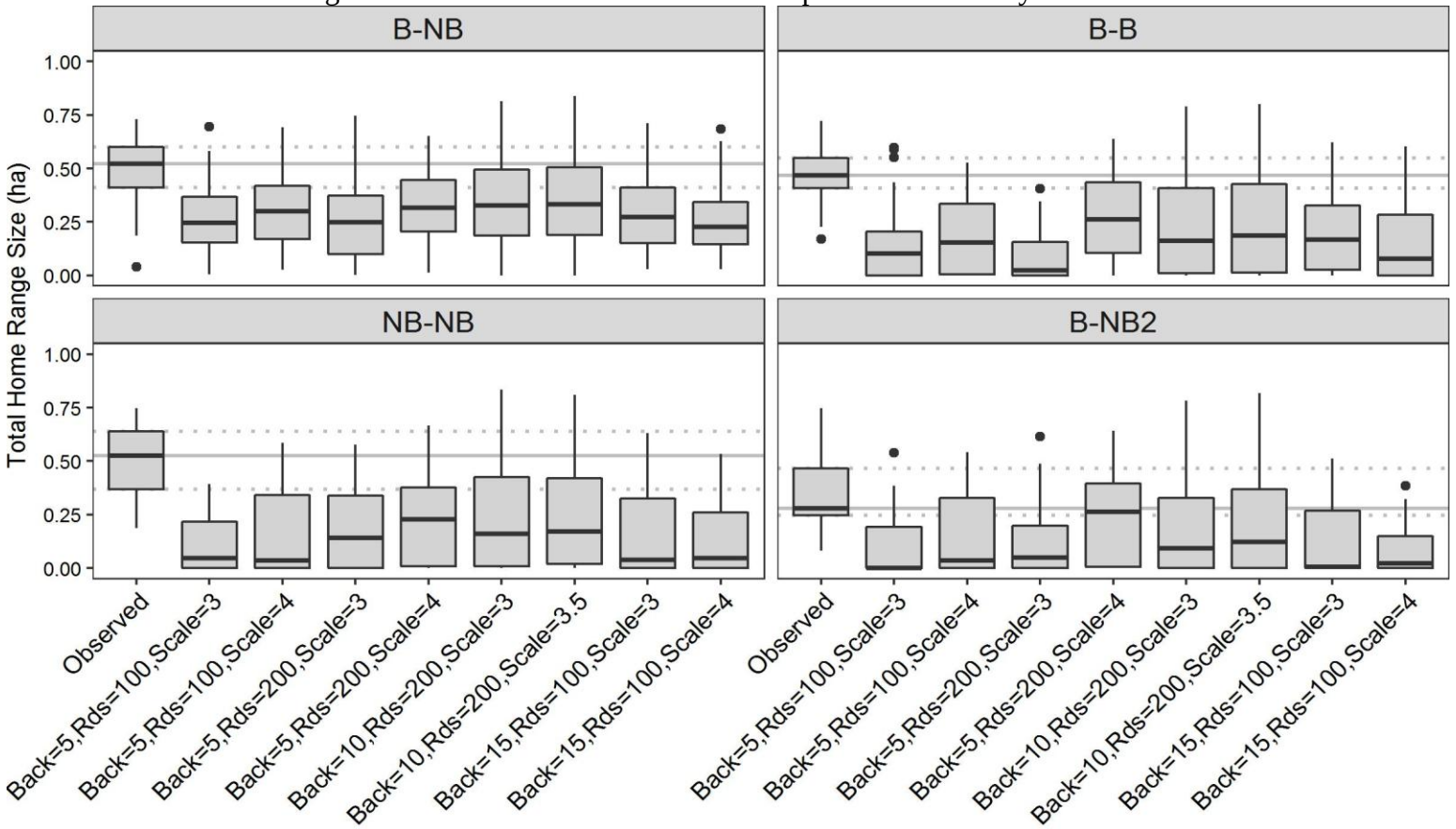

APPENDIX U. WEEKLY SURVIVAL ESTIMATES AS A FUNCTION OF LANDSCAPE COVARIATES

Survival was estimated as a function of roads, urban, and development (Dvlp) measured within 400, 1,100, and 1,100 m radius Uniform kernels, respectively, centered on each agent's total home range centroid using known-fate models. BackS represents background daily survival while Rd/UrbS represents road/urban crossing daily survival. Error bars and dashed lines are 95% CI around observed estimates and predicted values from the simulated data, respectively.

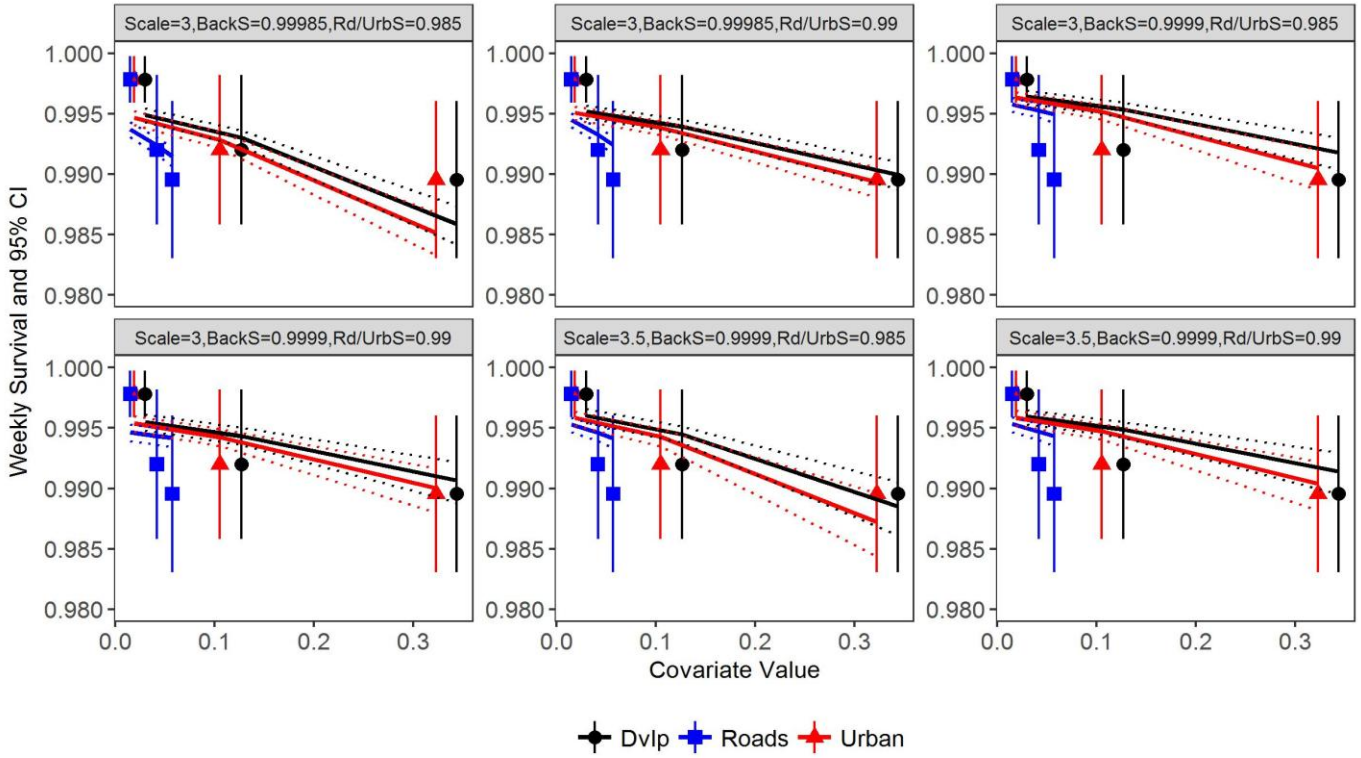

APPENDIX V. CHARACTERISTIC SCALES FOR SIMULATED EIS OCCUPANCY AS A FUNCTION OF MULTI-SCALE LANDSCAPE COVARIATES.

Occupancy was measured using 999 randomly placed plots with 1.013 m radii. Landscape covariates were measured using concentric Uniform kernels with radii from 677–3,077 m.ConsLands are the proportion of conservation lands. Roads_EQ are roads with all three road classes given equal weight, and Roads_SE are roads with primary and secondary roads given five times the weight as tertiary roads.

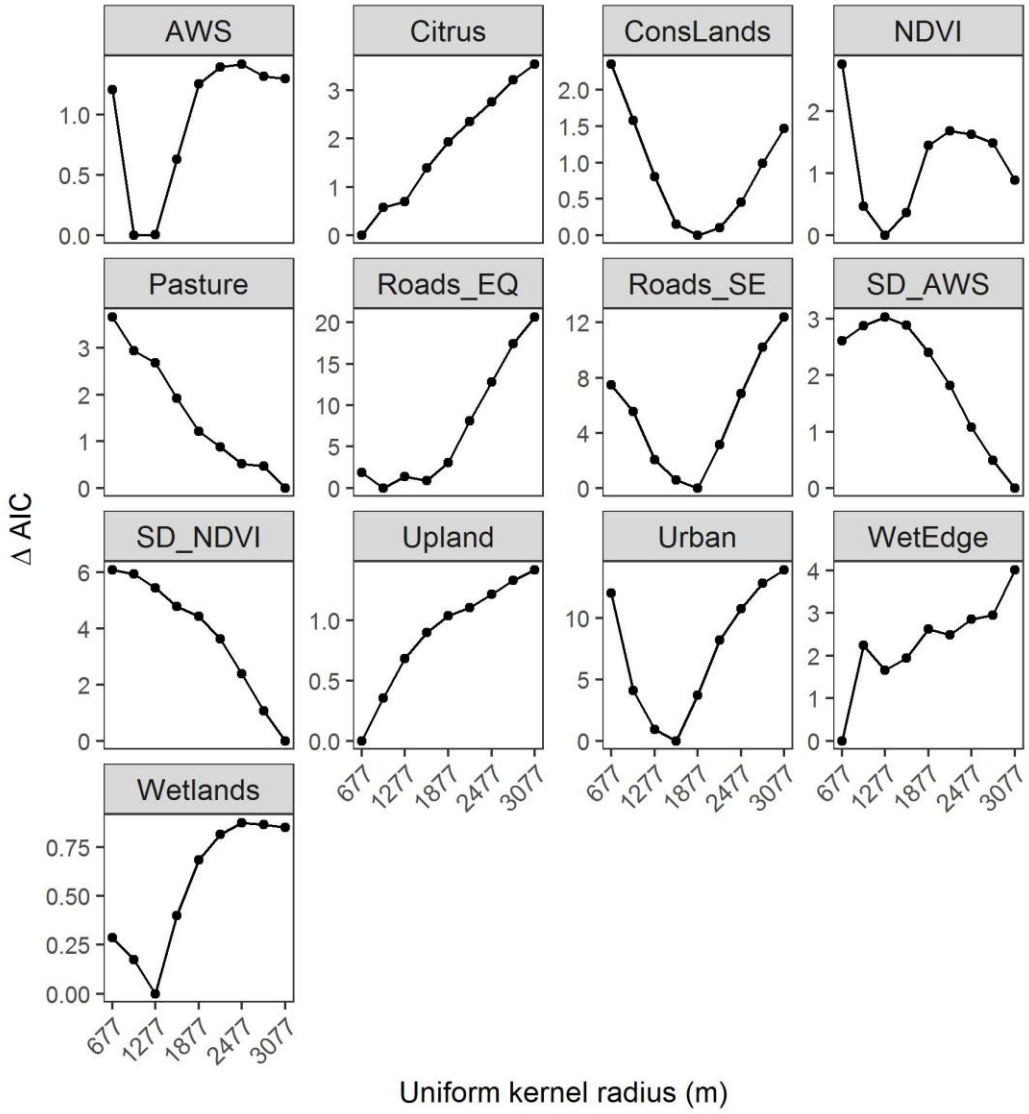

APPENDIX W. SUMMARY GENETIC DIVERSITY STATISTICS ACROSS ALL SAMPLES (N = 107) INCLUDING PUTATIVE DUPLICATES.

Statistics are presented for each of the 15 loci examined: A = number of alleles, A_R = allelic richness, H_O = observed heterozygosity, H_E = expected heterozygosity, HWP = *P* value for test of Hardy-Weinberg proportions using sequential Bonferroni correction, F_{IS} = inbreeding coefficient, F_{IS} *P* = *P* value for test significance of F_{IS} using sequential Bonferroni correction, nulls = estimated percentage of null alleles.

Locus	A	A_R	H_O	H_E	HWP	F_{IS}	F_{IS} *P*	nulls
Dry24	7	6.93	0.62	0.71	0.8208	0.14	0.0440	6.02%
Dry30	6	5.47	0.54	0.65	0.3645	0.17	0.0799	6.79%
Dry44	5	4.92	0.54	0.57	1.0000	0.05	1.0000	1.79%
Dry55	5	5.00	0.47	0.47	1.0000	0.00	1.0000	-0.28%
Dry68	7	6.86	0.54	0.72	0.0000	0.25	0.0150	11.96%
Dry06	8	7.65	0.63	0.63	1.0000	0.01	1.0000	0.06%
Dry48	12	11.31	0.67	0.73	1.0000	0.08	0.4615	3.30%
Dry58	14	13.63	0.74	0.87	0.0000	0.16	0.0150	7.62%
Dry59	10	9.14	0.59	0.72	0.0384	0.19	0.0240	8.35%
Dry65	8	7.66	0.39	0.46	1.0000	0.14	0.1349	4.49%
Dry69	6	5.92	0.62	0.63	1.0000	0.01	1.0000	0.33%
Dry05	8	7.65	0.65	0.68	0.0840	0.05	1.0000	1.68%
Dry14	5	4.75	0.36	0.61	0.0000	0.41	0.0150	18.17%
Dry35	8	8.00	0.74	0.79	1.0000	0.07	0.4336	3.20%
Dry70	6	5.93	0.64	0.73	0.0385	0.12	0.1349	5.29%

APPENDIX X. SUMMARY GENETIC DIVERSITY STATISTICS FROM SAMPLES WITHIN AND OUTSIDE OF THE ARCHBOLD BIOLOGICAL STATION (ABS)

Statistics are presented for each of the 15 loci examined: HWP = *P* value for test of Hardy-Weinberg proportions using sequential Bonferroni correction, F_{IS} = inbreeding coefficient, F_{IS} *P* = *P* value for test significance of F_{IS} using sequential Bonferroni correction.

	ABS (n = 62)			Other (n = 40)		
	HWP	F_{IS}	F_{IS} *P*	HWP	F_{IS}	F_{IS} *P*
Dry24	1.0000	0.08	0.8389	0.1056	0.23	0.1739
Dry30	1.0000	0.14	0.5961	0.5423	0.21	0.2815
Dry44	1.0000	0.03	1.0000	1.0000	0.02	1.0000
Dry55	1.0000	-0.01	1.0000	1.0000	-0.05	1.0000
Dry68	0.0030	0.22	0.0993	0.0286	0.23	0.0497
Dry06	1.0000	-0.02	1.0000	1.0000	-0.02	1.0000
Dry48	1.0000	0.06	0.9041	0.6408	-0.06	1.0000
Dry58	0.4200	0.10	0.3229	0.0126	0.14	0.1788
Dry59	0.4499	0.14	0.5563	0.5423	0.16	0.1739
Dry65	1.0000	0.11	0.6706	1.0000	0.11	0.9509
Dry69	1.0000	0.01	1.0000	1.0000	-0.01	1.0000
Dry05	0.5560	0.04	1.0000	1.0000	0.01	1.0000
Dry14	0.0336	0.34	0.0993	0.0000	0.44	0.0497
Dry35	1.0000	0.09	0.6706	1.0000	0.00	1.0000
Dry70	0.3185	0.16	0.3229	0.5423	0.07	1.0000

APPENDIX Y. COMPARISON OF ISOLATION-BY-DISTANCE TESTS ACROSS DATA SETS.

Estimates of the intercept and slope and 95% CI from MLPE linear mixed-effects models and Mantel's *r* comparing genetic distance to Euclidean geographic distance. Genetic distance was calculated using weighted principle components axes. Data sets with 107 samples include potential duplicates, data sets with 102 samples exclude potential duplicates, and data sets with 88 samples exclude potential duplicates and juveniles. Data sets with 13 loci exclude Dry14 and Dry68, those with 12 loci exclude Dry14, Dry68, and Dry30, and those with 11 loci exclude Dry14, Dry68, Dry58, and Dry59.

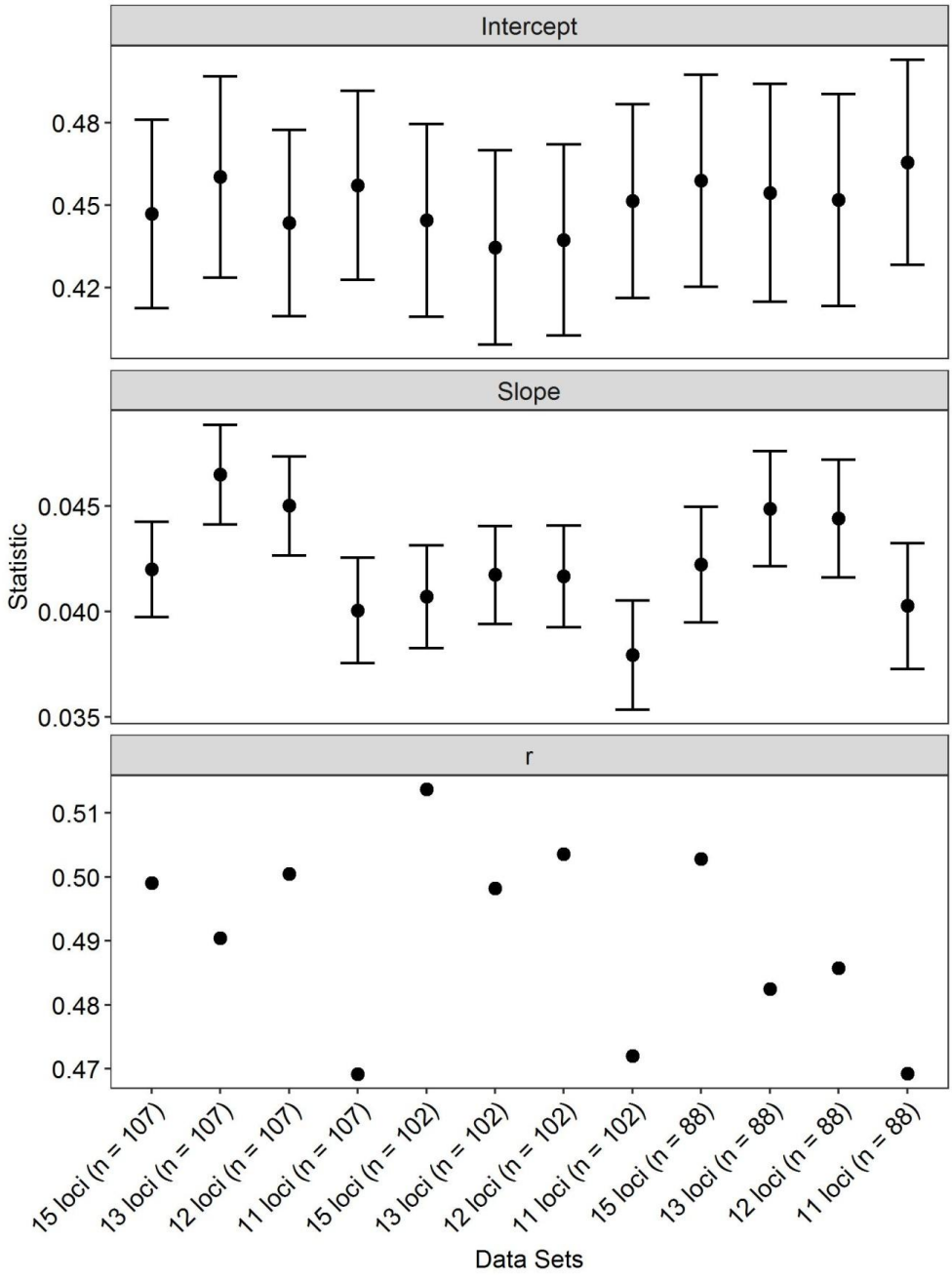
Intercept
0.48
0.45
0.42
Slope
0.045
0.040
0.035
Statistic
r
0.51
0.50
0.49
0.48
0.47
15 loci (n = 107)
13 loci (n = 107)
12 loci (n = 107)
11 loci (n = 107)
15 loci (n = 102)
13 loci (n = 102)
12 loci (n = 102)
11 loci (n = 102)
15 loci (n = 88)
13 loci (n = 88)
12 loci (n = 88)
11 loci (n = 88)
Data Sets

APPENDIX Z. ESTIMATES OF THE INTERCEPT AND SLOPE AND 95% CI FROM MLPE LINEAR MIXED-EFFECTS MODELS AND MANTEL'S *R* COMPARING GENETIC DISTANCE TO EUCLIDEAN GEOGRAPHIC DISTANCE.

Genetic distance was calculated using weighted principle components axes. Data sets included all samples excluding Archbold Biological Station (ABS) (Other, n = 40), samples within ABS (ABS, n = 62), Other samples excluding juveniles (n = 39), and ABS samples excluding juveniles (n = 49). Data sets with 13 loci exclude Dry14 and Dry68, those with 12 loci exclude Dry14, Dry68, and Dry30, and those with 11 loci exclude Dry14, Dry68, Dry58, and Dry59.

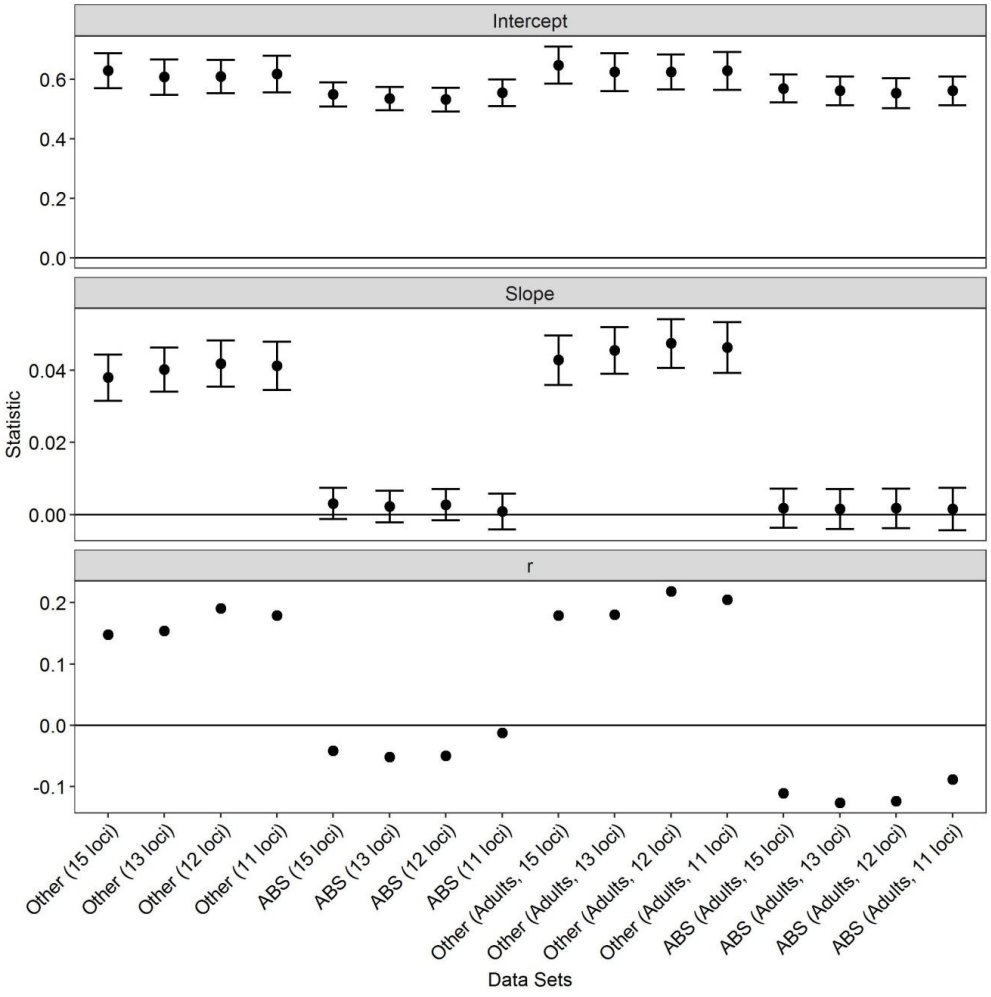

APPENDIX AA. GENETIC AUTOCORRELATION COEFFICIENTS

CALCULATED WITH DIFFERENT NUMBERS OF LOCI

Genetic autocorrelation coefficients calculated at different bin widths (km) with and without juveniles and different numbers of loci. Analyses were run across all samples and separately by each sex (adults only). Values marked in bold had bootstrapped 95% CI that were greater than zero. Data sets with 13 loci exclude Dry14 and Dry68, those with 12 loci exclude Dry14, Dry68, and Dry30, and those with 11 loci exclude Dry14, Dry68, Dry58, and Dry59.

All individuals (n = 102)								
Bin (km)	15 loci	15 loci, Adults	13 loci	13 loci, Adults	12 loci	12 loci, Adults	11 loci	11 loci, Adults
2	**0.061**	**0.066**	**0.062**	**0.072**	**0.060**	**0.072**	**0.056**	**0.065**
4	**0.040**	**0.043**	**0.037**	**0.042**	**0.034**	**0.040**	**0.035**	**0.041**
6	**0.038**	**0.044**	**0.036**	**0.040**	**0.034**	**0.038**	**0.030**	**0.029**
8	**0.022**	**0.030**	**0.021**	**0.031**	**0.021**	**0.030**	**0.023**	**0.034**
10	**0.021**	**0.028**	**0.022**	**0.029**	**0.026**	**0.032**	0.014	**0.025**
12	**0.021**	**0.024**	**0.021**	**0.022**	**0.024**	**0.025**	**0.017**	**0.020**
14	-0.012	-0.003	-0.005	0.003	-0.004	0.005	-0.006	0.000

Bin (km)	15 loci	15 loci, Adults	13 loci	13 loci, Adults	12 loci	12 loci, Adults	11 loci	11 loci, Adults
3	**0.051**	**0.056**	**0.051**	**0.059**	**0.049**	**0.058**	**0.046**	**0.053**
6	**0.042**	**0.047**	**0.039**	**0.045**	**0.037**	**0.043**	**0.035**	**0.038**
9	**0.021**	**0.029**	**0.021**	**0.029**	**0.022**	**0.030**	**0.020**	**0.030**
12	**0.021**	**0.026**	**0.023**	**0.026**	**0.025**	**0.028**	**0.018**	**0.024**
15	-0.014	-0.008	-0.004	0.000	-0.004	0.001	-0.006	-0.003
18	-0.032	-0.028	-0.028	-0.026	-0.026	-0.023	-0.032	-0.032
21	-0.027	-0.019	-0.021	-0.014	-0.026	-0.018	-0.023	-0.017

Bin (km)	15 loci	15 loci, Adults	13 loci	13 loci, Adults	12 loci	12 loci, Adults	11 loci	11 loci, Adults
4	**0.050**	**0.055**	**0.049**	**0.057**	**0.047**	**0.056**	**0.045**	**0.053**
8	**0.029**	**0.037**	**0.028**	**0.035**	**0.027**	**0.034**	**0.027**	**0.032**
12	**0.021**	**0.025**	**0.022**	**0.025**	**0.025**	**0.028**	**0.016**	**0.023**
16	-0.017	-0.012	-0.008	-0.006	-0.007	-0.003	-0.009	-0.007
20	-0.025	-0.016	-0.019	-0.013	-0.022	-0.014	-0.022	-0.019

Adult males (n = 45)				
Bin (km)	15 loci	13 loci	12 loci	11 loci
2	**0.057**	**0.056**	**0.050**	**0.051**
4	**0.043**	**0.041**	**0.034**	**0.039**
6	**0.057**	**0.049**	**0.043**	**0.038**
8	0.019	0.019	0.016	0.025
10	**0.054**	**0.047**	**0.056**	0.031
12	0.025	0.026	0.027	0.027
14	-0.037	-0.024	-0.020	-0.042

Bin (km)	15 loci	13 loci	12 loci	11 loci
3	**0.048**	**0.050**	**0.043**	**0.043**
6	**0.057**	**0.048**	**0.042**	**0.042**
9	**0.024**	**0.021**	**0.021**	**0.023**
12	**0.040**	**0.039**	**0.041**	**0.033**
15	-0.033	-0.023	-0.020	-0.044
18	-0.037	-0.028	-0.024	-0.025
21	-0.014	-0.003	-0.002	0.000

Bin (km)	15 loci	13 loci	12 loci	11 loci
4	**0.050**	**0.048**	**0.042**	**0.045**
8	**0.038**	**0.034**	**0.029**	**0.032**
12	**0.039**	**0.036**	**0.041**	**0.029**
16	-0.042	-0.032	-0.029	-0.045
20	-0.009	0.001	0.003	0.001

Adult females (n = 36)				
Bin (km)	15 loci	13 loci	12 loci	11 loci
2	**0.039**	**0.055**	**0.059**	**0.072**
4	**0.064**	**0.059**	**0.062**	**0.064**
6	0.024	0.024	0.029	0.006
8	0.018	0.023	0.023	0.030
10	0.000	0.009	0.002	-0.007
12	-0.024	-0.027	-0.028	-0.027
14	-0.026	-0.025	-0.029	-0.002

Bin (km)	15 loci	13 loci	12 loci	11 loci
3	**0.051**	**0.058**	**0.062**	**0.067**
6	**0.033**	**0.036**	**0.038**	0.031
9	0.013	0.014	0.013	0.014

12	-0.015	-0.007	-0.012	-0.012
15	-0.020	-0.008	-0.006	0.008
18	-0.020	-0.028	-0.029	-0.037
21	-0.037	-0.040	-0.048	-0.060

Bin (km)	15 loci	13 loci	12 loci	11 loci
4	**0.050**	**0.057**	**0.060**	**0.068**
8	**0.021**	**0.023**	**0.026**	0.019
12	-0.011	-0.008	-0.012	-0.016
16	0.001	0.010	0.012	0.020
20	-0.035	-0.038	-0.043	-0.055

APPENDIX AB. MODEL RANKINGS FOR RAW RESOURCE SELECTION FUNCTION (RSF) AND SCALE-INTEGRATED RESOURCE SELECTION FUNCTION (SRSF) SURFACES USING EXPONENTIATED VALUES.

RSF surfaces reflect second- and third-order habitat selection (Level II and III, respectively) while SRSF surfaces are the normalized product of Level II and Level III surfaces. Level II surfaces were estimated with and without urban land cover. Level III surfaces were estimated for breeding (Brd.) and non-breeding (NonBrd.) seasons for each sex. The number of model parameters is given by K, *w* is the AIC_c model weight, Avg. Rank is the average model ranking across 1,000 bootstrap iterations, π is the proportion of bootstrap iterations where the model was the top model, mR^2 is the marginal R^2, and cR^2 is the conditional R^2.

Surface	*K*	AIC_c	ΔAIC_c	*w*	Avg. Rank	π	mR2	cR2
Level II	2	-14769.17	0.00	1.0000	1.00	0.9910	0.12	0.77
Level II (w/Urban)	2	-14748.86	20.31	0.0000	2.00	0.0085	0.10	0.77
Female NonBrd. SRSF (w/Urban)	2	-14722.37	46.80	0.0000	3.03	0.0001	0.09	0.76
Female Brd. SRSF (w/Urban)	2	-14722.23	46.94	0.0000	4.37	0.0001	0.09	0.76
Female Brd. SRSF	2	-14722.23	46.94	0.0000	4.60	0.0001	0.09	0.76
Female NonBrd. SRSF	2	-14721.83	47.34	0.0000	6.00	0.0000	0.09	0.76
Male NonBrd. SRSF	2	-14721.52	47.65	0.0000	7.01	0.0000	0.09	0.76
Male NonBrd. SRSF (w/Urban)	2	-14721.44	47.73	0.0000	8.06	0.0000	0.09	0.76
Female Brd. Level III	2	-14721.32	47.85	0.0000	9.04	0.0000	0.09	0.76
Male NonBrd. Level III	2	-14721.29	47.88	0.0000	9.94	0.0000	0.09	0.76
Female NonBrd. Level III	2	-14721.24	47.93	0.0000	10.95	0.0000	0.09	0.76
Male Brd. SRSF	2	-14721.18	47.99	0.0000	12.12	0.0000	0.09	0.76
Male Brd. SRSF (w/Urban)	2	-14721.16	48.01	0.0000	13.03	0.0000	0.09	0.76
Male Brd. Level III	2	-14721.15	48.02	0.0000	13.84	0.0000	0.09	0.76

APPENDIX AC. MODEL RANKINGS FOR RESOURCE SELECTION FUNCTION (RSF) AND SCALE-INTEGRATED RESOURCE SELECTION FUNCTION (SRSF) SURFACES USING EXPONENTIATED VALUES OPTIMIZED USING RESISTANCEGA.

RSF surfaces reflect second- and third-order habitat selection (Level II and III, respectively) while SRSF surfaces are the normalized product of Level II and Level III surfaces. Level II surfaces were estimated with and without urban land cover. Level III surfaces were estimated for breeding (Brd.) and non-breeding (NonBrd.) seasons for each sex. The number of model parameters is given by K, *w* is the AIC_c model weight, Avg. Rank is the average model ranking across 1,000 bootstrap iterations, π is the proportion of bootstrap iterations where the model was the top model, mR^2 is the marginal R^2, and cR^2 is the conditional R^2.

Surface	*K*	AIC_c	ΔAIC_c	*w*	Avg. Rank	π	mR2	cR2
Level II (w/Urban)	4	-14903.3	0	1.00	1.02	0.97	0.33	0.85
Level II	4	-14870	33.35	0	1.98	0.03	0.29	0.84
Female NonBrd. SRSF (w/Urban)	4	-14737.1	166.17	0	3.07	0	0.09	0.77
Female Brd. SRSF (w/Urban)	4	-14735.5	167.76	0	4.27	0	0.09	0.77
Female Brd. SRSF	4	-14735.4	167.95	0	4.66	0	0.09	0.77
Female NonBrd. SRSF	4	-14727.8	175.51	0	6	0	0.09	0.77
Male NonBrd. SRSF	4	-14721.4	181.92	0	7	0	0.09	0.76
IBD	2	-14721.3	182.02	0	NA	NA	0.09	0.76
Male NonBrd. SRSF (w/Urban)	4	-14719.70	183.56	0	8	0	0.08	0.76
Female Brd. Level III	4	-14717.2	186.07	0	9.71	0	0.08	0.76
Male NonBrd. Level III	4	-14717	186.3	0	10.17	0	0.09	0.76
Male Brd. Level III	4	-14717	186.31	0	11.66	0	0.09	0.76
Male Brd. SRSF	4	-14717	186.31	0	12.01	0	0.09	0.76
Male Brd. SRSF (w/Urban)	4	-14717	186.31	0	11.96	0	0.09	0.76
Female NonBrd. Level III	4	-14717	186.32	0	13.49	0	0.09	0.76

APPENDIX AD. OPTIMIZED FUNCTIONAL TRANSFORMATIONS FOR THE AIC_C-BEST RSF/SRSF SURFACES USING PREDICTED AND EXPONENTIAL SURFACES.

The Best Predicted Optimized surface was the SRSF surface for breeding season females including urban while the Best Exponential Optimized surface was the Level II RSF including urban.

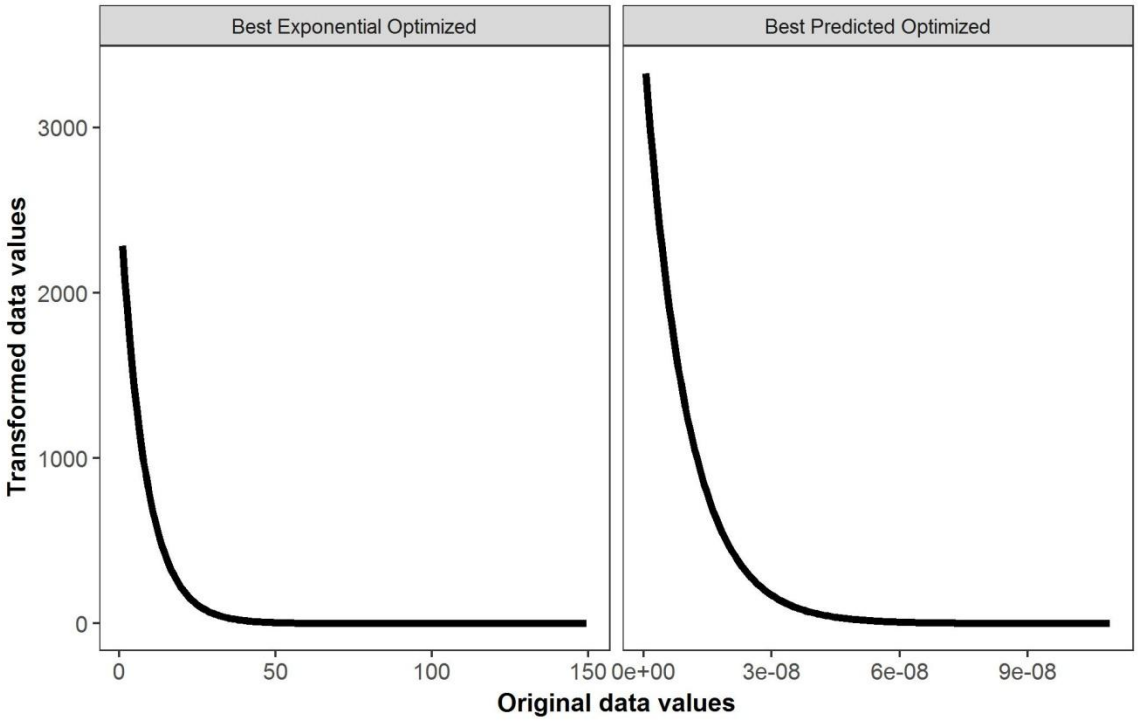

APPENDIX AE. MODEL RANKINGS FOR INDIVIDUAL LAND COVER SURFACES

Each surface was smoothed with Gaussian kernels with 60, 600, 1200, and 1800 m bandwidths. Water_prop was included in each optimization. *w* is the AIC_c model weight, Avg. Rank is the average model ranking across 1,000 bootstrap iterations, π is the proportion of bootstrap iterations where the model was the top model, mR^2 is the marginal R^2, and cR^2 is the conditional R^2. Water and Other are the percent contributions of Water_prop and the smoothed land cover surface, respectively. Total Delta and Total *w* are the ΔAIC_c and model weight across all individual land cover surfaces.

Landscape Feature	Scale	AIC_c	ΔAIC_c	*w*	mR^2	cR^2	Water	Other	π	Avg. Rank	Total Δ	Total *w*
Wetland Edge	1200	-14945.85	0.00	0.5730	0.30	0.82	0.003	0.996	23.40	1.80	0.00	0.5730
Wetland Edge	1800	-14945.21	0.64	0.4161	0.30	0.80	0.003	0.996	64.20	1.51	0.64	0.4161
Wetland Edge	600	-14937.92	7.93	0.0109	0.34	0.84	0.004	0.996	12.40	2.69	7.93	0.0109
Wetland Edge	60	-14866.39	79.46	0.0000	0.18	0.78	0.114	0.885	0.00	4.00	79.46	0.0000
Undeveloped	1800	-14918.17	0.00	0.8921	0.25	0.80	0.124	0.875	72.20	1.51	27.68	0.0000
Undeveloped	1200	-14912.55	5.62	0.0537	0.24	0.81	0.121	0.878	2.10	2.44	33.30	0.0000
Undeveloped	60	-14912.06	6.11	0.0420	0.25	0.82	0.140	0.859	17.40	2.89	33.79	0.0000
Undeveloped	600	-14909.58	8.59	0.0122	0.24	0.81	0.110	0.890	8.30	3.16	36.27	0.0000
Wetland	60	-14905.49	0	0.9875	0.35	0.80	0.468	0.532	72.6	1.423	40.36	0.0000
Wetland	1800	-14896.36	9.13	0.0103	0.27	0.79	0.433	0.566	23	2.197	49.49	0.0000
Wetland	1200	-14893.33	12.16	0.0023	0.34	0.83	0.430	0.569	4.2	2.485	52.52	0.0000
Wetland	600	-14880.00	25.54	0.0000	0.27	0.80	0.450	0.549	0.2	3.895	65.9	0.0000

		14879.95		0			2	8				
		-		0.992		0.7	0.431	0.568	65.9			
SD NDVI	1800	14902.20	0.00	1	0.15	7	2	8	0	1.49	43.65	0.0000
		-		0.005		0.8	0.270	0.729	22.3			
SD NDVI	600	14891.88	10.32	7	0.27	1	8	2	0	2.45	53.97	0.0000
		-		0.001		0.8	0.144	0.855	11.0			
SD NDVI	60	14889.06	13.14	4	0.26	2	8	2	0	3.07	56.79	0.0000
		-		0.000		0.7	0.394	0.605				
SD NDVI	1200	14887.93	14.27	8	0.15	7	4	6	0.80	3.00	57.92	0.0000
		-		0.925		0.8	0.514	0.485	44.6			
Urban	600	14898.06	0.00	7	0.29	2	1	9	0	1.79	47.79	0.0000
		-		0.069		0.8	0.500	0.499	21.0			
Urban	1200	14892.89	5.17	8	0.29	2	3	7	0	2.35	52.96	0.0000
		-		0.004		0.7	0.454	0.545	34.4			
Urban	1800	14887.43	10.63	6	0.23	8	3	7	0	1.95	58.42	0.0000
		-		0.000		0.7	0.513	0.487				
Urban	60	14868.54	29.52	0	0.23	9	0	0	0.00	3.91	77.31	0.0000
		-		0.994		0.7	0.513	0.486	94.9			
Pasture	1200	14851.31	0.00	5	0.16	8	1	9	0	1.06	94.54	0.0000
		-		0.004		0.7	0.223	0.776				
Pasture	1800	14840.33	10.98	1	0.12	7	5	5	0.00	2.31	105.52	0.0000
		-		0.001		0.7	0.207	0.792				
Pasture	600	14838.07	13.24	3	0.13	7	5	5	5.00	2.74	107.78	0.0000
		-		0.000		0.7	0.423	0.576				
Pasture	60	14831.37	19.94	0	0.13	6	6	4	0.10	3.90	114.48	0.0000

APPENDIX AF. MULTI-SURFACE OPTIMIZATION MODEL RANKINGS

Scale indicates the bandwidth (m) of the Gaussian kernel used to smooth each land cover surface. Pseudo Opt. indicates pseudo-optimized multi-scale optimizations. Water_prop was included in each optimization. *w* is the AIC_c model weight, Avg. Rank is the average model ranking across 10,000 bootstrap iterations, π is the proportion of bootstrap iterations where the model was the top model, mR^2 is the marginal R^2, and cR^2 is the conditional R^2. The following columns indicate the proportional contribution of each surface to the final optimized resistance surface: UN = undeveloped uplands, UR = urban, SD = SD NDVI, WT = wetland, WE = wetland edge, PA = pasture, WA = water.

Surface	Scale	Δ AIC_c	*w*	Avg. Rank	π	mR2	cR2	UN	UR	SD	WT	WE	PA	WA
Upland + Urban + SD NDVI	1800	0.00	0.92	1.93	66.42	0.33	0.80	0.20	0.26	0.51	NA	NA	NA	0.03
Upland + Urban + Wetland	Pseudo Opt.	37.84	0.00	5.63	13.36	0.34	0.80	0.57	0.14	NA	0.19	NA	NA	0.10
Upland + Urban + SD NDVI	Pseudo Opt.	5.06	0.07	3.68	7.48	0.35	0.83	0.25	0.17	0.54	NA	NA	NA	0.04
Upland + Urban + Wetland	1800	42.96	0.00	6.53	4.78	0.40	0.81	0.23	0.24	NA	0.53	NA	NA	0.01
Upland + SD NDVI + Wetland Edge	1800	11.83	0.00	4.02	3.75	0.28	0.81	0.16	NA	0.42	NA	0.40	NA	0.02
Upland + Urban + Wetland	1200	40.91	0.00	6.51	2.29	0.37	0.81	0.26	0.19	NA	0.52	NA	NA	0.02
Upland + Wetland + Pasture	1200	56.69	0.00	10.25	0.74	0.34	0.83	0.29	NA	NA	0.50	NA	0.14	0.07
Upland + Wetland + Pasture	Pseudo Opt.	64.20	0.00	10.69	0.56	0.30	0.80	0.63	NA	NA	0.17	NA	0.09	0.11
Upland + Urban + Wetland	600	39.72	0.00	7.62	0.49	0.38	0.83	0.46	0.11	NA	0.34	NA	NA	0.10
Upland + SD NDVI + Wetland Edge	600	53.89	0.00	10.73	0.12	0.28	0.82	0.34	NA	0.17	NA	0.47	NA	0.01
Upland + Wetland +	1800	65.68	0.00	12.10	0.01	0.31	0.82	0.46	NA	NA	0.37	NA	0.13	0.04

Pasture														
Upland + Urban + SD NDVI	1200	30.12	0.00	6.22	0.00	0.31	0.80	0.23	0.25	0.51	NA	NA	NA	0.01
Upland + SD NDVI + Wetland Edge	1200	46.08	0.00	8.85	0.00	0.28	0.81	0.12	NA	0.25	NA	0.63	NA	0.01
Upland + Urban + SD NDVI	600	57.37	0.00	10.54	0.00	0.26	0.79	0.32	0.18	0.47	NA	NA	NA	0.03
Upland + Wetland + Pasture	600	95.73	0.00	14.71	0.00	0.24	0.81	0.72	NA	NA	0.08	NA	0.14	0.06

BIBLIOGRAPHY

Abom R, Bell K, Hodgson L, Schwarzkopf L (2012) Moving day and night: highly labile diel activity patterns in a tropical snake. Biotropica 44:554-559

Abrahamson WG, Johnson AF, Layne JN, Peroni PA (1984) Vegetation of the Archbold Biological Station, Florida: an example of the southern Lake Wales Ridge. Fla Sci 47:209-250

Adamack AT, Gruber B (2014) PopGenReport: simplifying basic population genetic analyses in R. Methods Ecol Evol 5:384-387

Addicott JF, Aho JM, Antolin MF, Padilla DK, Richardson JS, Soluk DA (1987) Ecological neighborhoods: scaling environmental patterns. Oikos 49:340-346

Adriaensen F, Chardon JP, De Blust G, Swinnen E, Villalba S, Gulinck H, Matthysen E (2003) The application of 'least-cost' modelling as a functional landscape model. Landsc Urban Plan 64:233-247

Akcakaya HR (2002) RAMAS GIS: linking spatial data with population viability analysis (version 4.0). Applied Biomathematics, Setauket, New York, U.S.A.

Aldridge RD, Duvall D (2002) Evolution of the mating season in the pitvipers of North America. Herpetol Monogr 16:1-25

Allendorf FW, Luikart G, Aitken SN (2013) Conservation and The Genetics of Populations. Wiley-Blackwell, Oxford, United Kingdom

Anderson CD, Epperson BK, Fortin MJ, Holderegger R, James PMA, Rosenberg MS, Scribner KT, Spear S (2010) Considering spatial and temporal scale in landscape-genetic studies of gene flow. Mol Ecol 19:3565-3575

Anderson CD, Rosenberg MS (2011) Variation in association with anthropogenic habitat edges exhibited by the Timber Rattlesnake (*Crotalus horridus*) in St. Louis County, Missouri. J Herpetol 45:50-55

Anderson DP, Forester JD, Turner MG, Frair JL, Merrill EH, Fortin D, Mao JS, Boyce MS (2005) Factors influencing female home range sizes in elk (*Cervus elaphus*) in North American landscapes. Landscape Ecol 20:257-271

Anderson MJ (2001) A new method for non-parametric multivariate analysis of variance. Austral Ecol 26:32-46

Andrews KM, Gibbons JW (2008) Roads as catalysts of urbanization: snakes on roads face differential impacts due to inter- and intraspecific ecological attributes. In: Mitchell JC, Jung Brown RE, Bartholomew B (eds), Urban herpetology. Society for the Study of Amphibians and Reptiles, Salt Lake City, pp 145-153

Angelone S, Kienast F, Holderegger R (2011) Where movement happens: scale-dependent landscape effects on genetic differentiation in the European tree frog. Ecography 34:714-722

Anguiano MP, Diffendorfer JE (2015) Effects of fragmentation on the spatial ecology of the California kingsnake (*Lampropeltis californiae*). J Herpetol 49:420-427

Auffenberg W, Franz R (1982) The status and distribution of the gopher tortoise (*Gopherus polyphemus*). In: Bury RB (ed), North American tortoises: conservation and ecology. U.S. Fish and Wildlife Service, Washington, D.C., pp 95-126

Avgar T, Lele SR, Keim JL, Boyce MS (2017) Relative selection strength: quantifying effect size in habitat- and step-selection inference. Ecology and Evolution 7:5322-5330

Balkenhol N, Gugerli F, Cushman SA, Waits LP, Coulon A, Arntzen JW, Holderegger R, Wagner HH (2009) Identifying future research needs in landscape genetics: where to from here? Landscape Ecol 24:455-463

Balkenhol N, Pardini R, Cornelius C, Fernandes F, Sommer S (2013) Landscape-level comparison of genetic diversity and differentiation in a small mammal inhabiting different fragmented landscapes of the Brazilian Atlantic Forest. Conserv Genet 14:355-367

Balkenhol N, Cushman S, Storfer A, Waits L (eds) (2016) Landscape Genetics: Concepts, Methods, and Applications. Wiley Blackwell, Chichester

Banks SC, Peakall R (2012) Genetic spatial autocorrelation can readily detect sex-biased dispersal. Mol Ecol 21:2092-2105

Barbet-Massin M, Jiguet F, Albert CH, Thuiller W (2012) Selecting pseudo-absences for species distribution models: how, where and how many? Methods Ecol Evol 3:327-338

Bates D, Maechler M, Bolker B, Walker S (2014) lme4: Linear Mixed-Effects Models Using Eigen and S4. R package version 1.1-7. http://CRAN.R-project.org/package=lme4.

Bateson M (2002) Recent advances in our understanding of risk-sensitive foraging preferences. Proc Nutr Soc 61:509-516

Bauder JM, Barnhart P (2014) Factors affecting the accuracy and precision of triangulated radio telemetry locations of Eastern Indigo Snakes (*Drymarchon couperi*). Herpetol Rev 45:590-597

Bauder JM, Breininger DR, Bolt MR, Legare ML, Jenkins CL, McGarigal K (2015) The role of the bandwidth matrix in influencing kernel home range estimates for snakes using VHF telemetry data. Wildl Res 42:437-453

Bauder JM, Breininger DR, Bolt MR, Legare ML, Jenkins CL, Rothermel BB, McGarigal K (2016a) Seasonal variation in eastern indigo snake (*Drymarchon couperi*) movement patterns and space use in peninsular Florida at multiple temporal scales. Herpetologica 72:214-226

Bauder JM, Breininger DR, Bolt MR, Legare ML, Jenkins CL, Rothermel BB, McGarigal K (2016b) The influence of sex and season on conspecific spatial overlap in a large, actively-foraging colubrid snake. PLoS ONE 11:e0160033

Bauder JM, Stevenson DJ, Sutherland CS, Jenkins CL (2017) Occupancy of potential overwintering habitat on protected lands by two imperiled snake species in the coastal plain of the southeastern United States. J Herpetol 51:73-88

Bauder JM, Breininger DR, Bolt MR, Legare ML, Jenkins CL, Rothermel BB, McGarigal K (2018) Multi-level, multi-scale habitat selection by a wide-ranging ranging federally threatened snake. Landscape Ecol 33:743-763

Bauduin S, McIntire E, St-Laurent MH, Cumming S (2016) Overcoming challenges of sparse telemetry data to estimate caribou movement. Ecol Model 335:24-34

Beatty WS, Beasley JC, Rhodes OE (2014) Habitat selection by a generalist mesopredator near its historical range boundary. Can J Zool 92:41-48

Beier P, Majka DR, Spencer WD (2008) Forks in the road: choices in procedures for designing wildland linkages. Conserv Biol 22:836-851

Beissinger SR, Westphal MI (1998) On the use of demographic models of population viability in endangered species management. J Wildl Manage 62:821-841

Bellamy C, Scott C, Altringham J (2013) Multiscale, presence-only habitat suitability models: fine-resolution maps for eight bat species. J Appl Ecol 50:892-901

Beninde J, Feldmeier S, Werner M, Peroverde D, Schulte U, Hochkirch A, Veith M (2016) Cityscape genetics: structural vs. functional connectivity of an urban lizard population. Mol Ecol 25:4984-5000

Bernardino FS, Dalrymple GH (1992) Seasonal activity and road mortality of the snakes of the Pa-Hay-Okee wetlands of Everglades National Park, USA. Biol Conserv 62:71-75

Bertona M, Chiaraviglio M (2003) Reproductive biology, mating aggregations, and sexual dimorphism of the argentine boa constrictor (*Boa constrictor occidentalis*). J Herpetol 37:510-516

Beyer HL, Ung R, Murray DL, Fortin MJ (2013) Functional responses, seasonal variation and thresholds in behavioural responses of moose to road density. J Appl Ecol 50:286-294

Blouin-Demers G, Weatherhead PJ (2001a) An experimental test of the link between foraging, habitat selection and thermoregulation in black rat snakes *Elaphe obsoleta obsoleta*. J Anim Ecol 70:1006-1013

Blouin-Demers G, Weatherhead PJ (2001b) Habitat use by black rat snakes (*Elaphe obsoleta obsoleta*) in fragmented forests. Ecology 82:2882-2896

Blouin-Demers G, Weatherhead PJ (2002) Implications of movement patterns for gene flow in black rat snakes (*Elaphe obsoleta*). Can J Zool 80:1162-1172

Bolker BM, Deutschman DH, Hartvigsen G, Smith DL (1997) Individual-based modelling: What is the difference? Trends Ecol Evol 12:111-111

Bonnot TW, Thompson FR, Millspaugh JJ (2011) Extension of landscape-based population viability models to ecoregional scales for conservation planning. Biol Conserv 144:2041-2053

Bonnot TW, Thompson FR, Millspaugh JJ, Jones-Farrand DT (2013) Landscape-based population viability models demonstrate importance of strategic conservation planning for birds. Biol Conserv 165:104-114

Borger L, Franconi N, De Michele G, Gantz A, Meschi F, Manica A, Lovari S, Coulson T (2006) Effects of sampling regime on the mean and variance of home range size estimates. J Anim Ecol 75:1393-1405

Bowyer RT, Kie JG (2006) Effects of scale on interpreting life-history characteristics of ungulates and carniovers. Divers Distrib 12:244-257

Boyce MS (1992) Population viability analysis. Annu Rev Ecol Syst 23:481-506

Boyce MS, Vernier PR, Nielsen SE, Schmiegelow FKA (2002) Evaluating resource selection functions. Ecol Model 157:281-300

Boyce MS, Mao JS, Merrill EH, Fortin D, Turner MG, Fryxell J, Turchin P (2003) Scale and heterogeneity in habitat selection by elk in Yellowstone National Park. Ecoscience 10:421-431

Boyce MS (2006) Scale for resource selection functions. Divers Distrib 12:269-276

Breininger DR, Legare ML, Smith RB (2004) Eastern indigo snakes (*Drymarchon couperi*) in Florida: influence of edge on species viability. In: Akcakaya H, Burgman M, Kindvall O, Wood C, Sjögren-Gulve P, Hatfield J, McCarthy M (eds), Species conservation and management: case studies. Oxford University Press, New York, pp 299-311

Breininger DR, Bolt MR, Legare ML, Drese JH, Stolen ED (2011) Factors influencing home-range sizes of eastern indigo snakes in central Florida. J Herpetol 45:484-490

Breininger DR, Mazerolle MJ, Bolt MR, Legare ML, Drese JH, Hines JE (2012) Habitat fragmentation effects on annual survival of the federally protected eastern indigo snake. Anim Conserv 15:361-368

Brook BW, O'Grady JJ, Chapman AP, Burgman MA, Akcakaya HR, Frankham R (2000) Predictive accuracy of population viability analysis in conservation biology. Nature 404:385-387

Brown GP, Weatherhead PJ (1999) Female distribution affects mate searching and sexual selection in male northern water snakes (*Nerodia sipedon*). Behav Ecol Sociobiol 47:9-16

Brown GP, Shine R (2002) Reproductive ecology of a tropical natricine snake, *Tropidonophis mairii* (Colubridae). Journal of Zoology 258:63-72

Brown GP, Shine R, Madsen T (2005) Spatial ecology of slatey-grey snakes (*Stegonotus cucullatus*, Colubridae) on a tropical Australian floodplain. J Trop Ecol 21:605-612

Brown JL (1969) Territorial behavior and population regulation in birds: a review and re-evaluation. The Wilson Bulletin 81:293-329

Brownie C, Hines JE, Nichols JD, Pollock KH, Hestbeck JB (1993) Capture-recapture studies for multiple strata including non-Markovian transitions. Biometrics 49:1173-1187

Burnham KP, Anderson DR (2002) Model Selection and Multimodel Inference. Springer, New York

Calenge C (2006) The package adehabitat for the R software: a tool for the analysis of space and habitat use by animals. Ecol Model 197:516-519

Cardwell MD (2008) The reproductive ecology of Mohave rattlesnakes. Journal of Zoology 274:65-76

Carfagno GLF, Weatherhead PJ (2008) Energetics and space use: intraspecific and interspecific comparisons of movements and home ranges of two Colubrid snakes. J Anim Ecol 77:416-424

Carpenter FL, MacMillen RE (1976) Threshold model of feeding territoriality and test with a Hawaiian Honeycreeper. Science 194:639-642

Carter J, Finn JT (1999) MOAB: a spatially explicit, individual-based expert system for creating animal foraging models. Ecol Model 119:29-41

Carter N, Levin S, Barlow A, Grimm V (2015) Modeling tiger population and territory dynamics using an agent-based approach. Ecol Model 312:347-362

Castellon TD, Rothermel BB, Nomani SZ (2015) A comparison of line-transect distance sampling methods for estimating gopher tortoise population densities. Wildl Soc Bull 39:804-812

Castillo JA, Epps CW, Davis AR, Cushman SA (2014) Landscape effects on gene flow for a climate-sensitive montane species, the American pika. Mol Ecol 23:843-856

Chapron G, Wikenros C, Liberg O, Wabakken P, Flagstad O, Milleret C, Mansson J, Svensson L, Zimmermann B, Akesson M, Sand H (2016) Estimating wolf (*Canis lupus*) population size from number of packs and an individual based model. Ecol Model 339:33-44

Charland MB, Gregory PT (1995) Movements and habitat use in gravid and nongravid female garter snakes (Colubridae, *Thamnophis*). Journal of Zoology 236:543-561

Chaverri G, Gamba-Rios M, Kunz TH (2007) Range overlap and association patterns in the tent-making bat *Artibeus watsoni*. Anim Behav 73:157-164

Chetkiewicz CLB, Clair CCS, Boyce MS (2006) Corridors for conservation: Integrating pattern and process. Annu Rev Ecol Evol Syst 37:317-342

Christman SP (1988) Endemism in Florida's interior sand pine scrub. Florida Game and Fresh Water Fish Commission, Nongame Wildlife Program, Final Report, Tallahasse, Florida,

Clark RW (2004) Timber rattlesnakes (Crotalus horridus) use chemical cues to select ambush sites. J Chem Ecol 30:607-617

Clark RW, Brown WS, Stechert R, Zamudio KR (2008) Integrating individual behaviour and landscape genetics: the population tructure of timber rattlesnake hibernacula. Mol Ecol 17:719-730

Clark RW, Brown WS, Stechert R, Zamudio KR (2010) Roads, interrupted dispersal, and genetic diversity in timber rattlesnakes. Conserv Biol 24:1059-1069

Clarke RT, Rothery P, Raybould AF (2002) Confidence limits for regression relationships between distance matrices: Estimating gene flow with distance. J Agric Biol Environ Stat 7:361-372

Committee FGD (2013) Classification of wetlands and deepwater habitats of the United States. FGDC-STD-004-2013. Second Edition. Wetlands Subcommittee, Federal Geographic Data Committee and U.S. Fish and Wildlife Service, Washington, DC.

Compton BW, Rhymer JM, McCollough M (2002) Habitat selection by wood turtles (*Clemmys insculpta*): an application of paired logistic regression. Ecology 83:833-843

Compton BW, McGarigal K, Cushman SA, Gamble LR (2007) A resistant-kernel model of connectivity for amphibians that breed in vernal pools. Conserv Biol 21:788-799

Conant R, Collins JT (1998) A Field Guide to Reptiles and Amphibians: Eastern and Central North America. Houghton Mifflin Company, New York, New York, U.S.A.

Cooch E, White G (eds) (2017) Program Mark: A Gentle Introduction. Available at http://www.phidot.org/software/mark/docs/book/. Accessed 1 July 2017.

Corey B, Doody JS (2010) Anthropogenic influences on the spatial ecology of a semi-arid python. Journal of Zoology 281:293-302

Coster SS, Babbitt KJ, Cooper A, Kovach AI (2015) Limited influence of local and landscape factors on finescale gene flow in two pond-breeding amphibians. Mol Ecol 24:742-758

Cottone AM, Bauer AM (2013) The vernal spatial ecology and mating behaviors of the rhombic skaapsteker, *Psammophylax rhombeatus rhombeatus* (Serpentes: Psammophiidae), from the Western Cape, South Africa. Copeia 2013:194-200

Coulon A, Morellet N, Goulard M, Cargnelutti B, Angibault J-M, Hewison JM (2008) Inferring the effects of landscape structure on roe deer (*Capreolus capreolus*) movements using a step selection function. Landscape Ecol 23:603-614

Coulson T, Mace GM, Hudson E, Possingham H (2001) The use and abuse of population viability analysis. Trends in Ecology and Evolution 16:219-221

Croak BM, Crowther MS, Webb JK, Shine R (2013) Movements and habitat use of an endangered snake, *Hoplocephalus bungaroides* (Elapidae): implications for conservation. PLoS ONE 8:e61711. doi:10.1371/journal.pone.0061711

Cushman SA, McKelvey KS, Hayden J, Schwartz MK (2006) Gene flow in complex landscapes: testing multiple hypotheses with causal modeling. The American Naturalist 168:486-499

Cushman SA, McKelvey KS, Schwartz MK (2009) Use of empirically derived source-destination models to map regional conservation corridors. Conserv Biol 23:368-376

Cushman SA, Landguth EL (2010) Scale dependent inference in landscape genetics. Landscape Ecol 25:967-979

Dalrymple GH, Steiner TM, Nodell RJ, Bernardino FS (1991) Seasonal activity of the snakes of Long Pine Key, Everglades National Park. Copeia:294-302

DeCesare NJ, Hebblewhite M, Schmiegelow F, Hervieux D, McDermid GJ, Neufeld L, Bradley M, Whittington J, Smith KG, Morgantini LE, Wheatley M, Musiani M (2012) Transcending scale dependence in identifying habitat with resource selection functions. Ecol Appl 22:1068-1083

DeCesare NJ, Hebblewhite M, Bradley M, Hervieux D, Neufeld L, Musiani M (2014) Linking habitat selection and predation risk to spatial variation in survival. J Anim Ecol 83:343-352

Diffendorfer JE, Rochester C, Fisher RN, Brown TK (2005) Movement and space use by Coastal Rosy Boas (*Lichanura trivirgata roseofusca*) in Coastal Southern California. J Herpetol 39:24-36

Dobson AP, Rodgriguez JP, Roberts WM, Wilcove DS (1997) Geographic distribution of endangered species in the United States. Science 275:550-553

Doncaster CP, MacDonald DW (1991) Drifting territoriality in the red fox *Vulpes vulpes*. J Anim Ecol 60:423-439

Dray S, Dufour AB (2007) The ade4 package: Implementing the duality diagram for ecologists. Journal of Statistical Software 22:1-20

Dungan JL, Perry JN, Dale MRT, Legendre P, Citron-Pousty S, Fortin MJ, Jakomulska A, Miriti M, Rosenberg MS (2002) A balanced view of scale in spatial statistical analysis. Ecography 25:626-640

Dunning JB, Stewart DJ, Danielson BJ, Noon BR, Root TL, Lamberson RH, Stevens EE (1995) Spatially explicit population models - current forms and future uses. Ecol Appl 5:3-11

Duong T, Hazelton ML (2003) Plug-in bandwidth matrices for bivariate kernel density estimation. Journal of Nonparametric Statistics 15:17-30

Duong T (2007) ks: kernel density estimation and kernel discriminant analysis for multivariate data in R. Journal of Statistical Software 21:1-16

Duong T (2014) ks: kernel smoothing. R package version 1.9.3. http://CRAN.R-project.org/package=ks.

Duvall D, Chiszar D, Hayes WK, Leonhardt JK, Goode MJ (1990) Chemical and behavioral ecology of foraging in prairie rattlesnakes (*Crotalus viridis viridis*). J Chem Ecol 16:87-101

Duvall D, Schuett GW (1997) Straight-line movement and competitive mate searching in prairie rattlesnakes, *Crotalus viridis viridis*. Anim Behav 54:329-334

Eide NE, Jepsen JU, Prestrud P (2004) Spatial organization of reproductive Arctic foxes *Alopex lagopus*: responses to changes in spatial and temporal availability of prey. J Anim Ecol 73:1056-1068

Elliot NB, Cushman SA, Macdonald DW, Loveridge AJ (2014) The devil is in the dispersers: predictions of landscape connectivity change with demography. J Appl Ecol 51:1169-1178

Emaresi G, Pellet J, Dubey S, Hirzel AH, Fumagalli L (2011) Landscape genetics of the Alpine newt (*Mesotriton alpestris*) inferred from a strip-based approach. Conserv Genet 12:41-50

Enge KM, Stevenson DJ, Elliot MJ, Bauder JM (2013) The historical and current distribution of the eastern indigo snake (*Drymarchon couperi*). Herpetol Conserv Biol 8:288-307

Epps CW, Palsboll PJ, Wehausen JD, Roderick GK, Ramey RR, McCullough DR (2005) Highways block gene flow and cause a rapid decline in genetic diversity of desert bighorn sheep. Ecol Lett 8:1029-1038

Epps CW, Wehausen JD, Bleich VC, Torres SG, Brashares JS (2007) Optimizing dispersal and corridor models using landscape genetics. J Appl Ecol 44:714-724

ESRI (2014) Soil Survey Geographic Database (SSURGO) Downloader 2014. ESRI. <http://www.arcgis.com/home/item.html?id=4dbfecc52f1442eeb368c435251591ec>. Accessed 15 Jul 2015.

ESRI (2015) Soil Survey Geographic Database (SSURGO) Downloader 2015. ESRI. <http://www.arcgis.com/home/item.html?id=4dbfecc52f1442eeb368c435251591ec>. Accessed 15 Jul 2015.

Fahrig L (2003) Effects of habitat fragmentaiton on biodiversity. Annual Review of Ecology, Evolution, and Systematics 34:487-515

Fahrig L, Rytwinski T (2009) Effects of roads on animal abundance: an empirical review and synthesis. Ecol Soc 14:21

Fearn S, Schwarzkopf L, Shine R (2005) Giant snakes in tropical forests: a field study of the Australian scrub python, *Morelia kinghorni*. Wildl Res 32:193-201

Ferreras P, Beltran JF, Aldama JJ, Delibes M (1997) Spatial organization and land tenure system of the endangered Iberian lynx (*Lynx pardinus*). Journal of Zoology 243:163-189

Fieberg J, Kochanny CO (2005) Quantifying home-range overlap: The importance of the utilization distribution. J Wildl Manage 69:1346-1359

Fieberg J (2014) Home range overlap indices implemented using kernel density estimators with plug-in smoothing parameters and Program R., University of Minnesota Digital Conservancy. Retrieved from <http://hdl.handle.net/11299/163012>.

Firth D (1993) Bias reduction of maximum likelihood estimates. Biometrika 80:27-38

Fischer J, Lindenmayer DB (2000) An assessment of the published results of animal relocations. Biol Conserv 96:1-11

Fitzgerald M, Shine R, Lemckert F (2002) Spatial ecology of arboreal snakes (*Hoplocephalus stephensii*, Elapidae) in an eastern Australian forest. Austral Ecol 27:537-545

Florida Department of Environmental Protection (2017) Florida forever: five year plan, 2017. In: Florida Department of Environmental Protection T, Florida (ed). Florida Department of Environmental Protection, Tallahassee, Florida,

Florida Fish and Wildlife Conservation Commission and Florida Natural Areas Inventory (2014) Cooperative land cover map. Version 3.0 Vector. . <http://www.fnai.org/LandCover.cfm>. Accessed 1 Feb 2015.

Florida Natural Areas Inventory (2018) Florida Conservation Lands. <http://fnai.org/gisdata.cfm>. Accessed 14 Aug 2018.

Folt B, Bauder J, Spear S, Stevenson D, Hoffman M, Oaks J, Steen D, Jenkins C, Guyer C (In review) Phylogenetic, population genetic, and morphological analyses reveal evidence for one species of Eastern Indigo Snake (*Drymarchon couperi*). Zool J Linn Soc

Fortin D, Beyer HL, Boyce MS, Smith DW, Duchesne T, Mao JS (2005) Wolves influence elk movements: behavior shapes a trophic cascade in Yellowstone National Park. Ecology 86:1320-1330

Frankham R, Ballou JD, Eldridge MDB, Lacy RC, Ralls K, Dudash MR, Fenster CB (2011) Predicting the probability of outbreeding depression. Conserv Biol 25:465-475

Fryxell JM, Falls JB, Falls EA, Brooks RJ, Dix L, Strickland MA (1999) Density dependence, prey dependence, and population dynamics of martens in Ontario. Ecology 80:1311-1321

Galpern P, Manseau M, Hettinga P, Smith K, Wilson P (2012a) Allelematch: an R package for identifying unique multilocus genotypes where genotyping error and missing data may be present. Molecular Ecology Resources 12:771-778

Galpern P, Manseau M, Wilson P (2012b) Grains of connectivity: analysis at multiple spatial scales in landscape genetics. Mol Ecol 21:3996-4009

Galpern P, Manseau M (2013) Finding the functional grain: comparing methods for scaling resistance surfaces. Landscape Ecol 28:1269-1281

Gardiner LE, Somers CM, Martino JA, Parker DL, Poulin RG (2013) Balancing the dumbbell: Summer habitats need protection in addition to winter dens for northern snake communities. J Wildl Manage 77:975-982

Gaston A, Ciudad C, Mateo-Sanchez MC, Garcia-Vinas JI, Lopez-Leiva C, Fernandez-Landa A, Marchamalo M, Cuevas J, de la Fuente B, Fortin MJ, Saura S (2017) Species' habitat use inferred from environmental variables at multiple scales: How much we gain from high-resolution vegetation data? Int J Appl Earth Obs 55:1-8

Gehrt SD, Fritzell EK (1998) Resource distribution, female home range dispersion and male spatial interactions: group structure in a solitary carnivore. Anim Behav 55:1211-1227

Gehrt SD, Anchor C, White LA (2009) Home range and landscape use of coyotes in a metropolitan landscape: conflict or coexistence? J Mammal 90:1045-1057

George AD, Thompson FR, Faaborg J (2015) Isolating weather effects from seasonal activity patterns of a temperate North American Colubrid. Oecologia 178:1251-1259

Gese EM (2001) Territorial defense by coyotes (*Canis latrans*) in Yellowstone National Park, Wyoming: who, how, where, when, and why. Can J Zool 79:980-987

Giam X, Olden JD (2016) Quantifying variable importance in a multimodel inference framework. Methods Ecol Evol 7:388-397

Gillies CS, Beyer HL, St. Clair CC (2011) Fine-scale movement decisions of tropical forest birds in a fragmented landscape. Ecol Appl 21:944-954

Gillingham JC (1987) Social behavior. In: Seigel RA, Collins JT, Novak SS (eds), Snakes: Ecology and Evolutionary Biology. MacMillan Publishing Company, New York, New York, pp 184-209

Giuggioli L, Potts JR, Harris S (2011) Animal interactions and the emergence of territoriality. PLoS ONE 7:e1002008

Glaudas X, Rodriguez-Robles JA (2011) Vagabond males and sedentary females: spatial ecology and mating system of the speckled rattlesnake (*Crotalus mitchellii*). Biol J Linn Soc 103:681-695

Godwin J, Wines M, Stiles J, Stiles S, Guyer C, Rush EM (2011) Reintroduction of the Eastern Indigo Snake (*Drymarchon couperi*) into Conecuh National Forest. 2008-2011 Final report submitted to the Alabama Department of Conservation and Natural Resources and The Orianne Society.

Goudet J, Perrin N, Waser P (2002) Tests for sex-biased dispersal using bi-parentally inherited genetic markers. Mol Ecol 11:1103-1114

Graf RF, Bollmann K, Suter W, Bugmann H (2005) The importance of spatial scale in habitat models: capercaillie in the Swiss Alps. Landscape Ecol 20:703-717

Grand J, Cushman SA (2004) A multi-scale analysis of species-environment relationships: breeding birds in a pitch pine-scrub oak *(Pinus rigida-Quercus ilicifolia*) community. Biol Conserv 115:173-173

Graves BM, Duvall D (1993) Reproduction, rookery use, and thermoregulation in free-ranging, pregnant *Crotalus v. viridis*. J Herpetol 27:33-41

Graves BM, Duvall D (1995) Aggregation of Squamate reptiles associated with gestation, oviposition, and parturition. Herpetol Monogr 9:102-119

Greene HW (1997) Snakes: The Evolution of Mystery in Nature. University of California Press, Berkeley, California, U.S.A.

Gregory PT (1982) Reptilian hibernation. In: Gans C (ed), Biology of the Reptilia. Academic Press, New York,

Gregory PT (1984) Communal denning in snakes. In: Seigel RA, Hunt LE, Knight JL, Malaret L, Zushlag NL (eds), Vertebrate Ecology and Systematics-A tribute to Henry S. Fitch. Museum of Natural History, The University of Kansas, Lawrence, Kansas, pp 57-75

Gregory PT, Macartney JM, Larsen KW (1987) Spatial patterns and movements. In: Seigel RA, Collins JT, Novak SS (eds), Snakes: Ecology and Evolutionary Biology. Macmillan Publishing Company, New York, NY, pp 366-395

Gregory PT (2009) Northern lights and seasonal sex: the reproductive ecology of cool-climate snakes. Herpetologica 65:1-13

Grimm V, Railsback SF (2005) Individual-based Modeling and Ecology. Princeton University Press, Princeton, New Jersey, U.S.A.

Grimm V, Revilla E, Berger U, Jeltsch F, Mooij WM, Railsback SF, Thulke HH, Weiner J, Wiegand T, DeAngelis DL (2005) Pattern-oriented modeling of agent-based complex systems: Lessons from ecology. Science 310:987-991

Grimm V, Berger U, Bastiansen F, Eliassen S, Ginot V, Giske J, Goss-Custard J, Grand T, Heinz SK, Huse G, Huth A, Jepsen JU, Jorgensen C, Mooij WM, Muller B, Pe'er G, Piou C, Railsback SF, Robbins AM, Robbins MM, Rossmanith E, Ruger N, Strand E, Souissi S, Stillman RA, Vabo R, Visser U, DeAngelis DL (2006) A standard protocol for describing individual-based and agent-based models. Ecol Model 198:115-126

Grimm V, Berger U, DeAngelis DL, Polhill JG, Giske J, Railsback SF (2010) The ODD protocol A review and first update. Ecol Model 221:2760-2768

Grimm V, Railsback SF (2012) Pattern-oriented modelling: a 'multi-scope' for predictive systems ecology. Philosophical Transactions of the Royal Society B-Biological Sciences 367:298-310

Grolemond G, Wickman H (2011) Dates and times made easy with lubridate. Journal of Statistical Software 40:1-25

Gross J, Elvinger F, Hungerford LL, Gehrt SD (2012) Racoon use of the urban matrix in the Baltimore Metropolitan Area, Maryland. Urban Ecosyst 15:667-682

Hardin JW, Hilbe JM (2003) Generalized estimating equations. Chapman and Hall/CRC, Boca Raton

Harris S, Cresswell WJ, Forde PG, Trewhella WJ, Woollard T, Wray S (1990) Home-range analysis using radio-tracking data - a review of problems and techniques particularly as applied to they study of mammals. Mammal Rev 20:97-123

Harvey DS, Weatherhead PJ (2006) A test of the hierarchical model of habitat selection using eastern massasauga rattlesnakes (*Sistrurus c. catenatus*). Biol Conserv 130:206-216

Herfindal I, Tremblay JP, Hansen BB, Solberg EJ, Heim M, Saether BE (2009) Scale dependency and functional response in moose habitat selection. Ecography 32:849-859

Hijmans RJ (2017) raster: geographic data analysis and modeling. R package version 2.6-7. http://CRAN.R-project.org/package=raster.

Hoctor T, O'Brien M, Oetting J (2010) Heartland ecological assessment report. The Nature Conservancy, Babson Park, Florida. 36 pages.,

Hogg JT, Forbes SH, Steele BM, Luikart G (2006) Genetic rescue of an insular population of large mammals. Proceedings of the Royal Society B-Biological Sciences 273:1491-1499

Holbrook JD, Squires JR, Olson LE, DeCesare NJ, Lawrence RL (2017) Understanding and predicting habitat for wildlife conservation: the case of Canada lynx at the range periphery. Ecosphere 8:e01939. 10.1002/ecs2.1939

Holland JD, Bert DD, Fahrig L (2004) Determining the spatial scale of a species' response to habitat. Bioscience 54:227-233

Holm S (1979) A simple sequentially rejective multiple test procedure. Scandinavian Journal of Statistics 6:65-70

Hoss SK, Guyer C, Smith LL, Schuett GW (2010) Multiscale influences of landscape composition and configuration on the spatial ecology of eastern diamond-backed rattlesnakes (*Crotalus adamanteus*). J Herpetol 44:110-123

Huang W-S, Greene HW, Chang T-J, Shine R (2011) Territoriality behavior in Taiwanese kukrisnakes (*Oligodon formosanus*). Proceedings of the National Academy of Sciences 108:7455-7459

Hyslop NL (2007) Movements, habitat use, and survival of the threatened eastern indigo snake (*Drymarchon couperi*) in Georgia. University of Georgia

Hyslop NL, Cooper RJ, Meyers JM (2009a) Seasonal shifts in shelter and microhabitat use of *Drymarchon couperi* (Eastern Indigo Snake) in Georgia. Copeia 2009:458-464

Hyslop NL, Meyers JM, Cooper RJ, Norton TM (2009b) Survival of radio-implanted *Drymarchon couperi* (eastern indigo snake) in relation to body size and sex. Herpetologica 65:199-206

Hyslop NL, Stevenson DJ, Macey JN, Carlile LD, Jenkins CL, Hostetler JA, Oli MK (2012) Survival and population growth of a long-lived threatened snake species, *Drymarchon couperi* (Eastern Indigo Snake). Popul Ecol 54:145-156

Hyslop NL, Meyers JM, Cooper RJ, Stevenson DJ (2014) Effects of body size and sex of *Drymarchon couperi* (Eastern Indigo Snake) on habitat use, movements, and home range size in Georgia. J Wildl Manage 78:101-111

Irvin E, Duren KR, Buler JJ, Jones W, Gonzon AT, Williams CK (2013) A multi-scale occupancy model for the Grasshopper Sparrow in the Mid-Atlantic. J Wildl Manage 77:1564-1571

Jaquiery J, Broquet T, Hirzel AH, Yearsley J, Perrin N (2011) Inferring landscape effects on dispersal from genetic distances: how far can we go? Mol Ecol 20:692-705

Jellen BC, Aldridge RD (2014) It takes two to tango: female movement facilitates male mate location in wild northern watersnakes (*Nerodia sipedon*). Behaviour 151:421-434

Jellen BC, Graham SP, Aldridge RD, Earley RL (2014) Oestrus in a secretive species: endogenous estradiol varies throughout the shed cycle and influences attractiveness in wild northern watersnakes (*Nerodia sipedon*). Behaviour 151:403-419

Jenkins CL (2007) Ecology and conservation of rattlesnakes in sagebrush steppe ecosystems: landscape disturbance, small mammal communities, and Great Basin rattlesnake reproduction. Idaho State University

Johnson CJ, Seip DR, Boyce MS (2004) A quantitative approach to conservation planning: using resource selection functions to map the distribution of mountain caribou at multiple spatial scales. J Appl Ecol 41:238-251

Johnson CJ, Nielsen SE, Merrill EH, McDonald TL, Boyce MS (2006) Resource selection functions based on use availability-data: theoretical motivation and evaluation of methods. J Wildl Manage 70:347-357

Johnson DH (1980) The comparison of usage and availability measurements for evaluating resource preference. Ecology 61:65-71

Johnson PCD (2014) Extension of Nakagawa & Schielzeth's R_GLMM² to random slopes models. Methods Ecol Evol 5:944-946

Jombart T (2008) adegenet: a R package for the multivariate analysis of genetic markers. Bioinformatics 24:1403-1405

Jorgensen D, Gates CC, Whiteside DP (2008) Movements, migrations, and mechanisms: a review of radiotelemetry studies of prairie (*Crotalus v. viridis*) and western (*Crotalus oreganus*) rattlesnakes. In: Hayes WK, Beaman KR, Cardwell MD, Bush SP (eds), The Biology of Rattlesnakes. Loma Linda University Press, Loma Linda, California, U.S.A., pp 303-316

Kalinowski ST, Taper ML, Marshall TC (2007) Revising how the computer program CERVUS accommodates genotyping error increases success in paternity assignment. Mol Ecol 16:1099-1106

Kawula R (2014) Florida land cover classification system: final report. State Wildlife Grant, SWG T-13 (FWRI Grant # 6325). Center for Spatial Analysis, Fish and Wildlife Research Institute, Florida Fish and Wildlife Conservation Commission, Tallahassee, Florida,

Keeley ATH, Beier P, Gagnon JW (2016) Estimating landscape resistance from habitat suitability: effects of data source and nonlinearities. Landscape Ecol 31:2151-2162

Keller D, Holderegger R, van Strien MJ (2013) Spatial scale affects landscape genetic analysis of a wetland grasshopper. Mol Ecol 22:2467-2482

Keller D, Holderegger R, van Strien MJ, Bolliger J (2015) How to make landscape genetics beneficial for conservation management? Conserv Genet 16:503-512

Keller LF, Waller DM (2002) Inbreeding effects in wild populations. Trends Ecol Evol 17:230-241

Keogh JS, Webb JK, Shine R (2007) Spatial genetic analysis and long-term mark-recapture data demonstrate male-biased dispersal in a snake. Biol Lett 3:33-35

Kie JG, Bowyer RT, Nicholson MC, Boroski BB, Loft ER (2002) Landscape heterogeniety at differing scales: effects on spatial distribution of mule deer. Ecology 83:530-544

King MB, Duvall D (1990) Prairie rattlesnake seasonal migrations: episodes of movemnt, vernal foraging and sex differences. Anim Behav 39:924-935

Kivimaki I, Shimbo M, Saerens M (2014) Developments in the theory of randomized shortest paths with a comparison of graph node distances. Physica a-Statistical Mechanics and Its Applications 393:600-616

Klug PE, Fill J, With KA (2011) Spatial ecology of eastern yellow-bellied racer (*Coluber constrictor flaviventris*) and Great Plains rat snake (*Pantherophis emoryi*) in a contiguous tallgrass-prairie landscape. Herpetologica 67:428-439

Knight GR (2010) Development of a cooperative land cover map: final report. Florida's Wildlife Legacy Initiative Project 08009.

Knopff AA, Knopff KH, Boyce MS, St. Clair CC (2014) Flexible habitat selection by cougars in response to anthropogenic development. Biol Conserv 178:136-145

Koenig J, Shine R, Shea G (2001) The ecology of an Australian reptile icon: how do blue-tongued lizards (*Tiliqua scincoides*) survive in suburbia? Wildl Res 28:215-227

Kosmidis I (2017) brglm: bias reduction in binary-response generalized linear models. R package version 0.6.1. http://CRAN.R-project.org/package=brglm.

Kraemer P, Gerlach G (2017) Demerelate: calculating interindividual relatedness for kinship analysis based on codominant diploid genetic markers using R. Molecular Ecology Resources 17:1371-1377

Kramer-Schadt S, Revilla E, Wiegand T (2005) Lynx reintroductions in fragmented landscapes of Germany: projects with a future or misunderstood wildlife conservation? Biol Conserv 125:169-182

Krysko KL, Nunez CA, Lippi CA, Smith DJ, Granatosky MC (2016) Pliocene-Pleistocene lineage diversifications in the Eastern Indigo Snake (Drymarchon couperi) in the Southeastern United States. Mol Phylogenet Evol 98:111-122

Kwiatkowski MA, Schuett GW, Repp RA, Nowak EM, Sullivan BK (2008) Does urbanization influence the spatial ecology of Gila monsters in the Sonoran Desert? Journal of Zoology 276:350-357

Laake JL (2013) RMark: an R interface for analysis of capture-recapture data with MARK. AFSC Processed Rep 2013-01, 25p. Alaska Fish. Sci. Cent., NOAA, Natl. Mar. Fish. Serv., 7600 Sand Point Way NE, Seattle WA 98115.,

Landguth EL, Cushman SA (2010) CDPOP: a spatially explicit cost distance population genetics program. Molecular Ecology Resources 10:156-161

Larsen KW (1987) Movements and behavior of migratory garter snakes, *Thamnophis sirtalis*. Can J Zool 65:2241-2247

Laver PN, Kelly MJ (2008) A critical review of home range studies. J Wildl Manage 72:290-298

Law BS, Dickman CR (1998) The use of habitat mosaics by terrestrial vertebrate fauna: implications for conservation and management. Biodivers Conserv 7:323-333

Layne JN, Steiner TM (1996) Eastern indigo snake (*Drymarchon corais couperi*): summary of research conducted on Archbold Biological Station. Report prepared under order 43910-6-0134 to the U.S. Fish and Wildlife Service. Jackson, Mississippi, pp. 64 pp.

Leblond M, Frair J, Fortin D, Dussault C, Ouellet J-P, Courtois R (2011) Assessing the influence of resource covariates at multiple spatial scales: an application to forest-dwelling caribou faced with intensive human activity. Landscape Ecol 26:1433-1446

Lele SR, Keim JL (2006) Weighted distributions and estimation of resource selection probability functions. Ecology 87:3021-3028

Lelievre H, Le Henanff M, Blouin-Demers G, Naulleau G, Lourdais O (2010) Thermal strategies and energetics in two sympatric colubrid snakes with contrasted exposure. Journal of Comparative Physiology B 180:415-425

Lelievre H, Moreau C, Blouin-Demers G, Bonnet X, Lourdais O (2012) Two syntopic Colubrid snakes differ in their energetic requiremens and in their use of space. Herpetologica 68:358-364

LeMaster MP, Moore IT, Mason RT (2001) Conspecific trailing behaviour of red-sided garter snakes, Thamnophis sirtalis parietalis, in the natural environment. Anim Behav 61:827-833

Lenth RV (1981) On finding the source of a signal. Technometrics 23:149-154

Letcher BH, Priddy JA, Walters JR, Crowder LB (1998) An individual-based, spatially-explicit simulation model of the population dynamics of the endangered red-cockaded woodpecker, *Picoides borealis*. Biol Conserv 86:1-14

Levin SA (1992) The problem of pattern and scale in ecology. Ecology 73:1943-1967

Lewison RL, Carter J (2004) Exploring behavior of an unusual megaherbivore: a spatially explicit foraging model of the hippopotamus. Ecol Model 171:127-138

Lister BC, Aguayo AG (1992) Seasonality, predation, and the behavior of a tropical mainland anole. J Anim Ecol 61:717-733

Lopez-Bao JV, Rodriguez A, Delibes M, Fedriani JM, Calzada J, Ferreras P, Palomares F (2014) Revisiting food-based models of territoriality in solitary predators. J Anim Ecol 83:934-942

Lowe WH, Allendorf FW (2010) What can genetics tell us about population connectivity? Mol Ecol 19:3038-3051

Lukacs PM, Burnham KP, Anderson DR (2010) Model selection bias and Freedman's paradox. Annals of the Institute of Statistical Mathematics 62:117-125

MacDonald DW, Mosser A, Gittleman JL (2010) Felid society. In: MacDonald DW andLoveridge AJ (eds), Biology and Conservation of Wild Felids. Oxford University Press Inc., Oxford, New York, pp 126-160

Maciel AP, Di-Bernardo M, Hartz SM, Oliveira RB, Pontes GMF (2003) Seasonal and daily activity patterns of *Liophis poecilogyrus* (Serpentes: Colubridae) on the north coast of Rio Grande do Sul, Brazil. Amphib-Reptilia 24:189-200

Madsen T, Shine R, Loman J, Hakansson T (1993) Determinants of mating success in male adders, *Vipera berus*. Anim Behav 45:491-499

Madsen T, Shine R (1996a) Seasonal migration of predators and prey - a study of pythons and rats in tropical Australia. Ecology 77:149-156

Madsen T, Shine R (1996b) Determinants of reproductive output in female water pythons (*Liasis fuscus*: Pythonidae). Herpetologica 52:146-159

Maher CR, Lott DF (1995) Defininitions of territoriality used in the study of variation in vertebrate spacin systems. Anim Behav 49:1581-1597

Maher CR, Lott DF (2000) A review of ecological determinants of territoriality within vertebrate species. Am Midl Nat 143:1-29

Malishev M, Bull CM, Kearney MR (2018) An individual-based model of ectotherm movement integrating metabolic and microclimatic constraints. Methods Ecol Evol 9:472-489

Manel S, Schwartz MK, Luikart G, Taberlet P (2003) Landscape genetics: combining landscape ecology and population genetics. Trends in Ecology and Evolution 18:189-197

Manly BFJ, McDonald L, Thomas DL, McDonald TL, Erickson WP (2002) Resource Seleciton by Animals: Statistical Design and Analysis for Field Studies. Kluwer Academic Publishers, Secaucus, NJ, USA

Mantel N (1967) The detection of disease clustering and a generalized regression approach. Cancer Research 27:209-220

Marques OAV, Muniz-Da-Silva DF, Barbo FE, Cardoso SRT, Maia DC, Almeida-Santos SM (2014) Ecology of the colubrid snake *Spilotes pullatus* from the Atlantic Forest of southeastern Brazil. Herpetologica 70:407-416

Martin AE, Fahrig L (2012) Measuring and selecting scales of effect for landscape predictors in species-habitat models. Ecol Appl 22:2277-2292

Martin BT, Czesny S, Wahl DH, Grimm V (2016) Scale-dependent role of demography and dispersal on the distribution of populations in heterogeneous landscapes. Oikos 125:667-673

Martino JA, Poulin RG, Parker DL, Somers CM (2012) Habitat selection by grassland snakes at northern range limits: Implications for conservation. J Wildl Manage 76:759-767

Marzluff JM, Millspaugh JJ, Hurvitz P, Handcock MS (2004) Relating resources to a probabilistic measure of space use: forest fragments and Stellar's jays. Ecology 85:1411-1427

Masek JG, Vermote EF, N.E. S, Wolfe R, Hall FG, Huemmrich KF, Gao F, Kutler J, Lim T-K (2006) A Landsat surface reflectance dataset for North America, 1990-2000. IEEE Geoscience and Remote Sensing Letters 3:68-72

Mateo-Sanchez MC, Balkenhol N, Cushman S, Perez T, Dominguez A, Saura S (2015a) A comparative framework to infer landscape effects on population genetic structure: are habitat suitability models effective in explaining gene flow? Landscape Ecol 30:1405-1420

Mateo-Sanchez MC, Balkenhol N, Cushman S, Perez T, Dominguez A, Saura S (2015b) Estimating effective landscape distances and movement corridors: comparison of habitat and genetic data. Ecosphere 6

May PG, Farrell TM, Heulett ST, Pilgrim MA, Bishop LA, Spence DJ, Rabatsky AM, Campbell MG, Aycrigg AD, Richardson WE (1996) Seasonal abundance and activity of a rattlesnake (*Sistrurus miliarius barbouri*) in central Florida. Copeia:389-401

Mayor SJ, Schneider DC, Schaefer JA, Mahoney SP (2009) Habitat selection at multiple scales. Ecoscience 16:238-247

McArdle BH, Anderson MJ (2001) Fitting multivariate models to community data: A comment on distance-based redundancy analysis. Ecology 82:290-297

McClure CJW, Rolek BW, Hill GE (2012) Predicting occupancy of wintering migratory birds: is microhabitat information necessary? Condor 114:482-490

McCue MD (2007) Western diamondback rattlesnakes demonstrate physiological and biochemical strategies for tolerating prolonged starvation. Physiol Biochem Zool 80:25-34

McGarigal K, Wan HY, Zeller KA, Timm BC, Cushman SA (2016) Multi-scale habitat selection modeling: a review and outlook. Landscape Ecol 31:1161-1175

McLane AJ, Semeniuk C, McDermid GJ, Marceau DJ (2011) The role of agent-based models in wildlife ecology and management. Ecol Model 222:1544-1556

McLoughlin PD, Ferguson SH, Messier F (2000) Intraspecific variation in home range overlap with habitat quality: A comparison among brown bear populations. Evol Ecol 14:39-60

McNew LB, Gregory AJ, Sandercock BK (2013) Spatial heterogeneity in habitat selection: Nest site selection by greater prairie-chickens. J Wildl Manage 77:791-801

McRae BH (2006) Isolation by resistance. Evolution 60:1551-1561

McRae BH, Dickson BG, Keitt TH, Shah VB (2008) Using circuit theory to model connectivity in ecology, evolution, and conservation. Ecology 89:2712-2724

Meyer CB, Thuiller W (2006) Accuracy of resource selection functions across spatial scales. Divers Distrib 12:288-297

Meyer CB (2007) Does scale matter in predicting species distributions? Case study with the marbled murrelet. Ecol Appl 17:1474-1483

Milanesi P, Holderegger R, Bollmann K, Gugerli F, Zellweger F (2017a) Three-dimensional habitat structure and landscape genetics: a step forward in estimating functional connectivity. Ecology 98:393-402

Milanesi P, Holderegger R, Caniglia R, Fabbri E, Galaverni M, Randi E (2017b) Expert-based versus habitat-suitability models to develop resistance surfaces in landscape genetics. Oecologia 183:67-79

Millette KL, Keyghobadi N (2014) The relative influence of habitat amount and configuration on genetic structure across multiple spatial scales. Ecology and Evolution 5:73-86

Mitrovich MJ, Diffendorfer JE, Fisher RN (2009) Behavioral response of the coachwhip (*Masticophis flagellum*) to habitat fragment size and isolation in an urban landscape. J Herpetol 43:646-656

Moler PE (1985) Home range and seasonal activity of the eastern indigo snake, *Drymarchon corais couperi*, in northern Flordia. Final Preformance Report, Statewide Wildlife Research, Study No. E-1-06. pp. 26 pp.

Moler PE (1992) Eastern indigo snake. In: Moler PE (ed), Rare and endangered biota of Florida, volume III, Amphibians and Reptiles. University Press of Florida, Gainesville, pp 181-186

Moore JA, Gillingham JC (2006) Spatial ecology and multi-scale habitat selection by a threatened rattlesnake: the eastern massasauga (*Sistrurus catenatus catenatus*). Copeia 2006:742-751

Morellet N, Bonenfant C, Borger L, Ossi F, Cagnacci F, Heurich M, Kjellander P, Linnell JDC, Nicoloso S, Sustr P, Urbano F, Mysterud A (2013) Seasonality, weather and climate affect home range size in roe deer across a wide latitudinal gradient within Europe. J Anim Ecol 82:1326-1339

Moser BW, Garton EO (2007) Effects of telemetry location error on space-use estimates using a fixed kernel density estimator. J Wildl Manage 71:2421-2426

Moulis R (1976) Autecology of the eastern indigo snake, *Drymarchon corais couperi*. Bulletin of the New York Herpetological Society 12:14-23

Muller JW, Hardin ED, Jackson DR, Gatewood SE, Caire N (1989) Summary report of the vascular plants, animals, and plant communities endemic to Florida. In: Program FGaFWFCNW (ed). Florida Game and Fresh Water Fish Commission Nongame Wildlife Program, Tech. Rep. No. 7, pp. 113 pp. + viii

Mumme RL, Schoech SJ, Woolfenden GW, Fitzpatrick JW (2000) Life and death in the fast lane: Demographic consequences of road mortality in the Florida scrub jay. Conserv Biol 14:501-512

Murphy MA, Evans JS, Storfer A (2010) Quantifying *Bufo boreas* connectivity in Yellowstone National Park with landscape genetics. Ecology 91:252-261

Myers RL (1990) Scrub and high pine. In: Myers RL andEwel JJ (eds), Ecosystems of Florida. University of Central Florida Press, Orlando,

Myers RL, Ewel JJ (eds) (1990) Ecosystems of Florida. University of Florida Press, Orlando

Nagy KA (2005) Field metabolic rate and body size. J Exp Biol 208:1621-1625

Nakagawa S, Schielzeth H (2013) A general and simple method for obtaining R2 from generalized linear mixed-effects models. Methods Ecol Evol 4:133-142

Newberry SL, Jensen JB, Stevenson DJ (2009) *Drymarchon couperi* (eastern indigo snake). Nesting habitat and egg depredation. Herpetol Rev 40:97

Nielson SE, Boyce MS, Stenhouse GB, Munro RHM (2002) Modeling grizzly bear habitats in the Yellowhead Ecosystem of Alberta: Taking autocorrelation seriously. Ursus 13:45-56

Nowak EM, Theimer TC, Schuett GW (2008) Functional and numerical responses of predators: where do vipers fit in the traditional paradigms? Biological Reviews 83:601-620

Oksanen J, Blanchet FG, Kindt R, Legendre P, Minchin PR, O'Hara RB, Simpson GL, Solymos P, Stevens MHH, Wagner H (2015) vegan: community ecology package. R package version 2.2-1 http://CRAN.R-project.org/package=vegan.

Oli MK, Dobson FS (2003) The relative importance of life-history variables to population growth rate in mammals: Cole's prediction revisited. Am Nat 161:422-440

Olsen MT, Andersen LW, Dietz R, Teilmann J, Harkonen T, Siegismund HR (2014) Integrating genetic data and population viability analyses for the identification of harbour seal (Phoca vitulina) populations and management units. Mol Ecol 23:815-831

Ostfeld RS (1986) Territoriality and mating system of California voles. J Anim Ecol 55:691-706

Ostfeld RS (1990) The ecology of territoriality in small mammals. Trends Ecol Evol 5:411-415

Owen-Smith N (1977) On territoriality in ungulates and an evolutionary model. The Quarterly Review of Biology 52:1-38

Oyler-McCance SJ, Fedy BC, Landguth EL (2013) Sample design effects in landscape genetics. Conserv Genet 14:275-285

Paradis E (2010) pegas: an R package for population genetics with an integrated-modular approach. Bioinformatics 26:419-420

Parker WS, Plummer MV (1987) Population ecology. In: Seigel RA, Collins JT, Novak SS (eds), Snakes: Ecology and Evolutionary Biology. Macmillan Publsihing Company, New York, pp 253-301

Pattishall A, Cundall D (2009) Habitat use by synurbic watersnakes (*Nerodia sipedon*). Herpetologica 65:183-198

Peakall R, Ruibal M, Lindenmayer DB, Tonsor S (2003) Spatial autocorrelation analysis offers new insights into gene flow in the Australian bush rat, *Rattus fuscipes*. Evolution 57:1182-1195

Peakall R, Smouse PE (2006) GenAlEx 6: genetic analysis in Excel. Population genetic software for teaching and research. Mol Ecol Notes 6:288-295, doi: 10.1111/j.1471-8286.2005.01155.x

Peakall R, Smouse PE (2012) GenAIEx 6.5: genetic analysis in Excel. Population genetic software for teaching and research - an update. Bioinformatics 28:2537-2539, doi:10.1093/bioinformatics/bts460

Pearson D, Shine R, Williams A (2005) Spatial ecology of a threatened python (*Morelia spilota imbricata*) and the effects of anthropogenic habitat change. Austral Ecol 30:261-274

Peterman WE, Connette GM, Semlitsch RD, Eggert LS (2014) Ecological resistance surfaces predict fine-scale genetic differentiation in a terrestrial woodland salamander. Mol Ecol 23:2402-2413

Peterman WE (2018) ResistanceGA: An R package for the optimization of resistance surfaces using genetic algorithms. Methods Ecol Evol 9:1638-1647

Peterson CR, Gibson AR, Dorcas ME (1993) Snake thermal ecology: causes and consequences in body-temperature variation In: Seigel RA andCollins JT (eds), Snakes: Ecology and Behavior. McGraw Hill, Inc., New York, pp 241-314

Pinheiro J, Bates D, DebRoy S, Sarkar D (2013) nlme: Linear and nonlinear mixed effects models. R Package Version 3.1–111. Available at http://CRAN.R-project.org/package=nlme.

Plummer MV, Congdon JD (1994) radiotelemetric study of activity and movements of racers (*Coluber constrictor*) associated with a Carolina bay in South Carolina. Copeia 1994:20-26

Plummer MV, Congdon JD (1996) Rates of metabolism and water flux in free-ranging racers, *Coluber constrictor*. Copeia 1996:8-14

Polfus JL, Hebblewhite M, Heinemeyer K (2011) Identifying indirect habitat loss and avoidance of human infrastructure by northern mountain woodland caribou. Biol Conserv 144:2637-2646

Pough FH (1980) Advantages of ectotherm for tetrapods. Am Nat 115:92-112

Powell RA (1979) Mustelid spacing patterns - variations on a theme by *Mustella*. Zeitschrift Fur Tierpsychologie-Journal of Comparative Ethology 50:153-165

Powell RA (1993) Why do some forest carnivores exhibit intrasexual territoriality and what are the consequences for management? Proceedings of the International Union of Game Biologists 21:268-273

Powell RA (1994) Structure and spacing of *Martes* populations. In: Buskirk SW, Harestad AS, Raphael MG, Powell RA (eds), Martens, Sables, and Fishers: Biology and Conservation. Cornell University Press, Ithaca, New York, USA, pp 101-121

Proctor MF, McLellan BN, Strobeck C, Barclay RMR (2005) Genetic analysis reveals demographic fragmentation of grizzly bears yielding vulnerably small populations. Proceedings of the Royal Society B-Biological Sciences 272:2409-2416

Putman BJ, Lind C, Taylor EN (2013) Does size matter? Factors influencing the spatial ecology of Northern Pacific Rattlesnakes (*Crotalus oreganus oreganus*) in Central California. Copeia:485-492

R Core Team (2017) R: a language and environment for statistical computing. R Foundation for Statistical Computing, Vienna, Austria. http://www.R-project.org/. Accessed 1 October 2017,

Railsback SF, Harvey BC (2002) Analysis of habitat-selection rules using an individual-based model. Ecology 83:1817-1830

Railsback SF, Grimm V (2011) Agent-Based and Individual-Based Modeling: A Practical Introduction. Princeton University Press, New Jersey

Reding DM, Cushman SA, Gosselink TE, Clark WR (2013) Linking movement behavior and fine-scale genetic structure to model landscape connectivity for bobcats (*Lynx rufus*). Landscape Ecol 28:471-486

Reed RN, Douglas ME (2002) Ecology of the Grand Canyon rattlesnake (*Crotalus viridis abyssus*) in the Little Colorado River Canyon, Arizona. Southwest Nat 47:30-39

Reinert HK, Cundall D (1982) An improved surgical implantation method for radio-tracking snakes. Copeia 1982:702-705

Reinert HK (1984) Habitat variation within sympatric snake populations. Ecology 65:1673-1682

Reinert HK, Zappalorti RT (1988a) Field observation of the association of adult and neonatal timber rattlesnakes, *Crotalus horridus*, with possible evidence for conspecific trailing. Copeia:1057-1059

Reinert HK, Zappalorti RT (1988b) Timber rattlesnake (*Crotalus horridus*) of the Pine Barrens - their movement patterns and habitat preference. Copeia:964-978

Richardson JL, Brady SP, Wang IJ, Spear SF (2016) Navigating the pitfalls and promise of landscape genetics. Mol Ecol 25:849-863

Riley SPD, Sauvajot RM, Fuller TK, York EC, Kamradt DA, Bromley C, Wayne RK (2003) Effects of urbanization and habitat fragmentation on bobcats and coyotes in southern California. Conserv Biol 17:566-576

Rivera PC, Gardenal CN, Chiaraviglio M (2006) Sex-biased dispersal and high levels of gene flow among local populations in the Argentine boa constrictor, *Boa constrictor occidentalis*. Austral Ecol 31:948-955

Robinson SK, Thompson FR, Donovan TM, Whitehead DR, Faaborg J (1995) Regional forest fragmentation and the nesting success of migratory birds. Science 267:1987-1990

Rodriguez-Robles JA (2003) Home ranges of gopher snakes (*Pituophis catenifer*, Colubridae) in central California. Copeia:391-396

Roffler GH, Schwartz MK, Pilgrim KL, Talbot SL, Sage GK, Adams LG, Luikart G (2016) Identification of landscape features influencing gene flow: How useful are habitat selection models? Evolutionary Applications 9:805-817

Rogers LL (1987) Effects of food-supply and kinship on social behavior, movements, and population growth of black bears in northeastern Minnesota. Wildl Monogr 97:1-72

Rossmanith E, Blaum N, Grimm V, Jeltsch F (2007) Pattern-oriented modelling for estimating unknown pre-breeding survival rates: the case of the lesser spotted woodpecker (*Picoides minor*). Biol Conserv 135:555-564

Rousset F (2008) GENEPOP'007: a complete re-implementation of the GENEPOP software for Windows and Linux. Molecular Ecology Resources 8:103-106

Row JR, Blouin-Demers G (2006) Thermal quality influences habitat selection at multiple spatial scales in milksnakes. Ecoscience 13:443-450

Row JR, Blouin-Demers G, Weatherhead PJ (2007) Demographic effects of road mortality in black ratsnakes (*Elaphe obsoleta*). Biol Conserv 137:117-124

Row JR, Blouin-Demers G, Lougheed SC (2012) Movements and habitat use of eastern foxsnakes (*Pantherophis gloydi*) in two areas varying in size and fragmentation. J Herpetol 46:94-99

Row JR, Oyler-McCance SJ, Fike JA, O'Donnell MS, Doherty KE, Aldridge CL, Bowen ZH, Fedy BC (2015) Landscape characteristics influencing the genetic structure of greater sage-grouse within the stronghold of their range: a holistic modeling approach. Ecology and Evolution 5:1955-1969

Ruben JA (1976) Aerobic and anaerobic metabolism during activity in snakes. Journal of Comparative Physiology 109:147-157

Said S, Gaillard J-M, Duncan P, Guillon N, Guillon N, Servanty S, Pellerin M, Lefeuvre K, Martin C, van Laere G (2005) Ecological correlates of home-range size in spring–summer for female roe deer (*Capreolus capreolus*) in a deciduous woodland. Journal of Zoology 267:301-308

Salek M, Drahnikova L, Tkadlec E (2015) Changes in home range sizes and population densities of carnivore species along the natural to urban habitat gradient. Mammal Rev 45:1-14

Sandell M (1989) The mating tactics and spacing patterns of solitary carnivores. In: Gittleman JL (ed), Carnivore Behavior, Ecology, and Evolution. Cornell University Press, Ithaca, NY, USA, pp 164-182

Scott ML, Whiting MJ, Webb JK, Shine R (2013) Chemosensory discrimination of social cues mediates space use in snakes, *Cryptophis nigrescens* (Elapidae). Anim Behav 85:1493-1500

Scrucca L (2013) GA: a package for genetic algorithms in R. Journal of Statistical Software 53:1-37

Secor SM (1994) Ecological significane of movements and activity range for the sidewinder, *Crotalus cerastes*. Copeia 1994:631-645

Secor SM, Nagy KA (1994) Bioenergetic correlates of foraging mode for the snakes *Crotalus cerastes* and *Masticophis flagellum*. Ecology 75:1600-1614

Segelbacher G, Cushman SA, Epperson BK, Fortin MJ, Francois O, Hardy OJ, Holderegger R, Taberlet P, Waits LP, Manel S (2010) Applications of landscape genetics in conservation biology: concepts and challenges. Conserv Genet 11:375-385

Service USFaW (2008) Eastern indigo snake *Drymarchon couperi* 5 year review: summary and evaluation. U.S. Fish and Wildlife Service, Jackson, pp. 33

Sexton JP, Strauss SY, Rice KJ (2011) Gene flow increases fitness at the warm edge of a species' range. Proc Natl Acad Sci U S A 108:11704-11709

Shafer ABA, Northrup JM, White KS, Boyce MS, Cote SD, Coltman DW (2012) Habitat selection predicts genetic relatedness in an alpine ungulate. Ecology 93:1317-1329

Shamblin BM, Alstad TI, Stevenson DJ, Macey JN, Snow F, Nairn CJ (2011) Isolation and characterization of microsatellite markers from the threatened eastern indigo snake (*Drymarchon couperi*). Conservation Genetics Resources 3:303-306

Shine R, Madsen T (1996) Is thermoregulation unimportant for most reptiles? An example using water pythons (*Liasis fuscus*) in tropical Australia. Physiol Zool 69:252-269

Shine R, Phillips B, Waye H, LeMaster M, Mason RT (2003) Chemosensory cues allow courting male garter snakes to assess body length and body condition of potential mates. Behav Ecol Sociobiol 54:162-166

Shine R, Bonnet X (2009) Reproductive biology, population viability, and options for field management. In: Mullin SJ andSeigel RA (eds), Snakes: Ecology and Conservation. Cornell University Press, Ithaca, New York,

Shirk AJ, Wallin DO, Cushman SA, Rice CG, Warheit KI (2010) Inferring landscape effects on gene flow: a new model selection framework. Mol Ecol 19:3603-3619

Shirk AJ, Raphael MG, Cushman SA (2014) Spatiotemporal variation in resource selection: insights from the American marten (*Martes americana*). Ecol Appl 24:1434-1444

Shirk AJ, Landguth EL, Cushman SA (2017) A comparison of individual-based genetic distance metrics for landscape genetics. Molecular Ecology Resources:1-10

Shirk AJ, Landguth EL, Cushman SA (2018) A comparison of regression methods for model selection in individual-based landscape genetic analysis. Molecular Ecology Resources 18:55-67

Short-Bull RA, Cushman SA, Mace R, Chilton T, Kendall KC, Landguth EL, Schwartz MK, McKelvey K, Allendorf FW, Luikart G (2011) Why replication is important in landscape genetics: American black bear in the Rocky Mountains. Mol Ecol 20:1092-1107

Slip DJ, Shine R (1988) Habitat use, movemens and activity patterns of free-ranging diamond pythons, *Morelia spilota spilota* (Serpentes, Boidae) - a radiotelemetric study. Aust Wildl Res 15:515-531

Smith CC (1968) Adaptive nature of social organization in genus of 3 squirrels *Tamiasciurus*. Ecol Monogr 38:31-64

Smith CF, Shuett GW, Earley RL, Schwenk K (2009) The spatial and reproductive ecology of the copperhead (*Agkistrodon contortrix*) at the northeastern extreme of its range. Herpetol Monogr 23:45-73

Smith CF, Schuett GW, Amarello M (2015) Male mating success in a North American pitviper: influence of body size, testosterone, and spatial metrics. Biol J Linn Soc 115:185-194

Smith CR (1987) Ecology of juvenile and gravid eastern indigo snakes in north Florida. Auburn University

Smith HM (1941) Zoology: A review of the subspecies of the eastern indigo snake (*Drymarchon corais*). J Wash Acad Sci 31:466-481

Smouse PE, Peakall R (1999) Spatial autocorrelation analysis of individual multiallele and multilocus genetic structure. Heredity 82:561-573

South Florida Water Management District (2004) Land Cover Land Use 2004. <http://www.sfwmd.gov/gisapps/sfwmdxwebdc/dataview.asp>. Accessed 1 Jun 2015.

Southwest Florida Water Management District (2004) LU04. <http://www.swfwmd.state.fl.us/data/gis/libraries/physical_dense/lu04.htm>. Accessed Jun 1 2015.

Southworth H, Heffernan JE (2013) texmex: statistical modeling of extreme values. R package version 2.1. http://CRAN.R-project.org/package=texmex.

Speake DW, McGlincy JA, Colvin TR (1978) Ecology and management of the eastern indigo snake in Georgia: a progress report. In: Odum R andLanders L (eds), Proceedings of the Third Southeastern Nongame and Endangered Wildlife Symposium. Georgia Department of Natural Resources, Game and Fish Division Technical Bulletin WL4, Athens, pp. 64-73

Speake DW, McGlincy D, Smith C (1987) Captive breeding and experimental reintroducion of the eastern indigo snake. Proceedings of the Third Southeastern Nongame and Endangered Wildlife Symposium 3:84-90

Spear SF, Balkenhol N, Fortin M-J, McRae BH, Scribner K (2010) Use of resistance surfaces for landscape genetic studies: considerations for parameterization and analysis. Mol Ecol 19:3576-3591

Spear SF, Cushman SA, McRae BH (2016) Resistance surface modeling in landscape genetics. In: Balkenhol N, Cushman S, Storfer A, Waits L (eds), Landscape Genetics: Concepts, Methods, Applications. Wiley-Blackwell, Chichester,

Sperry JH, Weatherhead PJ (2009a) Sex differences in behavior associated with sex-biased mortality in an oviparous snake species. Oikos 118:627-633

Sperry JH, Weatherhead PJ (2009b) Does prey availability determine seasonal patterns of habitat selection in Texas ratsnakes? J Herpetol 43:55-64

Sperry JH, Blouin-Demers G, Carfagno GLF, Weatherhead PJ (2010) Latitudinal variation in seasonal activity and mortality in ratsnakes (*Elaphe obsoleta*). Ecology 91:1860-1866

Sperry JH, Weatherhead PJ (2012) Individual and sex-based differences in behaviour and ecology of rat snakes in winter. Journal of Zoology 287:142-149

Squires JR, DeCesare NJ, Olson LE, Kolbe JA, Hebblewhite M, Parks SA (2013) Combining resource selection and movement behavior to predict corridors for Canada lynx at their southern range periphery. Biol Conserv 157:187-195

St. John's River Water Management District [SJRWMD] (2002) SJRWMD land use and land cover. ≤http://www.sjrwmd.com/gisdevelopment/docs/themes.html>. Accessed 1 Jun 2015.

Stamps JA (1983) Sexual selection, sexual dimorphism, and territoriality. In: Huey RB, Pianka ER, Schoener TW (eds), Lizard Ecology: Studies of a Model Organism. Harvard University Press, Cambridge, Massachusetts, U.S.A., pp 169-204

Steen DA, Smith LL (2009) Eastern kingsnake (*Lampropeltis getula getula*) home ranges exhibit limited overlap. Southeast Nat 8:553-558

Steen DA, McClure CJW, Brock JC, Rudolph DC, Pierce JB, Lee JR, Humphries WJ, Gregory BB, Sutton WB, Smith LL, Baxley DL, Stevenson DJ, Guyer C (2012) Landscape-level influences of terrestrial snake occupancy within the southeastern United States. Ecol Appl 22:1084-1097

Steiner TM, Bass OL, Jr., Kushlan JA (1983) Status of the eastern indigo snake in southern Florida national parks and vicinity. Report SFRC-83/01. National Park Service, South Florida Research Center, Everglades National Park, Homestead,

Stevenson DJ, Dyer KJ, Willis-Stevenson BA (2003) Survey and monitoring of the eastern indigo snake in Georgia. Southeast Nat 2:393-408

Stevenson DJ, Enge KM, Carlile LD, Dyer KJ, Norton TM, Hyslop NL, Kilte RA (2009) An eastern indigo snake (*Drymarchon couperi*) mark-recapture study in southeastern Georgia. Herpetol Conserv Biol 4:30-42

Stevenson DJ, Bolt MR, Smith DJ, Enge KM, Hyslop NL, Norton TM, Dyer KJ (2010) Prey records for the eastern indigo snake (*Drymarchon couperi*). Southeast Nat 9:1-18

Stevenson DJ, Hyslop NL (2010) *Drymarchon couperi* (eastern indigo snake). Long-distance interpopulation movement. Herpetol Rev 41:91-92

Stewart BP, Nelson TA, Laberee K, Nielsen SE, Wulder MA, Stenhouse G (2013) Quantifying grizzly bear selection of natural and anthropogenic edges. J Wildl Manage 77:957-964

Stodola KW, Ward MP (2017) The emergent properties of conspecific attraction can limit a species' ability to track environmental change. Am Nat 189:726-733

Storfer A, Murphy MA, Evans JS, Goldberg CS, Robinson S, Spear SF, Dezzani R, Delmelle E, Vierling L, Waits LP (2007) Putting the 'landscape' in landscape genetics. Heredity 98:128-142

Swain HM, Martin PA (2014) Saving the Florida scrub ecosystem: translating science into conservation action. In: Levitt JN (ed), Conservation catalysts: the academy of nature's agent. Lincoln Institute of Land Policy, Cambridge, pp 63-96

Tack JD, Noon BR, Bowen ZH, Strybos L, Fedy BC (2017) No substitute for survival: perturbation analyses using golden eagle population model reveal limits to managing for take. J Raptor Res 51:258-272

Theodoratus DH, Chiszar D (2000) Habitat selection and prey odor in the foraging behavior of western rattlesnakes (*Crotalus viridis*). Behaviour 137:119-135

Therneau T (2015) A package for survival analysis in S. R package version 2.38. http://CRAN.R-project.org/package=survival.

Thompson CM, McGarigal K (2002) The influence of research scale on bald eagle habitat selection along the lower Hudson River, New York (USA). Landscape Ecol 17:569-586

Thurfjell H, Ciuti S, Boyce MS (2014) Applications of step-selection functions in ecology and conservation. Movement ecology 2:4-4

Tille Y, Matei A (2016) sampling: survey sampling. R package version 2.8 http://CRAN.R-project.org/package=sampling.

Timm BC, McGarigal K, Cushman SA, Ganey JL (2016) Multi-scale Mexican spotted owl (*Strix occidentalis lucida*) nest/roost habitat selection in Arizona and a comparison with single-scale modeling results. Landscape Ecol 31:1209-1225

Timmerman WW (1995) Home range, habitat use, and behavior of the eastern diamondback rattlesnake (*Crotalus adamanteus*) on the Ordway Preserve. Bull Fla Mus Nat Hist 38:127-158

Topping CJ, Hoye TT, Odderskaer P, Aebischer NJ (2010) A pattern-oriented modelling approach to simulating populations of grey partridge. Ecol Model 221:729-737

Toral GM, Stillman RA, Santoro S, Figuerola J (2012) The importance of rice fields for glossy ibis (*Plegadis falcinellus*): Management recommendations derived from an individual-based model. Biol Conserv 148:19-27

Trierweiler C, Mullie WC, Drent RH, Exo KM, Komdeur J, Bairlein F, Harouna A, de Bakker M, Koks BJ (2013) A Palaearctic migratory raptor species tracks shifting prey availability within its wintering range in the Sahel. J Anim Ecol 82:107-120

Trumbo DR, Spear SF, Baumsteiger J, Storfer A (2013) Rangewide landscape genetics of an endemic Pacific northwestern salamander. Mol Ecol 22:1250-1266

Turner MG, Gardner RH (2015) Landscape Ecology in Theory and Practice: Pattern and Process. Springer-Verlag, New York

Turner WR, Wilcove DS, Swain HM (2006a) Assessing the effectiveness of reserve acquisition programs in protecting rare and threatened species. Conserv Biol 20:1657-1669

Turner WR, Wilcove DS, Swain HM (2006b) State of the scrub: conservation progress, management responsibilities, and land acquisition priorities for imperiled species of Florida's Lake Wales Ridge.

U. S. Census Bureau (2016) 2016 TIGER/Line shapefiles technical documentation. U.S. Census Bureau. https://www2.census.gov/geo/pdfs/maps-data/data/tiger/tgrshp2016/TGRSHP2016_TechDoc.pdf. Accessed 15 Jul 2017.

U. S. Fish and Wildlife Service (1978) Endangered and threatened plants: listing of the eastern indigo snake as a threatened species. Federal Register 43:4026-4028

U. S. Fish and Wildlife Service (2008) Eastern indigo snake (*Drymarchon couperi*) 5-year review: summary and evaluation. United States Fish and Wildlife Service, Southeast region, Mississippi Ecological Services Field Office, Jackson, Mississippi,

U. S. Fish and Wildlife Service (2014) National wetlands inventory website. U.S. Fish and Wildlife Service. <http://www.fws.gov/wetlands/>. Accessed 15 Jun 2015.

U. S. Geologic Survey (1990) Digital line graphs from 1:24,000-scale maps: Data users guide. National Mapping Program, Techncal Instructions, Data Users Guide 1, Department of the Interior, U.S. Geological Survey,

U. S. Geologic Survey (2014) Hydrography: national hydrography dataset. U.S. Geologic Survey. <http://nhd.usgs.gov/index.html>. Accessed 1 Jul 2015.

U.S. Geological Survey (1990) Digital line graphs from 1:24,000-scale maps: Data users guide. In: National Mapping Program TI, Data Users Guide 1 (ed). Department of the Interior, U.S. Geological Survey,

van Etten J (2017) R Package gdistance: distances and routes on geographical grids. Journal of Statistical Software 76:1-21

Van Oosterhout C, Hutchinson WF, Wills DPM, Shipley P (2004) MICRO-CHECKER: software for identifying and correcting genotyping errors in microsatellite data. Mol Ecol Notes 4:535-538

van Strien MJ, Keller D, Holderegger R (2012) A new analytical approach to landscape genetic modelling: least-cost transect analysis and linear mixed models. Mol Ecol 21:4010-4023

van Strien MJ, Keller D, Holderegger R, Ghazoul J, Kienast F, Bolliger J (2014) Landscape genetics as a tool for conservation planning: predicting the effects of landscape change on gene flow. Ecol Appl 24:327-339

Venables WN, Ripley BD (2002) Modern Applied Statistics with S. Springer, New York

Villard MA, Metzger JP (2014) Beyond the fragmentation debate: a conceptual model to predict when habitat configuration really matters. J Appl Ecol 51:309-318

Villemey A, Peterman WE, Richard M, Ouin A, van Halder I, Stevens VM, Baguette M, Roche P, Archaux F (2016) Butterfly dispersal in farmland: a replicated landscape genetics study on the meadow brown butterfly (*Maniola jurtina*). Landscape Ecol 31:1629-1641

Waldron JL, Lanham JD, Bennett SH (2006) Using behaviorally-based seasons to investigate canebrake rattlesnake (*Crotalus horridus*) movement patterns and habitat selection. Herpetologica 62:389-398

Wang IJ, Savage WK, Shaffer HB (2009) Landscape genetics and least-cost path analysis reveal unexpected dispersal routes in the California tiger salamander (Ambystoma californiense). Mol Ecol 18:1365-1374

Wang M, Grimm V (2007) Home range dynamics and population regulation: An individual-based model of the common shrew *Sorex ayaneus*. Ecol Model 205:397-409

Wasserman TN, Cushman SA, Schwartz MK, Wallin DO (2010) Spatial scaling and multi-model inference in landscape genetics: Martes americana in northern Idaho. Landscape Ecol 25:1601-1612

Watkins A, Noble J, Foster RJ, Harmsen BJ, Doncaster CP (2015) A spatially explicit agent-based model of the interactions between jaguar populations and their habitats. Ecol Model 306:268-277

Weatherhead PJ, Hoysak DJ (1989) Spatial and activity patterns of black rat snakes (*Elaphe obsoleta*) from radiotelemetry and recapture data. Can J Zool 67:463-468

Webb JK, Shine R (1997) A field study of the spatial ecology and movements of a threatened snake species, *Hoplocephalus bungaroides*. Biol Conserv 82:203-217

Webb JK, Brook BW, Shine R (2002) What makes a species vulnerable to extinction? Comparative life-history traits of two sympatric snakes. Ecol Res 17:59-67

Webb JK, Scott ML, Whiting MJ, Shine R (2015) Territoriality in a snake. Behav Ecol Sociobiol 69:1657-1661

Weckworth BV, Musiani M, DeCesare NJ, McDevitt AD, Hebblewhite M, Mariani S (2013) Preferred habitat and effective population size drive landscape genetic patterns in an endangered species. Proceedings of the Royal Society B-Biological Sciences 280

Weekley CW, Menges ES, Pickert RL (2008) An ecological map of Florida's Lake Wales Ridge: a new boundary delineation and an assessment of post-Columbian habitat loss. Fla Sci 71:45-64

Wheatley M, Johnson C (2009) Factors limiting our understanding of ecological scale. Ecol Complex 6:150-159

Whitaker PB, Shine R (2000) Sources of mortality of large elapid snakes in an agricultural landscape. J Herpetol 34:121-128

Whitaker PB, Shine R (2003) A radiotelemetric study of movements and shelter-site selection by free-ranging brownsnakes (*Pseudonaja textilis*, Elapidae). Herpetol Monogr 17:130-144

White GC, Garrott RA (1990) Analysis of Wildlife Radio-tracking Data. Academic Press, Inc., San Diego

White PJ, Ralls K (1993) Reproduction and spacing patterns of kit foxes relative to changing prey availability. J Wildl Manage 57:861-867

White WA (1970) The geomorphology of the Florida peninsula. Bureau of Geology, Florida Department of Natural Resources, Tallahassee, Florida,

Wiegand T, Jeltsch F, Hanski I, Grimm V (2003) Using pattern-oriented modeling for revealing hidden information: a key for reconciling ecological theory and application. Oikos 100:209-222

Wiegand T, Knauer F, Kaczensky P, Naves J (2004) Expansion of brown bears (*Ursus arctos*) into the eastern Alps: a spatially explicit population model. Biodivers Conserv 13:79-114

Wiens JA (1989) Spatial scaling in ecology. Funct Ecol 3:385-397

Williams BK, Nichols JD, Conroy MJ (2002) Analysis and Management of Animal Populations. Academic Press, New York, New York, U.S.A.

Wilson D, Heinsohn R, Legge S (2006) Age- and sex-related differences in the spatial ecology of a dichromatic tropical python (*Morelia viridis*). Austral Ecol 31:577-587

Winiarski KJ, Peterman WE, McGarigal K (In review-a) Evaluation of the R package 'ResistanceGA': a promising approach towards the accurate optimization of landscape resistance surfaces.

Winiarski KJ, Whiteley AR, Peterman WE, McGarigal K (In review-b) Multi-scale resistant kernel surfaces derived from inferred gene flow: an application with vernal pool breeding amphibians.

Wolff JO (1997) Population regulation in mammals: an evolutionary perspective. J Anim Ecol 66:1-13

Wood S (2015) mgcv: Mixed GAM computation vehicle with GCV/AIC/REML smoothness estimation. R package Version 1.8–5. Available at http://CRAN.R-project.org/package=mgcv.

Wood SN (2011) Fast stable restricted maximum likelihood and marginal likelihood estimation of semiparametric generalized linear models. Journal of the Royal Statistical Society Series B-Statistical Methodology 73:3-36

Wronski T, Apio A, Baranga J, Plath M (2006) Scent marking and territorial defence in male bushbuck (*Tragelaphus scriptus*). Journal of Zoology 270:49-56

Wuster W, Yrausquin JL, Mijares-Urrutia A (2001) A new species of indigo snake from north-western Venezuela (Serpentes: Colubridae: *Drymarchon*). Herpetol J 11:157-165

Zeller KA, McGarigal K, Whiteley AR (2012) Estimating landscape resistance to movement: a review. Landscape Ecol 27:777-797

Zeller KA, McGarigal K, Beier P, Cushman SA, Vickers TW, Boyce WM (2014) Sensitivity of landscape resistance estimates based on point selection functions to scale and behavioral state: pumas as a case study. Landscape Ecol 29:541-557

Zeller KA, McGarigal K, Cushman SA, Beier P, Vickers TW, Boyce WM (2016) Using step and path selection functions for estimating resistance to movement: pumas as a case study. Landscape Ecol 31:1319-1335

Zeller KA, Vickers TW, Ernest HB, Boyce WM (2017) Multi-level, multi-scale resource selection functions and resistance surfaces for conservation planning: Pumas as a case study. PLoS ONE 12: e0179570

Zeller KA, Jennings MK, Vickers TW, Ernest HB, Cushman SA, Boyce WM, Bolliger J (2018) Are all data types and connectivity models created equal? Validating common connectivity approaches with dispersal data. Divers Distrib 24:868-879

Zhu Z, Woodcock CE (2012) Object-based cloud and cloud shadow detection in Landsat imagery. Remote Sens Environ 118:83-94

Zhu Z, Wang SX, Woodcock CE (2015) Improvement and expansion of the Fmask algorithm: cloud, cloud shadow, and snow detection for Landsats 4-7, 8, and Sentinel 2 images. Remote Sens Environ 159:269-277

Zurell D, Grimm V, Rossmanith E, Zbinden N, Zimmermann NE, Schroder B (2012) Uncertainty in predictions of range dynamics: black grouse climbing the Swiss Alps. Ecography 35:590-603

Zweifel-Schielly B, Kreuzer M, Ewald KC, Suter W (2009) Habitat selection by an Alpine ungulate: the significance of forage characteristics varies with scale and season. Ecography 32:103-113

Zwick PD, Carr MH (2006) Florida 2060: a population distribution scenario for the state of Florida.